Avantek
HIGH-FREQUENCY TRANSISTOR PRIMER

PART I

ELECTRICAL CHARACTERISTICS

Transistors have been used at frequencies above 1 GHz since about 1960. The technology has increased such that both circuit and project engineers look to transistors for new system requirements at frequencies below 6 GHz. New techniques are being evaluated that should result in X-band transistors in the near future. The purpose of the primer is to introduce microwave designers to the terminology used in describing the characteristics of high frequency transistors. An understanding of the capabilities and limitations of these transistors should result in better performing, more reliable circuits.

TABLE OF CONTENTS

INTRODUCTION

This primer is a short glossary and brief explanation of transistor terms commonly used in Avantek transistor data sheets, advertisements, and other technical communications. Some of these terms are simple, virtually self-explanatory and are included here primarily for the sake of completeness. Others are more specialized and potentially ambiguous due to a lack of terminology standardization in the high-frequency transistor area. These latter types receive more treatment here.

I. TRANSISTOR STRUCTURE TYPES

All current Avantek transistors are of the Bi-polar NPN Silicon Planar Expitaxial type. Briefly, the significance of each of these descriptive terms is as follows:

A. Bi-polar

A word which in its broad sense identifies the basic structure shown schematically in Figure 1; the familiar three semiconductor-region structure. Bi-polar specifically means that charge carriers of both negative (electrons) and positive (holes) polarities are involved in the transistor action. In way of contrast, unipolar types include the junction-gate and insulated-gate field-effect transistors which are basically one- or two-semiconductor-region structures in which carriers of a single polarity dominate.

B. NPN

An abbreviation of negative - positive - negative which identifies the regions of the structure as to polarity (of the dominant or majority carrier in each region). The second polarity-type is PNP. (See Figure 1.)

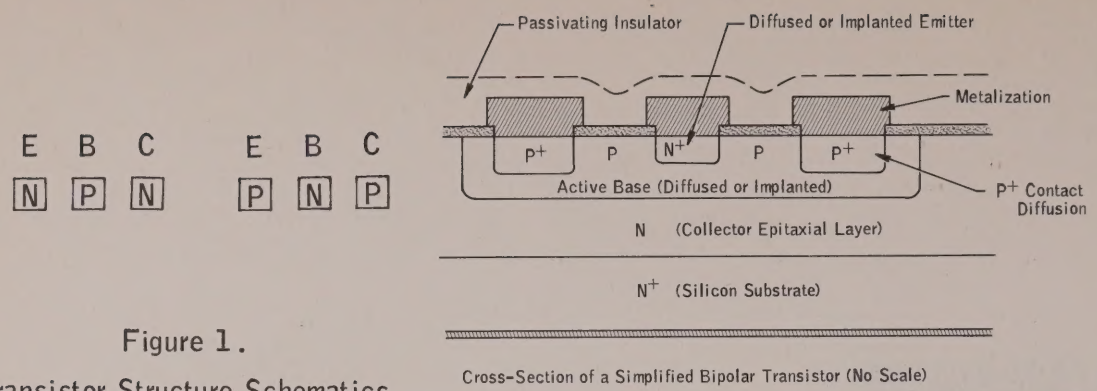

Figure 1.
Transistor Structure Schematics

C. Silicon

Silicon is one of two elements from the fourth column of the periodic table which are in widespread use for transistor fabrication (the other is germanium). Other materials used include the compound, gallium arsenide. Silicon is in predominant use because it results in the most favorable compromise among high-frequency, high-temperature, high-reliability, and ease-of-fabrication attributes of the usable semiconductor materials.

D. Planar

A term which denotes that both emitter-base and base-collector junctions of the transistor intersect the device surface in a common plane (hence, a better term might be co-planar). However, the real significance of the so-called planar structure is that the technique of diffusing dopants through an oxide mask, used in fabricating such a structure, results in the junctions being formed beneath a protective oxide layer. These protected junctions are less prone to surface problems sometimes associated with other types of structures, such as the mesa.

E. Epitaxial

This term, as it is commonly used, is actually a shortening of the term epitaxial-collector. That is, the collector region of the transistor is formed by the epitaxial technique rather than by diffusion which is commonly used to form the base and emitter regions. The epitaxial layer is formed by condensing a single-crystal film of semiconductor material upon a wafer or substrate which is usually of the same material. Thus, an epitaxial (collector) transistor is one in which the collector region is formed upon a low-resistivity silicon substrate. Subsequently, the base and emitter regions are diffused into the "epi" layer. The

epitaxial technique lends itself to precise tailoring of collector-region thickness and resistivity with consequent improved device performance and uniformity.

II. MAXIMUM RATINGS

Maximum ratings may be defined as limiting values of externally applied stresses (voltage, current, temperature, etc.) normally under control of the user which if exceeded may result in irreversible damage to the device. The user who exceeds the maximum ratings does so necessarily at his own risk. These ratings are set by the manufacturer on the basis of many considerations such as life tests, breakdown voltages, etc., in order to define to the user certain operating conditions which are safe for each and every transistor of a given type.

Unfortunately, due to the cost of establishing certain ratings (which must eventually be reflected in product prices) the ratings given do not always encompass all conceivable operating conditions. For example, device dissipation ratings typically are complete only for the case of continuous dissipation (as opposed to peak dissipation in pulse applications). In practice, the ratings given should be sufficient for the majority of applications of a particular device. In certain applications, more information must be obtained by the user himself and/or through applications assistance from the manufacturer. The following ratings typically appear on Avantek transistor data sheets and provide adequate information for most applications of these devices.

A. Voltage Ratings

These ratings are usually derived from and usually coincide with the minimum device breakdown voltages. However, since this coincidence does not necessarily occur, it has become common practice to include both maximum voltage ratings and minimum breakdown voltages on data sheets.

It can be argued that such practice erodes the meaning of maximum ratings. Since, strictly speaking, maximum ratings should not be exceeded under any circumstances, strict adherence to voltage ratings would preclude measurement

of breakdown voltages of any but marginal devices. In practice, voltage ratings are usually maximum operating voltages and no damage results if they are exceeded only to measure the breakdown voltages provided that care is taken to insure that the specified low currents for these measurements are not exceeded.

B. Current Ratings

Maximum current ratings are arrived at from various considerations such as bonding-wire current-carrying ability, overall transistor performance degradation, etc. Maximum ratings are usually given only for collector current (except, in some cases for switching devices) since safely limiting collector current usually insures that base and emitter currents are also safely limited.

C. Dissipation Ratings

In addition to the individual ratings on voltage and current discussed above, there is also a limit to the voltage-current products which can be safely handled by a transistor. That is, there is a power dissipation rating which must also be adhered to. Since the dissipation capabilities of a device are a function of the temperature of the external environment, this rating is a function of that temperature. For the DC case, this temperature dependence is usually the only significant functional dependence of this rating. In the AC case, that is when device dissipation varies significantly with time, dissipation capabilities become a generally complex function of waveshape. In the latter case, in addition to an average dissipation rating (which coincides with the DC rating) there exists a peak dissipation rating which is a function of waveshape (e.g., a function of pulse width and pulse period in the case of rectangular waveforms). Due to the complexity of the general AC case, transistors are seldom characterized completely enough to include complete AC rating information. Most transistors are rated only in terms of maximum continuous dissipation (that is the maximum DC and maximum average dissipation). This rating is typically specified in terms of a maximum continuous dissipation at or below some stated reference temperature (usually 25°C) and a linear derating factor to be applied

at higher temperatures. These two quantities define the maximum continuous dissipation rating curve shown graphically in Figure 2, or expressed analytically as:

$$P_{T(max)}\ T_X = P_{T(max)}\ T_{XI}\ ;\ T_X \leq T_{XI}$$

$$P_{T(max)}\ T_X = P_{T(max)}\ T_{XI} - K_{JX}\Delta T_X\ ;\ T_{XI} < T_X < T_{X(max)}$$

Where

T_X = Temperature of External Reference Point

$P_{T(max)}\ T_X$ = Maximum Total Dissipation, a function of T_X

T_{XI} = Reference Temperature below which $P_{T(max)}$ is constant

K_{JX} = Linear Derating Factor

$T_{X(max)}$ = Maximum Junction Temperature

ΔT_X = $T_X - T_{XI}$

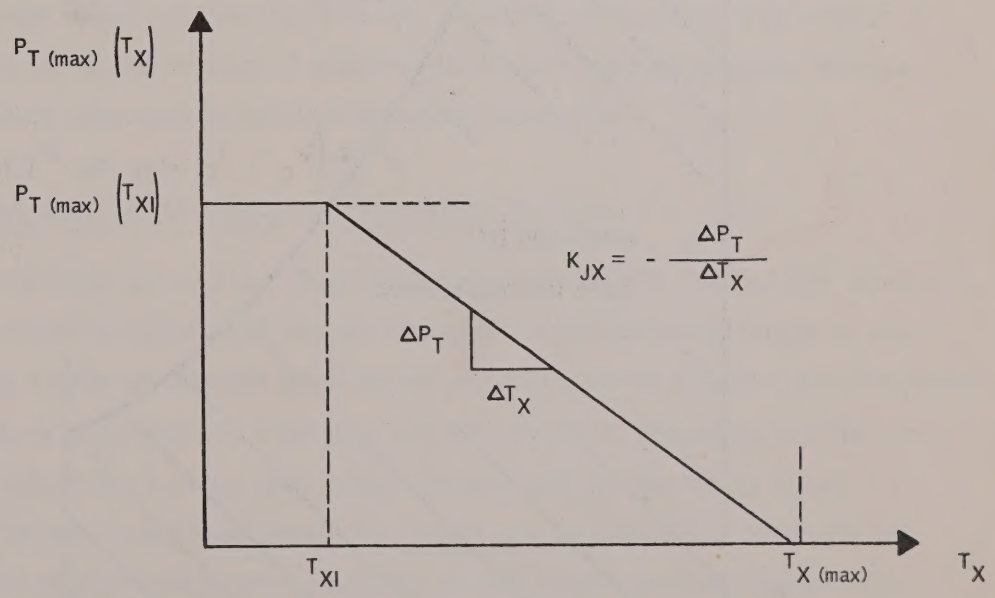

Figure 2

Continuous Dissipation Rating Curve

Two external temperature reference points are commonly used:

1. Air ambient, T_A (or free-air; that is no forced air cooling), which is the air temperature in proximity to the transistor case as mounted in its "normal" manner and,

2. Case ambient, T_C, which is the temperature of the point on the transistor package at which it is most effective to heat sink the transistor. Which reference point is used depends on the application.

In summary, the continuous dissipation rating (usually based on a V·I product), and the collector voltage and current ratings define a DC safe operating area as sketched in Figure 3.

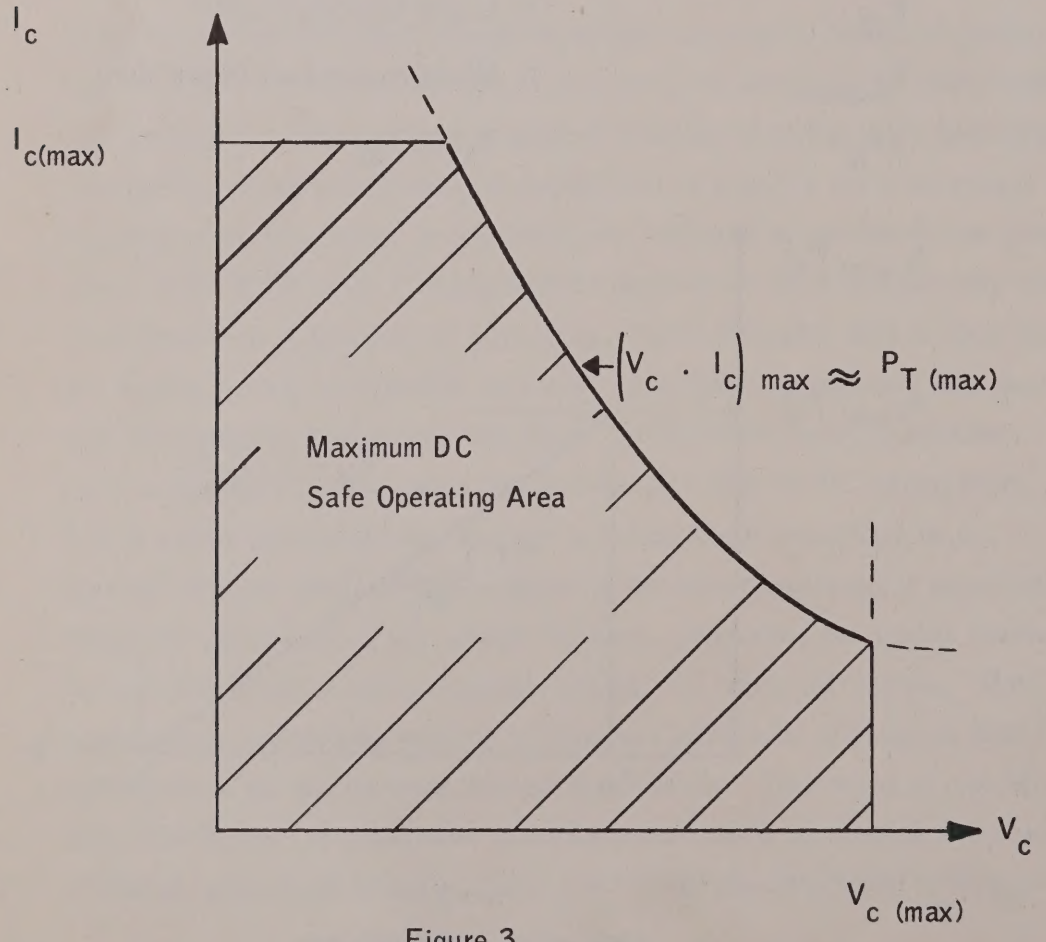

Figure 3

D. Junction Temperature Rating

Another temperature reference point implicit in the above discussion of dissipation ratings is transistor junction temperature. The maximum external reference temperature, $T_{X(max)}$ corresponds to maximum internal junction temperature, since at $T_{X(max)}$ the power dissipation must be derated to zero. Strictly speaking, junction temperature does not properly classify as a maximum rating since it is not an external stress under direct control of the user (as opposed to power dissipation and external operating temperature which are). Thus, a more appropriate terminology for this rating would be maximum operating temperature. However, since it is a limiting factor in transistor dissipation capabilities and its use simplifies time-varying thermal analysis, this rating still appears on many transistor data sheets as a junction temperature rating.

E. Storage Temperature Rating

This rating defines the range of temperature over which the transistor may be stored (in the non-operating state) without damage. Because of possible electrical-temperature interactions, storage temperature range and operating temperature range do not necessarily coincide. However, in practice, they usually do coincide and in the absence of stated restrictions on operating range, storage temperature range may be taken as operating range also.

III. ELECTRICAL AND PERFORMANCE CHARACTERISTICS

Electrical characteristics may be described as uniquely defined, measurable electrical properties of the transistor which are not a function of the measuring circuit or apparatus (except insofar as standard terminations and measurement accuracy are concerned). Performance, or operating characteristics are also electrical properties but they are, in general, not unique because their values depend upon the measuring circuit (in particular, the source and load impedance, which may be arbitrary). As might be expected, the terms are often used somewhat loosely (and sometimes interchangeably), especially in some cases where there are only subtle differences involved. The terms are generally used on transistor data sheets to segregate (for emphasis)

under performance or operating characteristics those properties most directly applicable for the primary intended application.

A. Performance (Operating) Characteristics

Of the numerous performance characteristics which can be specified for high-frequency transistors, perhaps the most fundamental and pertinent characteristics are:

1. Power gain and noise figure, for small-signal applications;

2. Power gain, power output and efficiency, for large-signal applications.

All of these characteristics are, of course, functions of frequency, bias, temperature, etc., and to completely characterize a transistor over its full frequency, bias, and temperature ranges would be prohibitively costly. Consequently, characterization data is given only for restricted ranges of these variables. This data should portray sufficiently the capabilities of a particular device for its primary intended applications. As in the case of maximum ratings, some applications may require additional characterization by the user himself or through applications assistance from the manufacturer.

1. Power Gain

a. G_{max}

Of the various definitions for the measure of power flow in an active two-port device, such as a transistor, two are unique enough to allow specification without recourse to specifying the complete measuring circuit in detail. One of these definitions is termed maximum available gain, G_{max}; it is the power gain obtained when the input and output ports are simultaneously conjugately matched to source and load impedances, respectively. Implicit in this definition is the

assumption that the two-port is unconditionally stable, i.e., no combinations of input/output tuning can result in increasing gain to the point of oscillation.

b. $|S_{21}|^2$

The other unique power gain is the gain realized when the transistor is inserted between a source and load with identical impedances (in practice usually 50 + j0 ohms). This particular insertion or transducer gain happens to coincide with the usual definition of the two-port forward scattering parameter, S_{21}. More precisely, it is equal to the magnitude-squared of this parameter and is therefore often identified by the symbol $|S_{21}|^2$. For wideband applications, $|S_{21}|^2$ is important since wideband terminations "not-too-different" from 50 ohms are more easily realized than are wideband transforming networks which provide the matching required for G_{max}.

2. Noise Figure

A common measure of the noise generated by an active two-port device, noise which sets a lower limit on amplifier sensitivity, is the noise factor, F.

This may be defined as $F = \frac{\text{Input signal-noise ratio}}{\text{Output signal-noise ratio}}$,

or more generally, $F = \frac{\text{Total output noise power}}{\text{Output noise power due to Source Resistance}}$

At high frequencies, spot noise factor or noise factor for small fractional bandwidth (say 1%) is used and is usually expressed as noise figure, NF, in decibels, i.e.,

$$NF = 10 \log F$$

As already discussed, noise figure is a function of source impedance (as

well as functions of frequency, bias, etc.) and hence, there is an infinity of noise figures associated with a given device corresponding to the infinity of possible impedances which may be presented to the device output. The only unique one, in the sense that it does not involve arbitrary source impedances is NF_{min}, the minimum noise figure obtained (at given bias and frequency) when the input is tuned to optimize this parameter. It is this noise figure which is usually given on Avantek data sheets.

In practical amplifiers, involving more than one stage, overall noise factor F_0 is given by:

$$F_0 = F_1 + \frac{F_2 - 1}{G_1} + \cdots + \frac{F_n - 1}{G_{(n-1)}}$$

where n = number of stages

G_n = gain of nth stage

F_n = noise factor of nth stage

This expression emphasizes the important fact that for low noise amplifiers, the first stage must be designed for as low noise figure and as high gain as possible. (Note that the noise contribution of the second stage is divided (reduced) by the gain of the first stage.) Since the optimum source impedances and bias currents for optimum gain and noise figure do not often coincide, very careful circuit design is required to minimize overall noise figure.

3. Power Output

This characteristic is important for both amplifier and oscillator transistors. In both cases, it is extremely circuit sensitive. For amplifiers, maximum useful output is often limited to that power output level at which gain has compressed 1 dB, an indicator of the upper limit on linearity range. For oscillators, it is merely a quantitative measure of RF power output for a given DC input power.

4. Efficiency

In the most general sense, this characteristic expresses as a percentage, the ratio of RF power output to the total circuit input power, both DC and RF. That is efficiency, η, is given by:

$$\eta = \frac{P_0}{P_i + P_{DC}} \cdot 100$$

where P_0 = RF output power

P_i = RF input power

P_{DC} = total DC power input

Since for oscillator transistors there is no RF power input, and for amplifier transistors the maximum input RF power is calculable from the power gain and power output specifications, the inclusion of P_i in efficiency is redundant. Moreover, since the major portion of the DC power is dissipated by the transistor collector, a more restricted definition of efficiency is pertinent. This parameter, termed collector efficiency, η_c is given by:

$$\eta_c = \frac{P_0}{P_{CC}} \cdot 100$$

where $P_{CC} = V_{CC} \cdot I_{CC}$

V_{CC} = collector supply voltage

I_{CC} = collector supply current

B. Electrical Characteristics

Electrical characteristics may be conveniently classified into two main types, DC and AC.

1. DC Characteristics

The importance of DC characteristics of high frequency transistors lies

primarily in biasing and reliability considerations. However, certain DC characteristics are also directly related to high-frequency performance. For example, high-frequency noise figure is affected by the DC current gain. The DC characteristics which are discussed here are those usually found on high-frequency transistor data sheets.

a. $V_{(BR)CBO}$, I_{CBO}

These two parameters serve to characterize the reverse-biased collector-base p-n junction and are defined as follows, with the aid of Figure 4a. The collector-base breakdown voltage, $V_{(BR)CBO}$, identifies the voltage at which collector current tends to increase without limit, usually due to the high electric field developed across the junction. This voltage sets a limit on the maximum transistor operating voltage and as mentioned before under maximum ratings, usually is the basis for the collector-base maximum voltage rating. $V_{(BR)CBO}$ should be specified at a value of $I_C = I_{C1}$ in the figure, which is within the avalanche (or high-slope) region of the reverse characteristic - typical values of I_{C1} are in $1 - 10$ μA region for high-frequency transistors.

To further define the quality of the reverse V-I characteristic a specification is usually placed on collector cutoff current, I_{CBO}, measured at some value of collector-base voltage less than $V_{(BR)CBO}$. For a good quality ("sharp" instead of soft, see Figure 4a) silicon junction, I_{CBO} is in the nano ampere range.

b. $V_{(BR)EBO}$, I_{EBO}

These two parameters characterize the reverse-biased emitter-base p-n junction in an analogous manner to the collector-base junction parameters $V_{(BR)CBO}$ and I_{CBO}. No further discussion will be given here.

c. $V_{BR(CEO)}$, I_{CEO}

The collector-emitter breakdown voltage and cutoff current are somewhat more complex in nature than either the collector-base or emitter-base parameters. In the latter two, only a single p-n diode is involved. In the collector-emitter case, two diodes are involved. Moreover, each is influenced by the other through transistor action, since the reverse current of the collector-base diode flows through the emitter-base junction as forward current. Thus the collector-base reverse current is amplified by the DC current gain of the transistor resulting in:

1) I_{CEO} being greater than I_{CBO} (for a given voltage).

2) Typically the familiar negative-resistance region in the V-I characteristic as shown in Figure 4c.

Consequently $V_{BR(CEO)}$ is typically specified at collector currents one to three orders of magnitude higher than in the case of $V_{BR(CBO)}$ and $V_{BR(EBO)}$ in order to establish the minimum value of this characteristic.

d. h_{FE}

This parameter is simply the DC common-emitter current gain; i.e., the ratio of collector current to base current at some specified collector voltage and current.

2. AC Characteristics

Of the numerous AC characteristics which are defined for transistors, only relatively few are commonly used in characterizing high-frequency transistors. Some of the more pertinent parameters are briefly covered here.

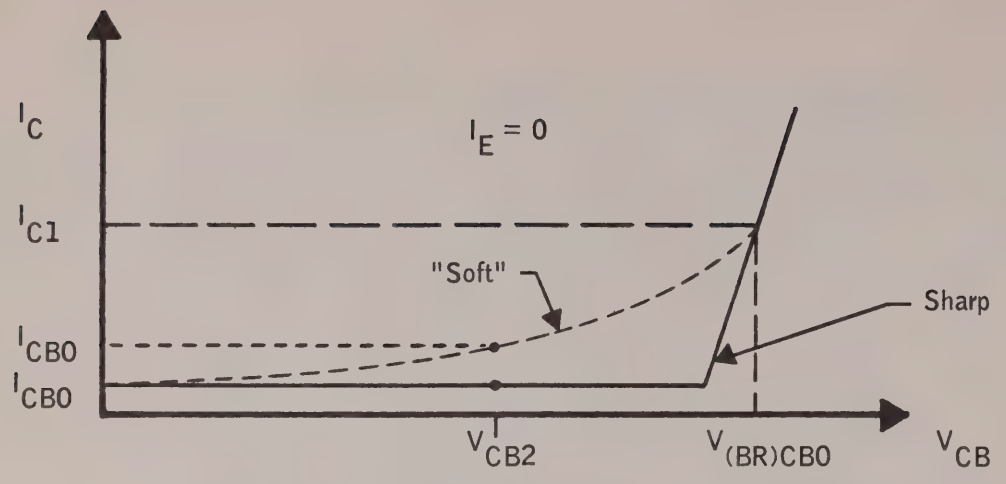

(a) COLLECTOR-BASE

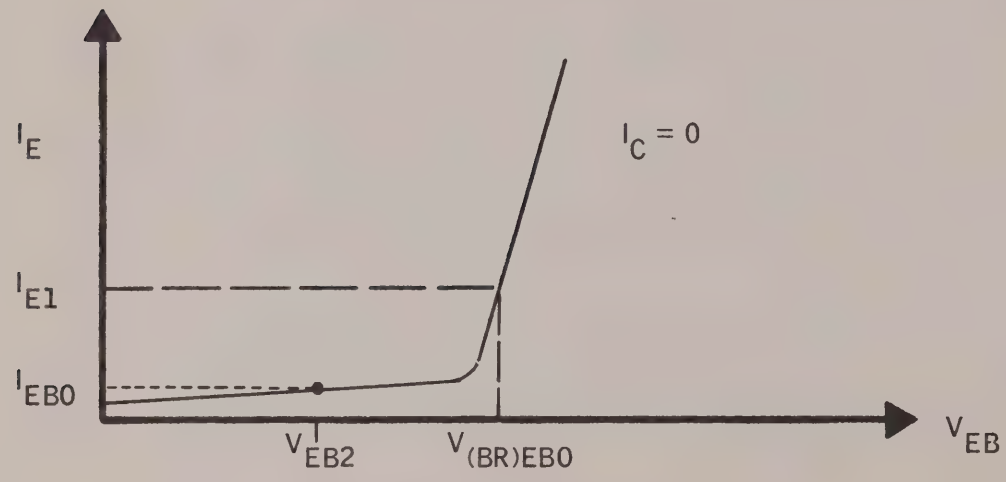

(b) EMITTER-BASE

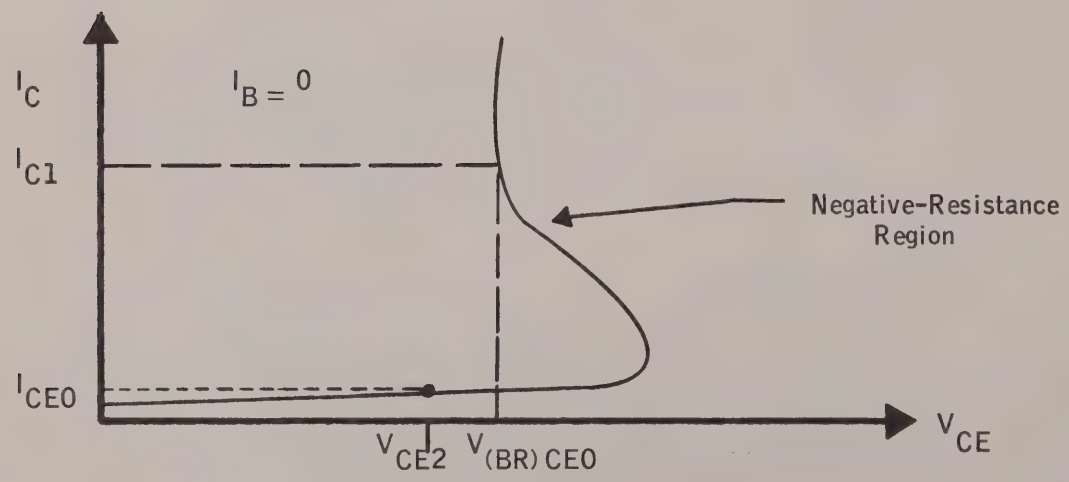

(c) COLLECTOR-EMITTER

Figure 4 - Transistor Reverse V-I Characteristics

a. S-Parameters

By far the most useful and conveniently measured set of two-port parameters for transistor high-frequency (say, 100 MHz and above) characterization is the s-parameter or scattering-matrix set. These parameters completely and uniquely define the small-signal gain and input/ouput immitance properties of any linear "black-box". (By definition, a transistor or any active device is linear under small-signal conditions.) However, these parameters reveal nothing (except possible indirectly and approximately) about large-signal behavior or about noise behavior. Simply interpreted (more general definitions and other interpretations abound in the technical literature), the s-parameters are merely insertion gains, forward and reverse; and reflection coefficients, input and output, with driven and non-driven ports both terminated in equal impedances, usually 50 ohms, real. Such an interpretation tends to make s-parameters very attractive, once some familiarity is gained, at high (especially microwave) frequencies, since the power flow or gain and reflection-coefficient concepts are more intuitively meaningful than voltage and current conceptual schemes. It should also be mentioned that s-parameters can be converted through straight-forward matrix transformations to other two-port parameter sets; e.g., h-, y-, or z-parameters.

Proceeding with more specific definitions, the s-parameters are defined analytically by:

$$b_1 = s_{11} a_1 + s_{12} a_2$$

$$b_2 = s_{21} a_1 + s_{22} a_2$$

or, in matrix form,

$$\begin{bmatrix} b_1 \\ b_2 \end{bmatrix} = \begin{bmatrix} s_{11} & s_{12} \\ s_{21} & s_{22} \end{bmatrix} \begin{bmatrix} a_1 \\ a_2 \end{bmatrix}$$

where (referring to Figure 5)

a_1 = (incoming power at port 1)$^{1/2}$

b_1 = (outgoing power at port 1)$^{1/2}$

a_2 = (incoming power at port 2)$^{1/2}$

b_2 = (outgoing power at port 2)$^{1/2}$

E_1, E_2 = Electrical Stimuli at Port 1, Port 2

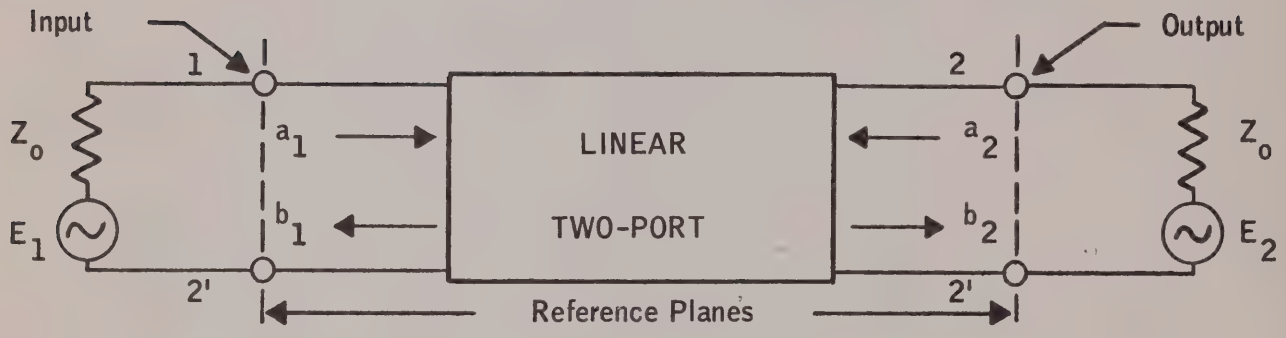

Figure 5 - Two-Port s-parameter Definition Schematic

From the figure and defining linear equations, for $E_2 = 0$, then $a_2 = 0$, and (skipping numerous rigorous steps)

$$S_{11} = \frac{b_1}{a_1} = \left[\frac{\text{Outgoing Input Power}}{\text{Incoming Input Power}}\right]^{1/2}$$

$$= \frac{\text{Reflected Voltage}}{\text{Incident Voltage}}$$

$$= \text{Input Reflection Coefficient}$$

$$S_{21} = \frac{b_2}{a_1} = \left[\frac{\text{Outgoing Output Power}}{\text{Incoming Input Power}}\right]^{1/2}$$

$$= \left[\frac{\text{Output Power}}{\text{Available Input Power}}\right]^{1/2}$$

$$= \left[\text{Forward Transducer Gain}\right]^{1/2}$$

or more precisely in the case of S_{21},

$$\text{Forward Transducer Gain} = G_{TF} = \left|S_{21}\right|^2$$

$$Z_i = Z_o$$

Similarly, at port 2, for $E_1 = 0$, then $a_1 = 0$, and

$$S_{22} = \frac{b_2}{a_2} = \text{Output Reflection Coefficient}$$

$$S_{12} = \frac{b_1}{a_2} = (\text{Reverse Transducer Gain})^{1/2}$$

or

$$G_{TR} = |S_{12}|^2$$

Some measuring systems used actually "read-out", the magnitude of the s-parameter, in decibels. Since the most useful form of s-parameters for circuit design is when the magnitude is in ratio form, the following simple relationships are important.

$$|S_{11}|_{dB} = 10 \log |S_{11}|^2$$
$$= 20 \log |S_{11}|$$
$$|S_{22}|_{dB} = 20 \log |S_{22}|$$
$$|S_{21}|_{dB} = 10 \log |S_{21}|^2$$
$$= 20 \log |S_{21}|$$
$$= 10 \log G_{TF} = G_{TF}|_{dB}$$
$$|S_{12}|_{dB} = 10 \log |S_{12}|^2$$
$$= 20 \log |S_{12}|$$
$$= 10 \log |G_{TR}| = G_{TR}|_{dB}$$

b. Transition Frequency

One of the better known, but perhaps least understood, figures-of-merit for high-frequency transistors is the so-called transition frequency, f_T. Part of the misunderstanding which appears to exist is due to the use of a misleading (but common, for historical reasons) terminology of "short-circuit gain-bandwidth product" for this parameter.

By definition f_T is that characteristic frequency described by the equation:

$$f_T = |h_{fe}| \cdot f_{meas}$$

where

$|h_{fe}|$ = magnitude of small-signal common-emitter short-circuit current gain, h_{fe}

f_{meas} = frequency of measurement, chosen such that $2 \lesssim |h_{fe}| \lesssim \frac{h_{feo}}{2}$

h_{feo} = the low-frequency value of h_{fe}

To varying degrees of approximation, depending on transistor type, f_T is the frequency at which $|h_{fe}|$ approximates unity. It is not, in general, the frequency at which $|h_{fe}|$ is precisely equal to unity. To clarify these points further, consider the plot of $|h_{fe}|$ against frequency sketched in Figure 6.

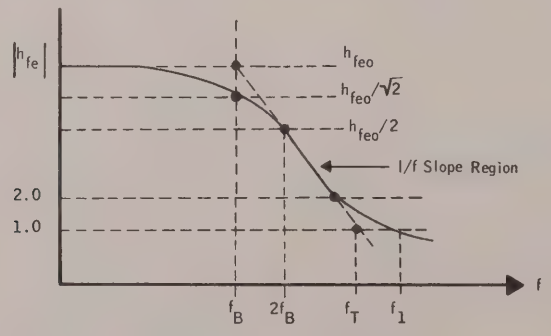

Figure 6 - $|h_{fe}|$ Frequency Characteristic

At low frequencies, $f << f_B$ $|h_{fe}|$ is constant and equal to h_{feo}.

At f_B, $|h_{fe}|$ has decreased to 0.707 h_{feo} ; i.e., f_B is the 3 dB cutoff frequency for common-emitter short-circuit current gain, h_{fe}.

For frequencies such that

$$2 f_B < f < f_T$$

h_{fe} varies inversely proportional to frequency. That is, the f_T defining relationship holds:

$$|h_{fe}| \cdot f_{meas} = \text{constant} = f_T$$

At frequencies approaching f_T, other parameters, especially package parasitics, can cause $|h_{fe}|$ to depart significantly from this 1/f variation. Therefore, the frequency, f_1, at which $|h_{fe}|$ actually equals unity can be somewhat different from f_T.

Applying this frequency-gain characteristic to common-emitter wideband, low-pass amplifiers gives rise to the terminology of f_T being a "gain-bandwidth product". However, this is an optimistic approximation at best, since the product of low-frequency circuit gain and the 3 dB cutoff frequency is reduced from f_T by an amount depending on circuit impedances.

The real significance of f_T lies in the fact that it is a measure of certain internal transistor parameters which do, in fact, affect high frequency performance; for example, gain (though not in the convenient quantitative manner implied by the gain-bandwidth product terminology). In particular, good high-frequency noise performance requires that f_T be high. Thus, f_T is included on transistor data sheets as a figure of merit primarily, not as a parameter to be used directly in design.

c. Collector-Base Time Constant, $r_b' C_c$

This is an internal device parameter which relates only somewhat indirectly to high frequency performance. It is primarily a measure of internal feedback within the transistor. It also relates to transistor high frequency impedance. As the name shows, it is a measure of transistor base resistance and collector capacitance in combination; however, except for certain low frequency transistors, it can not be considered a simple two-element lumped R-C time constant implied by the terminology. (In high frequency transistors, both base resistance and collector capacitance must be considered distributed when considered in detail). As a figure-of-merit, it is included on transistor data sheets to indicate how well base resistance and collector capacitance have been minimized. It also allows the estimation of certain gain properties of the transistor. (see f_{max} parameter, following).

d. Collector-Base Capacitance, C_{cb}

This parameter is simply the total collector base p–n junction capacitance measured at a low frequency (typically, 1 MHz) where it can be considered a single lumped element. For high-frequency transistors it is, of course, desirable that C_{cb} be small from bandwidth and stability considerations as well as from gain considerations alone.

e. Maximum Frequency of Oscillation, f_{max}

This is another figure-of-merit parameter, as opposed to measurable parameters directly usable in the applications of transistors. Its importance stems from the following approximate relationships(which will not be derived here);

$$f_{max} \approx \left(\frac{f_T}{8\pi r_b' C_c} \right)^{1/2}$$

$$G_{max} \approx \left(\frac{f_{max}}{f_{oper}} \right)^2$$

These expressions illustrate in a quantitative way the importance and the interrelationship between high f_T and low $r_b'C_c$ insofar as high frequency gain is concerned. However, since they are approximations and since their derivation involves several assumptions not always valid, they must be interpreted with caution. For example, the expression for G_{max} is obviously not applicable at low frequencies, since as $f \rightarrow 0$, $G_{max} \rightarrow \infty$, according to this expression. As a rule of thumb, the G_{max} expression is a reasonable approximation for frequencies such that,

$$5 > \frac{f_{max}}{f_{oper}} > 1.$$

For accurate analysis of transistor gain and stability, a complete set of two-port parameters must be employed in exact expressions, such as those from which the approximations shown above were derived.

GLOSSARY OF MICROWAVE TRANSISTOR TERMINOLOGY

$V_{(BR)CBO}$	Breakdown voltage of a reverse biased collector base juntion. Measured with the emitter open.
$V_{(BR)EBO}$	Breakdown voltage of a reversed biased emitter base junction. Measured with the collector open.
$V_{(BR)CEO}$	Breakdown voltage between the collector and emitter terminals. Measured with the base open.
I_{CBO}	Leakage current of a reverse biased collector base junction. Measured with the emitter open.
I_{EBO}	Leakage current of a reverse biased emitter base junction. Measured with the collector open.
h_{fe}	DC common emitter current gain
C_{cb}	Collector base junction capacitance. Measured with the emitter connected to the guarded terminal of a three terminal measurement system.
f_T	Transition Frequency. The frequency at which the magnitude of the small signal common emitter short circuit current gain approximates unity.
$r_b' C_c$	The collector base time constant.
f_{max}	Maximum frequency of oscillation. The frequency at which G_{max} approximates unity.
$P_{T(max)}$	Maximum continuous power dissipation below a reference temperature (usually 25°C).
$T_{J(max)}$	Maximum allowable transistor junction temperature.
$I_{C(max)}$	Maximum allowable collector current without destruction or degradation of the transistor.
NF	A measure of the noise generated by the transistor.
G_{max}	The maximum available power gain (MAG) when the transistor is unconditionally stable and input and output parts are simultaneously conjugately matched.
S_{11}	Input reflection coefficient
S_{12}	Reverse transfer coefficient
S_{21}	Forward transfer coefficient
S_{22}	Output reflection coefficient
P_o	Amplifier -- The power output at the one (1) dB gain compression point. Oscillator -- A measure of the RF power output.

DOMESTIC REPRESENTATIVES

ALABAMA
Beacon Electronic Associates
11309 S. Memorial Parkway,
Suite B
Huntsville, AL 35803
(205) 881-5031

ARIZONA
The Thorson Company
2505 E. Thomas Road
Phoenix, AZ 85016
(602) 956-5300

CALIFORNIA (Southern)
Cain Technology
522 S. Sepulveda Blvd., Suite 112
Los Angeles, CA 90049
(213) 476-2251

CALIFORNIA (Northern)
Cain-White & Company
Foothill Office Center
105 Fremont Avenue
Los Altos, CA 94022
(415) 948-6533

COLORADO
The Thorson Company
5290 Yale Circle
Denver, CO 80222
(303) 759-0809

DC and VIRGINIA
Applied Engineering Consultants
Washington, DC
(301) 953-2808
(301) 953-2809

FLORIDA
Beacon Electronic Associates
P.O. Box 1278
Maitland, FL 32751
(305) 647-3498

Beacon Electronic Associates
1041 W. Commercial Blvd., Suite 202
Fort Lauderdale, FL 33309
(305) 776-6074

GEORGIA
Beacon Electronic Associates
2285 Peachtree Road, NE
Atlanta, GA 30309
(404) 351-3654

ILLINOIS (Northern)
DyTec/Central, Inc.
121 S. Wilke Road
Suite 304
Arlington Heights, IL 60035
(312) 394-3380

ILLINOIS (Southern)
DyTec/South, Inc.
10534 Natural Bridge Road
St. Louis, MO 63134
(314) 423-1234

IOWA (Eastern)
DyTec/Central, Inc.
121 S. Wilke Road
Suite 304
Arlington Heights, IL 60035
(312) 394-3380

IOWA (Southern)
DyTec/South, Inc.
10534 Natural Bridge Road
St. Louis, MO 63134
(314) 423-1234

KANSAS
DyTec/South, Inc.
6300 W. 75th Street
Overland Park, KS 66204
(913) 432-5596

MARYLAND
Applied Engineering Consultants
9051 Baltimore National Pike
Building 3, Office A
Ellicott City, MD 21043
(301) 465-1272

MASSACHUSETTS
R.J. Sickles Associates
12 Cambridge St. (Rt. 3)
Burlington, MA 01803
(617) 272-7285

MICHIGAN
Comtel Instruments Company
17500 West McNichols Road
Detroit, MI 48235
(313) 255-1970

MISSOURI (East)
DyTec/South, Inc.
10534 Natural Bridge Road
St. Louis, MO 63134
(314) 423-1234

MISSOURI (West)
DyTec/South, Inc.
6300 W. 75th Street
Overland Park, KS 66204
(913) 432-5596

NEBRASKA
DyTec/South, Inc.
10534 Natural Bridge Road
St. Louis, MO 63134
(314) 423-1234

NEW JERSEY (Northern)
Technical Marketing Associates
2460 Lemoine Avenue
Fort Lee, NJ 07024
(201) 224-6911

NEW MEXICO
The Thorson Company
2201 San Pedro Drive, NE
Building 2, Suite 107
Albuquerque, NM 87110
(505) 265-5655

NEW YORK (Metropolitan)
Technical Marketing Associates
2460 Lemoine Avenue
Fort Lee, NJ 07024
(201) 224-6911

NEW YORK (Upper State)
Robtron
2-4 Fennell Street, Suite 209
Skaneateles, NY 13152
(315) 685-5731

NORTH and SOUTH CAROLINA
Beacon Electronic Associates
122 W. Woodlawn Road
Suite A-106
Charlotte, NC 28210
(704) 525-7412

OHIO
Comtel Instruments Company
5827 Mayfield Road
Cleveland, OH 44124
(216) 442-8080

Comtel Instruments Company
1717 Big Hill Road A6
P.O. Box 2036 Kettering
Dayton, OH 45439
(513) 298-7573

PENNSYLVANIA
Comtel Instruments Company
No. 2 Parkway Center
Pittsburgh, PA 15220
(412) 922-5720

Eastern Instrumentation of
Philadelphia
613 W. Cheltenham Avenue
Philadelphia, PA 19126
(215) 927-7777

TEXAS
The Thorson Company
4400 Sigma Road
Dallas, TX 75240
(214) 233-5744

The Thorson Company
6655 Hillcroft, Suite 224
Houston, TX 77036
(713) 771-3504

WASHINGTON
The Thorson Company
One Lake Bellevue Drive
Bellevue, WA 98005
(206) 455-9180

WISCONSIN
DyTec/Central, Inc.
121 S. Wilke Road
Suite 304
Arlington Heights, IL 60035
(312) 394-3380

INTERNATIONAL REPRESENTATIVES

AUSTRALIA
General Electronic Services Pty. Ltd.
99 Alexander Street, Crows Nest
New South Wales, 2065
Phone: 439-2488
Telex: Servo 25486

BELGIUM
Simac Electronics B.V.
148, Boulevard du Triomphe
1160 Brussels
Phone: 02/672.45.56
Telex: 23662 SIMEIP B

CANADA
R.D.B. Sheppard Agencies Ltd.
P.O. Box 8
Georgetown, Ontario L7G 4T1
Phone: (416) 877-9846
Telex: 06-97500 SHEP GTWN

DENMARK
Nordisk Elektronik A/S
Transformervej 17
DK-2730 Herlev
Phone: (01) 96 95 96
Telex: 35200 NORDEL DK

FRANCE
PRANA
142, av. de la Republique
91230 Montgeron (Essonne)
Phone: 16(1)903.55.46
Telex: PUBLI A 210311 F
(Public Code 1616)

INDIA
Hinditron Services Pvt. Ltd.
69/A,L. Jagmohandas Marg
Bombay 400 006
Phone: 36 53 44
Telex: Tekhind 0112326

ISRAEL
M.T.I. Engineering Ltd.
182 Ben Yehuda Street
P.O. Box 16349
Tel-Aviv
Phone: 24 40 90
Telex: 32200 MTI IL

ITALY
SISTREL
Societa Italiana Strumenti
Elettronici, S.p.A
Via Giuseppe Armellini 37
00143 Roma
Phone: 5915551
Telex: 68356 SISTREL

JAPAN
Toko Trading Inc.
Kyodo (Shin-Aoyama) Bldg. 9-15
Minami-Aoyama 5-Chome
Minato-Ku
Tokyo
Phone: (03) 409-5831
Telex: Tokotrad J24686

THE NETHERLANDS
Simac Electronics B.V.
veenstraat 20
Veldhoven
Phone: 040-533725
Telex: 51037 Simac NI

NORWAY
Nordisk Elektronik AB
Mustadsvei 1
Oslo 2
Phone: 55 38 93
Telex: 16963 Ajco N

REPUBLIC OF SOUTH AFRICA
South Continental Devices (Pty) Ltd.
Box 56420 Pinegowrie, 2123
Phone: 48-7125, 9229, 9260
Telex: 8-3324 SA

SINGAPORE, MALAYSIA
Masia Ltd.
3rd Floor
First National City Bank Building
28/30 Medan Pasar, P.O. Box 2197
Kuala Lumpur, Malaysia
Phone: 80011
Telex: Samia MA30966

SWEDEN
Nordisk Elektronik AB
Fack
S-10380 Stockholm
Phone: (08) 24 83 40
Telex: 10547 Nortron S

SWITZERLAND
Telemeter Electronic AG
Gerechtigkeitsgasse 25
Postfach
CH-8027 Zurich
Phone: 051 25 78 72
Telex: 57287 Telzu CH

TAIWAN
Sun Moon Star Co., Ltd.
164 Min Shen East Road
P.O. Box 1273
Taipei, Taiwan 104
Republic of China
Phone: 588521-5.510521
Telex: 22199 SMSCO

UNITED KINGDOM
Walmore Electronics, Ltd.
11-15 Betterton Street
Drury Lane
London WC 2H 9BS
Phone: 01-836 1228
Telex: Walrad 28752

WEST GERMANY-AUSTRIA
Telemeter Electronic GmbH
885 Donauworth-Riedlingen
Posthof 4 (West Germany)
Phone: (0906) 5091
Telex: 51856 Teldo D

YUGOSLAVIA
Belram S.A.
Avenue des Mimosas 83
1150 Brussels (Belgium)
Phone: 34 33 32
Telex: 21790 Belram B

Avantek

Advanced solid-state products • 3175 Bowers Avenue, Santa Clara, California 95051 • Phone (408) 249-0700 • TWX 910-339-9274 • Cable: Avantek

ATP-1018/9-75

PRINTED IN U.S.A.

Avantek
HIGH-FREQUENCY TRANSISTOR PRIMER

PART II

NOISE & S-PARAMETER
CHARACTERIZATION

TABLE OF CONTENTS

INTRODUCTION

This Primer is a short summary of the S-parameter and noise parameters commonly used on Avantek transistor data sheets and their functional relationships to noise figure, gain, stability, impedance matching and other parameters necessary for high frequency circuit design. Much of this information has been published in various journals over the years. The intent of this Primer is to provide a short, concise booklet containing the key functional relationships necessary for circuit design.

I. S-PARAMETERS

By far the most accurate and conveniently measured microwave two-port parameters are the scattering parameters. These parameters completely and uniquely define the small signal gain and the input/output immitance properties of any linear two-port network. Simply interpreted, the scattering parameters are merely insertion gains, forward and reverse, and reflection coefficients, input and output, with the driven and non-driven ports both terminated in equal impedances; usually 50 ohms, real. This type of measurement system is particularly attractive because of the relative ease in obtaining highly accurate 50 ohm measurement hardware at microwave frequencies.

Proceeding more specifically, S-parameters are defined analytically by:

$$b_1 = s_{11}a_1 + s_{12}a_2$$

$$b_2 = s_{21}a_1 + s_{22}a_2$$

or, in matrix form,

$$\begin{bmatrix} b_1 \\ b_2 \end{bmatrix} = \begin{bmatrix} s_{11} & s_{12} \\ s_{21} & s_{22} \end{bmatrix} \begin{bmatrix} a_1 \\ a_2 \end{bmatrix}$$

where (referring to Figure 1):

a_1 = (Incoming power at Port 1)$^{1/2}$

b_1 = (outgoing power at Port 1)$^{1/2}$

a_2 = (incoming power at Port 2)$^{1/2}$

b_2 = (outgoing power at Port 2)$^{1/2}$

E_1, E_2 = Electrical Stimuli at Port 1, Port 2

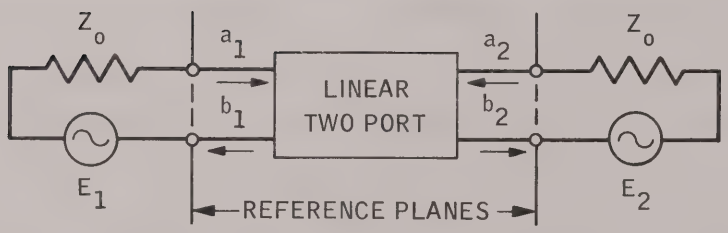

Figure 1 - S-Parameters Definition Schematic

From Figure 1 and defining linear equations for $E_2 = 0$, then $a_2 = 0$, and:

$$s_{11} = \frac{b_1}{a_1} = \left[\frac{\text{Outgoing Input Power}}{\text{Incoming Input Power}}\right]^{1/2} \qquad (1)$$

$$= \frac{\text{Reflected Voltage}}{\text{Incident Voltage}}$$

$$= \text{Input Reflection Coefficient}$$

$$s_{21} = \frac{b_2}{a_1} = \left[\frac{\text{Outgoing Output Power}}{\text{Incoming Input Power}}\right]^{1/2} \qquad (2)$$

$$= \left[\text{Forward Transducer Gain}\right]^{1/2}$$

or in the case of s_{21}:

$$\text{Forward Transducer Gain} = |s_{21}|^2 \tag{3}$$

Similarly at Port 2 for $E_1 = 0$, $a_2 = 0$:

$$s_{12} = \left[\frac{\text{Outgoing Input Power}}{\text{Incoming Output Power}}\right]^{1/2} = \frac{b_1}{a_2} = \text{Reverse Transducer Gain} \tag{4}$$

$$s_{22} = \left[\frac{\text{Outgoing Output Power}}{\text{Incoming Output Power}}\right]^{1/2} = \frac{b_2}{a_2} = \text{Output Reflection Coefficient} \tag{5}$$

Since many measurement systems actually "read out" the magnitude of S-parameters in decibels, the following relationships are particularly useful:

$$|s_{11}|_{dB} = 10 \log |s_{11}|^2 = 20 \log |s_{11}| \tag{6}$$

$$|s_{22}|_{dB} = 20 \log |s_{22}| \tag{7}$$

$$|s_{21}|_{dB} = 20 \log |s_{21}| \tag{8}$$

$$|s_{12}|_{dB} = 20 \log |s_{12}| \tag{9}$$

Using scattering parameters, it is possible to calculate the reflection coefficients and transducer gains for arbitrary load and source impedances where the load and source impedances are described by their reflection coefficients Γ_L and Γ_s respectively:

$$s'_{11} = \frac{b_1}{a_1} = \frac{s_{11}(1-s_{22}\Gamma_L) + s_{21}s_{12}\Gamma_L}{1 - s_{22}\Gamma_L}$$

$$= s_{11} + \frac{s_{21}s_{12}\Gamma_L}{1 - s_{22}\Gamma_L} \qquad (10)$$

$$s'_{22} = \frac{b_2}{a_2} = \frac{s_{22}(1-s_{11}\Gamma_s) + s_{21}s_{12}\Gamma_s}{1 - s_{11}\Gamma_s}$$

$$= s_{22} + \frac{s_{21}s_{12}\Gamma_s}{1 - s_{11}\Gamma_s} \qquad (11)$$

$$\text{Transducer Power Gain} = \frac{\text{Power Delivered to Load}}{\text{Power Available from Source}}$$

$$= \left|\frac{b_2}{b_s}\right|^2 (1 - |\Gamma_s|^2)(1 - |\Gamma_L|^2)$$

$$= \frac{|s_{21}|^2 (1 - |\Gamma_s|^2)(1 - |\Gamma_L|)^2}{|(1 - s_{11}\Gamma_s)(1 - s_{22}\Gamma_L) - s_{12}s_{21}\Gamma_L\Gamma_s|^2} \qquad (12)$$

2. FUNCTIONAL RELATIONSHIPS

With this information, the functional relationships to gain, stability, input and output matching impedance can be readily derived from S-parameters.

Since much of the literature[1, 2, 3] gives the complete derivation of these relationships, the mathematics of their derivation is omitted and Table 1 lists the most useful relationships required for circuit design.

TABLE I

1. Available Power Gain = $\frac{\text{Power Available from Network}}{\text{Power Available from Generator}}$

$$G_A = \frac{|s_{21}|^2 (1 - |\Gamma_s|^2)}{(1 - |s_{22}|^2) + |\Gamma_s|^2 (|s_{11}|^2 - |D|^2) - 2\,\mathrm{Re}(\Gamma_s C_1)}$$

2. Stability

$$K = \frac{1 + |D|^2 - |s_{11}|^2 - |s_{22}|^2}{2\,|s_{12} s_{21}|}$$

3. Maximum Stable Gain

$$G_{msg} = \left|\frac{s_{21}}{s_{12}}\right|$$

4. Maximum Available Gain (for $K > 1$)

$$G_{max} = \left|\frac{s_{21}}{s_{12}} (K + \sqrt{K^2 - 1})\right|$$

Use minus sign when B_1 is positive, plus sign when B_1 is negative. See page 6 for definition of B_1.

5. Unilateral Power Gain

$$U = \frac{|s_{11} s_{21} s_{12} s_{22}|}{|1 - |s_{11}|^2|\,|1 - |s_{22}|^2}$$

6. Source and Load Match for Maximum Available Power Gain

$$\Gamma_{ms} = C_1^* \left[\frac{B_1 \pm \sqrt{B_1^2 - 4\,|C_1|^2}}{2\,|C_1|^2}\right]$$

Use minus sign when B_i is positive, plus sign when B_i is negative. See page 6 for definition of B_1 and B_2.

$$\Gamma_{mL} = C_2^* \left[\frac{B_2 \pm \sqrt{B_2^2 - 4\,|C_2|^2}}{2\,|C_2|^2}\right]$$

$$D = \det[s] = s_{11}s_{22} - s_{12}s_{21}$$

$$B_1 = 1 + |s_{11}|^2 - |s_{22}|^2 - |D|^2$$

$$B_2 = 1 + |s_{22}|^2 - |s_{11}|^2 - |D|^2$$

$$C_1 = s_{11} - D(s_{22}^*)$$

$$C_2 = s_{22} - D(s_{22}^*)$$

TABLE II

y and h Parameters in Terms of S-Parameters

$$y_{11} = \frac{s_{12}s_{21} + (1 - s_{11})(1 + s_{22})}{(1 + s_{11})(1 + s_{22}) - s_{21}s_{12}} Z_o^{-1}$$

$$y_{21} = \frac{-2s_{21}}{(1 + s_{11})(1 + s_{22}) - s_{21}s_{12}} Z_o^{-1}$$

$$y_{12} = \frac{-2s_{12}}{(1 + s_{11})(1 + s_{22}) - s_{21}s_{12}} Z_o^{-1}$$

$$y_{22} = \frac{s_{21}s_{12} + (1 + s_{11})(1 - s_{22})}{(1 + s_{11})(1 + s_{22}) - s_{12}s_{21}} Z_o^{-1}$$

$$h_{11} = \frac{(1 + s_{11})(1 + s_{22}) - s_{21}s_{12}}{(1 - s_{11})(1 + s_{22}) + s_{12}s_{21}} Z_o$$

$$h_{21} = \frac{-2s_{21}}{(1 - s_{11})(1 + s_{22}) + s_{12}s_{21}}$$

$$h_{12} = \frac{+2 s_{12}}{(1 - s_{11})(1 + s_{22}) + s_{12} s_{21}}$$

$$h_{22} = \frac{(1 - s_{11})(1 - s_{22}) - s_{12} s_{21}}{(1 - s_{11})(1 + s_{22}) + s_{12} s_{21}} \; Z_o^{-1}$$

3. STABILITY

A two port network is unconditionally stable if there exists no combination of passive load or source impedances which will allow the circuit to oscillate. In terms of S-parameters, unconditional stability is assured if the following equations are simultaneously satisfied:

$$|s_{11}| < 1 \tag{13}$$

$$|s_{22}| < 1 \tag{14}$$

$$\left| \frac{|s_{12} s_{22}| - |C_1^*|}{|s_{11}|^2 - |D|^2} \right| > 1 \tag{15}$$

$$\left| \frac{|s_{12} s_{21}| - |C_2^*|}{|s_{22}|^2 - |D|^2} \right| > 1 \tag{16}$$

Under these conditions, Rollett's Stability Factor, $K > 1$ and Maximum Available Gain is real and defined (Equation 4, Table I):

When $K < 1$, the 2 port network is potentially unstable, but there may exist areas of the Γ_s and Γ_L plane in which the real part of the total impedance in the input (or output) loop is positive and the network is conditionally stable. The regions of instability occur within the stability circles, the centers and

radii of which are defined by,

rs_1 = Center of the stability circle on the input plane

$$= \frac{C_1^*}{|s_{11}|^2 - |D|^2} \tag{17}$$

Rs_1 = Radius of stability circle on the input plane

$$= \left[\frac{|s_{12}s_{21}|}{|s_{11}|^2 - |D|^2}\right] \tag{18}$$

rs_2 = Center of the stability circle on the output plane

$$= \frac{C_2^*}{|s_{22}|^2 - |D|^2} \tag{19}$$

Rs_2 = Radius of the stability circle on the output plane

$$Rs_2 = \left[\frac{|s_{12}s_{21}|}{|s_{22}|^2 - |D|^2}\right] \tag{20}$$

Figure 2 is a typical example of the input plane of a conditionally stable network and the location of the stability circle. The shaded area represents the area of the input plane in which instability (or oscillation) occurs.

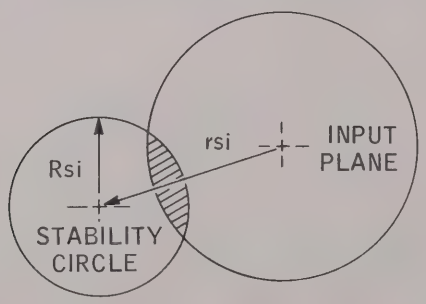

Figure 2

4. GAIN CONTOURS

By manipulating Equation 1, Table 1, circles of constant power gain can be generated in the Γ_s plane.

Equation 1, Table 1 may be expressed as:

$$G_A = |s_{21}|^2 G_1 \tag{21}$$

where

$$G_1 = \frac{|1 - |\Gamma_s|^2|}{(1 - |s_{22}|^2) + |\Gamma_s|^2(|s_{11}|^2 - |D|^2) - 2\mathrm{Re}\,\Gamma_s C_1} \tag{22}$$

The radius and location of a constant G_1 gain circle is given by:

$$r_g = \frac{(1 - 2K|s_{12}s_{21}|G_1 + |s_{12}s_{21}|^2 G_1^2)^{1/2}}{1 + M_1 G_1} \tag{23}$$

$$R_g = \left(\frac{G_1}{1 + M_1 G_1}\right) C_1^* \tag{24}$$

where

$$M_1 = |s_{11}|^2 - |D|^2 \tag{25}$$

Figures 3 and 4 are typical examples of gain contour plots on a Smith Chart. In this case, the contours are of a typical AT-4641 transistor measured at 2 GHz and 4 GHz. Figure 3 shows the typical plot when $K > 1$ and the transistor is unconditionally stable, and maximum available gain is uniquely defined at a single point.

Figure 4 shows a typical plot when $K < 1$ and the device is potentially unstable. In this case $|r_g|$ is greater than unity and gain circle center falls outside the unit circle and maximum available power gain is undefined.

However, it is possible to plot contours. The 15.4 dB gain contour represents the maximum stable gain of the device defined as $G_{msg} = |s_{21}/s_{12}|$. By presenting the input with an impedance lying outside of this gain contour, the output impedance of the device is positive and may be conjugately matched to realize the specified gain.

To realize the specified gain for any arbitrary Γ_s, the output matching impedance is obtained by conjugately matching s'_{22} (Equation 11) or

$$\Gamma_L = \left[s_{22} + \frac{s_{21} s_{12} \Gamma_s}{1 - s_{11} \Gamma_s} \right]^* \qquad (26)$$

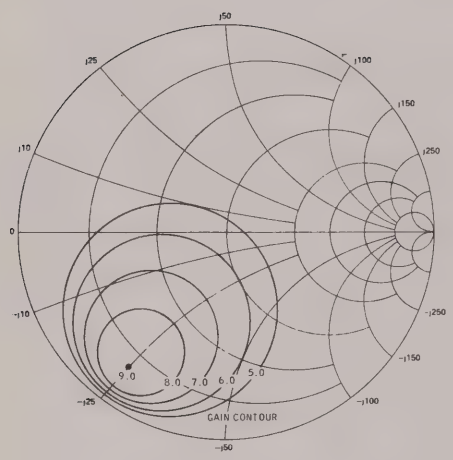

Figure 3.
Frequency = 4 GHz, 10 V 5 mA

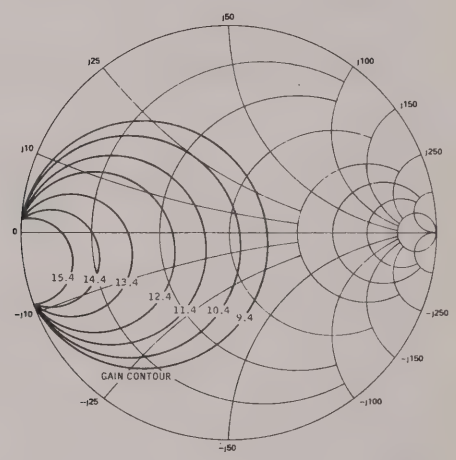

Figure 4.
Frequency = 2 GHz, 10 V 5 mA

5. NOISE CHARACTERIZATION

While S-Parameters completely define the stability, gain and power matching conditions of a linear two port network, they are not sufficient to describe the noise behavior of a noisy, linear, two port network such as a small signal transistor. Another set of parameters, namely noise parameters are required, in addition to S-Parameters to describe the noisy linear two port.

The noise figure of a linear two port as a function of source admittance may be represented by:[3]

$$F = F_{opt} + \frac{R_n}{G_s}\left[(G_{opt} - G_s)^2 + (B_{opt} - B_s)^2\right] \qquad (27)$$

where:

$G_s + jB_s$ = the source admittance presented to the two port

$G_{opt} + jB_{opt}$ = the source admittance at which optimum noise figure occurs

R_n = an empirical constant relating the sensitivity of the noise figure to source admittance, with dimensions of resistance.

It may be noted that for an arbitrary noise figure measurement with a known source admittance, Equation (1) has four unknowns, F_{opt}, R_n, G_{opt}, and B_{opt}. By chosing four known values of source admittance, a set of four linear equations are formed and the solution of the four unknowns can be found.

Equation (1) may be transformed to:

$$F = F_{opt} + \frac{R_n |Y_{opt}|^2}{G_s} - 2R_n G_{opt} + \frac{R_n |Y_s|^2}{G_s} - 2R_n B_{opt}\left(\frac{B_s}{G_s}\right) \qquad (28)$$

Let:

$$X_1 = F_{opt} - 2R_n G_{opt} \tag{29}$$

$$X_2 = R_n |Y_{opt}|^2 \tag{30}$$

$$X_3 = R_n \tag{31}$$

$$X_4 = R_n B_{opt} \tag{32}$$

Then the generalized equation may be written as:

$$F_i = X_1 + \frac{1}{G_{si}} X_2 + \frac{|Y_{si}|^2}{G_{si}} X_3 - 2\left(\frac{G_{si}}{B_{si}}\right) X_4 \tag{33}$$

Or, in matrix form:

$$[F] = [A]\,[X] \tag{34}$$

and the solution becomes:

$$[X] = [A]^{-1}\,[F] \tag{35}$$

These parameters completely characterize the noise behavior of the two port network.

Direct measurement of these noise parameters by this method would be possible only if the receiver on the output of the two port were noiseless and insensitive to its input admittance. In actual practice, the receiver itself behaves as a noisy two port network and can be characterized in the same manner. What is actually being measured is the system noise figure of the two port and the receiver.

The two port noise figure, however, can be calculated using the system formula:

$$F_{1i} = F_{(sys)i} - \frac{F_2 - 1}{G_{1i}} \tag{36}$$

Where:

F_{1i} = Two port noise figure when driven from the ith source admittance

F_2 = Second stage noise figure (or receiver noise figure)

$F_{(sys)i}$ = System noise figure when driven from the ith source

G_{1i} = Available gain of the two port when driven from the ith source.

It is important to note that F_2 is assumed to be independent of the impedance of the first stage two port, which means that an isolator must be inserted between the first stage two port and the receiver.

Thus, it becomes apparent that to do a complete two port noise characterization, the system noise characterization, the receiver noise characterization, and the gain of the two port must be measured. In addition, any losses in the input matching networks must be carefully accounted for, because they add directly to the measured noise figure reading.

Figure 5 shows a generalized block diagram of a typical noise figure setup used to obtain noise parameters

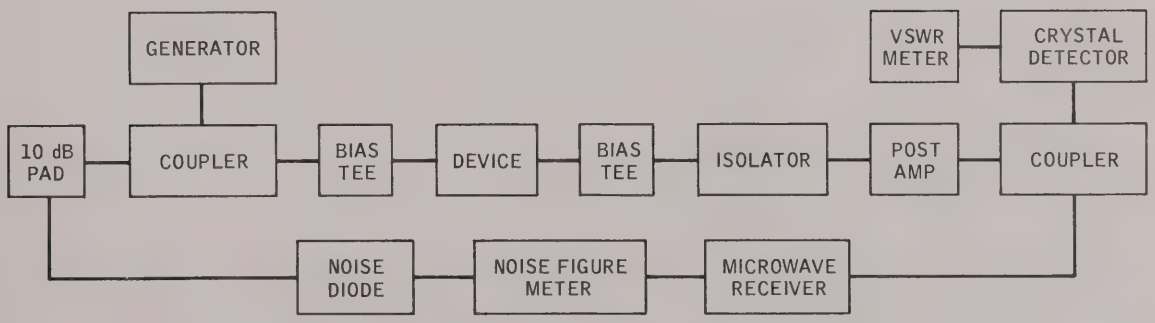

Figure 5

6. NOISE CONTOURS

Noise figure can be graphically presented on a Smith Chart of the input plane much the same as gain. This graphical representation can be presented in the impedance plane (Z plane), admittance plane (y plane) or reflection coefficient plane (Γ plane), all of which can be functionally related to each other. Since the noise parameters were derived in terms of admittance parameters, the noise contours will be derived in terms of normalized admittance parameters, which may be easily converted into the Z plane by a 180° angular rotation.

If we define the normalized admittances as:

$$y_s = g_s + jb_s = \frac{1}{Y_o} (G_s + jB_s) \tag{37}$$

$$y_{opt} = g_{opt} + jb_{opt} = \frac{1}{Y_o} (G_{opt} + jB_{opt}) \tag{38}$$

where: Y_o is the real characteristic admittance of the input transmission line.

From the literature,[3] it can be shown that the center of the circle of constant noise figure ($F_i \geq F_{opt}$) is:

$$R_{Fi} = \frac{\left[(1 - g_{opt}^2 - b_{opt}^2)^2 + 4b_{opt}^2 \right]^{1/2}}{(1 + g_{opt})^2 + b_{opt}^2 + 2\delta_{Fi}} \tag{39}$$

where:

$$\delta_{Fi} = \frac{F_i - F_{opt}}{2R_n Y_o} \tag{40}$$

The angle of the vector is:

$$\theta = \tan^{-1} \left[\frac{2b_{opt}}{1 - g_{opt}^2 - b_{opt}^2} \right] \tag{41}$$

The radius of the circle of constant noise figure is given by:

$$r_{Fi} = \frac{2N_i}{(1 + g_{opt})^2 + b_{opt}^2 + 2\delta_{Fi}} \tag{42}$$

when:

$$N_i = \frac{1}{Y_o} \left[\frac{G_{opt}}{R_n} (F_i - F_{opt}) + \frac{1}{4R_n^2} (F_i - F_{opt})^2 \right]^{1/2} \tag{43}$$

Figure 6 shows a typical plot of noise figure of the AT-4641 transistor plotted in the impedance plane.

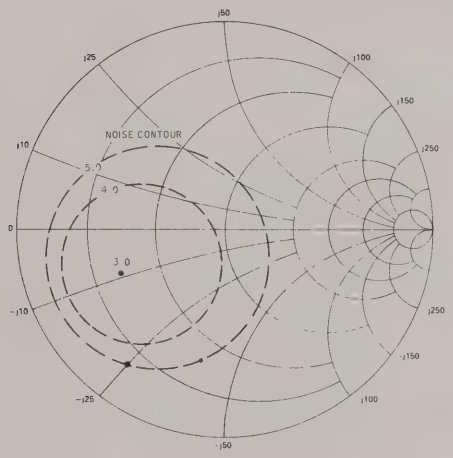

Figure 6
4 GHz Noise Contour - AT-4641

7. NOISE AND GAIN CONTOURS

All practical amplifiers involve more than one internal noise generator, and as a result have an optimum noise source which is not the same as the optimum gain source. From a practical point of view, it becomes desirable to know what the tradeoffs between noise figure and gain involve. This tradeoff is best shown by plotting both the gain and noise circles on the same chart.

By taking the gain contours developed in Section 4 and the noise contours developed in Section 6 and superimposing them on the same Smith Chart, the gain and noise figure tradeoffs become readily apparent.

Figure 7 shows the noise and gain contours of the AT-4641 transistor plotted in the input impedance plane.

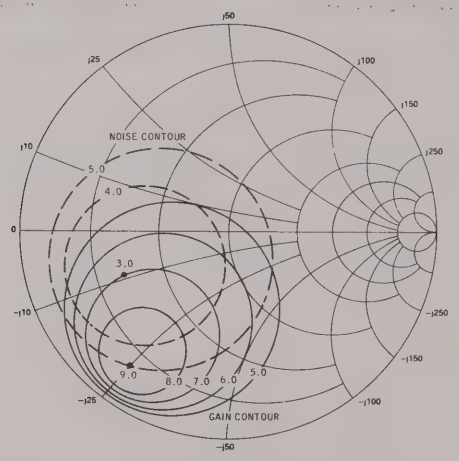

Figure 7.
4 GHz Contours - AT-4641

With this chart, the circuit designer can easily pick his input matching conditions which will result in the optimum compromise for simultaneously meeting his gain, VSWR and noise figure requirements.

Again, to realize the specified gain for any arbitrary point on the input plane, the output matching impedance is obtained by conjugately matching s'_{22} (Equation 11):

$$\Gamma_L = \left[s_{22} + \frac{s_{21} s_{12} \Gamma_s}{1 - s_{11} \Gamma_s} \right]^* \qquad (44)$$

SUMMARY

In the previous sections of this booklet, the basic techniques for developing a graphical display of the input plane of a noisy linear two port network have been described, and a number of specific examples were shown. This technique may be used to graphically describe any noisy linear two port network at any microwave frequency, provided that the following parameters are known at the desired frequency and, in the case of a transistor, at the desired bias conditions.

$$s_{11}, s_{21}, s_{12}, s_{22}, F_{opt}, Y_{opt}, R_n$$

REFERENCES

1. Kurokawa, K , IEEE Trans MTT, March 1965

2. Bodway, G.E., Two Port Power Flow Analysis Using Generalized Scattering Parameters, Microwave Journal, Vol. 10, No. 6, May 1967

3. Fukui, H., Available Power Gain, Noise Figure and Noise Measure of Two Ports and their Graphical Representation, IEEE Trans. on CT, Vol. CT-13, No. 2, pp 137-142.

Domestic Representatives

ALABAMA
Beacon
11309 S. Memorial Parkway, Suite B
Huntsville, AL 35803
(205) 881-5031

ARIZONA
The Thorson Company
2505 E. Thomas Road
Phoenix, AZ 85016
(602) 956-5300

CALIFORNIA
Cain Technology
522 S. Sepulveda Blvd., Suite 107
Los Angeles, CA 90049
(213) 476-2251

Cain-White & Company
Foothill Office Center
105 Fremont Avenue
Los Altos, CA 94022
(415) 948-6533

COLORADO
The Thorson Company
5290 Yale Circle
Denver, CO 80222
(303) 759-0809

DC and VIRGINIA
Applied Engineering Consultants
Washington, DC
(301) 953-2808
(301) 953-2809

FLORIDA
Beacon
P.O. Box 1278
Maitland, FL 32751
(305) 647-3498

Beacon
1041 W. Commercial Blvd., Suite 202
Fort Lauderdale, FL 33309
(305) 776-6074

GEORGIA
Beacon
2285 Peachtree Road, NE
Atlanta, GA 30309
(404) 351-3654

ILLINOIS
Cozzens/Cudahy, Inc.
1301 North Rand Road
Des Plaines, IL 60016
(312) 298-3600

Cozzens/Cudahy, Inc.
10534 Natural Bridge Road
St. Louis, MO 63134
(314) 423-1234

INDIANA
Cozzens/Cudahy, Inc.
21 Beachway Drive
Indianapolis, IN 46224
(317) 244-2456

KANSAS
E.I.R. Company
6811 W. 63rd Street, Suite 114
Shawnee Mission, KS 66202
(913) 362-0919

MARYLAND
Applied Engineering Consultants
9051 Baltimore National Pike
Building 3, Office A
Ellicott City, MD 21043
(301) 465-1272

MASSACHUSETTS
Tritek, Inc.
155 Middlesex Turnpike
Burlington, MA 01803
(617) 272-4550

MICHIGAN
Micro Sales Corporation
7522 Emily
Detroit, MI 48234
(313) 482-1229

MINNESOTA
Cozzens/Cudahy, Inc.
10800 Lyndale Avenue, South
Minneapolis, MN 55420
(612) 884-4336

MISSISSIPPI
Beacon
P.O. Box 423
Hernando, MS 38632
(601) 368-9008

MISSOURI
E.I.R. Company
47 Village Square Shopping Center
Hazelwood, MO 63024
(314) 895-4100

NEW JERSEY (L.I. & N.Y.C.)
Technical Marketing Associates
2460 Lemoine Avenue
Fort Lee, NJ 07024
(201) 224-6911

NEW MEXICO
The Thorson Company
2201 San Pedro Drive, N.E.
Building 2, Suite 107
Albuquerque, NM 87110
(505) 265-5655

NEW YORK
Robtron
2-4 Fennell Street, Suite 209
Skaneateles, NY 13152
(315) 685-5731

NORTH CAROLINA
Beacon
4502 Bromley Road
Greensboro, NC 27406
(919) 674-9432

OHIO
Micro Sales Corporation
P.O. Box 450
44 East Franklin Street
Centerville, OH 45459
(513) 433-8171

Micro Sales Corporation
P.O. Box 523
Medina, OH 44256
(216) 725-4560

PENNSYLVANIA
Eastern Instrumentation of Philadelphia
613 W. Cheltenham Avenue
Philadelphia, PA 19126
(215) 927-7777

SOUTH CAROLINA
Beacon
217 Green Gate Lane
Spartanburg, SC 29302
(803) 582-4613

TEXAS
The Thorson Company
4400 Sigma Road
Dallas, TX 75240
(214) 233-5744

The Thorson Company
6655 Hillcroft, Suite 224
Houston, TX 77036
(713) 771-3504

WASHINGTON
The Thorson Company
One Lake Bellevue Drive
Bellevue, WA 98005
(206) 455-9180

International Representatives

AUSTRALIA
General Electronic Services Pty. Ltd.
99 Alexander Street, Crows Nest
New South Wales, 2065
Phone: 439-2488
Telex: Servo 25486

BELGIUM
Simac Electronics B.V.
148, Boulevard du Triomphe
1160 Brussels
Phone: 02/672.45.56

CANADA
R.D.B. Sheppard Agencies Ltd.
P.O. Box 8
Georgetown, Ontario L7G 4T1
Phone: (416) 877-9846
Telex: 06-97500 SHEP GTWN

DENMARK
Nordisk Elektronik A/S
Transformervej 17
DK-2730 Herlev
Phone: (01) 96 95 96
Telex: 19219

FRANCE
Salies, S.A.
65-67 Avenue Jean Jaures
91 Palaiseau
Phone: 920 40 10+
Telex: Salies 69287F

INDIA
Hinditron Services Pvt. Ltd.
69/A, L. Jagmohandas Marg
Bombay 400 006
Phone: 36 53 44
Telex: Tekhind 0112326

ISRAEL
M.T.I. Engineering Ltd.
182 Ben Yehuda Street
P.O. Box 16349
Tel-Aviv
Phone: 24 40 90
Telex: 32200 MTI IL

ITALY
Vianello, S.p.A.
Via L. Anelli, 13
1-20122 Milano
Milano
Phone: 5483811 or 5483081
Telex: 31123 Vianello

NORWAY
Nordisk Elektronik AB
Mustadsvei 1
Oslo 2
Phone: 55 38 93
Telex: 16963 Ajco N

REPUBLIC OF SOUTH AFRICA
South Continental Devices (Pty) Ltd.
Box 56420 Pinegowrie, 2123
Phone: 48-7125, 9229, 9260
Telex: 8-3324 SA

JAPAN
Toko Trading Inc.
Kyodo (Shin-Aoyama) Bldg 9-15
Minami-Aoyama 5-Chome
Minato-Ku
Tokyo
Phone: (03) 409-5831
Telex: Tokotrad J24686

THE NETHERLANDS
Simac Electronics B.V.
Eindhovenseweg 58
Steensel
Phone: (04970)-2011
Telex: 51037 Simac NI

SPAIN
Rema Leo Haag, S.A.
General Sanjurjo No. 18
Madrid 3
Phone: 253 40 03
Telex: 42838 REMA E

SINGAPORE MALAYSIA
Masia Ltd.
3rd Floor
First National City Bank Building
28/30 Medan Pasar, P.O. Box 2197
Kuala Lumpur, Malaysia
Phone: 80011
Telex: Samia MA30966

SWEDEN
Nordisk Elektronik AB
Fack
S-10380 Stockholm
Phone: (08) 24 83 40
Telex: 10547 Nortron S

SWITZERLAND
Telemeter Electronic AG
Gerechtigkeitsgasse 25
Postfach
CH-8027 Zurich
Phone: 051 25 78 72
Telex: 57287 Telzu CH

TAIWAN
Sun Moon Star Co., Ltd.
164 Min Shen East Road
P.O. Box 1273
Taipei, Taiwan 104
Republic of China
Phone: 588521-5.510521
Telex: 22199 SMSCO

UNITED KINGDOM
Walmore Electronics, Ltd.
11-15 Betterton Street
Drury Lane
London WC 2H 9BS
Phone: 01-836 1228
Telex: Walrad 28752

WEST GERMANY - AUSTRIA
Telemeter Electronic GmbH
885 Donauworth-Riedlingen
Posthof 4 (West Germany)
Phone: (0906) 5362
Telex: 51856 Teldo D

YUGOSLAVIA
Belram S.A.
Avenue des Mimosas 83
1150 Brussels (Belgium)
Phone: 34 33 32
Telex: 21790 Belram B

Avantek

Advanced solid-state products • 3175 Bowers Avenue, Santa Clara, California 95051 • Phone (408) 249-0700 • TWX 910-339-9274 • Cable: Avantek

ATP-1019/9-75

PRINTED IN U.S.A.

Avantek HIGH-FREQUENCY TRANSISTOR PRIMER

PART III

THERMAL PROPERTIES

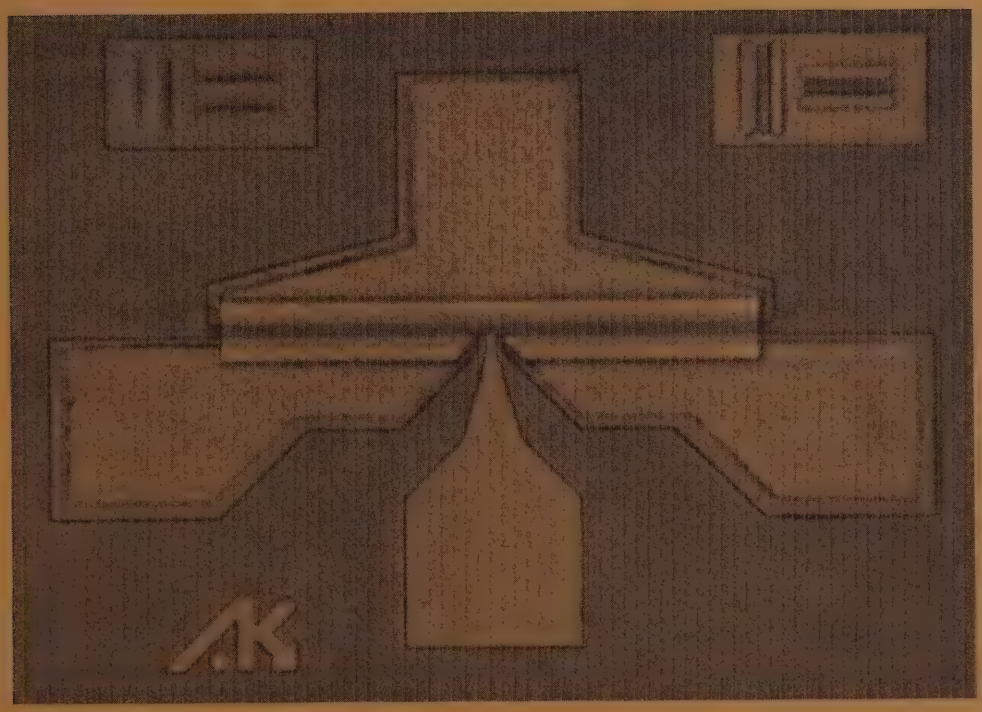

This is the third part of the Avantek High Frequency Transistor Primer series. It is intended as an introduction to the thermal characteristics of GaAs FET and silicon bipolar transistors for the microwave engineer. The contents are based on the questions most often asked of members of the Avantek transistor group.

Using the information in this primer should enable the engineer to make the basic calculations necessary to assure that the transistors he uses will be operated at a safe temperature for long term reliability. Further discussion on the subject of transistor thermal characteristics and heat flow calculations is provided in the literature referenced in the appendix.

The other parts of the High Frequency Transistor Primer currently available are: Part I, Electrical Characteristics (of bipolar microwave transistors) and Part II, Noise and S Parameter Characterization. Work is also underway on Part IV, GaAs FET Characteristics.

For copies of any of the Avantek High Frequency Transistor Primer volumes, contact your closest Avantek factory representative (see list on back cover), or the Avantek Publications Department in Santa Clara.

TABLE OF CONTENTS

I. THERMAL RESISTANCE

A. DEFINITION

A transistor, bipolar or FET, has a maximum temperature which cannot be exceeded without destroying the device or at least shortening its life. The heat is generated in a bipolar transistor directly under the emitters and very close to the upper surface of the die. In microwave FET's heat is also dissipated near the surface, under the gate, near the drain end. For all practical purposes, the heat can be considered as generated on the top surface of the chip or die.

The ability of a transistor to dissipate heat depends upon a factor called the thermal resistance, which may be designated as Θ, or Θ_{th} or R_{th}. It is defined as follows:

$$\text{Temp. Rise} \triangleq \text{Power Dissipated} \times \text{Thermal Resistance}$$

$$\Delta T = P_D \Theta \qquad \text{(Eq. 1A)}$$

$$\Theta \triangleq \frac{\Delta T}{P_D} \qquad \text{(Eq. 1B)}$$

Note that Θ has the dimensions of °C/watt. The reciprocal of thermal resistance is thermal conductance. Equation 1A can be used to calculate the temperature rise at the surface of a chip due to P_D watts being dissipated, with the bottom of chip held at a constant temperature. Junction temperature, T_j is given as:

$$T_j = T_A + \text{Temp. rise due to heating}$$

$$T_j = T_A + P_D \Theta \qquad \text{(Eq. 2)}$$

where T_A is ambient temperature.

Figure 1 shows a cross section of a chip on a mount. As can be seen, there are actually three thermal resistances involved, and

$$T_j = T_A + P_D \left(\Theta_{chip} + \Theta_{solder} + \Theta_{mount}\right)$$

Note that the thermal resistances add just like electrical resistances in series. We will now see how thermal resistance is calculated.

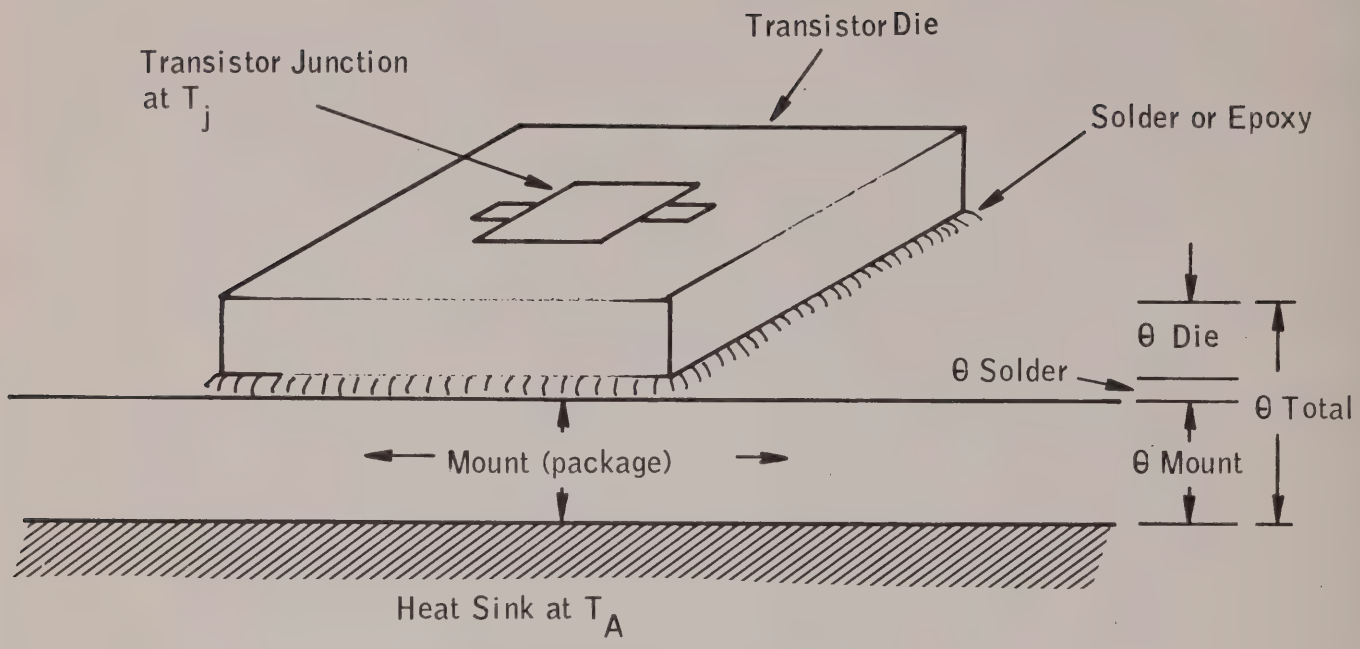

FIGURE 1 - TRANSISTOR THERMAL RESISTANCES

TABLE I

THERMAL CONDUCTIVITY (K_{TH}) OF SOME MATERIALS USED IN TRANSISTORS

Material	K_{TH} W/cm°C
Silicon	1.00-1.46
GaAs (Gallium Arsenide)	0.44
Copper	4.05
Gold	3.09
Kovar	0.2
Sapphire	.25
Al_2O_3 (Aluminum Oxide)	.188
BeO (Beryllium Oxide)	2.34
Silver	4.14

B. CALCULATION OF THERMAL RESISTANCE

All materials will conduct heat to some degree, some much better than others. Silver is the best metallic heat conductor and plastics tend to be relatively poor heat conductors. BeO (beryllia) is the best ceramic heat conductor and is often used in high power transistor packages.

When thermal resistance is calculated, the physical size and placement of the chip and mount are all important. There are two general cases for thermal resistance [1].

Case I - "Columnar" Heat Flow (Fig. 2)*

Figure 2 shows that if the thickness of the material is small compared to the lateral dimensions of the device and die, the heat will flow in a vertical "column." The thermal resistance is then:

$$\Theta_{col} = \frac{F}{K_{TH}\ Area} = \frac{F}{K_{TH}\ 4CD} \qquad \text{(Eq. 3)}$$

Example: A silicon transistor 20 x 20 mils is fabricated on a die 50 mils square and 5 mils thick. Then 2D = 2C = 20 mils, 2B = 2A = 50 mils, and F = 5 mils.

$$\frac{F}{B} = \frac{5}{25} = 0.2;\ \frac{F}{D} = \frac{5}{10} = 0.50$$

Heat flow is, therefore, essentially columnar.

20 mils = 0.051 cm

5 mils = 0.0127 cm

Let K_{TH} = 1.0 W/cm°C

$$\Theta = \frac{.0127}{1.0\ (.051)^2} = 4.88\ °C/W$$

Case II - "Spreading" Heat Flow (Fig. 3)

If the material is thick compared to the device size, and the device dimensions are less than 20% of the die side dimension, then flow is said to be essentially spreading. Figure 3 illustrates this case and

* The notation using a 2X multiplier for the dimensions is consistent with the figures in the reference.

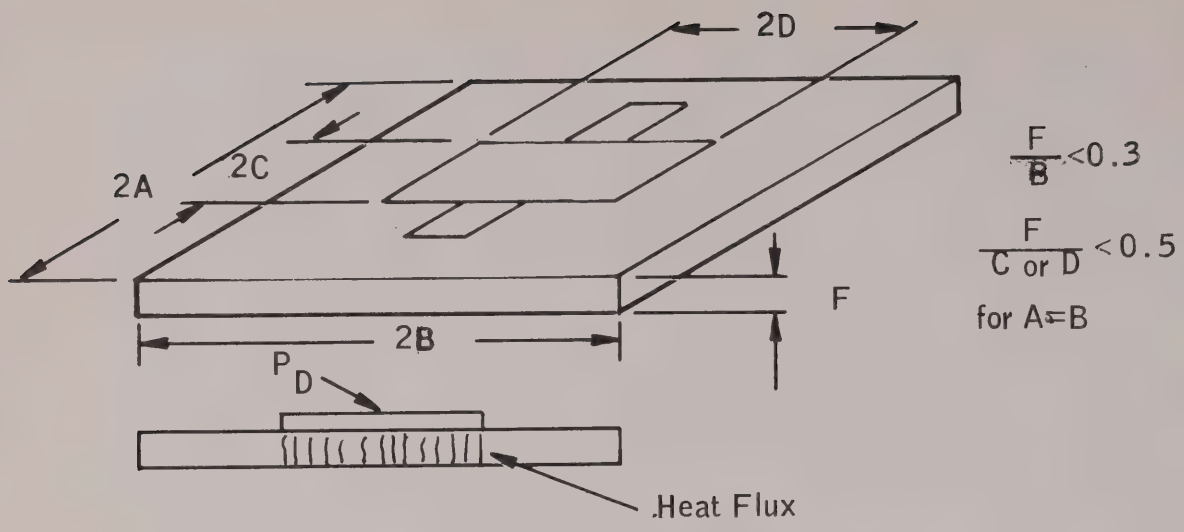

FIGURE 2 - COLUMNAR HEAT FLOW
See Page 619, Reference [1]

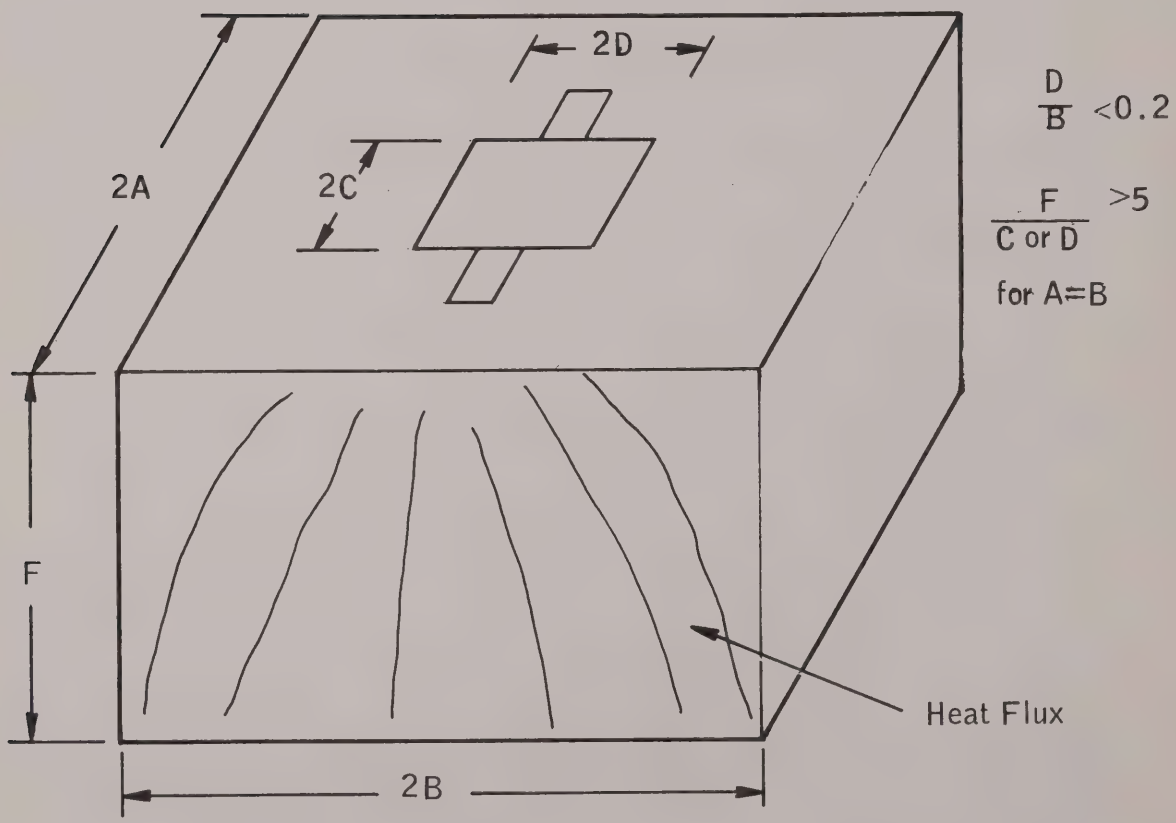

FIGURE 3 - SPREADING HEAT FLOW
See Page 619, Reference [1]

shows how the heat "spreads out" instead of flowing in a vertical column. For this case:

$$\Theta_{sp} = \frac{1}{K_{TH}\pi r}, \quad r = \frac{C+D}{2} \qquad \text{(Eq. 4)}$$

Note that r is the radius of a circle whose diameter is the average of the transistor dimensions.

Most transistor dimensions fall into a range of values which are intermediate between spreading and columnar flow, and the general equations for heat flow in 3 dimensions, X, Y, and Z, must be solved using the three-dimensional Laplace equation:

$$\frac{\partial^2 T}{\partial X^2} + \frac{\partial^2 T}{\partial Y^2} + \frac{\partial^2 T}{\partial Z^2} = 0 \qquad \text{(Eq. 5)}$$

Linstead and Surty [2] solved Eq. 5 for a number of different geometries and presented the results in a series of normalized charts (Fig. 4, 5, 6). The use of these charts will be demonstrated using the Avantek M-4 geometry (i.e., AT-4641). The dimensional notation corresponds to Fig. 3.

The dimensions of the M-4 transistor are 1.1 x 3.0 mils; the die is 10 mils square and about 5 mils thick. Therefore, in Fig. 5:

$$2A = 2B = 0.01" = 0.0254 \text{ cm}$$
$$2D = 0.003" = 0.00762 \text{ cm}$$
$$2C = 0.0011" = 0.0028 \text{ cm}$$
$$F = 0.005" = 0.0127 \text{ cm}$$
$$\frac{A}{F} = 1, \ \frac{A}{B} = 1, \ \frac{C}{A} = 0.11, \ \frac{D}{C} \cong 3$$

In Fig. 5, at C/A = 0.11 and on the A/F = 1 curve read

$$\frac{\Theta K_{TH} CD}{F} = 0.046$$

Therefore:

$$\Theta = \frac{.046F}{K_{TH}CD} = \frac{0.046\ (.0127)}{1.00\ (.0014)(.0038)} = 109° \text{ C/W}$$

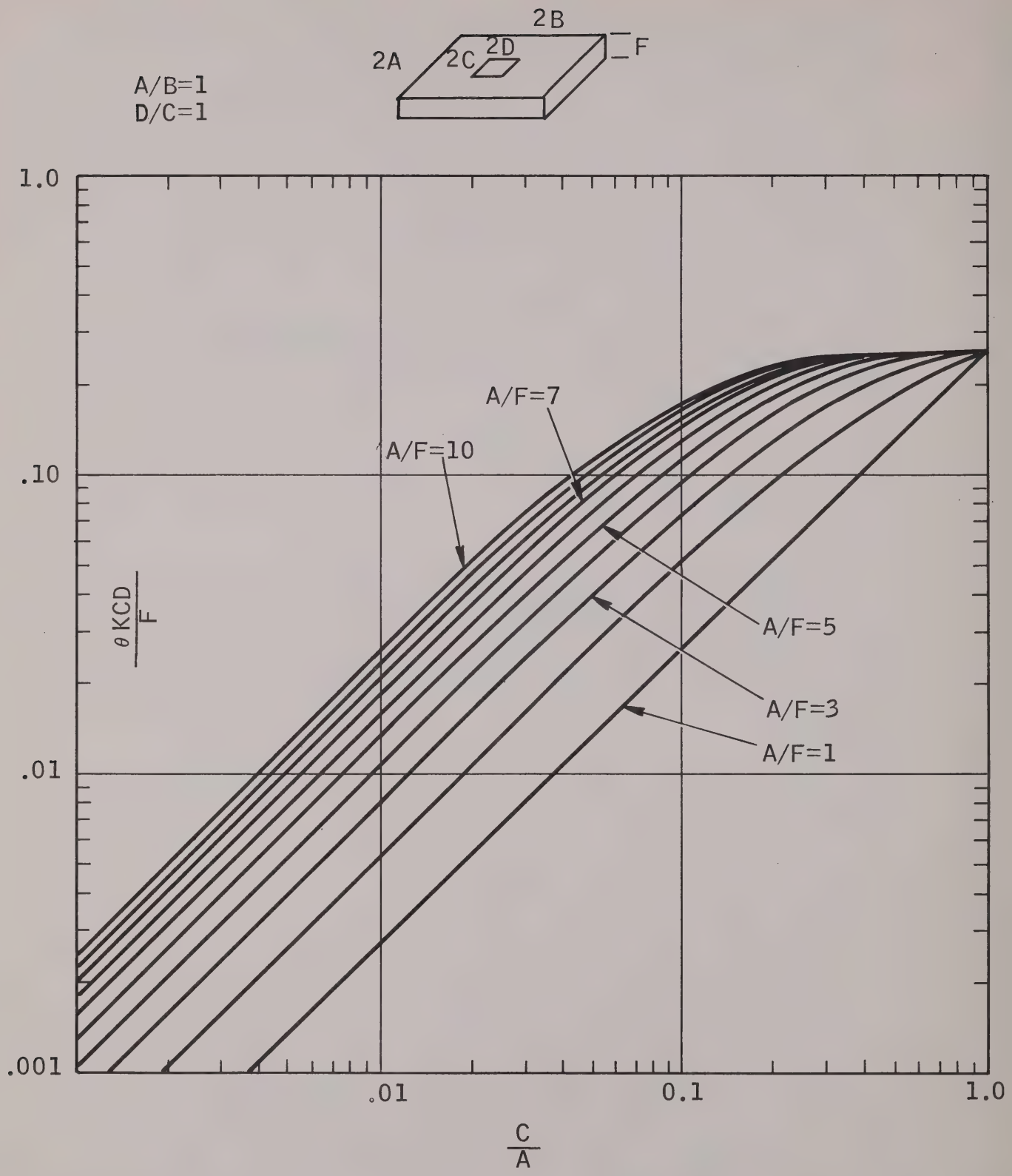

FIGURE 4 - THERMAL RESISTANCE CURVES

Thermal resistance curves for semi-conductor chips from R.D. Linsted & R.J. Surty, "IEEE Transactions on Electron Devices", Volume - ED 19, No. 1, January 1972, pp. 41-44, Reproduced courtesy of the Institure for Electrical and Electronics Engineers. (Figs. 4, 5 & 6)

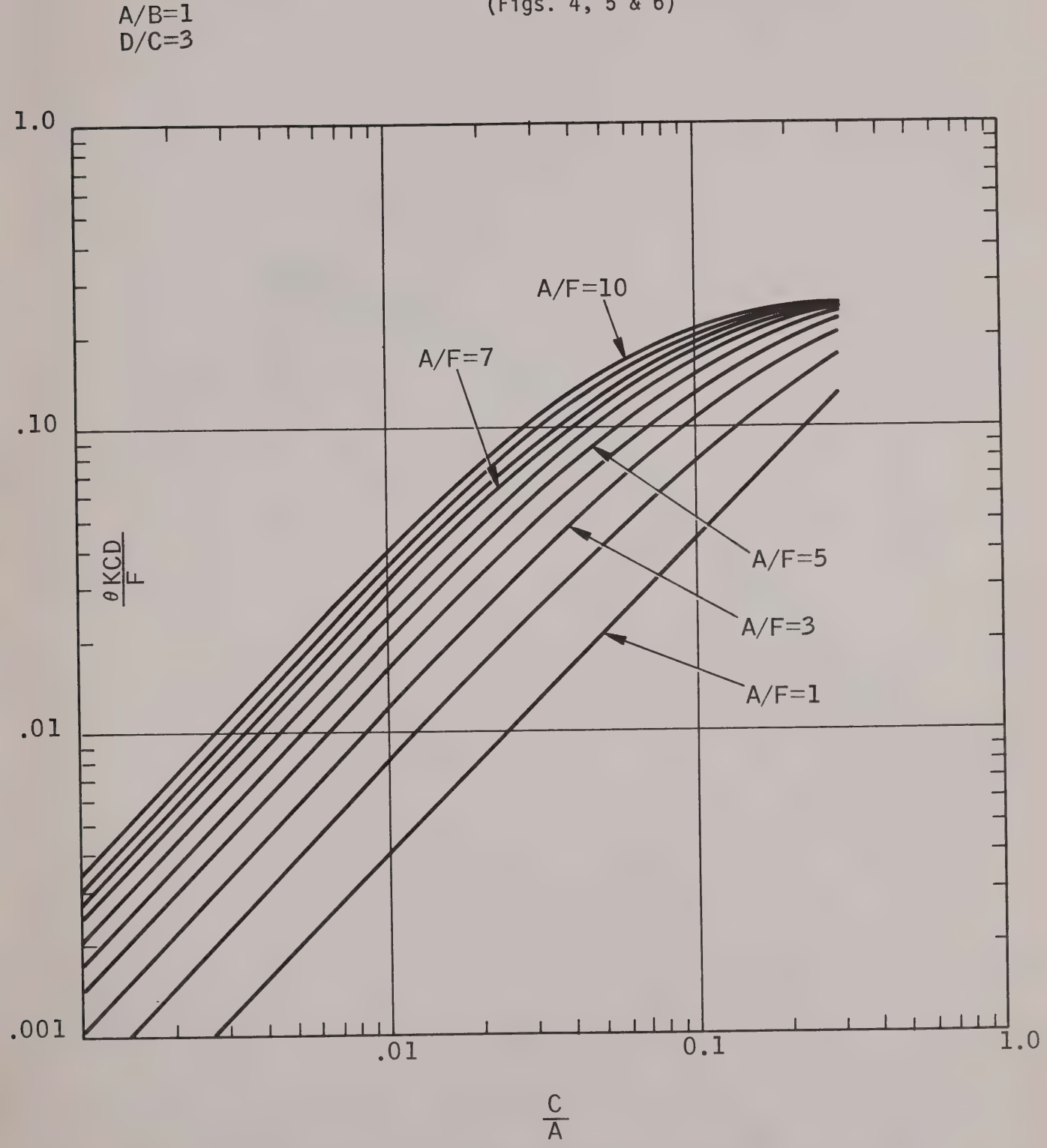

FIGURE 5 - THERMAL RESISTANCE CURVES

A/B=1
D/C=5

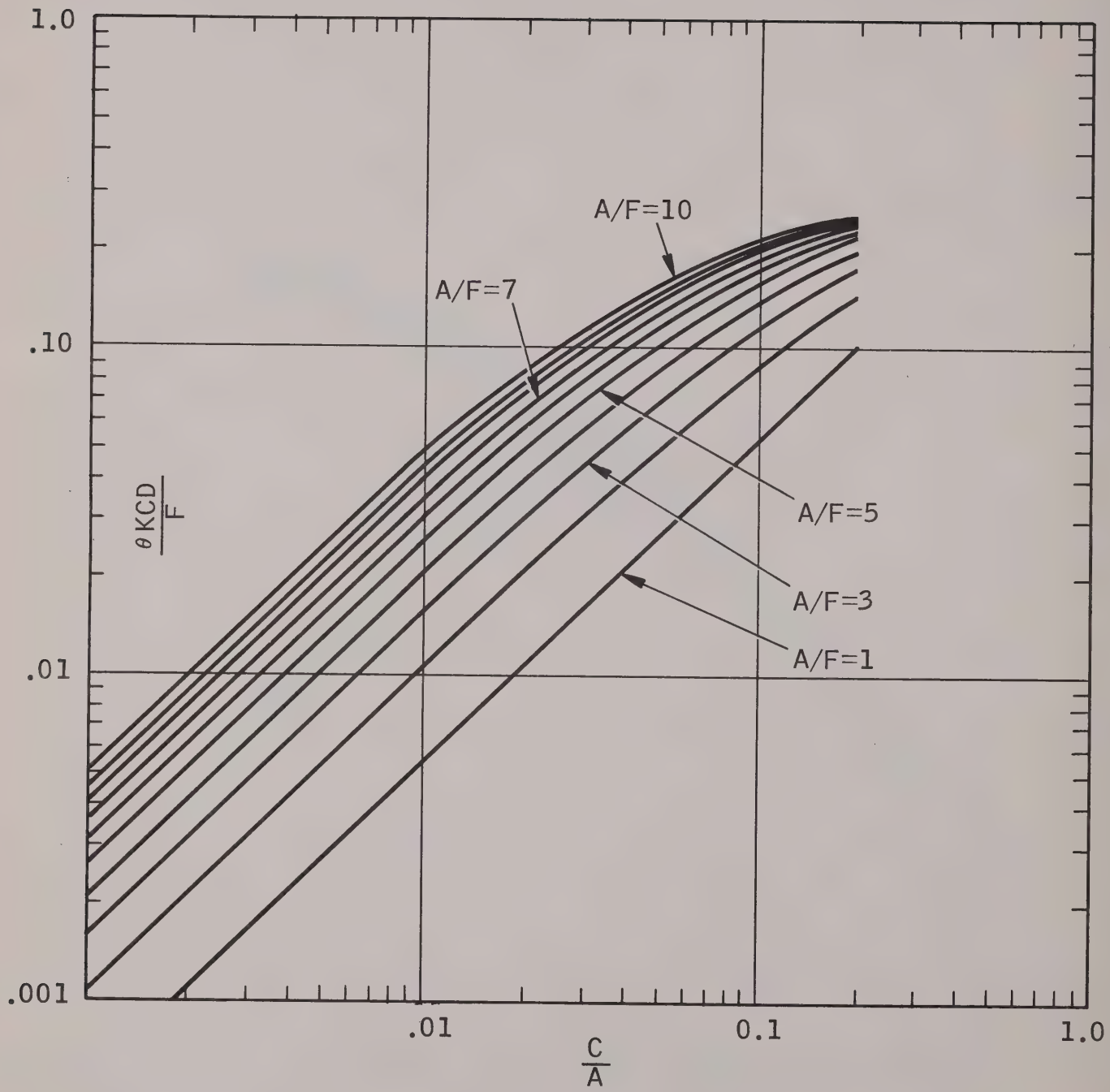

FIGURE 6 - THERMAL RESISTANCE CURVES

A similar calculation made for other Avantek bipolar transistor geometries give the following results:

M-2	Θ = 97°C/W (i.e., AT-0025, -0045, -2625)
M-1, M-10	Θ = 47°C/W (i.e., AT-0017/-0017A, AT-2715)

The thermal resistance for a FET cannot be calculated from the charts of Linstead and Surty since the heat source is a long thin line, not a small rectangle. Thermal resistance for a long thin line can be approximated by the analogy between fringing capacitance for an electrical conductor and thermal heat flow spreading. Since the capacitance per unit length of a transmission line is $(120\ \pi\varepsilon)/Zo$, formulas for transmission line characteristic impedance may be used to calculate thermal resistance. Using the formula for stripline characteristic impedance given by Cohn [3] and the equivalent ideal line as shown by Oliver [4], one can derive the following equation for FET thermal resistance:

$$\Theta W_g = \frac{K(k)}{2\ K_{TH}\ [K(k')]} * \qquad \text{(Eq. 6)}$$

Where:

$$k = \operatorname{sech}\left(\frac{\pi L_g}{4F}\right) \qquad \text{(Eq. 7)}$$

$$k' = \tanh\left(\frac{\pi L_g}{4F}\right) \qquad \text{(Eq. 8)}$$

K = complete elliptic integral of 1st kind
L_g = gate length in cm
F = die thickness in cm $\cong$ .0125 cm
W_g = gate width in cm
$K_{TH} \cong 0.44$, for GaAs

---

* Equation 6 is valid for single line gates. Devices with multiple gates (like power FETs) could have a higher thermal resistance. This is because the gates are thermally "coupled," i.e., there is heat transfer between gate segments.

Using these numbers, ΘW_g has been calculated for gate lengths of 0.1 to 4 μm and is shown in Fig. 7. Thermal resistance for three FETs has been calculated and is shown in Table II.

TABLE II

THERMAL RESISTANCE CALCULATED FOR THREE DIFFERENT FETS

DEVICE	L_g (μm)	W_g (μm)	ΘW_g FROM FIG. 7 (°C cm/W)	Θ (°C/W)
M-104	0.5	150	5.17	345
M-107	0.5	300	5.17	172
M-105	1.0	500	4.68	93.6

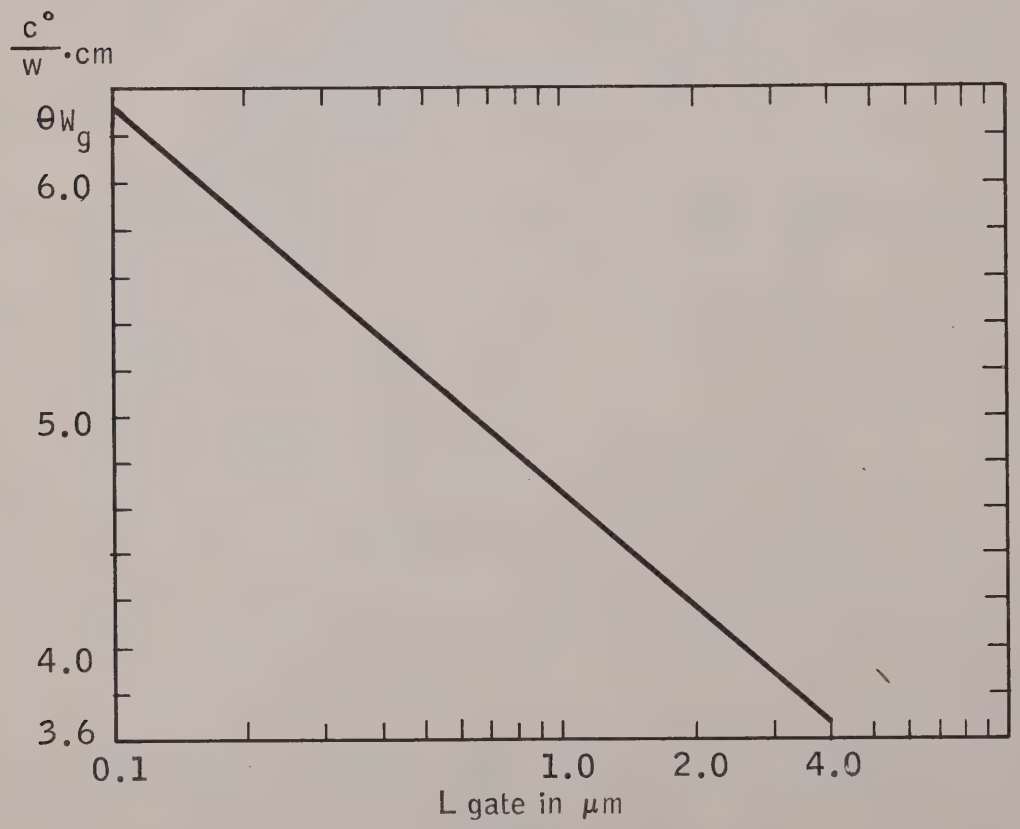

FIGURE 7 - THERMAL RESISTANCE X GATE WIDTH VS. GATE LENGTH FOR GaAs FETS ON 5 MIL THICK DIE

II. THERMAL TIME CONSTANT

If a pulse of power is supplied to a semiconductor device, the temperature of the junction does not rise instantaneously. In other words, the die has a thermal time constant. Figure 8A illustrates the effect; 8B shows the electrical analog of several time constants in cascade (i.e., in series).

Semiconductor junction temperature as a function of time can be given as: *

$$T_j = P_D\Theta\left[\frac{4}{\pi^{\frac{3}{2}}}\right]\left[\frac{t}{\tau}\right]^{\frac{1}{2}} + T_A \qquad \text{for } t<\tau \qquad \text{(Eq. 9)}$$

τ = thermal time constant
t = time

Note that the temperature is proportional to the square root of time and, thus, the RC analog is not exact. It has also been found that Eq. 9 is only accurate during the early part of the pulse, and is not correct for the entire duration, particularly near the end as the temperature approaches equilibrium, i.e., as t approaches τ.

The thermal time constant can be estimated by:

$$\tau = \left[\frac{2F}{\pi}\right]^2\left[\frac{\rho C}{K_{TH}}\right] \qquad \text{(Eq. 10)}$$

Where:

F = die thickness
ρ = density of semiconductor
K_{TH} = thermal conductivity
C = specific heat of semiconductor

The constant $\frac{\rho C}{K_{TH}}$ will be calculated for two semiconductors, silicon and GaAs.

1. Silicon (Si)

ρ = 2.33 gr/cc
C = 0.7 J/gr°C $\cong$ 0.7 W-sec/gr°C
$K_{TH} \cong$ 1.00 W/cm°C

* This is Eq. (9.64a) in reference [1].

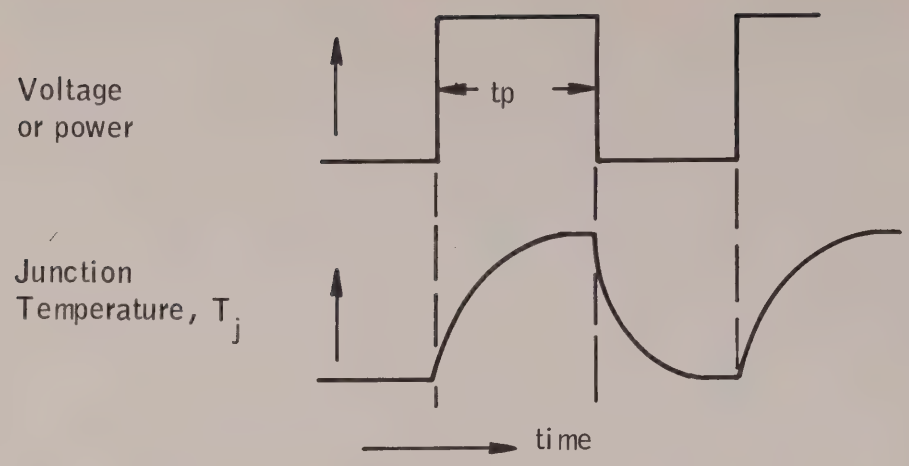

A. JUNCTION TEMPERATURE VS. TIME FOR $\tau < t_p$

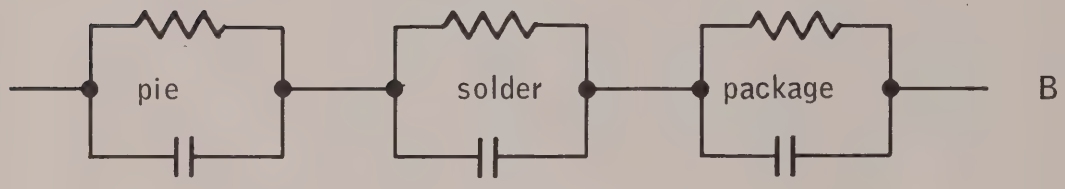

B. TIME CONSTANTS IN CASCADE

FIGURE 8 - THERMAL TIME CONSTANT

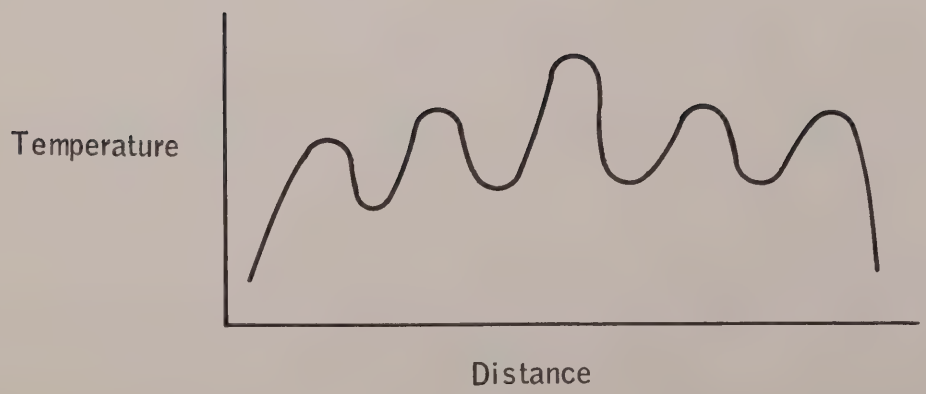

FIGURE 9 - TEMPERATURE VS. DISTANCE ACROSS A LARGE MULTI-FINGER DIE

$$\text{Then } \frac{\rho C}{K_{TH}} = \frac{2.33 \times 0.7}{1.0} = 1.63 \text{ sec/cm}^2$$

2. Gallium Arsenide (GaAs)

ρ = 5.31 gr/cc

C = 0.35 J/gr°C = 0.35 W-sec/gr°C

K_{TH} = 0.44 w/cm°C

$$\text{Then } \frac{\rho C}{K_{TH}} = \frac{5.31 \times .35}{0.44} = 4.22 \text{ sec/cm}^2$$

The following examples of a pulsed <u>silicon</u> transistor will show the importance of the thermal time constant.

Let: Θ = 50°C/W

T_A = 25°C

P_D = 5 watts, peak

F = 5 mils = .0125 cm

Use the following pulse lengths:

(1) 10 μsec

(2) 100 μsec

(3) C.W.

Calculate τ, the thermal time constant

$$\tau = \left[\frac{2F}{\pi}\right]^2 \left[\frac{\rho C}{K_{TH}}\right] = \left[\frac{2(0.0125)}{\pi}\right]^2 [1.63]$$

$$= 103 \text{ μs} = 1.03 \times 10^{-4} \text{ sec}$$

Then:

a. $$T_j = 5(50) \left[\frac{4}{\tau^{\frac{3}{2}}}\right] \left[\frac{10^{-5}}{1.03 \times 10^{-4}}\right]^{\frac{1}{2}} + 25$$

= 56 + 25 = 81°C for a pulse length of 10 μsec.

Or:

$$b. \quad T_j = 5(50)\left[\frac{4}{\tau^{\frac{3}{2}}}\right]\left[\frac{10^{-4}}{1.03 \times 10^{-4}}\right]^{\frac{1}{2}} + 25$$

$$= 202°C \text{ for a pulse length of } 100\ \mu sec.$$

Or:

$$c. \quad T_j = 5(50) + 25$$

$$= 275°\ C \text{ for CW}$$

Note that a Gallium Arsenide device under otherwise the same conditions would have a much higher temperature.

$$\Theta = 50\left(\frac{1}{.44}\right) = 113°C/W$$

$$\tau = 103\left(\frac{4.22}{1.63}\right) = 267\ \mu sec$$

1. Therefore, with a 10 μsec pulse

$$T_j = 5(113)\left[\frac{4}{\pi^{\frac{3}{2}}}\right]\left[\frac{10^{-5}}{2.67 \times 10^{-4}}\right]^{\frac{1}{2}} + 25$$

$$= 103°C$$

2. Or, with a 100 μsec pulse

$$T_j = 248°C$$

3. Or, under CW conditions

$$T_j = 113 \times 5 + 25 = 590°C$$

The result above shows that pulses short compared to τ give a very small temperature rise, while the long pulses result in a temperature rise closer to the CW condition. Pulse lengths greater than 2τ result in essentially the CW temperature.

III. MEASUREMENT OF THERMAL RESISTANCE

There are two basic approaches to the measurement of Θ, the thermal resistance. A method considered by some to be the most basic uses an infrared scanner to measure the surface temperature by its infrared emission. This system has both advantages and disadvantages.

INFRARED MEASUREMENT OF Θ

Advantages	Disadvantages
1. Reads peak (not average, locates "hot spot" temperature to 0.3 mil accuracy.	1. High cost.
2. Can give temperature profiles of larger devices.	2. Slow.
	3. Destructive (uses constant emissivity coating on die).

A temperature profile of a large device will be similar to Fig. 9 where the temperature peaks occur at the emitters.

The second method of temperature measurement depends on the temperature dependence of the forward voltage across a diode. This can be emitter-base voltage of a bipolar or the gate-source voltage of a FET.

For a bipolar transistor:

$$I_E = A_e q n_i^2 \frac{D_B}{N_B} \left[\exp \frac{qV_{be}}{kT_j} - 1 \right] \qquad \text{(Eq. 11)}$$

Where:

I_E = emitter current
V_{be} = emitter-base voltage
V_j = temperature
A_e = emitter area
n_i, D_B, N_B = material constants

Using the M-4 geometry, V_{be} is found to have a slope of ≈1.6 MV/°C for I_E = 1 ma. Therefore, by measuring V_{be}, the junction temperature can be

determined. The temperature thus measured is an average and does not indicate the peak temperature as the thermal scan method can.

Measuring temperature by the ΔV_{be} method is very simple. The device to be tested is biased to a constant low "measuring" current; e.g., 1 ma. It is then momentarily pulsed to a higher current (pulse length>>τ). V_{be} is then measured immediately after the device returns to the lower current condition. The delay should be less than 1% τ. V_{be} is then compared to the low current "cold" value.

$$\Theta = \frac{\Delta T}{\Delta P_D} = \frac{\frac{1}{mV/C} \cdot (\Delta V_{be})^*}{VI_{Hi} - VI_{meas}} \qquad * \text{ in mV} \qquad \text{(Eq. 12)}$$

For example, an M-4 device is pulsed from 1 ma and 10 volts to 30 ma and 10 volts. V_{be} changes from 0.704 volts (cold) to 0.653 volts (hot). Note that the temperature reduces V_{be}; current increases V_{be}. Calculate Θ:

$$\Theta = \frac{C^\circ}{mV} \cdot \frac{\Delta V_{be}}{\Delta P_D} = \frac{1}{1.6} \times \frac{704-653}{(.03-.001)\ 10} = 110^\circ C/W$$

The instrumentation for the measurement includes a pulse generator, oscilloscope (with Tektronix type W plug-in), and power supply. Figure 10 shows simplified test setups for bipolar and FET. Note that in the case of the FET, the gate bias is negative in the higher power dissipating mode and positive in the measuring mode.

Avantek uses a Θ_{jc} test set to measure ΔV_{be} semi-automatically on bipolar transistors. The test set uses a sample-and-hold circuit to remember V_{be} and displays it on a digital voltmeter. Thus, for special applications, devices can be screened individually for Θ_{jc}.

IV. GENERAL COMMENTS ON THERMAL RATINGS

The thermal resistance may be stated in a number of ways, the most common of which is Θ_{jc}, the thermal resistance between the junction and the external case (or package). It includes:

$$\Theta_{jc} = \Theta_{die} + \Theta_{solder} + \Theta_{case}$$

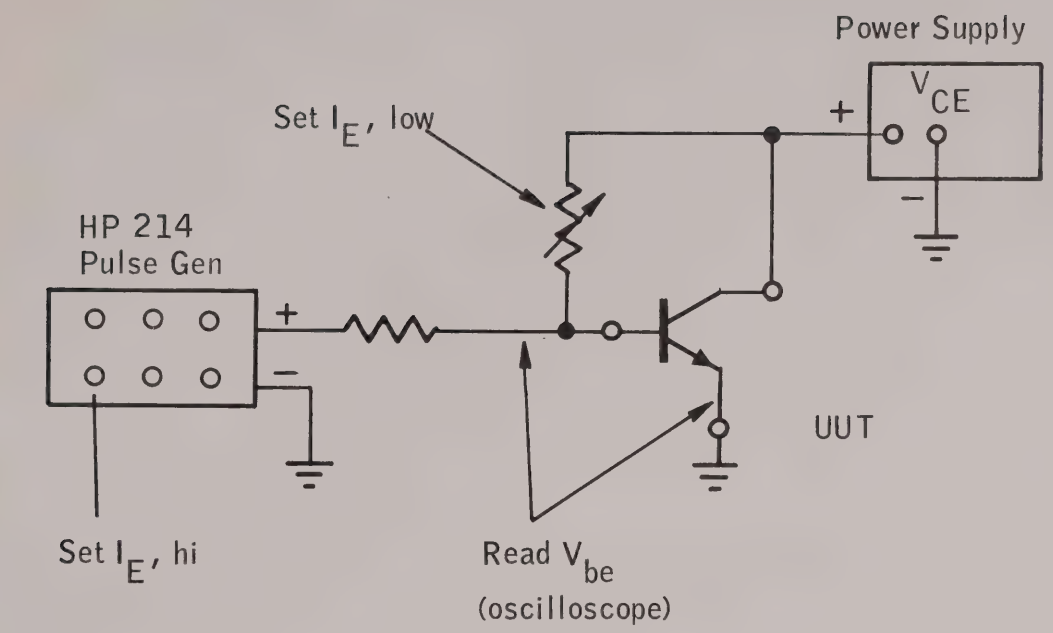

A. BIPOLAR SETUP

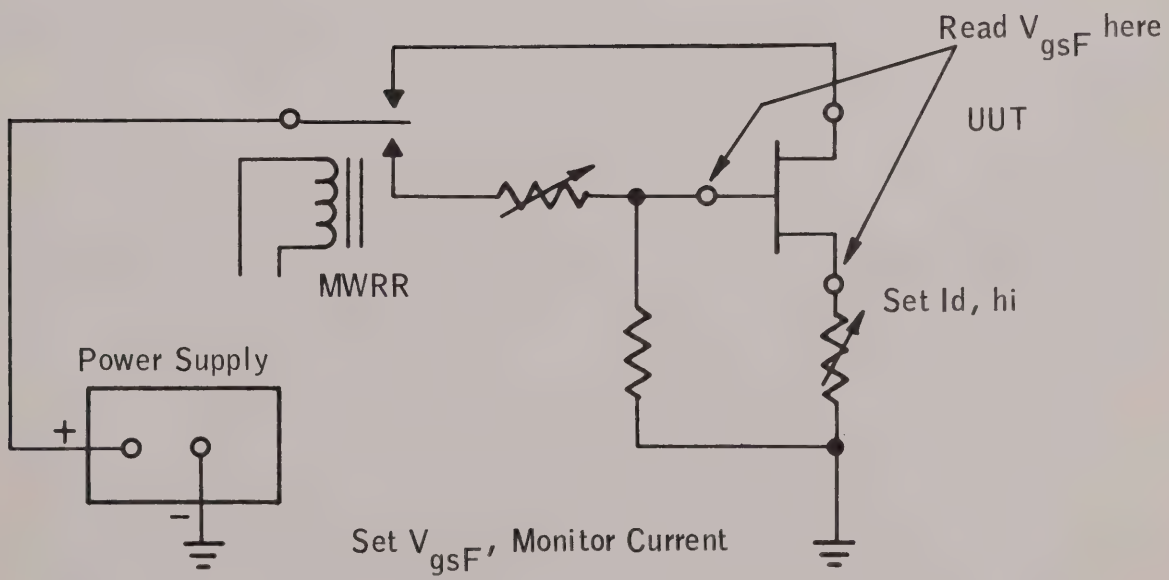

B. FET SETUP

FIGURE 10- SIMPLIFIED TEST SETUPS FOR MEASURING THERMAL RESISTANCE OF (A) BIPOLAR TRANSISTORS AND (B) FETS

The free air thermal resistance is much higher since the case is not tied to a sink, but must lose heat by radiation and convection. If the device is sinked by the leads only, then Θ has a value between Θ_{jc} and Θ free air.

Derating curves are determined as follows: The maximum dissipation in the case of a bipolar is determined from what is called the "safe operating area." Within that area the VI product is such that secondary breakdown will not occur. The maximum dissipated power is then computed from this characteristic and would always be less than the maximum voltage times the maximum current. A typical value for P_{Dmax} for a small-signal microwave transistor is 100-200 mw.

Figure 11 shows a derating curve. P_{max} is determined from the safe operating area as explained above. The maximum junction temperature is determined from reliability studies and can vary depending upon the MTBF desired. A value of 200°C is typical for silicon bipolar transistors. The breakpoint in the curve is where the junction is at 200°C and the power is P_{max}; i.e.,

$$Tx = 200 - P_{Dmax}\Theta$$

When the temperature of the case is greater than T_x, the dissipation is no longer determined by the safe operating area but is a function of the thermal resistance and the maximum junction temperature.

Since microwave FET's are a relatively new product, parameters like safe operating area, T_{jmax}, etc., have not yet been standardized. However, reliability tests indicate that an FET operated at T_j = 100°C will have an MTBF of over 10^8 hours; at 200°C it will be over 10^5 hours.

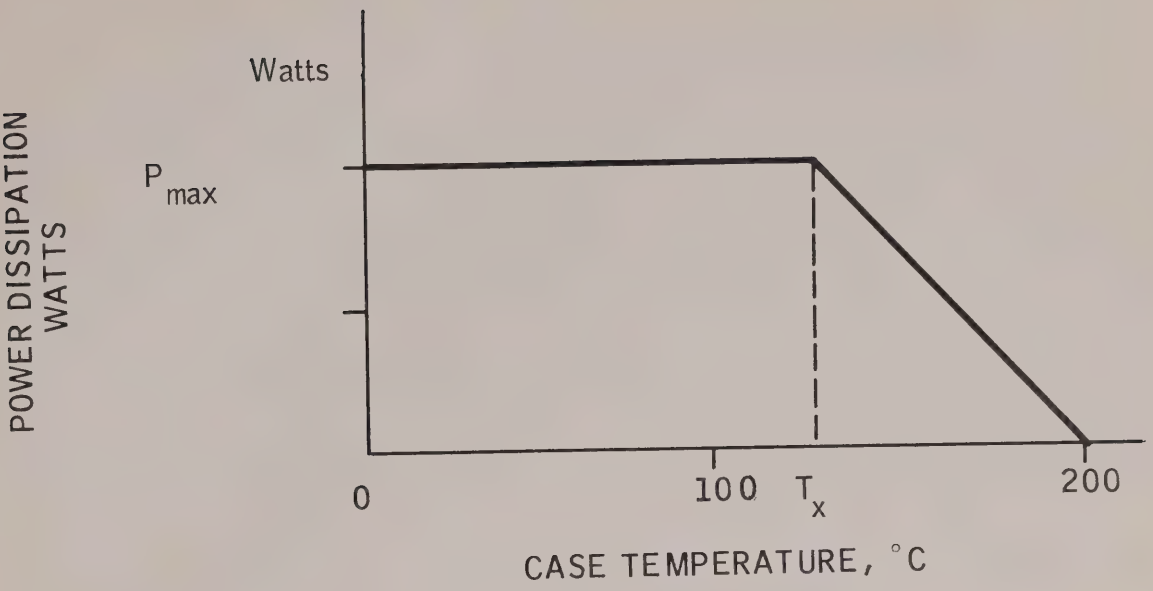

FIGURE 11 - POWER DERATING CURVE

SUMMARY OF SYMBOLS

Symbol		Units
ΔT	= temperature rise	°C
P_D	= power dissipation	watts
Θ	= thermal resistance	°C/watt
T_j	= junction temperature	°C
T_A	= ambient temperature	°C
K_{TH}	= thermal conductivity	watts/cm · °C
L	= gate length (of FET)	cm
F	= die (chip) thickness	cm
τ	= thermal time constant	seconds
t	= time	seconds
ρ	= density of material	gram/m^3
c	= specific heat	watt sec/gram · °C
t_p	= pulse width	seconds
I_E	= emitter current	amperes
V_{be}	= emitter-base voltage	volts
A_e	= emitter area	cm^2
n_i	= intrinsic carrier density	cm^{-3}
D_B	= diffusion constant for minority carriers in base	$cm^2 sec^{-1}$
N_B	= free carrier density in base	cm^{-3}

REFERENCES

1. Pritchard, R.L.; Electrical Characteristics of Transistors, McGraw-Hill, New York, 1967; Chapter 9.4

2. Linstead, R.D. and Surty, R.J.; "Steady State Junction Temperatures of Semiconductor Chips," IEEE Transactions on Electron Devices, Vol. Ed. 19, No. 1, Jan 1972; pp. 41-44.

3. Cohn, S.B.; IRE Transactions on Microwave Theory and Techniques, Vol. MTT-2, No. 2, July 1954; pp. 52-57.

4. Oliver, A.A.; IRE Transactions on Microwave Theory and Techniques, Vol. MTT-3, March 1955; pp. 134-143.

DOMESTIC REPRESENTATIVES

ALABAMA
Beacon Electronic Associates
11309 S. Memorial Parkway,
Suite B
Huntsville, AL 35803
(205) 881-5031

ARIZONA
The Thorson Company
2505 E. Thomas Road
Phoenix, AZ 85016
(602) 956-5300

CALIFORNIA (Northern)
Cain-White & Company
Foothill Office Center
105 Fremont Avenue
Los Altos, CA 94022
(415) 948-6533

CALIFORNIA (Southern)
Cain Technology
522 S. Sepulveda Blvd., Suite 112
Los Angeles, CA 90049
(213) 476-2251

Cain Technology
1046 N. Tustin
Suite K
Orange County, CA 92667
(714) 997-7311

COLORADO
The Thorson Company
5290 Yale Circle
Denver, CO 80222
(303) 759-0809

DC and VIRGINIA
Applied Engineering Consultants
Washington, DC
(301) 953-2808
(301) 953-2809

FLORIDA
Beacon Electronic Associates
235 S. Maitland
Maitland, FL 32751
(305) 647-3498

Beacon Electronic Associates
6842 NW 20 Avenue
Fort Lauderdale, FL 33309
(305) 971-7320

Beacon Electronic Associates
25 Anastasia Drive
Ft. Walton Beach, FL 32548
(904) 244-1550

GEORGIA
Beacon Electronic Associates
2285 Peachtree Road, NE
Atlanta, GA 30309
(404) 351-3654

ILLINOIS (Northern)
Dy Tec/Central, Inc.
121 S. Wilke Road
Suite 304
Arlington Heights, IL 60035
(312) 394-3380

ILLINOIS (Southern)
Dy Tec/South, Inc.
300 Brooks Drive, Suite 102
Hazelwood, MO 63042
(314) 731-5400

IOWA (Eastern)
Dy Tec/Central, Inc.
121 S. Wilke Road
Suite 304
Arlington Heights, IL 60035
(312) 394-3380

IOWA (Southern)
Dy Tec/South, Inc.
300 Brooks Drive, Suite 102
Hazelwood, MO 63042
(314) 731-5400

INDIANA
DyTec/Central, Inc.
4129 Oakleaf Drive
Fort Wayne, IN 46805
(219) 485-0845

KANSAS
Dy Tec/South, Inc.
6300 W. 75th Street
Overland Park, KS 66204
(913) 384-2710

MARYLAND
Applied Engineering Consultants
9051 Baltimore National Pike
Building 3, Office A
Ellicott City, MD 21043
(301) 465-1272

MASSACHUSETTS
R.J. Sickles Associates
12 Cambridge St. (Rt. 3)
Burlington, MA 01803
(617) 272-7285

MICHIGAN
Comtel Instruments Company
17500 West McNichols Road
Detroit, MI 48235
(313) 255-1970

MISSOURI (East)
Dy Tec/South, Inc.
300 Brooks Drive, Suite 102
Hazelwood, MO 63042
(314) 731-5400

MISSOURI (West)
Dy Tec/South, Inc.
6300 W. 75th Street
Overland Park, KS 66204
(913) 384-2710

NEBRASKA
Dy Tec/South, Inc.
300 Brooks Drive, Suite 102
Hazelwood, MO 63042
(314) 731-5400

NEW JERSEY (Northern)
Technical Marketing Associates
2460 Lemoine Avenue
Fort Lee, NJ 07024
(201) 224-6911

NEW MEXICO
The Thorson Company
2201 San Pedro Drive, NE
Building 2, Suite 107
Albuquerque, NM 87110
(505) 265-5655

NEW YORK (Metropolitan)
Technical Marketing Associates
2460 Lemoine Avenue
Fort Lee, NJ 07024
(201) 224-6911

NEW YORK (Upper State)
Robtron
2-4 Fennell Street, Suite 209
Skaneateles, NY 13152
(315) 685-5731

NORTH and SOUTH CAROLINA
Beacon Electronic Associates
122 W. Woodlawn Road
Suite A-106
Charlotte, NC 28210
(704) 525-7412

OHIO
Comtel Instruments Company
5827 Mayfield Road
Cleveland, OH 44124
(216) 442-8080

Comtel Instruments Company
1717 Big Hill Road A6
P.O. Box 2036 Kettering
Dayton, OH 45439
(513) 298-7573

OREGON
The Thorson Company
7000 SW Hampton Street
Suite 207
Portland, OR 97223
(503) 620-0958

PENNSYLVANIA
Comtel Instruments Company
No. 2 Parkway Center
Pittsburgh, PA 15220
(412) 922-5720

Eastern Instrumentation of
Philadelphia
613 W. Cheltenham Avenue
Philadelphia, PA 19126
(215) 927-7777

TEXAS
The Thorson Company
300 Huntland Drive
Austin, TX 78752
(515) 451-7527

The Thorson Company
4445 Alpha Road
Dallas, TX 75240
(214) 233-5744

The Thorson Company
6655 Hillcroft, Suite 224
Houston, TX 77036
(713) 771-3504

WASHINGTON
The Thorson Company
One Lake Bellevue Drive
Bellevue, WA 98005
(206) 455-9180

WISCONSIN
Dy Tec/Central, Inc.
121 S. Wilke Road
Suite 304
Arlington Heights, IL 60035
(312) 394-3380

INTERNATIONAL REPRESENTATIVES

AUSTRALIA
General Electronic Services Pty. Ltd.
99 Alexander Street, Crows Nest
New South Wales, 2065
Phone: 439-2488
Telex: Servo 25486

BELGIUM
Simac Electronics B.V.
148 Boulevard du Triomphe
1160 Brussels
Phone: 02/672.45.56
Telex: 23662 SIMEIP B

CANADA
R.D.B. Sheppard Agencies Ltd.
P.O. Box 8
Georgetown, Ontario L7G 4T1
Phone: (416) 877-9846
Telex: 06-97500 SHEP GTWN

FRANCE
PRANA
3. rue de la Grange
F 91230 Montgeron (Essonne)
Phone: 16(I)903.55.46
Telex: 692116 F

INDIA
Hinditron Services Pvt. Ltd.
69/A,L. Jagmohandas Marg
Bombay 400 006
Phone: 36 53 44
Telex: Tekhind 0112326

"Hinditron House"
412 Rajmahal Vilas Extension
12th Main Road
Bangalore 560 006 India
Telex: 043-741

ISRAEL
M.T.I. Engineering Ltd.
182 Ben Yehuda Street
P.O. Box 16349
Tel-Aviv
Phone: 24 40 90
Telex: 32200 MTI IL

ITALY
SISTREL
Societa Italiana Strumenti
Elettronici, S.p.A.
Via Giuseppe Armellini 37
00143 Roma
Phone: 5915551
Telex: 68356 SISTREL

JAPAN
Toko Trading Inc.
Kyodo (Shin-Aoyama) Bldg. 9-15
Minami-Aoyama 5-Chome
Minato-Ku
Tokyo
Phone: (03) 409-5831
Telex: Tokotrad J24686

THE NETHERLANDS
Simac Electronics B.V.
veenstraat 20
Veldhoven
Phone: 040-533725
Telex: 51037 Simac NI

REPUBLIC OF SOUTH AFRICA
South Continental Devices (Pty) Ltd.
Box 56420 Pinegowrie, 2123
Phone: 48-7125, 9229, 9260
Telex: 8-3324 SA

SINGAPORE, MALAYSIA
Masia Ltd.
3rd Floor
First National City Bank Building
28/30 Medan Pasar, P.O. Box 2197
Kuala Lumpur, Malaysia
Phone: 80011
Telex: Samia MA30966

SWEDEN, SCANDINAVIA
Walmore Electronics AB
Fack
S-162 10 Vallingby, Sweden
Phone: 468-380130
Telex: 17880

SWITZERLAND
Telemeter Electronic AG
Gerechtigkeitsgasse 25
Postfach
CH-8027 Zurich
Phone: 051 25 78 72
Telex: 57287 Telzu CH

TAIWAN
Sun Moon Star Co., Ltd.
164 Min Shen East Road
P.O. Box 1273
Taipei, Taiwan 104
Republic of China
Phone: 588521-5.510521
Telex: 22199 SMSCO

UNITED KINGDOM
Walmore Electronics, Ltd.
11-15 Betterton Street
Drury Lane
London WC 2H 9BS
Phone: 01-836 1228
Telex: Walrad 28752

WEST GERMANY-AUSTRIA
Telemeter Electronic GmbH
885 Donauworth-Riedlingen
Posthof 4 (West Germany)
Phone: (0906) 5091
Telex: 51856 Teldo D

YUGOSLAVIA
Belram S.A.
Avenue des Mimosas 83
1150 Brussels (Belgium)
Phone: 34 33 32
Telex: 21790 Belram B

Avantek

Advanced solid-state products • 3175 Bowers Avenue, Santa Clara, California 95051 • Phone (408) 249-0700 • TWX 910-339-9274 • Telex 34-6337

ATP-1040/1-78

Printed in U.S.A.

Intercept Point and Dynamic Range.

An article describing the concept of *intercept point* as an indicator of the spurious-free dynamic range of an amplifier was presented in the February 1, 1967 issue of *Electronic Design* magazine. A copy of this article along with an enlarged version of the useful intercept point nomograph appearing in the article is available from your local representative or by contacting Avantek.

If the fundamental input power (1) vs. output power response of an amplifier is plotted on a log-log scale, it will have a 1:1 slope (see fig. 1) in the linear operating region. A plot of the second-order intermodulation products (2) of most amplifiers, plotted on the same scale will have a slope of 2:1 and the third-order products (3) a slope of 3:1.

Since the third-order spurious products are the most troublesome, falling within the bandpass of even moderate bandwidth amplifiers, the intercept point is generally defined as the point where extensions of the first and third order responses intersect on the output power scale. Note that the second-order response plot will generally intersect near the same point as well, unless the amplifier design suppresses even-order responses (for example, uses push-pull stages).

When the amplifier is operating in the linear amplification range (i.e., below the 1 dB gain compression point), the levels of the spurious responses can be estimated accurately with a simple calculation or by using the nomograph.

Referring to the typical amplifier response curve of figure 1 the output power at 1 dB gain compression is +20 dBm and the intercept point is +30 dBm, a difference of 10 dB. Since the difference between the slope of the second order response curve and the fundamental curve is 1:1, the second order spurious products will be the same distance down from the fundamental as the fundamental is from the intercept point at any output power. Similarly, since the difference between the slope of the third order curve and the fundamental is 2:1, the third order products will be twice the distance down from the fundamental as the fundamental is from the intercept point at any output power in the linear range.

If the amplifier in figure 1 is driven to an output power of 0 dBm (30 dB down from the intercept point), the second order spurious products will be at -30 dBm, and the third order products at -60 dBm.

Notes:
(1) The input signal consists of two components, f_1 and f_2 closely spaced in frequency, but not so closely spaced that difference frequencies are not well bypassed.

(2) $f_1 \pm f_2$, $2f_1$ and $2f_2$. The second order intercept point is normally only important for amplifiers with an octave or more of bandwidth, otherwise second order products will not fall within the amplifier passband.

(3) $3f_1$, $3f_2$, $2f_1 \pm f_2$, $2f_2 \pm f_1$. The third order intercept point is important, since third order products will fall within the passband of virtually any amplifier capable of amplifying both f_1 and f_2. Unless otherwise indicated, the intercept point given in any Avantek data sheet is for third-order products.

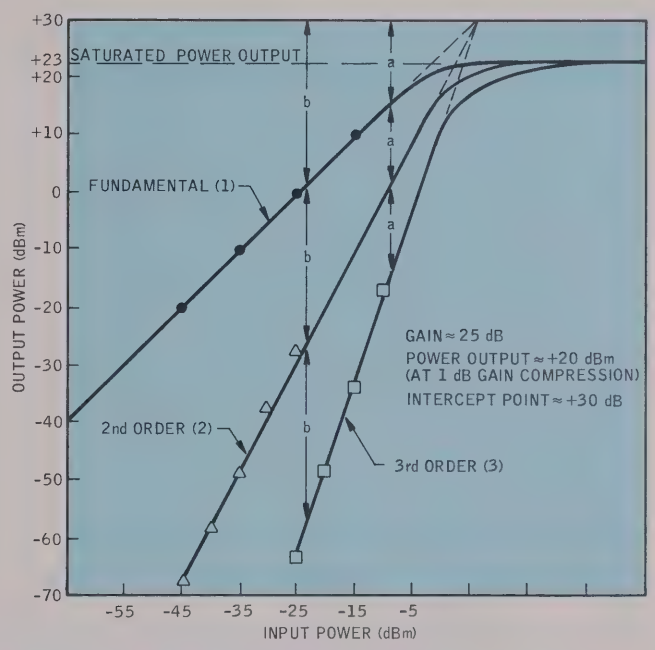

The plot of amplifier responses is a set of straight lines on the log-log scale. The slope of the line depends on the order; the fundamental has a slope of 1, the second order has a slope of 2 and the third order has a slope of 3. The intersection of the fundamental and third order yields the intercept point.

Figure 1. Intercept Point Response for a Typical Amplifier

Amplifier Dynamic Range

Once the intercept point of an amplifier is known, the spurious-free dynamic range can be calculated from the equation:

Spurious Free Dynamic Range (dB) =
$2/3\ (P_1 - P_0 - 10 \log BW - NF)$

Where: P_1 = *Input* intercept Point (obtained by subtracting the amplifier gain from the *output* intercept point given on data sheets)
P_0 = effective input noise power with no signal = -114 dBm/MHz
BW = System noise bandwidth* in MHz (controlled by any filtering or other

Guaranteed Specifications @25°C

Model	Frequency (MHz)	Gain (dB)	Spurious Free Dynamic Range (dB)	Typical 2nd Order Intercept Point (dBm)	Typical 3rd Order Intercept Point (dBm)	Power Output (dBm) (1 dB Compression)	Gain Flatness (dB)	Noise Figure (dB)	VSWR In	VSWR Out	Input Power* Volts DC	Input Power* Current (mA)	Case Drawing
ADM-110Δ	10-100	14.0	88	+70	+39	+23	±1.0	5.0	1.5	1.5	+15	150	GC-4
ADM-115Δ	10-100	30.0	83	+80	+47	+27	±1.0	5.5	1.5	1.5	+15	750	DM
ADM-150Δ	30-150	11.0	94	+65	+46	+33	±1.0	7.0	1.3	1.3	+24	800	DM
ADM-250Δ	20-250	29.0	82	+53	+46	+33	±1.0	5.0	2.0	2.0	+24	600	DM

Video and Pulse Amplifiers

All Avantek AV Series video and pulse amplifiers are unconditionally stable under all operating conditions including open and short circuited input and output terminals. The DC input connector is RFI shielded to prevent signals from entering through or radiating from the power supply line.

The optimized video amplifiers offer flat gain response extending from a few KHz to several hundred MHz. They are capable of amplifying complex waveforms without distortion and provide wide dynamic range, high output power and excellent input and output impedance match. Common applications include preamplification of low level signals applied to wideband oscilloscopes or spectrum analyzers as well as preamplifiers for ECM and spectrum survey receivers. They are also useful as post amplifiers to raise the level of signal and sweep generators and as coaxial line drivers for remote receivers or instruments.

The optimized pulse amplifiers are specifically designed and tuned for fast pulse risetime, minimum pulse droop and minimum overshoot. Their high output power capability and wide dynamic range makes them ideal for pulse distribution and instrumentation applications.

Guaranteed Specifications @25°C

Model	Frequency Response (MHz) Minimum	Gain (dB) Minimum	Gain Flatness ±dB) Maximum	Noise Figure (dB) Maximum	VSWR (50 ohms) Maximum In	VSWR (50 ohms) Maximum Out	Power Output for 1 dB Gain Compression (dBm) Minimum	Typical Intercept Point for IM Products (dBm)	Input Power* Volts DC	Input Power* Current (mA)	Case Drawing
AV-1T	0.01-300	29	±1.0	8.0	2.0	2.0	+19	+30	+28	200	FW
AV-4T	0.02-300	30	±1.0	8.0	2.0	2.5	+29	+38	+28	650	FX
AV-8T	0.002-400	30	±1.0	10.0	2.0	2.0	+29	+40 odd	+28	550	FXX
AV-6T	0.02-400	24	±1.0	8.5	2.5	2.5	+24	+35 odd +50 even	+28	325	FX

Model	Rise Time Max.	Noise Level Max. Input	Gain (dB) Min.	Output Level Min.	Pulse Droop Max.	Input & Output Impedance	Input Power* Volts DC	Input Power* Current (mA)	Pulse Overshoot (Typ)	Case Drawing
AV-3T	1.25 ns SSRT	30 μV	29	±2.3 V Peak	20% (8μs pulse)	50 ohms	+28	200	5%	FW
AV-5T	1.25 ns SSRT, Max. 1.60 ns LSRT, Typ.	25 μV	30	±9 V Peak	15% (2.5 μs pulse)	50 ohms	+28	650	8%	FX
AV-7T	1.1 ns SSRT, Max. 1.25 ns LSRT, Typ.	30 μV	24	±5 V Peak	15% (4.5 μs pulse)	50 ohms	+28	325	8%	FX
AV-9T	0.9 ns SSRT, Max. 1.0 ns LSRT, Typ.	25 μV	30	±9 V Peak	10% (10 μs pulse)	50 ohms	+28	550	3%	FXX

ΔPreliminary, contact factory.
*VDC @ ±1% regulation; mA, typical.

selectivity in the system, or by the amplifier bandwidth if no selectivity is provided)
NF = Amplifier Noise Figure in dB.

Sensitivity/Noise Floor of an Avantek Amplifier

The lowest input signal power level which will produce a detectable output from an amplifier is determined by the thermal noise generated within the amplifier itself. Any signal below this "noise floor" will cause an amplifier output with signal-to-noise ratio of less than one, which requires special techniques to recover useful information.

The following equation can be used to determine the thermal noise floor and thus the minimum signal that can provide a usable amplifier output:

$Pn = -114\ dBm + 10 \log BW + NF$

Pn = effective input noise power, or minimum usable input signal level

BW = Noise bandwidth* of amplifier or system in MHz

NF = Amplifier or system noise figure in dB

Noise Figure vs. Effective Noise Temperature (T_e)

The effective noise temperature of an amplifier may be calculated from noise figure with the equation:

$T_e(°K) = 290\ [\log^{-1}(NF/10)-1]$

Noise Figure vs. Noise Factor

The Noise factor of an amplifier may be calculated from the noise figure with the identity:

$F_N = \log^{-1}(NF/10)$
Where F_N = noise factor.

---

* Noise bandwidth is defined as: $BW = \frac{1}{G}\int G_f\,df$

where G_f is the differential available gain
G is the gain of the system under measurement
f is frequency

As a first order approximation of noise bandwidth, the bandwidth between the 3 dB down points on the gain response curve is generally used since it can be measured directly.

Note that neither the noise bandwidth nor the 3 dB bandwidth of an Avantek amplifier can be determined from the published data (which indicates *flat* gain response). In many applications the overall bandwidth is limited by external filtering or other selectivity. In those cases the amplifier bandwidth is not important.

Phase Linearity, Group Delay and Distortion

In an ideal transmission of "infinite" bandwidth such as free space or (in most cases) a well-terminated coaxial transmission line, the phase of a signal passing through the transmission path is directly related to the signal frequency and the propagation velocity. A plot of frequency vs. phase would result in a straight line with a slope dependent on the propagation velocity and effective electrical length of the path. In this ideal case, the phase delay term defined by equation 1 would remain constant regardless of the signal frequency.

When a single-frequency signal is applied to a filter, amplifier or other device with limited bandwidth, the phase delay becomes frequency-sensitive. The plot of phase vs. frequency is no longer a straight line and the phase delay (t_f) would vary as the frequency is changed.(See figure 2).

Phase linearity can be expressed as the maximum deviation from the ideal straight line phase vs frequency plot which would be produced by an ideal transmission line of similar electrical length, or simply by reference to a tabular listing of phase deviation at a number of discrete frequencies.

In most cases, the value of knowing the phase deviation for the single-frequency signal passing through a device is limited, since amplifiers are generally called upon to process signals consisting of many frequency components such as modulated or keyed carriers. In a simple case, this signal consists of two original frequency components and the resulting modulation envelope (or beat). Each of the two original frequencies applied to an amplifier may propagate at a different velocity and the modulation envelope at a third velocity. The latter is known as the group velocity. The more linear the phase shift of the amplifier, the less difference will exist between the velocities of the two original frequencies.

Group delay is an expression of the rate of change of the phase shift of the modulation envelope vs. changes in carrier frequency and is expressed in units of time through equation 2.

The group delay of an amplifier may be measured in several different ways. The frequency of a single-frequency signal may vary in increments and the corresponding change in the phase of the output signal measured (equation 3), or the phase shift of the modulation envelope may be measured as the carrier is swept through the frequency range of interest (equation 4).

The actual phase shift affecting all frequency components of the signals passing through an amplifier (or system) is relatively unimportant (except when several signal paths must be combined in or out of phase), but phase distortion affecting different fre-

quency components differently (as represented by dispersion) is vitally important. Phase distortion can result in intersymbol interference due to broadening of pulses in digital transmission or co-channel interference in systems carrying a number of FM or television channels.

For many Avantek communications amplifiers, the group delay characteristics are specified by the terms of the quadratic equation $t_d = Lx + Px^2 \pm R$, which describes a frequency vs. group delay curve similar to figure 3. In this equation L = the slope of the linear component of the curve (ns/MHz), P = the shape factor of the parabolic component of the curve (ns/MHz²) and R is the residual (ripple) component of the curve after the linear and parabolic components have been removed (ns P-P).

Avantek specifications guarantee maximum values for the Linear, Parabolic and Ripple components of many communications amplifiers. It should be noted however, that usually the overall group delay characteristics of a system in which a transistor amplifier is used will be primarily determined by the characteristics of other components in the signal path. For example, when an Avantek amplifier is used as the preamplifier in a satellite downlink receiving system the bandpass filter, mixer and IF amplifier characteristics of the receiver will largely determine the group delay of the system.

The phase response of Avantek amplifiers can be measured using the Hewlett-Packard 8542A Automatic Network Analyzer and the results supplied to customers at extra cost. In addition, phase matching is available for critical applications.

Equation 1 - Phase Delay vs. Frequency

$$t_f = \frac{\phi}{\omega}$$

Equation 2 - Group Delay vs. Frequency

$$t_d = \frac{d\phi}{d\omega}$$

Equation 3

$$t_d = \frac{\Delta\phi}{\Delta\omega}$$

Equation 4

$$t_d = \frac{\phi e}{fm \times 360°}$$

t_f = phase delay (in seconds)
ϕ = carrier phase shift (in radians)
ω = carrier frequency (radians/second)
t_d = group delay (in seconds)
ϕe = modulation envelope phase shift (in degrees)
fm = modulation frequency (Hz)

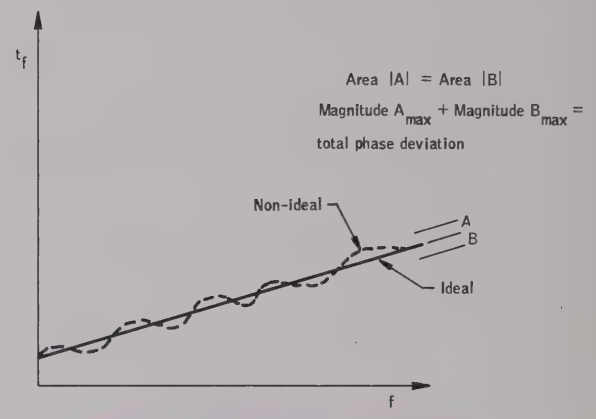

Fig. 2 — Phase Shift vs. Frequency

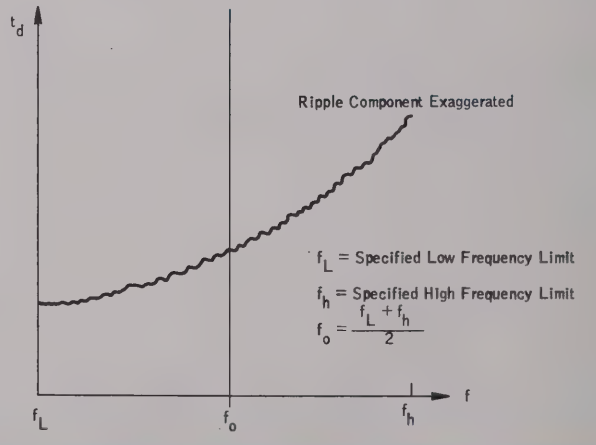

Fig. 3 - Combined Linear Parabolic and Ripple Components of Group Delay

AM-PM Conversion

As the input signal level applied to a transistor amplifier is increased until some degree of gain compression is produced, further increases in signal amplitude will result in a slight shift of the amplifier phase delay. This phenomenon is known as AM-PM conversion and can be thought of as a result of the change of the transistor operating parameters from the small-signal to large-signal conditions. Many

Avantek amplifiers include a guaranteed specification that AM-PM conversion will not exceed a certain value, on the order of a few tenths of a degree per dB increase in power output at a nominal power output level. If the input signal is further increased, the amount of AM-PM conversion will continue to increase reaching a maximum value when one of the amplifier stages is driven into full saturation. The maximum value will normally never exceed a few degrees/dB near amplifier saturation, and may generally be ignored.

Any limiters in a system are usually the major contributors to overall AM-PM conversion. Perhaps the worst case example is when a transistor amplifier is used in a receiving system in close proximity to a nearby transmitting system operating on a different frequency and the leakage power is sufficient to drive the limiters into their operating region. The result will usually be a noticeable slope in the baseband frequency response which will take place only when the transmitter is operating.

Bandwidth Limitation with External Filtering

The guaranteed frequency range of all Avantek amplifiers represents the range in which all guaranteed performance parameters are met and *not* the 3 dB down points on the amplifier gain curve. There is no way to determine the 3 dB points from the basic amplifier specifications, and the amplifier may continue to exhibit large amounts of gain over a considerably wider frequency range. If response to out-of-band signals is a problem in a system design, it may be necessary to provide external filtering to limit the overall system bandwidth to a known range.

Pulse Amplification

When linear amplifiers are used to amplify fast-resetime pulses or pulsed RF bursts, they may exhibit weaknesses in their transient response characteristics which can distort the pulse or envelope waveform. In general, for wideband small signal video amplifiers, the risetime behavior can be approximated from the emperical relationship:

$$T_R = \frac{0.35}{f_{3\,dB}}$$

Where T_R is the 10% to 90% risetime for small signal pulses. f_{3dB} is the upper 3 dB point on the amplifier gain vs. frequency curve.

Equally emperically, since Avantek small signal amplifiers are characterized with a guaranteed bandwidth in the flat portion of their gain vs. frequency response curve, the 0.35 factor can be disregarded and the following relationship may be used:

$$T'_R = \frac{1}{f_{h\ spec}}$$

Where $f_{h\ spec}$ is the specified upper guaranteed frequency limit.

In amplifiers designed for flat gain response over a wide frequency range, no provision has usually been made for optimization of pulse overshoot (the difference between the peak amplitude of the output pulse and the final amplitude at the pulse leading edge). Avantek AV Series pulse amplifiers are specifically designed to minimize overshoot (typically 3% to 8%), while the overshoot of other Avantek amplifiers is not normally specified or characterized.

Another important characteristic of a pulse amplifier is pulse droop (or sag), which is the amount that an amplitude of the output signal will decrease in a given amount of time, with a fixed DC level applied to the amplifier input. Although pulse droop characteristics are directly related to the lower 3 dB frequency of an amplifier, they are also affected by the coupling and bypassing networks making it difficult to quantify given the usual amplifier specifications.

The output pulse will be inverted by the AV-7, but not by the other AV series amplifiers. Models AV-4, -6 and -8 have symmetrical output stages to assure equal amplification of both positive and negative-going pulses.

Contact the factory for information on the number of stages and the suitability of other Avantek amplifiers for your particular pulse applications.

Single-Ended Vs. Balanced Amplification — Why Avantek Uses Both

Avantek engineers incorporate both single-ended and balanced amplification stages in their amplifier designs. In some products, both techniques are combined in the same amplifier, generally with a single-ended input and intermediate stages followed by a balanced output stage. Each design offers certain specific performance features as the following comparison will show.

Balanced Amplification

In a balanced microwave transistor stage, two identical amplification channels are used with quadrature (90°) couplers to equally divide the input signal and combine the output of the channels. The major advantage to the balanced amplifier stage is that, using the same transistors, a balanced stage can produce approximately twice the output power of a similar single-ended stage. In addition, the third-order intercept point is about 3 dB higher. Thus, with available microwave transistors, balanced amplification can provide significantly higher power output levels.

The quadrature couplers have the inherent ability to cancel reflected energy at both their input and output ports and tend to improve the VSWR of each stage in which they are used. This improved VSWR is

obtained without the need for trading off gain or noise figure in stage tuning. The degree of VSWR improvement depends on how well the two amplifier channels are matched and on the degree of balance of the coupler.

Single-Ended Amplification

In a single-ended stage, a single transistor provides the amplification. Since there is no input coupler to add loss, the noise figure of a single-ended stage may be lower than that of a balanced stage. Minimum-loss interstage coupling also means that a single-ended amplifier stage will generally produce a somewhat higher gain than the equivalent balanced stage.

One good example of the differences between amplifiers using all single ended stages and those using all balanced stages can be found by examining the performance of the similar Avantek AMG Series (single-ended) vs. the ABG Series (balanced). The noise figures and gains of the two series are comparable but the guaranteed input/output VSWR of the ABM series amplifiers is 1.5:1 (vs. 2.0:1), and the power output and intercept point are considerably higher.

All AMT-8000, -11000, -12000, 16000 and 18000 Series Amplifiers use balanced stages exclusively to produce a maximum power output at the C, X, and Ku-Bands while still maintaining their wide frequency ranges. The AM-7700/8400 Series communications band GaAs FET amplifiers (7.25 - 7.75 and 7.9 to 8.4 GHz) use single-ended stages (with an active biasing transistor for each stage). Isolators at both the input and output ports maintain VSWR at 1.25:1 maximum. Finally, the AM-5000/-6000 Series GaAs FET amplifiers (4.4 - 5.0 and 5.4 - 6.0 GHz) represent the combination of single-ended input and intermediate stages (with an input isolator) and a balanced amplifier stage for low output VSWR (1.25:1 maximum).

In each Avantek amplifier family the choice of transistor technology, single-ended or balanced stages (or a combination of both), and the use of isolators is all based on providing the right performance specifications for the specific application while maintaining an optimum ratio of performance to cost.

Notes

HEWLETT hp PACKARD

S-Parameter Techniques for Faster, More Accurate Network Design

ABSTRACT. Richard W. Anderson describes s-parameters and flowgraphs and then relates them to more familiar concepts such as transducer power gain and voltage gain. He takes swept-frequency data obtained with a network analyzer and uses it to design amplifiers. He shows how to calculate the error caused by assuming the transistor is unilateral. Both narrow band and broad band amplifier designs are discussed. Stability criteria are also considered.

This article originally appeared in the February 1967 issue of the Hewlett-Packard Journal.

LINEAR NETWORKS, OR NONLINEAR NETWORKS operating with signals sufficiently small to cause the networks to respond in a linear manner, can be completely characterized by parameters measured at the network terminals (ports) without regard to the contents of the networks. Once the parameters of a network have been determined, its behavior in any external environment can be predicted, again without regard to the specific contents of the network.

S-parameters are being used more and more in microwave design because they are easier to measure and work with at high frequencies than other kinds of parameters. They are conceptually simple, analytically convenient, and capable of providing a surprising degree of insight into a measurement or design problem. For these reasons, manufacturers of high-frequency transistors and other solid-state devices are finding it more meaningful to specify their products in terms of s-parameters than in any other way. How s-parameters can simplify microwave design problems, and how a designer can best take advantage of their abilities, are described in this article.

Two-Port Network Theory

Although a network may have any number of ports, network parameters can be explained most easily by considering a network with only two ports, an input port and an output port, like the network shown in Fig. 1. To characterize the performance of such a network, any of several parameter sets can be used, each of which has certain advantages.

Each parameter set is related to a set of four variables associated with the two-port model. Two of these variables represent the excitation of the network (independent variables), and the remaining two represent the response of the network to the excitation (dependent variables). If the network of Fig. 1 is excited by voltage sources V_1 and V_2, the network currents I_1 and I_2 will be related by the following equations (assuming the network behaves linearly):

$$I_1 = y_{11}V_1 + y_{12}V_2 \quad (1)$$

$$I_2 = y_{21}V_1 + y_{22}V_2 \quad (2)$$

In this case, with port voltages selected as independent variables and port currents taken as dependent variables, the relating parameters are called short-circuit admittance parameters, or y-parameters. In the absence of additional information, four measurements are required to determine the four parameters y_{11}, y_{21}, y_{12}, and y_{22}. Each measurement is made with one port of the network excited by a voltage source while the other port is short circuited. For example, y_{21}, the forward transadmittance, is the ratio of the current at port 2 to the voltage at port 1 with port 2 short circuited as shown in equation 3.

$$y_{21} = \left.\frac{I_2}{V_1}\right|_{V_2 = 0 \text{ (output short circuited)}} \quad (3)$$

If other independent and dependent variables had been chosen, the network would have been described, as before, by two linear equations similar to equations 1 and 2, except that the variables and the parameters describing their relationships would be different. However, all parameter sets contain the same information about a network, and it is always possible to calculate any set in terms of any other set.

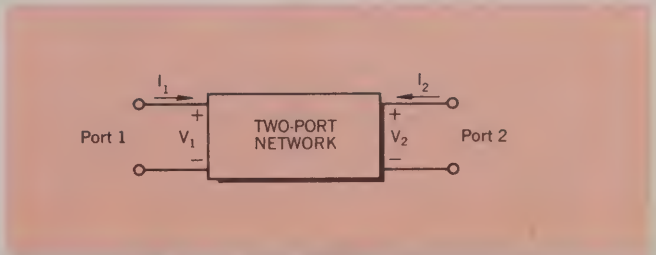

Fig. 1. *General two-port network.*

S-Parameters

The ease with which scattering parameters can be measured makes them especially well suited for describing transistors and other active devices. Measuring most other parameters calls for the input and output of the device to be successively opened and short circuited. This is difficult to do even at RF frequencies where lead inductance and capacitance make short and open circuits difficult to obtain. At higher frequencies these measurements typically require tuning stubs, separately adjusted at each measurement frequency, to reflect short or open circuit conditions to the device terminals. Not only is this inconvenient and tedious, but a tuning stub shunting the input or output may cause a transistor to oscillate, making the measurement difficult and invalid. S-parameters, on the other hand, are usually measured with the device imbedded between a 50Ω load and source, and there is very little chance for oscillations to occur.

Another important advantage of s-parameters stems from the fact that traveling waves, unlike terminal voltages and currents, do not vary in magnitude at points along a lossless transmission line. This means that scattering parameters can be measured on a device located at some distance from the measurement transducers, provided that the measuring device and the transducers are connected by low-loss transmission lines.

Generalized scattering parameters have been defined by K. Kurokawa.[1] These parameters describe the interrelationships of a new set of variables (a_i, b_i). The variables a_i and b_i are normalized complex voltage waves incident on and reflected from the i^{th} port of the network. They are defined in terms of the terminal voltage V_i, the terminal current I_i, and an arbitrary reference impedance Z_i, as follows

[1] K. Kurokawa, 'Power Waves and the Scattering Matrix,' IEEE Transactions on Microwave Theory and Techniques, Vol. MTT-13, No. 2, March, 1965.

$$a_i = \frac{V_i + Z_i I_i}{2\sqrt{|\mathrm{Re}\, Z_i|}} \tag{4}$$

$$b_i = \frac{V_i - Z_i^* I_i}{2\sqrt{|\mathrm{Re}\, Z_i|}} \tag{5}$$

where the asterisk denotes the complex conjugate.

For most measurements and calculations it is convenient to assume that the reference impedance Z_i is positive and real. For the remainder of this article, then, all variables and parameters will be referenced to a single positive real impedance Z_o.

The wave functions used to define s-parameters for a two-port network are shown in Fig. 2. The independent variables a_1 and a_2 are normalized incident voltages, as follows:

$$a_1 = \frac{V_1 + I_1 Z_o}{2\sqrt{Z_o}} = \frac{\text{voltage wave incident on port 1}}{\sqrt{Z_o}} = \frac{V_{i1}}{\sqrt{Z_o}} \tag{6}$$

$$a_2 = \frac{V_2 + I_2 Z_o}{2\sqrt{Z_o}} = \frac{\text{voltage wave incident on port 2}}{\sqrt{Z_o}} = \frac{V_{i2}}{\sqrt{Z_o}} \tag{7}$$

Dependent variables b_1 and b_2 are normalized reflected voltages:

$$b_1 = \frac{V_1 - I_1 Z_o}{2\sqrt{Z_o}} = \frac{\text{voltage wave reflected (or emanating) from port 1}}{\sqrt{Z_o}} = \frac{V_{r1}}{\sqrt{Z_o}} \tag{8}$$

$$b_2 = \frac{V_2 - I_2 Z_o}{2\sqrt{Z_o}} = \frac{\text{voltage wave reflected (or emanating) from port 2}}{\sqrt{Z_o}} = \frac{V_{r2}}{\sqrt{Z_o}} \tag{9}$$

The linear equations describing the two-port network are then:

$$b_1 = s_{11}a_1 + s_{12}a_2 \tag{10}$$

$$b_2 = s_{21}a_1 + s_{22}a_2 \tag{11}$$

The s-parameters s_{11}, s_{22}, s_{21}, and s_{12} are:

$$s_{11} = \left.\frac{b_1}{a_1}\right|_{a_2 = 0} = \text{Input reflection coefficient with the output port terminated by a matched load } (Z_L = Z_o \text{ sets } a_2 = 0). \tag{12}$$

$$s_{22} = \left.\frac{b_2}{a_2}\right|_{a_1 = 0} = \text{Output reflection coefficient with the input terminated by a matched load } (Z_S = Z_o \text{ and } V_S = 0). \tag{13}$$

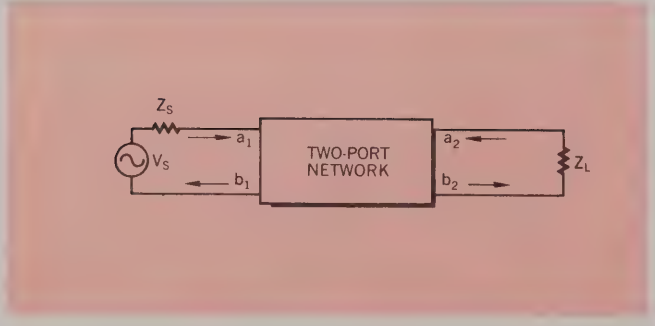

Fig. 2. *Two-port network showing incident* (a_1, a_2) *and reflected* (b_1, b_2) *waves used in s-parameter definitions.*

$$s_{21} = \left.\frac{b_2}{a_1}\right|_{a_2 = 0} = \text{Forward transmission (insertion) gain with the output port terminated in a matched load.} \quad (14)$$

$$s_{12} = \left.\frac{b_1}{a_2}\right|_{a_1 = 0} = \text{Reverse transmission (insertion) gain with the input port terminated in a matched load.} \quad (15)$$

Notice that

$$s_{11} = \frac{b_1}{a_1} = \frac{\frac{V_1}{I_1} - Z_o}{\frac{V_1}{I_1} + Z_o} = \frac{Z_1 - Z_o}{Z_1 + Z_o} \quad (16)$$

and

$$Z_1 = Z_o \frac{(1 + s_{11})}{(1 - s_{11})} \quad (17)$$

where $Z_1 = \frac{V_1}{I_1}$ is the input impedance at port 1.

This relationship between reflection coefficient and impedance is the basis of the Smith Chart transmission-line calculator. Consequently, the reflection coefficients s_{11} and s_{22} can be plotted on Smith charts, converted directly to impedance, and easily manipulated to determine matching networks for optimizing a circuit design.

The above equations show one of the important advantages of s-parameters, namely that they are simply gains and reflection coefficients, both familiar quantities to engineers. By comparison, some of the y-parameters described earlier in this article are not so familiar. For example, the y-parameter corresponding to insertion gain s_{21} is the 'forward transadmittance' y_{21} given by equation 3. Clearly, insertion gain gives by far the greater insight into the operation of the network.

Another advantage of s-parameters springs from the simple relationships between the variables a_1, a_2, b_1, and b_2, and various power waves:

$|a_1|^2$ = Power incident on the input of the network.
= Power available from a source of impedance Z_o.

$|a_2|^2$ = Power incident on the output of the network.
= Power reflected from the load.

$|b_1|^2$ = Power reflected from the input port of the network.
= Power available from a Z_o source minus the power delivered to the input of the network.

$|b_2|^2$ = Power reflected or emanating from the output of the network.
= Power incident on the load.
= Power that would be delivered to a Z_o load.

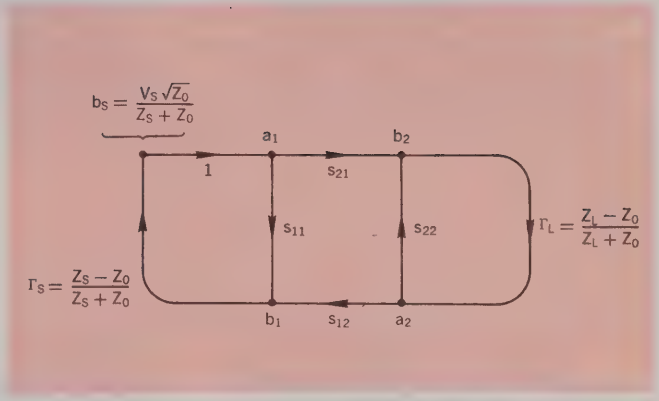

Fig. 3. *Flow graph of network of Fig. 2.*

Hence s-parameters are simply related to power gain and mismatch loss, quantities which are often of more interest than the corresponding voltage functions:

$$|s_{11}|^2 = \frac{\text{Power reflected from the network input}}{\text{Power incident on the network input}}$$

$$|s_{22}|^2 = \frac{\text{Power reflected from the network output}}{\text{Power incident on the network output}}$$

$$|s_{21}|^2 = \frac{\text{Power delivered to a } Z_o \text{ load}}{\text{Power available from } Z_o \text{ source}}$$
= Transducer power gain with Z_o load and source

$|s_{12}|^2$ = Reverse transducer power gain with Z_o load and source.

Network Calculations with Scattering Parameters

Scattering parameters turn out to be particularly convenient in many network calculations. This is especially true for power and power gain calculations. The transfer parameters s_{12} and s_{21} are a measure of the complex insertion gain, and the driving point parameters s_{11} and s_{22} are a measure of the input and output mismatch loss. As dimensionless expressions of gain and reflection, the parameters not only give a clear and meaningful physical interpretation of the network

performance but also form a natural set of parameters for use with signal flow graphs[2, 3]. Of course, it is not necessary to use signal flow graphs in order to use s-parameters, but flow graphs make s-parameter calculations extremely simple, and I recommend them very strongly. Flow graphs will be used in the examples that follow.

In a signal flow graph each port is represented by two nodes. Node a_n represents the wave coming into the device from another device at port n and node b_n represents the wave leaving the device at port n. The complex scattering coefficients are then represented as multipliers on branches connecting the nodes within the network and in adjacent networks. Fig. 3 is the flow graph representation of the system of Fig. 2.

Fig. 3 shows that if the load reflection coefficient Γ_L is zero ($Z_L = Z_o$) there is only one path connecting b_1 to a_1 (flow graph rules prohibit signal flow against the forward direction of a branch arrow). This confirms the definition of s_{11}:

$$s_{11} = \left.\frac{b_1}{a_1}\right|_{a_2 = \Gamma_L b_2 = 0}$$

The simplification of network analysis by flow graphs results from the application of the "non-touching loop rule." This rule applies a generalized formula to determine the transfer function between any two nodes within a complex system. The non-touching loop rule is explained in footnote 4.

[2] J. K. Hunton, 'Analysis of Microwave Measurement Techniques by Means of Signal Flow Graphs,' IRE Transactions on Microwave Theory and Techniques, Vol. MTT-8, No. 2, March, 1960.
[3] N. Kuhn, 'Simplified Signal Flow Graph Analysis,' Microwave Journal, Vol. 6, No. 11, Nov., 1963.

[4] The nontouching loop rule provides a simple method for writing the solution of any flow graph by inspection. The solution T (the ratio of the output variable to the input variable) is

$$T = \frac{\sum_k T_k \Delta_k}{\Delta}$$

where T_k = path gain of the k^{th} forward path

Δ = 1 − (sum of all individual loop gains) + (sum of the loop gain products of all possible combinations of two nontouching loops) − (sum of the loop gain products of all possible combinations of three nontouching loops) + ...

Δ_k = The value of Δ not touching the k_{th} forward path.

A path is a continuous succession of branches, and a forward path is a path connecting the input node to the output node, where no node is encountered more than once. Path gain is the product of all the branch multipliers along the path. A loop is a path which originates and terminates on the same node, no node being encountered more than once. Loop gain is the product of the branch multipliers around the loop.

For example, in Fig. 3 there is only one forward path from b_S to b_2 and its gain is s_{21}. There are two paths from b_S to b_1; their path gains are $s_{21}s_{12}\Gamma_L$ and s_{11} respectively. There are three individual loops, only one combination of two nontouching loops, and no combinations of three or more nontouching loops; therefore, the value of Δ for this network is

$$\Delta = 1 - (s_{11}\Gamma_S + s_{21}s_{12}\Gamma_L\Gamma_S + s_{22}\Gamma_L) + (s_{11}s_{22}\Gamma_L\Gamma_S).$$

The transfer function from b_S to b_2 is therefore

$$\frac{b_2}{b_S} = \frac{s_{21}}{\Delta}$$

Using scattering parameter flow-graphs and the non-touching loop rule, it is easy to calculate the transducer power gain with arbitrary load and source. In the following equations the load and source are described by their reflection coefficients Γ_L and Γ_S, respectively, referenced to the real characteristic impedance Z_o.

Transducer power gain

$$G_T = \frac{\text{Power delivered to the load}}{\text{Power available from the source}} = \frac{P_L}{P_{avS}}$$

$$P_L = P(\text{incident on load}) - P(\text{reflected from load})$$
$$= |b_2|^2 (1 - |\Gamma_L|^2)$$

$$P_{avS} = \frac{|b_S|^2}{(1 - |\Gamma_S|^2)}$$

$$G_T = \left|\frac{b_2}{b_s}\right|^2 (1 - |\Gamma_S|^2)(1 - |\Gamma_L|^2)$$

Using the non-touching loop rule,

$$\frac{b_2}{b_S} = \frac{s_{21}}{1 - s_{11}\Gamma_S - s_{22}\Gamma_L - s_{21}s_{12}\Gamma_L\Gamma_S + s_{11}\Gamma_S s_{22}\Gamma_L}$$

$$= \frac{s_{21}}{(1 - s_{11}\Gamma_S)(1 - s_{22}\Gamma_L) - s_{21}s_{12}\Gamma_L\Gamma_S}$$

$$G_T = \frac{|s_{21}|^2 (1 - |\Gamma_S|^2)(1 - |\Gamma_L|^2)}{|(1 - s_{11}\Gamma_S)(1 - s_{22}\Gamma_L) - s_{21}s_{12}\Gamma_L\Gamma_S|^2} \qquad (18)$$

Two other parameters of interest are:

1) Input reflection coefficient with the output termination arbitrary and $Z_S = Z_0$.

$$s'_{11} = \frac{b_1}{a_1} = \frac{s_{11}(1 - s_{22}\Gamma_L) + s_{21}s_{12}\Gamma_L}{1 - s_{22}\Gamma_L}$$

$$= s_{11} + \frac{s_{21}s_{12}\Gamma_L}{1 - s_{22}\Gamma_L} \qquad (19)$$

2) Voltage gain with arbitrary source and load impedances

$$A_V = \frac{V_2}{V_1} \qquad V_1 = (a_1 + b_1)\sqrt{Z_o} = V_{i1} + V_{r1}$$

$$V_2 = (a_2 + b_2)\sqrt{Z_o} = V_{i2} + V_{r2}$$

$$a_2 = \Gamma_L b_2$$

$$b_1 = s'_{11} a_1$$

$$A_V = \frac{b_2(1 + \Gamma_L)}{a_1(1 + s'_{11})} = \frac{s_{21}(1 + \Gamma_L)}{(1 - s_{22}\Gamma_L)(1 + s'_{11})} \qquad (20)$$

On p. 11 is a table of formulas for calculating many often-used network functions (power gains, driving point characteristics, etc.) in terms of scattering parameters. Also included in the table are conversion formulas between s-parameters and h-, y-, and z-parameters, which are other parameter sets used very often for specifying transistors at

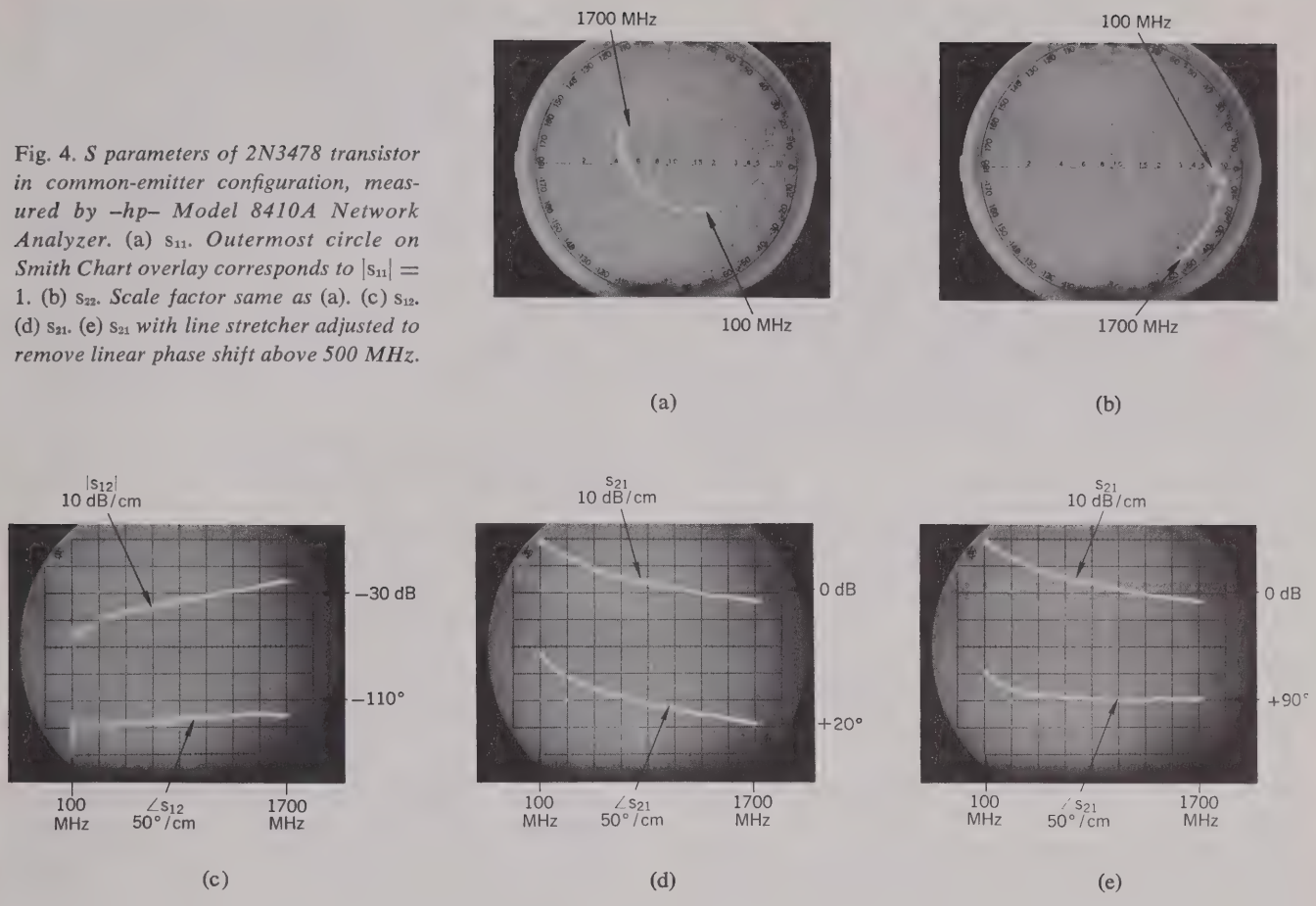

Fig. 4. *S parameters of 2N3478 transistor in common-emitter configuration, measured by –hp– Model 8410A Network Analyzer.* (a) s_{11}. *Outermost circle on Smith Chart overlay corresponds to* $|s_{11}| = 1$. (b) s_{22}. *Scale factor same as* (a). (c) s_{12}. (d) s_{21}. (e) s_{21} *with line stretcher adjusted to remove linear phase shift above 500 MHz.*

lower frequencies. Two important figures of merit used for comparing transistors, f_t and f_{max}, are also given, and their relationship to s-parameters is indicated.

Amplifier Design Using Scattering Parameters

The remainder of this article will show by several examples how s-parameters are used in the design of transistor amplifiers and oscillators. To keep the discussion from becoming bogged down in extraneous details, the emphasis in these examples will be on s-parameter design *methods,* and mathematical manipulations will be omitted wherever possible.

Measurement of S-Parameters

Most design problems will begin with a tentative selection of a device and the measurement of its s-parameters. Fig. 4 is a set of oscillograms containing complete s-parameter data for a 2N3478 transistor in the common-emitter configuration. These oscillograms are the results of swept-frequency measurements made with the new microwave network analyzer described elsewhere in this issue. They represent the actual s-parameters of this transistor between 100 MHz and 1700 MHz.

In Fig. 5, the magnitude of s_{21} from Fig. 4(d) is replotted on a logarithmic frequency scale, along with additional data on s_{21} below 100 MHz, measured with a vector voltmeter. The magnitude of s_{21} is essentially constant to 125 MHz, and then rolls off at a slope of 6 dB/octave. The phase angle of s_{21}, as seen in Fig. 4(d), varies linearly with frequency above about 500 MHz. By adjusting a calibrated line stretcher in the network analyzer, a compensating linear phase shift was introduced, and the phase curve of Fig. 4(e) resulted. To go from the phase curve of Fig. 4(d) to that of Fig. 4(e) required 3.35 cm of line, equivalent to a pure time delay of 112 picoseconds.

After removal of the constant-delay, or linear-phase, component, the phase angle of s_{21} for this transistor [Fig. 4(e)] varies from 180° at dc to +90° at high frequencies, passing through +135° at 125 MHz, the −3 dB point of the magnitude curve. In other words, s_{21} behaves like a single pole in the frequency domain, and it is possible to write a closed expression for it. This expression is

$$s_{21} = \frac{-s_{21_0} e^{-j\omega T_0}}{1 + j\frac{\omega}{\omega_0}} \qquad (21)$$

where

$$T_0 = 112 \text{ ps}$$
$$\omega = 2\pi f$$
$$\omega_0 = 2\pi \times 125 \text{ MHz}$$
$$s_{21_0} = 11.2 = 21 \text{ dB}$$

The time delay $T_0 = 112$ ps is due primarily to the transit time of minority carriers (electrons) across the base of this npn transistor.

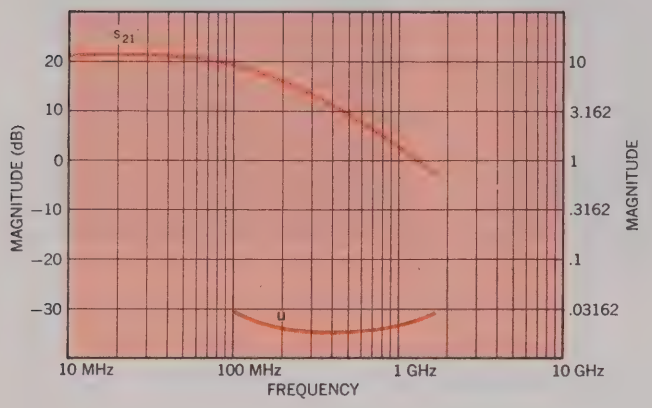

Fig. 5. Top curve: $|s_{21}|$ from Fig. 4 replotted on logarithmic frequency scale. Data below 100 MHz measured with –hp– 8405A Vector Voltmeter. Bottom curve: unilateral figure of merit, calculated from s parameters (see text).

Narrow-Band Amplifier Design

Suppose now that this 2N3478 transistor is to be used in a simple amplifier, operating between a 50Ω source and a 50Ω load, and optimized for power gain at 300 MHz by means of lossless input and output matching networks. Since reverse gain s_{12} for this transistor is quite small — 50 dB smaller than forward gain s_{21}, according to Fig. 4 — there is a possibility that it can be neglected. If this is so, the design problem will be much simpler, because setting s_{12} equal to zero will make the design equations much less complicated.

In determining how much error will be introduced by assuming $s_{12} = 0$, the first step is to calculate the unilateral figure of merit u, using the formula given in the table on p. 11, i.e.

$$u = \frac{|s_{11}s_{12}s_{21}s_{22}|}{|(1 - |s_{11}|^2)(1 - |s_{22}|^2)|} . \qquad (22)$$

A plot of u as a function of frequency, calculated from the measured parameters, appears in Fig. 5. Now if G_{Tu} is the transducer power gain with $s_{12} = 0$ and G_T is the actual transducer power gain, the maximum error introduced by using G_{Tu} instead of G_T is given by the following relationship:

$$\frac{1}{(1 + u)^2} < \frac{G_T}{G_{Tu}} < \frac{1}{(1 - u)^2} . \qquad (23)$$

From Fig. 5, the maximum value of u is about 0.03, so the maximum error in this case turns out to be about ±0.25 dB at 100 MHz. This is small enough to justify the assumption that $s_{12} = 0$.

Incidentally, a small reverse gain, or feedback factor, s_{12}, is an important and desirable property for a transistor to have, for reasons other than that it simplifies amplifier design. A small feedback factor means that the input characteristics of the completed amplifier will be independent of the load, and the output will be independent of the source impedance. In most amplifiers, isolation of source and load is an important consideration.

Returning now to the amplifier design, the unilateral expression for transducer power gain, obtained either by setting $s_{12} = 0$ in equation 18 or by looking in the table on p. 11, is

$$G_{Tu} = \frac{|s_{21}|^2(1 - |\Gamma_s|^2)(1 - |\Gamma_L|^2)}{|1 - s_{11}\Gamma_s|^2|1 - s_{22}\Gamma_L|^2} . \qquad (24)$$

When $|s_{11}|$ and $|s_{22}|$ are both less than one, as they are in this case, maximum G_{Tu} occurs for $\Gamma_S = s^*_{11}$ and $\Gamma_L = s^*_{22}$ (table, p. 11).

The next step in the design is to synthesize matching networks which will transform the 50Ω load and source impedances to the impedances corresponding to reflection coefficients of s^*_{11} and s^*_{22}, respectively. Since this is to be a single-frequency amplifier, the matching networks need not be complicated. Simple series-capacitor, shunt-inductor networks will not only do the job, but will also provide a handy means of biasing the transistor — via the inductor — and of isolating the dc bias from the load and source.

Values of L and C to be used in the matching networks are determined using the Smith Chart of Fig. 6. First, points corresponding to s_{11}, s^*_{11}, s_{22}, and s^*_{22} at 300 MHz are plotted. Each point represents the tip of a vector leading away from the center of the chart, its length equal to the magnitude of the reflection coefficient being plotted, and its angle equal to the phase of the coefficient. Next, a combination of constant-resistance and constant-conductance circles is found, leading from the center of the chart, representing 50Ω, to s^*_{11} and s^*_{22}. The circles on the Smith Chart are constant-resistance circles; increasing series capacitive reactance moves an impedance point counter-clockwise along these circles. In this case, the circle to be used for finding series C is the one passing through the center of the chart, as shown by the solid line in Fig. 6.

Increasing shunt inductive susceptance moves impedance points clockwise along constant-conductance circles. These circles are like the constant-resistance circles, but they are on another Smith Chart, this one being just the reverse of the one in Fig. 6. The constant-conductance circles for shunt L all pass through the leftmost point of the chart rather than the rightmost point. The circles to be used are those passing through s^*_{11} and s^*_{22}, as shown by the dashed lines in Fig. 6.

Once these circles have been located, the normalized values of L and C needed for the matching networks are calculated from readings taken from the reactance and susceptance scales of the Smith Charts. Each element's reactance or susceptance is the difference between the scale readings at the two end points of a circular arc. Which arc corresponds to which element is indicated in Fig. 6. The final network and the element values, normalized and unnormalized, are shown in Fig. 7.

Broadband Amplifier Design

Designing a broadband amplifier, that is, one which has nearly constant gain over a prescribed frequency range, is a matter of surrounding a transistor with external elements in order to compensate for the variation of forward gain $|s_{21}|$ with frequency. This can be done in either of two ways — first, negative feedback, or second, selective mismatching of the input and output circuitry. We will use the second method. When feedback is used, it is usually convenient to convert to y- or z-parameters (for shunt or series feedback respectively) using the conversion equations given in the table, p. 12, and a digital computer.

Equation 24 for the unilateral transducer power gain can be factored into three parts:

$$G_{Tu} = G_o G_1 G_2$$

where

$$G_o = |s_{21}|^2$$

$$G_1 = \frac{1 - |\Gamma_s|^2}{|1 - s_{11}\Gamma_s|^2}$$

$$G_2 = \frac{1 - |\Gamma_L|^2}{|1 - s_{22}\Gamma_L|^2} .$$

When a broadband amplifier is designed by selective mismatching, the gain contributions of G_1 and G_2 are varied to compensate for the variations of $G_o = |s_{21}|^2$ with frequency.

Suppose that the 2N3478 transistor whose s-parameters are given in Fig. 4 is to be used in a broadband amplifier which has a constant gain of 10 dB over a frequency range of 300 MHz to 700 MHz. The amplifier is to be driven from a 50Ω source and is to drive a 50Ω load. According to Fig. 5,

$$|s_{21}|^2 = 13 \text{ dB at } 300 \text{ MHz}$$
$$= 10 \text{ dB at } 450 \text{ MHz}$$
$$= 6 \text{ dB at } 700 \text{ MHz}.$$

To realize an amplifier with a constant gain of 10 dB, source and load matching networks must be found which will decrease the gain by 3 dB at 300 MHz, leave the gain the same at 450 MHz, and increase the gain by 4 dB at 700 MHz.

Although in the general case both a source matching network and a load matching network would be designed, $G_{1\,max}$ (i.e., G_1 for $\Gamma_S = s^*_{11}$) for this transistor is less than 1 dB over the frequencies of interest, which means there is little to be gained by matching the source. Consequently, for this example, only a load-matching network will be designed. Procedures for designing source-matching networks are identical to those used for designing load-matching networks.

The first step in the design is to plot s^*_{22} over the required frequency range on the Smith Chart, Fig. 8. Next, a set of constant-gain circles is drawn. Each circle is drawn for a single frequency; its center is on a line between the center of the Smith Chart and the point representing s^*_{22} at that frequency. The distance from the center of the Smith Chart to the center of the constant gain circle is given by (these equations also appear in the table, p. 11):

$$r_2 = \frac{g_2|s_{22}|}{1 - |s_{22}|^2(1 - g_2)}$$

where

$$g_2 = \frac{G_2}{G_{2\,max}} = G_2(1 - |s_{22}|^2).$$

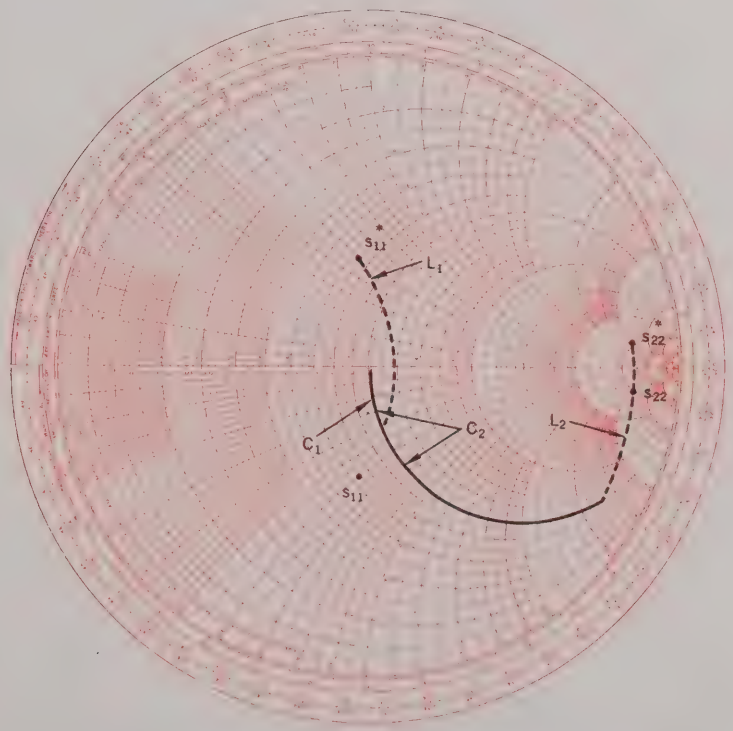

Fig. 6. *Smith Chart for 300-MHz amplifier design example.*

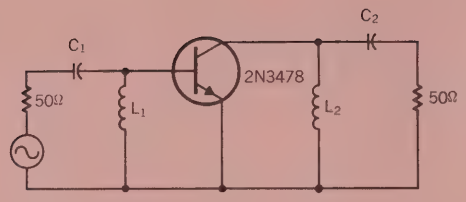

Calculations:

$$X_{L2} = \frac{50}{0.32} = 156\ \Omega$$

$$L_2 = \frac{156}{2\pi\ (0.3 \times 10^9)} = 83\ \text{nH}$$

$$C_2 = \frac{1}{2\pi\ (0.3 \times 10^9)\ (3.5)\ (50)} = 3\ \text{pF}$$

$$C_1 = \frac{3\ (3.5)}{0.42}\ \text{pF} = 25\ \text{pF}$$

$$L_1 = \frac{50}{1.01}\ \text{nH} = 26\ \text{nH}$$

Fig. 7. *300-MHz amplifier with matching networks for maximum power gain.*

The radius of the constant-gain circle is

$$\rho_2 = \frac{\sqrt{1 - g_2}\,(1 - |s_{22}|^2)}{1 - |s_{22}|^2\,(1 - g_2)}.$$

For this example, three circles will be drawn, one for $G_2 = -3$ dB at 300 MHz, one for $G_2 = 0$ dB at 450 MHz, and one for $G_2 = +4$ dB at 700 MHz. Since $|s_{22}|$ for this transistor is constant at 0.85 over the frequency range [see Fig. 4(b)], $G_{2\,max}$ for all three circles is $(0.278)^{-1}$, or 5.6 dB. The three constant-gain circles are indicated in Fig. 8.

The required matching network must transform the center of the Smith Chart, representing 50Ω, to some point on the −3 dB circle at 300 MHz, to some point on the 0 dB circle at 450 MHz, and to some point on the +4 dB circle at 700 MHz. There are undoubtedly many networks that will do this. One which is satisfactory is a combination of two inductors, one in shunt and one in series, as shown in Fig. 9.

Shunt and series elements move impedance points on the Smith Chart along constant-conductance and constant-resistance circles, as I explained in the narrow-band design example which preceded this broadband example. The shunt inductance transforms the 50Ω load along a circle of constant conductance and varying (with frequency) inductive susceptance. The series inductor transforms the combination of the 50Ω load and the shunt inductance along circles of constant resistance and varying inductive reactance.

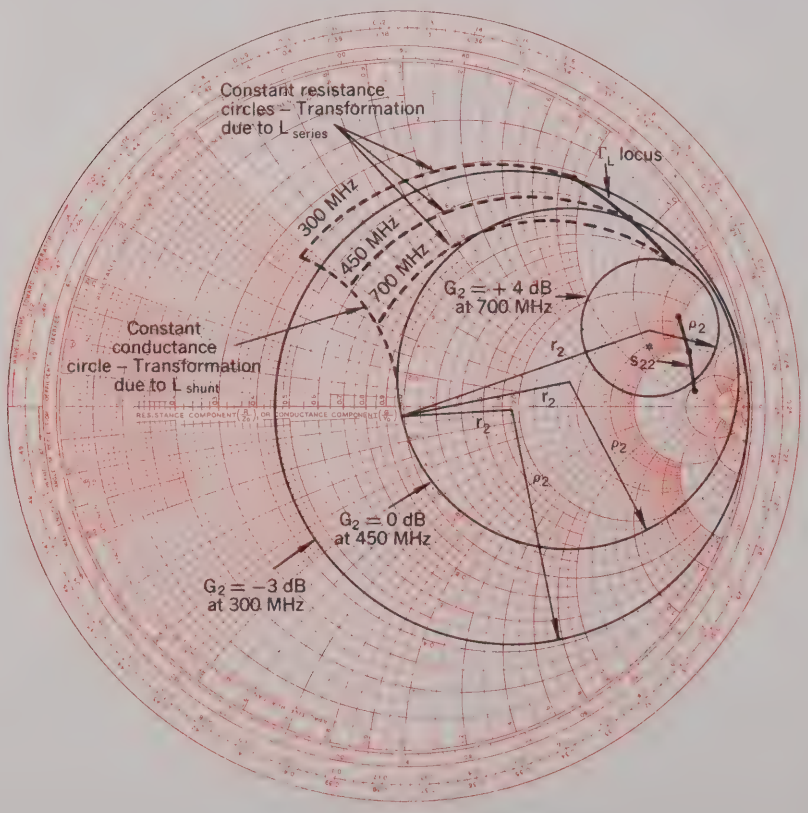

Fig. 8. *Smith Chart for broadband amplifier design example.*

Optimizing the values of shunt and series L is a cut-and-try process to adjust these elements so that

—the transformed load reflection terminates on the right gain circle at each frequency, and

—the susceptance component decreases with frequency and the reactance component increases with frequency. (This rule applies to inductors; capacitors would behave in the opposite way.)

Once appropriate constant-conductance and constant-resistance circles have been found, the reactances and susceptances of the elements can be read directly from the Smith Chart. Then the element values are calculated, the same as they were for the narrow-band design.

Fig. 10 is a schematic diagram of the completed broadband amplifier, with unnormalized element values.

Stability Considerations and the Design of Reflection Amplifiers and Oscillators

When the real part of the input impedance of a network is negative, the corresponding input reflection coefficient (equation 17) is greater than one, and the network can be used as the basis for two important types of circuits, reflection amplifiers and oscillators. A reflection amplifier (Fig. 11) can be realized with a circulator—a nonreciprocal three-port device — and a negative-resistance device. The circulator is used to separate the incident (input) wave from the larger wave reflected by the negative-resistance device. Theoretically, if the circulator is perfect and has a positive real characteristic impedance Z_o, an amplifier with infinite gain can be built by selecting a negative-resistance device whose input impedance has a real part equal to $-Z_o$ and an imaginary part equal to zero (the imaginary part can be set equal to zero by tuning, if necessary).

Amplifiers, of course, are not supposed to oscillate, whether they are reflection amplifiers or some other kind. There is a convenient criterion based upon scattering parameters for determining whether a device is stable or potentially unstable with given source and load impedances. Referring again to the flow graph of Fig. 3, the ratio of the reflected voltage wave b_1 to the input voltage wave b_s is

$$\frac{b_1}{b_s} = \frac{s'_{11}}{1 - \Gamma_s s'_{11}}$$

where s'_{11} is the input reflection coefficient with $\Gamma_s = 0$ (that is, $Z_s = Z_o$) and an arbitrary load impedance Z_L, as defined in equation 19.

If at some frequency

$$\Gamma_s s'_{11} = 1 \qquad (25)$$

the circuit is unstable and will oscillate at that frequency. On the other hand, if

$$|s'_{11}| < \left|\frac{1}{\Gamma_s}\right|$$

the device is unconditionally stable and will not oscillate, whatever the phase angle of Γ_s might be.

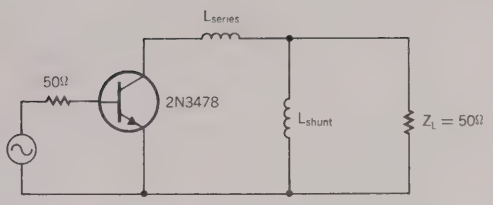

Fig. 9. *Combination of shunt and series inductances is suitable matching network for broadband amplifier.*

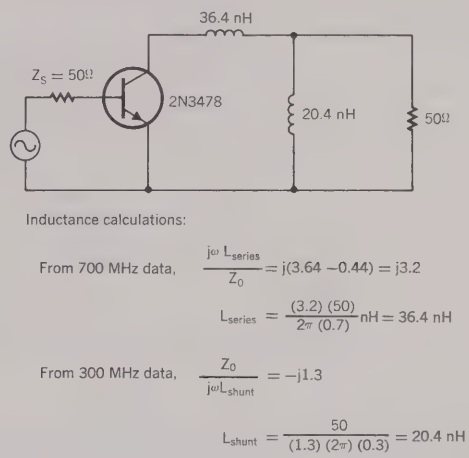

Fig. 10. *Broadband amplifier with constant gain of 10 dB from 300 MHz to 700 MHz.*

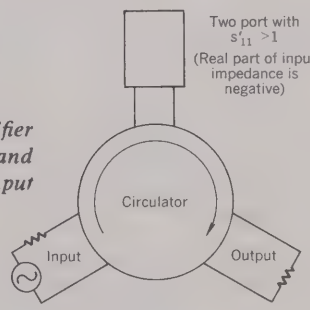

Fig. 11. *Reflection amplifier consists of circulator and transistor with negative input resistance.*

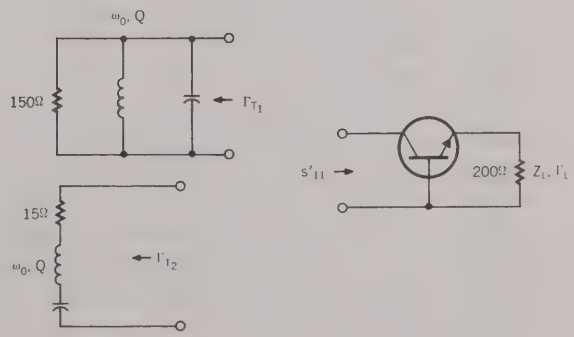

Fig. 12. *Transistor oscillator is designed by choosing tank circuit such that* $\Gamma_T s'_{11} = 1$.

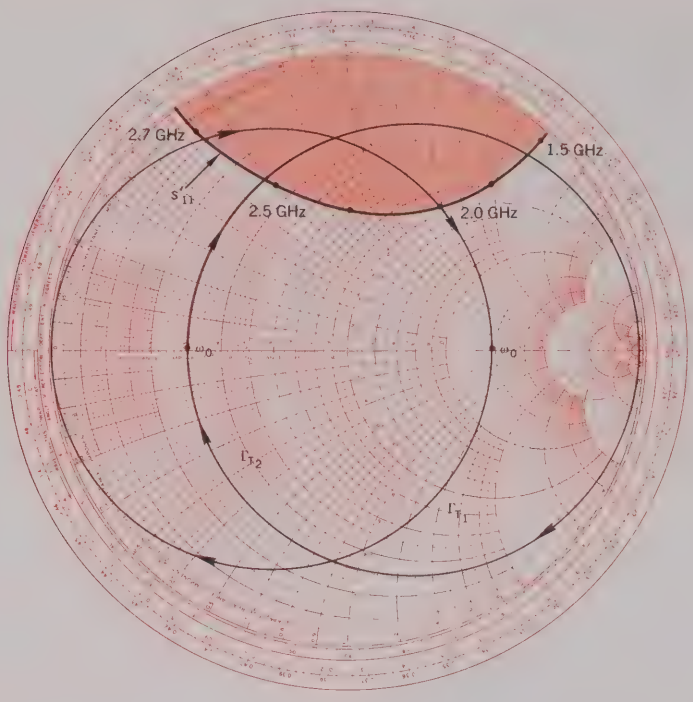

Fig. 13. *Smith Chart for transistor oscillator design example.*

As an example of how these principles of stability are applied in design problems, consider the transistor oscillator design illustrated in Fig. 12. In this case the input reflection coefficient s'_{11} is the reflection coefficient looking into the collector circuit, and the 'source' reflection coefficient Γ_S is one of the two tank-circuit reflection coefficients, Γ_{T1} or Γ_{T2}. From equation 19,

$$s'_{11} = s_{11} + \frac{s_{12}\, s_{21}\, \Gamma_L}{1 - s_{22}\, \Gamma_L}$$

To make the transistor oscillate, s'_{11} and Γ_S must be adjusted so that they satisfy equation 25. There are four steps in the design procedure:

—Measure the four scattering parameters of the transistor as functions of frequency.

—Choose a load reflection coefficient Γ_L which makes s'_{11} greater than unity. In general, it may also take an external feedback element which increases $s_{12}\, s_{21}$ to make s'_{11} greater than one.

—Plot $1/s'_{11}$ on a Smith Chart. (If the new network analyzer is being used to measure the s-parameters of the transistor, $1/s'_{11}$ can be measured directly by reversing the reference and test channel connections between the reflection test unit and the harmonic frequency converter. The polar display with a Smith Chart overlay will then give the desired plot immediately.)

—Connect either the series or the parallel tank circuit to the collector circuit and tune it so that Γ_{T1} or Γ_{T2} is large enough to satisfy equation 25 (the tank circuit reflection coefficient plays the role of Γ_S in this equation).

Fig. 13 shows a Smith Chart plot of $1/s'_{11}$ for a high-frequency transistor in the common-base configuration. Load impedance Z_L is 200Ω, which means that Γ_L referred to 50Ω is 0.6. Reflection coefficients Γ_{T1} and Γ_{T2} are also plotted as functions of the resonant frequencies of the two tank circuits. Oscillations occur when the locus of Γ_{T1} or Γ_{T2} passes through the shaded region. Thus this transistor would oscillate from 1.5 to 2.5 GHz with a series tuned circuit and from 2.0 to 2.7 GHz with a parallel tuned circuit.

—Richard W. Anderson

Additional Reading on S-Parameters

Besides the papers referenced in the footnotes of the article, the following articles and books contain information on s-parameter design procedures and flow graphs.

—F. Weinert, 'Scattering Parameters Speed Design of High-Frequency Transistor Circuits,' Electronics, Vol. 39, No. 18, Sept. 5, 1966.

—G. Fredricks, 'How to Use S-Parameters for Transistor Circuit Design,' EEE, Vol. 14, No. 12, Dec., 1966.

—D. C. Youla, 'On Scattering Matrices Normalized to Complex Port Numbers,' Proc. IRE, Vol. 49, No. 7, July, 1961.

—J. G. Linvill and J. F. Gibbons, 'Transistors and Active Circuits,' McGraw-Hill, 1961. (No s-parameters, but good treatment of Smith Chart design methods.)

Useful Scattering Parameter Relationships

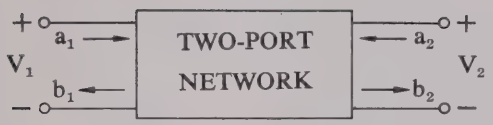

$$b_1 = s_{11}a_1 + s_{12}a_2$$

$$b_2 = s_{21}a_1 + s_{22}a_2$$

Input reflection coefficient with arbitrary Z_L

$$s'_{11} = s_{11} + \frac{s_{12}s_{21}\Gamma_L}{1 - s_{22}\Gamma_L}$$

Output reflection coefficient with arbitrary Z_S

$$s'_{22} = s_{22} + \frac{s_{12}s_{21}\Gamma_S}{1 - s_{11}\Gamma_S}$$

Voltage gain with arbitrary Z_L and Z_S

$$A_V = \frac{V_2}{V_1} = \frac{s_{21}(1 + \Gamma_L)}{(1 - s_{22}\Gamma_L)(1 + s'_{11})}$$

$$\text{Power Gain} = \frac{\text{Power delivered to load}}{\text{Power input to network}}$$

$$G = \frac{|s_{21}|^2(1 - |\Gamma_L|^2)}{(1 - |s_{11}|^2) + |\Gamma_L|^2(|s_{22}|^2 - |D|^2) - 2\,\mathrm{Re}\,(\Gamma_L N)}$$

$$\text{Available Power Gain} = \frac{\text{Power available from network}}{\text{Power available from source}}$$

$$G_A = \frac{|s_{21}|^2(1 - |\Gamma_S|^2)}{(1 - |s_{22}|^2) + |\Gamma_S|^2(|s_{11}|^2 - |D|^2) - 2\,\mathrm{Re}\,(\Gamma_S M)}$$

$$\text{Transducer Power Gain} = \frac{\text{Power delivered to load}}{\text{Power available from source}}$$

$$G_T = \frac{|s_{21}|^2(1 - |\Gamma_S|^2)(1 - |\Gamma_L|^2)}{|(1 - s_{11}\Gamma_S)(1 - s_{22}\Gamma_L) - s_{12}s_{21}\Gamma_L\Gamma_S|^2}$$

Unilateral Transducer Power Gain ($s_{12} = 0$)

$$G_{Tu} = \frac{|s_{21}|^2(1 - |\Gamma_S|^2)(1 - |\Gamma_L|^2)}{|1 - s_{11}\Gamma_S|^2\,|1 - s_{22}\Gamma_L|^2}$$

$$= G_0 G_1 G_2$$

$$G_0 = |s_{21}|^2$$

$$G_1 = \frac{1 - |\Gamma_S|^2}{|1 - s_{11}\Gamma_S|^2}$$

$$G_2 = \frac{1 - |\Gamma_L|^2}{|1 - s_{22}\Gamma_L|^2}$$

Maximum Unilateral Transducer Power Gain when $|s_{11}| < 1$ and $|s_{22}| < 1$

$$G_u = \frac{|s_{21}|^2}{|(1 - |s_{11}|^2)(1 - |s_{22}|)^2|}$$

$$= G_o\, G_{1\,\max}\, G_{2\,\max}$$

$$G_{i\,\max} = \frac{1}{1 - |s_{ii}|^2} \qquad i = 1, 2$$

This maximum attained for $\Gamma_S = s^*_{11}$ and $\Gamma_L = s^*_{22}$

Constant Gain Circles (Unilateral case: $s_{12} = 0$)

—center of constant gain circle is on line between center of Smith Chart and point representing s^*_{ii}

—distance of center of circle from center of Smith Chart:

$$r_i = \frac{g_i|s_{ii}|}{1 - |s_{ii}|^2(1 - g_i)}$$

—radius of circle:

$$\rho_i = \frac{\sqrt{1 - g_i}\,(1 - |s_{ii}|^2)}{1 - |s_{ii}|^2(1 - g_i)}$$

where: $i = 1, 2$

$$\text{and } g_i = \frac{G_i}{G_{i\,\max}} = G_i(1 - |s_{ii}|^2)$$

Unilateral Figure of Merit

$$u = \frac{|s_{11}s_{22}s_{12}s_{21}|}{|(1 - |s_{11}|^2)(1 - |s_{22}|^2)|}$$

Error Limits on Unilateral Gain Calculation

$$\frac{1}{(1 + u^2)} < \frac{G_T}{G_{Tu}} < \frac{1}{(1 - u^2)}$$

Conditions for Absolute Stability

No passive source or load will cause network to oscillate if a, b, and c are all satisfied.

a. $|s_{11}| < 1, |s_{22}| < 1$

b. $\left| \dfrac{|s_{12}s_{21}| - |M^*|}{|s_{11}|^2 - |D|^2} \right| > 1$

c. $\left| \dfrac{|s_{12}s_{21}| - |N^*|}{|s_{22}|^2 - |D|^2} \right| > 1$

Condition that a two-port network can be simultaneously matched with a positive real source and load:

$K > 1$ or $C < 1$

C = Linvill C factor

Linvill C Factor

$$C = K^{-1}$$

$$K = \frac{1 + |D|^2 - |s_{11}|^2 - |s_{22}|^2}{2\,|s_{12}s_{21}|}$$

Source and Load for Simultaneous Match

$$\Gamma_{mS} = M^* \left[\frac{B_1 \pm \sqrt{B_1^2 - 4\,|M|^2}}{2\,|M|^2} \right]$$

$$\Gamma_{mL} = N^* \left[\frac{B_2 \pm \sqrt{B_2^2 - 4\,|N|^2}}{2\,|N|^2} \right]$$

Where $B_1 = 1 + |s_{11}|^2 - |s_{22}|^2 - |D|^2$

$B_2 = 1 + |s_{22}|^2 - |s_{11}|^2 - |D|^2$

Maximum Available Power Gain

If $K > 1$,

$$G_{A\,max} = \left| \frac{s_{21}}{s_{12}} (K \pm \sqrt{K^2 - 1}) \right|$$

$K = C^{-1}$

C = Linvill C Factor

(Use minus sign when B_1 is positive, plus sign when B_1 is negative. For definition of B_1 see 'Source and Load for Simultaneous Match,' elsewhere in this table.)

$$D = s_{11}s_{22} - s_{12}s_{21}$$

$$M = s_{11} - D\,s^*_{22}$$

$$N = s_{22} - D\,s^*_{11}$$

s-parameters in terms of h-, y-, and z-parameters	h-, y-, and z-parameters in terms of s-parameters
$s_{11} = \dfrac{(z_{11}-1)(z_{22}+1) - z_{12}z_{21}}{(z_{11}+1)(z_{22}+1) - z_{12}z_{21}}$	$z_{11} = \dfrac{(1+s_{11})(1-s_{22}) + s_{12}s_{21}}{(1-s_{11})(1-s_{22}) - s_{12}s_{21}}$
$s_{12} = \dfrac{2z_{12}}{(z_{11}+1)(z_{22}+1) - z_{12}z_{21}}$	$z_{12} = \dfrac{2s_{12}}{(1-s_{11})(1-s_{22}) - s_{12}s_{21}}$
$s_{21} = \dfrac{2z_{21}}{(z_{11}+1)(z_{22}+1) - z_{12}z_{21}}$	$z_{21} = \dfrac{2s_{21}}{(1-s_{11})(1-s_{22}) - s_{12}s_{21}}$
$s_{22} = \dfrac{(z_{11}+1)(z_{22}-1) - z_{12}z_{21}}{(z_{11}+1)(z_{22}+1) - z_{12}z_{21}}$	$z_{22} = \dfrac{(1+s_{22})(1-s_{11}) + s_{12}s_{21}}{(1-s_{11})(1-s_{22}) - s_{12}s_{21}}$
$s_{11} = \dfrac{(1-y_{11})(1+y_{22}) + y_{12}y_{21}}{(1+y_{11})(1+y_{22}) - y_{12}y_{21}}$	$y_{11} = \dfrac{(1+s_{22})(1-s_{11}) + s_{12}s_{21}}{(1+s_{11})(1+s_{22}) - s_{12}s_{21}}$
$s_{12} = \dfrac{-2y_{12}}{(1+y_{11})(1+y_{22}) - y_{12}y_{21}}$	$y_{12} = \dfrac{-2s_{12}}{(1+s_{11})(1+s_{22}) - s_{12}s_{21}}$
$s_{21} = \dfrac{-2y_{21}}{(1+y_{11})(1+y_{22}) - y_{12}y_{21}}$	$y_{21} = \dfrac{-2s_{21}}{(1+s_{11})(1+s_{22}) - s_{12}s_{21}}$
$s_{22} = \dfrac{(1+y_{11})(1-y_{22}) + y_{12}y_{21}}{(1+y_{11})(1+y_{22}) - y_{12}y_{21}}$	$y_{22} = \dfrac{(1+s_{11})(1-s_{22}) + s_{12}s_{21}}{(1+s_{22})(1+s_{11}) - s_{12}s_{21}}$
$s_{11} = \dfrac{(h_{11}-1)(h_{22}+1) - h_{12}h_{21}}{(h_{11}+1)(h_{22}+1) - h_{12}h_{21}}$	$h_{11} = \dfrac{(1+s_{11})(1+s_{22}) - s_{12}s_{21}}{(1-s_{11})(1+s_{22}) + s_{12}s_{21}}$
$s_{12} = \dfrac{2h_{12}}{(h_{11}+1)(h_{22}+1) - h_{12}h_{21}}$	$h_{12} = \dfrac{2s_{12}}{(1-s_{11})(1+s_{22}) + s_{12}s_{21}}$
$s_{21} = \dfrac{-2h_{21}}{(h_{11}+1)(h_{22}+1) - h_{12}h_{21}}$	$h_{21} = \dfrac{-2s_{21}}{(1-s_{11})(1+s_{22}) + s_{12}s_{21}}$
$s_{22} = \dfrac{(1+h_{11})(1-h_{22}) + h_{12}h_{21}}{(h_{11}+1)(h_{22}+1) - h_{12}h_{21}}$	$h_{22} = \dfrac{(1-s_{22})(1-s_{11}) - s_{12}s_{21}}{(1-s_{11})(1+s_{22}) + s_{12}s_{21}}$

The h-, y-, and z-parameters listed above are all normalized to Z_o. If h′, y′, and z′ are the actual parameters, then

$z_{11}' = z_{11}Z_o$	$y_{11}' = \dfrac{y_{11}}{Z_o}$	$h_{11}' = h_{11}Z_o$
$z_{12}' = z_{12}Z_o$	$y_{12}' = \dfrac{y_{12}}{Z_o}$	$h_{12}' = h_{12}$
$z_{21}' = z_{21}Z_o$	$y_{21}' = \dfrac{y_{21}}{Z_o}$	$h_{21}' = h_{21}$
$z_{22}' = z_{22}Z_o$	$y_{22}' = \dfrac{y_{22}}{Z_o}$	$h_{22}' = \dfrac{h_{22}}{Z_o}$

Reprinted Compliments of
Hewlett-Packard Journal
Vol. 18, No. 6 FEB 1967

S. N. Prasad

Application Note 154

S-Parameter Design

HEWLETT hp PACKARD

APRIL 1972

Application Note 154

S-Parameter Design

Introduction

The need for new high frequency solid state circuit design techniques has been recognized both by microwave engineers and circuit designers. These engineers are being asked to design solid state circuits that will operate at higher and higher frequencies.

The development of microwave transistors and Hewlett-Packard's network analysis instrumentation systems that permit complete network characterization in the microwave frequency range have greatly assisted these engineers in their work.

The Hewlett-Packard Microwave Division's lab staff have developed a high frequency circuit design seminar to assist their counterparts in R&D labs throughout the world. This seminar has been presented in a number of locations in the United States and Europe.

From the experience gained in presenting this original seminar, we have developed a four-part video tape "S-Parameter Design Seminar." While the technology of high frequency circuit design is ever changing, the concepts upon which this technology has been built are relatively invariant.

The content of this "S-Parameter Design Seminar" is as follows:

A. S-Parameter Design Techniques—Part I (ID #800586)

1. "Basic Microwave Review—Part I"
   This portion of the seminar contains a review of:
   a) Transmission line theory
   b) S-parameters
   c) The Smith Chart
   d) The frequency response of RL - RC - RLC circuits
2. "Basic Microwave Review—Part II"
   This portion extends the basic concepts to:
   a) Scattering-Transfer or T-parameters
   b) Signal flow graphs
   c) Voltage and power gain relationships
   d) Stability considerations

B. S-Parameter Design Techniques—Part II (ID #800600)

1. "S-Parameter Measurements"
   In this portion, the characteristics of microwave transistors and the network analyzer instrumentation system used to measure these characteristics are explained.
2. "High Frequency Amplifier Design"
   The theory of Constant Gain and Constant Noise Figure Circles is developed in this portion of the seminar. This theory is then applied in the design of three actual amplifier circuits.

The style of this Application Note is somewhat informal since it is a verbatim transcript of these video tape programs.

Much of the material contained in this seminar, and in this Application Note, has been developed in greater detail in standard electrical engineering textbooks, or in other Hewlett-Packard application notes.

The value of this Application Note rests in its bringing together the high frequency circuit design concepts used today in R&D labs throughout the world.

We are confident that Application Note 154 and the video taped "S-Parameter Design Seminar" will assist you as you continue to develop new high frequency circuit designs.

Printed APRIL 1972

Revised May 1973

Chapter I
Basic Microwave Review -- I

Introduction

This first portion of Hewlett-Packard's S-Parameter Design Seminar introduces some fundamental concepts we will use in the analysis and design of high frequency networks.

These concepts are most useful at those frequencies where distributed rather than lumped parameters must be considered. We'll discuss: (1) Scattering or S-parameters, (2) Voltage and power gain relationships as well as (3) Stability criteria for two-port networks in terms of these S-parameters, and (4) Review the Smith Chart.

Network Characterization

S-parameters are basically a means for characterizing n-port networks. By reviewing some traditional network analysis methods we'll understand why an additional method of network characterization is necessary at higher frequencies.

Figure 1

A two-port device (Fig. 1) can be described by a number of parameter sets. We're all familiar with the H, Y, and Z-parameter sets (Fig. 2). All of these network parameters relate total voltages and total currents at each of the two ports. These are the network variables.

H-Parameters

$$V_1 = h_{11}I_1 + h_{12}V_2$$
$$I_2 = h_{21}I_1 + h_{22}V_2$$

Y-Parameters

$$I_1 = y_{11}V_1 + y_{12}V_2$$
$$I_2 = y_{21}V_1 + y_{22}V_2$$

Z-Parameters

$$V_1 = z_{11}I_1 + z_{12}I_2$$
$$V_2 = z_{21}I_1 + z_{22}I_2$$

Figure 2

The only difference in the parameter sets is the choice of independent and dependent variables. The parameters are the constants used to relate these variables.

To see how parameter sets of this type can be determined through measurement, let's focus on the H-parameters. H_{11} is determined by setting V_2 equal to zero—applying a short circuit to the output port of the network. H_{11} is then the ratio of V_1 to I_1—the input impedance of the resulting network. H_{12} is determined by measuring the ratio of V_1 to V_2—the reverse voltage gain—with the input port open circuited (Fig. 3). The important thing to note here is that both open and short circuits are essential for making these measurements.

$$h_{11} = \left.\frac{V_1}{I_1}\right|_{V_2 = 0}$$

$$h_{12} = \left.\frac{V_1}{V_2}\right|_{I_1 = 0}$$

Figure 3

Moving to higher and higher frequencies, some problems arise:

1. Equipment is not readily available to measure total voltage and total current at the ports of the network.
2. Short and open circuits are difficult to achieve over a broad band of frequencies.
3. Active devices, such as transistors and tunnel diodes, very often will not be short or open circuit stable.

Some method of characterization is necessary to overcome these problems. The logical variables to use at these frequencies are **traveling waves** rather than total voltages and currents.

Transmission Lines

Let's now investigate the properties of traveling waves. High frequency systems have a source of power. A portion of this power is delivered to a load by means of transmission lines (Fig. 4).

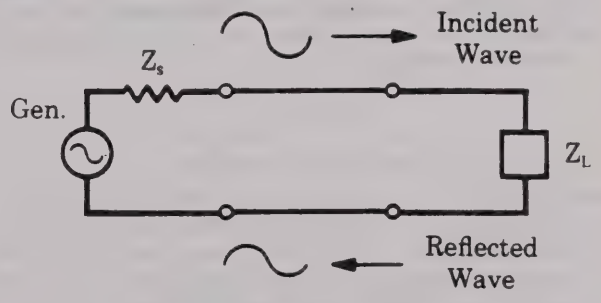

Figure 4

Voltage, current, and power can be considered to be in the form of waves traveling in both directions along this transmission line. A portion of the waves incident on the load will be reflected. It then becomes incident on the source, and in turn re-reflects from the source (if $Z_S \neq Z_0$), resulting in a standing wave on the line.

If this transmission line is uniform in cross section, it can be thought of as having an equivalent series impedance and equivalent shunt admittance per unit length (Fig. 5).

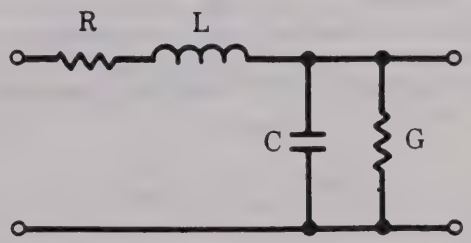

Uniform Transmission Line

Figure 5

A lossless line would simply have a series inductance and a shunt capacitance. The characteristic impedance of the lossless line, Z_o, is defined as $Z_o = \sqrt{L/C}$. At microwave frequencies, most transmission lines have a 50-ohm characteristic impedance. Other lines of 75, 90, and 300-ohm impedance are often used.

Although the general techniques developed in this seminar may be applied for any characteristic impedance, we will be using lossless 50-ohm transmission lines.

We've seen that the incident and reflected voltages on a transmission line result in a standing voltage wave on the line.

The value of this total **voltage** at a given point along the length of the transmission line is the sum of the incident and reflected waves at that point (Fig. 6a).

a) $V_t = E_{inc} + E_{refl.}$

b) $I_t = \dfrac{E_{inc} - E_{refl.}}{Z_o}$

Figure 6

The total **current** on the line is the **difference** between the incident and reflected voltage waves divided by the characteristic impedance of the line (Fig. 6b).

Another very useful relationship is the reflection coefficient, Γ. This is a measure of the quality of the impedance match between the load and the characteristic impedance of the line. The reflection coefficient is a complex quantity having a magnitude, rho, and an angle, theta (Fig. 7a). The better the match between the load and the characteristic impedance of the line, the smaller the reflected voltage wave and the smaller the reflection coefficient.

a) $\Gamma = \rho \angle \Theta$

$= \dfrac{E_{refl.}}{E_{inc.}}$

b) $\Gamma = \dfrac{Z_L - Z_o}{Z_L + Z_o}$

$= \dfrac{Y_o - Y_L}{Y_o + Y_L}$

Figure 7

This can be seen more clearly if we express the reflection coefficient in terms of load impedance or load admittance. The reflection coefficient can be made equal to zero by selecting a load, Z_L, equal to the characteristic impedance of the line (Fig. 7b).

To facilitate computations, we will often want to normalize impedances to the characteristic impedance of the transmission line. Expressed in terms of the reflection coefficient, the normalized impedance has this form (Fig. 8).

$z_N = \dfrac{Z_L}{Z_o}$

$= \dfrac{1 + \Gamma}{1 - \Gamma}$

Figure 8

S-Parameters

Having briefly reviewed the properties of transmission lines, let's insert a two-port network into the line (Fig. 9). We now have additional traveling waves that are interrelated. Looking at E_{r2}, we see that it is made up of that portion of E_{i2} reflected from the output port of the network as well as that portion of E_{i1} that is transmitted through the network. Each of the other waves are similarly made up of a combination of two waves.

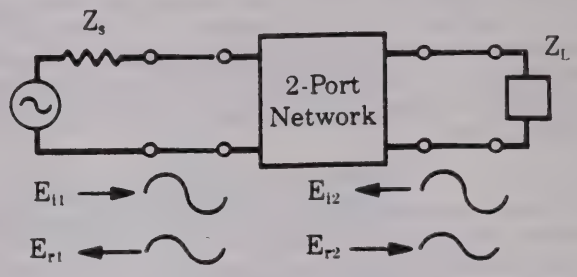

Figure 9

It should be possible to relate these four traveling waves by some parameter set. While the derivation of this parameter set will be made for two-port networks, it is applicable for n-ports as well. Let's start with the H-parameter set (Fig. 10).

H-Parameters

$V_1 = h_{11}I_1 + h_{12}V_2$
$I_2 = h_{21}I_1 + h_{22}V_2$

Figure 10

$V_1 = E_{i1} + E_{r1}$ $\quad$ $V_2 = E_{i2} + E_{r2}$

$I_1 = \dfrac{E_{i1} - E_{r1}}{Z_o}$ $\quad$ $I_2 = \dfrac{E_{i2} - E_{r2}}{Z_o}$

By substituting the expressions for total voltage and total current (Fig. 11) on a transmission line into this parameter set, we can rearrange these equations such that the incident traveling voltage waves are the independent variables; and the reflected traveling voltage waves are the dependent variables (Fig. 12).

$E_{r1} = f_{11}\,(h)\,E_{i1} + f_{12}\,(h)\,E_{i2}$

$E_{r2} = f_{21}\,(h)\,E_{i1} + f_{22}\,(h)\,E_{i2}$

Figure 12

The functions f_{11}, f_{21} and f_{12}, f_{22} represent a new set of network parameters relating traveling voltage waves rather than total voltages and total currents. In this case these functions are expressed in terms of H-parameters. They could have been derived from any other parameter set.

It is appropriate that we call this new parameter set "scattering parameters," since they relate those waves scattered or reflected from the network to those waves incident upon the network. These scattering parameters will commonly be referred to as S-parameters.

Let's go one step further. If we divide both sides of these equations by $\sqrt{Z_o}$, the characteristic impedance of the transmission line, the relationship will not change. It will, however, give us a change in variables (Fig. 13). Let's now define the new variables:

$$a_1 = \frac{E_{i1}}{\sqrt{Z_o}} \qquad a_2 = \frac{E_{i2}}{\sqrt{Z_o}}$$

$$b_1 = \frac{E_{r1}}{\sqrt{Z_o}} \qquad b_2 = \frac{E_{r2}}{\sqrt{Z_o}}$$

Figure 13

Notice that the square of the magnitude of these new variables has the dimension of power. $|a_1|^2$ can then be thought of as the incident power on port one. $|b_1|^2$ as power reflected from port one. These new waves can be called traveling power waves rather than traveling voltage waves. Throughout this seminar, we will simply refer to these waves as **traveling** waves.

Looking at the new set of equations in a little more detail, we see that the S-parameters relate these four waves in this fashion (Fig. 14).

$$b_1 = S_{11}\, a_1 + S_{12}\, a_2$$
$$b_2 = S_{21}\, a_1 + S_{22}\, a_2$$

Figure 14

S-Parameter Measurement

We saw how the H-parameters are measured. Let's now see how we go about measuring the S-parameters. For S_{11}, we terminate the output port of the network and measure the ratio b_1 to a_1 (Fig. 15). Terminating the output port in an impedance equal to the characteristic impedance of the transmission line is equivalent to setting $a_2 = 0$, since a traveling wave incident on this load will be totally absorbed. S_{11} is the input reflection coefficient of the network. Under the same conditions, we can measure S_{21}, the forward transmission through the network. This is the ratio of b_2 to a_1 (Fig. 16). This could either be the gain of an amplifier or the attenuation of a passive network.

$$S_{11} = \left.\frac{b_1}{a_1}\right|_{a_2 = 0}$$

Figure 15

$$S_{21} = \left.\frac{b_2}{a_1}\right|_{a_2 = 0}$$

Figure 16

By terminating the input side of the network, we set $a_1 = 0$. S_{22}, the output reflection coefficient, and S_{12}, the reverse transmission coefficient, can then be measured (Fig. 17).

$$S_{22} = \left.\frac{b_2}{a_2}\right|_{a_1 = 0}$$

$$S_{12} = \left.\frac{b_1}{a_2}\right|_{a_1 = 0}$$

Figure 17

A question often arises about the terminations used when measuring the S-parameters. Since the transmission line is terminated in the characteristic impedance of the line, does the network port have to be matched to that impedance as well? The answer is no!

To see why, let's look once again at the network enmeshed in the transmission line (Fig. 18). If the load impedance is equal to the characteristic impedance of the line, any wave traveling toward the load would be totally absorbed by the load. It would not reflect back to the network. This sets $a_2 = 0$. This condition is completely independent from the network's output impedance.

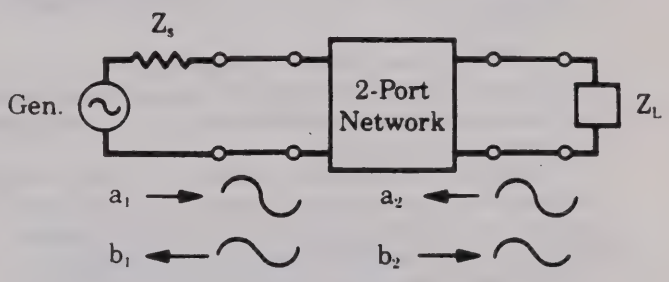

If: $Z_L = Z_0$, $a_2 = 0$

Figure 18

Multiple-Port Networks

So far we have just discussed two-port networks. These concepts can be expanded to multiple-port networks. To characterize a three-port network, for example, nine parameters would be required (Fig. 19). S_{11}, the input reflection coefficient at port one, is measured by terminating the second and third ports with an impedance equal to the characteristic impedance of the line at these ports. This again ensures that $a_2 = a_3 = 0$. We could go through the remaining S-parameters and measure them in a similar way, once the other two ports are properly terminated.

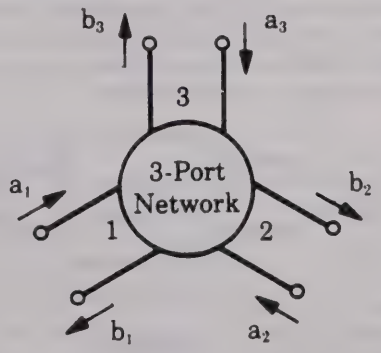

$$S_{11} = \left.\frac{b_1}{a_1}\right|_{a_2 = a_3 = 0}$$

Figure 19

What is true for two- and three-port networks is similarly true for n-port networks (Fig. 20). The number of measurements required for characterizing these more complex networks goes up as the square of the number of ports. The concept and method of parameter measurement, however, is the same.

$$\begin{bmatrix} b_1 \\ b_2 \\ \cdot \\ \cdot \\ \cdot \\ b_N \end{bmatrix} = \begin{bmatrix} S_{11} & S_{12} & \cdots & S_{1N} \\ S_{21} & S_{22} & \cdots & S_{2N} \\ \cdot & \cdot & & \cdot \\ \cdot & \cdot & & \cdot \\ \cdot & \cdot & & \cdot \\ S_{N1} & S_{N2} & \cdots & S_{NN} \end{bmatrix} \begin{bmatrix} a_1 \\ a_2 \\ \cdot \\ \cdot \\ \cdot \\ a_N \end{bmatrix}$$

Figure 20

Let's quickly review what we've done up to this point. We started off with a familiar network parameter set relating total voltages and total currents at the ports of the network. We then reviewed some transmission line concepts. Applying these concepts, we derived a new set of parameters for a two-port network relating the incident and reflected traveling waves at the network ports.

The Use of S-Parameters

To gain further insight into the use of S-parameters, let's see how some typical networks can be represented in terms of S-parameters.

A **reciprocal network** is defined as having identical transmission characteristics from port one to port two or from port two to port one (Fig. 21). This implies that the S-parameter matrix is equal to its transpose. In the case of a two-port network, $S_{12} = S_{21}$.

$$S = \tilde{S}$$
$$S_{ij} = S_{ji}$$

Figure 21

A **lossless network** does not dissipate any power. The power incident on the network must be equal to the power reflected or $\Sigma |a_n|^2 = \Sigma |b_n|^2$ (Fig. 22). In the case of a two-port, $|a_1|^2 + |a_2|^2 = |b_1|^2 + |b_2|^2$. This implies that the S-matrix is unitary as defined here. Where: I is the identity matrix and S* is the complex conjugate of the transpose of S. This is generally referred to as the hermetian conjugate of S. Typically, we will be using lossless networks when we want to place matching networks between amplifier stages.

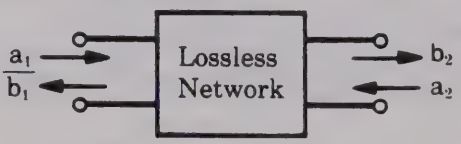

$$I - S^* S = 0$$

Figure 22

For a **lossy network,** the net power reflected is less than the net incident power (Fig. 23). The difference is the power dissipated in the network. This implies that the statement $I - S^* S$ is positive definite, or the eigenvalues for this matrix are in the left half plane so that the impulse response of the network is made up of decaying exponentials.

$$\Sigma |b_i|^2 < \Sigma |a_i|^2$$

$$I - S^* S > 0$$

Figure 23

Change in Reference Plane

Another useful relationship is the equation for changing reference planes. We often need this in the measurement of transistors and other active devices where, due to device size, it is impractical to attach RF connectors to the actual device terminals.

Imbedding the device in the transmission line structure, we can then measure the S-parameters at these two planes (Fig. 24). We've added a length of line, ϕ_1, to port one of the device and another length, ϕ_2, to port two.

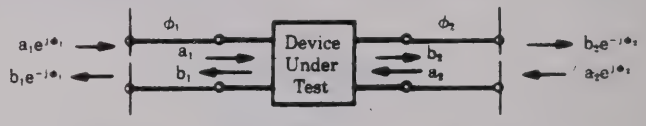

$$S' = \Phi S \Phi$$

$$\text{where: } \Phi = \begin{bmatrix} e^{-j\phi_1} & 0 \\ 0 & e^{-j\phi_2} \end{bmatrix}$$

Figure 24

The S-parameter matrix, S′, measured at these two planes is related to the S-parameter matrix of the device, S, by this expression. We've simply pre-multiplied and post-multiplied the device's S-parameter matrix by the diagonal matrix, Φ .

To see what's happening here, let's carry through the multiplication of the S_{11} term. It will be multiplied by $e^{-j\phi_1}$ twice, since a_1 travels through this length of line, ϕ_1, and gets reflected and then travels through it again (Fig. 25). The transmission term, S'_{21}, would have this form, since the input wave, a_1, travels through ϕ_1 and the transmitted wave, b_2, through ϕ_2. From the measured S-parameters, S′, we can then determine the S-parameters of the device, S, with this relationship (Fig. 26).

$$S'_{11} = S_{11}\, e^{-j2\phi_1}$$

$$S'_{21} = S_{21}\, e^{-j(\phi_1 + \phi_2)}$$

Figure 25

$$S = \Phi^{-1} S' \Phi^{-1}$$

Figure 26

Analysis of Networks Using S-Parameters

Let's now look at a simple example which will demonstrate how S-parameters can be determined analytically.

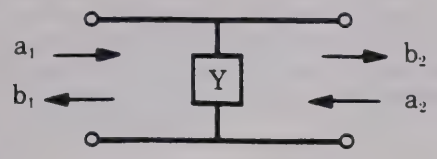

Figure 27

Using a shunt admittance, we see the incident and reflected waves at the two ports (Fig. 27). We first normalize the admittance and terminate the network in the normalized characteristic admittance of the system (Fig. 28a). This sets $a_2 = 0$. S_{11}, the input reflection coefficient of the terminated network, is then: (Fig. 28b).

To calculate S_{21}, let's recall that the total voltage at the input of a shunt element, $a_1 + b_1$, is equal to the total voltage at the output, $a_2 + b_2$ (Fig. 28c). Since the network is symmetrical and reciprocal, $S_{22} = S_{11}$ and $S_{12} = S_{21}$. We have then determined the four S-parameters for a shunt element.

a)

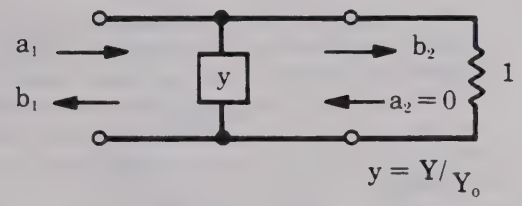

b) $$S_{11} = \frac{1 - y_T}{1 + y_T} = \frac{-y}{y + 2}$$

c) $$S_{21} = \frac{b_2}{a_1}\bigg|_{a_2 = 0} = \frac{a_1 + b_1}{a_1}\bigg|_{a_2 = 0} = 1 - \frac{y}{y + 2}$$

Figure 28

The Smith Chart

Another basic tool used extensively in amplifier design will now be reviewed. Back in the thirties, Phillip Smith, a Bell Lab engineer, devised a graphical method for solving the oft-repeated equations appearing in microwave theory. Equations like the one for reflection coefficient, $\Gamma = (Z - 1) / (Z + 1)$. Since all the values in this equation are complex numbers, the tedious task of solving this expression could be reduced by using Smith's graphical technique. The Smith Chart was a natural name for this technique.

This chart is essentially a mapping between two planes—the Z or impedance plane and the Γ or reflection coefficient plane. We're all familiar with the impedance plane—a rectangular coordinate plane having a real and an imaginary axis. Any impedance can be plotted in this plane. For this discussion, we'll normalize the impedance plane to the characteristic impedance (Fig. 29a).

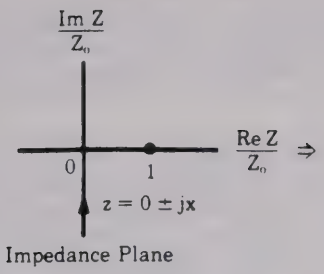

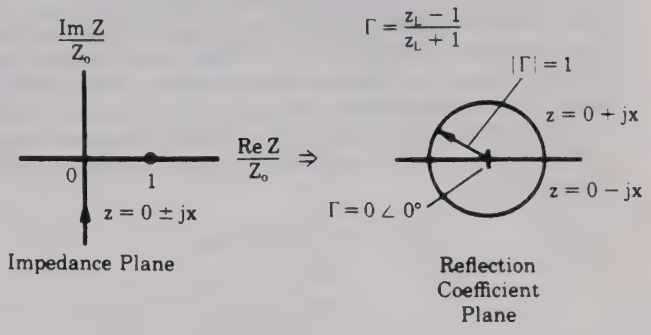

Figure 29

Let's pick out a few values in this normalized plane and see how they map into the Γ plane. Let $z = 1$. In a 50-ohm system, this means $Z = 50$ ohms. For this value, $|\Gamma| = 0$, the center of the Γ plane.

We now let z be purely imaginary; i.e., $z = jx$ where x is allowed to vary from minus infinity to plus infinity. Since $\Gamma = (jx - 1) / (jx + 1)$, $|\Gamma| = 1$ and its phase angle varies from 0 to 360°. This traces out a circle in the Γ plane (Fig. 29b). For positive reactance, jx positive, the impedance maps into the upper half circle. For negative reactance, the impedance maps into the lower half circle. The upper region is inductive and the lower region is capacitive.

Now let's look at some other impedance values. A constant resistance line, going through the point $z = 1$ on the real axis, maps into a circle in the Γ plane. The upper semicircle represents an impedance of $1 + jx$, which is inductive; the lower semicircle, an impedance of $1 - jx$ or capacitive (Fig. 30).

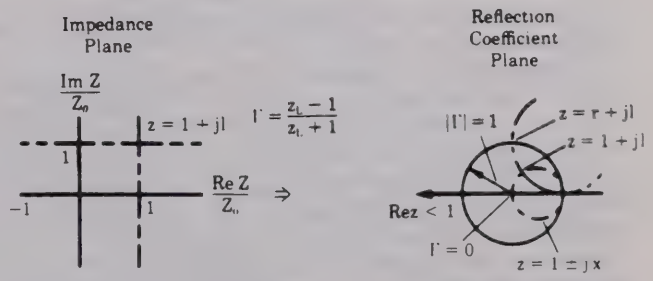

Figure 30

The constant reactance line, r + j1, also maps into the Γ plane as a circle. As we approach the imaginary axis in the impedance plane, Γ approaches the unit radius circle. As we cross the imaginary axis, the constant reactance circle in the Γ plane goes outside the unit radius circle.

If we now go back and look at z real, we see at $z = -1$, $\Gamma = \infty$. When z is real and less than one, we move out toward the unit radius circle in the Γ plane. When the real part of z goes negative, Γ continues along this circle of infinite radius. The entire region outside the unit radius circle represents impedances with negative real parts. We will use this fact later when working with transistors and other active devices which often have negative real impedances.

In the impedance plane, constant resistance and constant reactance lines intersect. They also cross in the Γ plane. There is a one-to-one correspondence between points in the impedance plane and points in the Γ plane.

The Smith Chart can be completed by continuing to draw other constant resistance and reactance circles (Fig. 31).

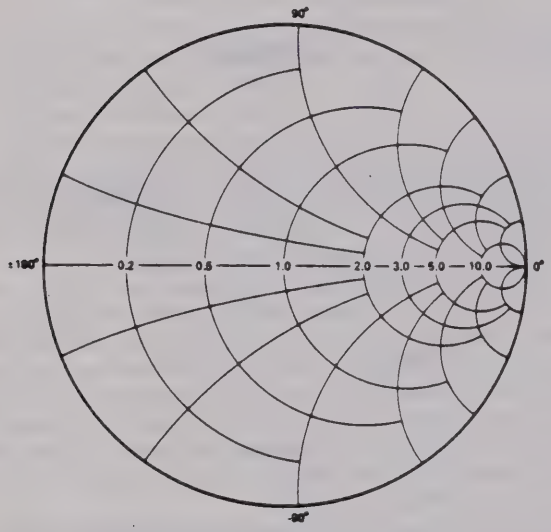

Figure 31

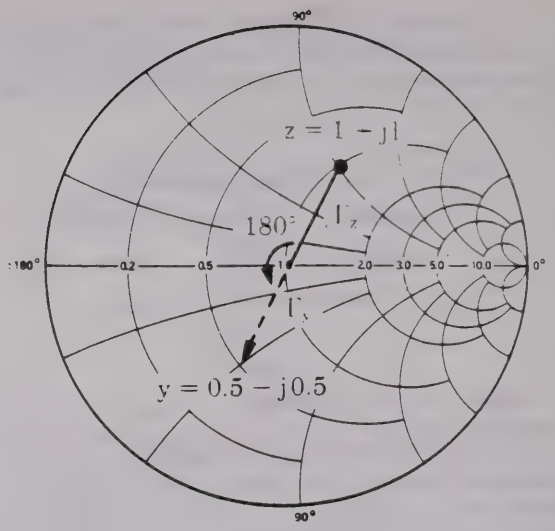

$$\Gamma_z = \frac{z-1}{z+1} \qquad \Gamma_y = \frac{1-y}{1+y} \qquad |y| = \frac{1}{|z|}$$

$$|\Gamma_z| = |\Gamma_y|$$

Figure 32

We can approach this impedance to admittance conversion in another way. Rather than rotate the Γ vector by 180°, we could rotate the Smith Chart by 180° (Fig. 33). We can call the rotated chart an admittance chart and the original an impedance chart. Now we can convert any impedance to admittance, or vice versa, directly.

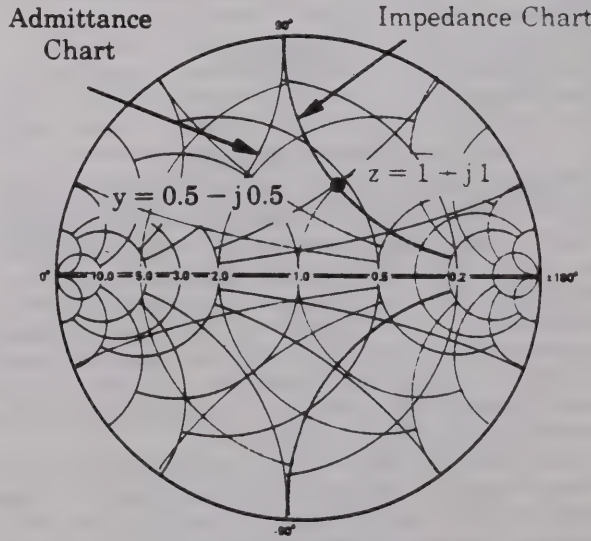

Figure 33

Applications of the Smith Chart

Let's now try a few examples with the Smith Chart to illustrate its usefulness.

1. **Conversion of impedance to admittance:** Converting a normalized impedance of 1 + j1 to an admittance can be accomplished quite easily. Let's first plot the point representing the value of z on the Smith Chart (Fig. 32). From these relationships, we see that while the magnitude of admittance is the reciprocal of the magnitude of impedance, the magnitude of Γ is the same—but its phase angle is changed by 180°. On the Smith Chart, the Γ vector would rotate through 180°. This point could then be read off as an admittance.

2. **Impedances with negative real parts:** Let's now take a look at impedances with negative real parts. Here again is a conventional Smith Chart defined by the boundary of the unit radius circle. If we have an impedance that is inductive with a negative real part, it would map into the Γ plane outside the chart (Fig. 34). One way to bring this point back onto the chart would be to plot the reciprocal of Γ, rather than Γ itself. This would be inconvenient since the phase angle would not be preserved. What was a map of an inductive impedance appears to be capacitive.

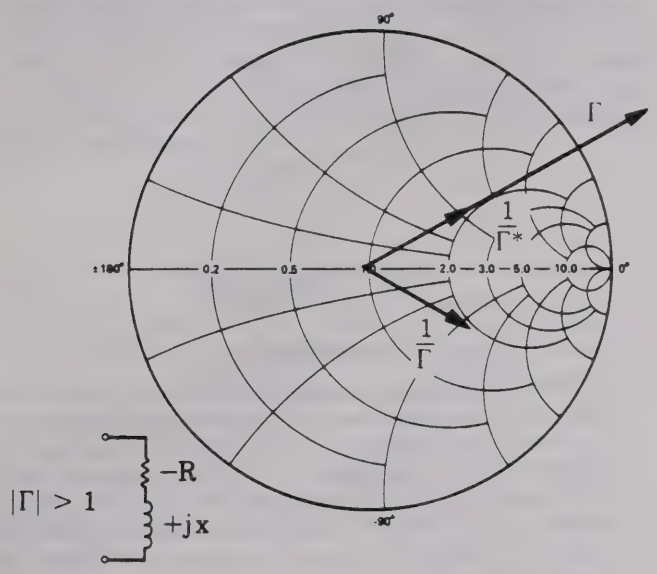

Figure 34

If we plot the reciprocal of the complex conjugate of Γ, however, the phase angle is preserved. This value lies along the same line as the original Γ. Typically in the Hewlett-Packard transistor data sheets, impedances of this type are plotted this way.

There are also compressed Smith Charts available that include the unit radius chart plus a great deal of the negative impedance region. This chart has a radius which corresponds to a reflection coefficient whose magnitude is 3.16 (Fig. 35).

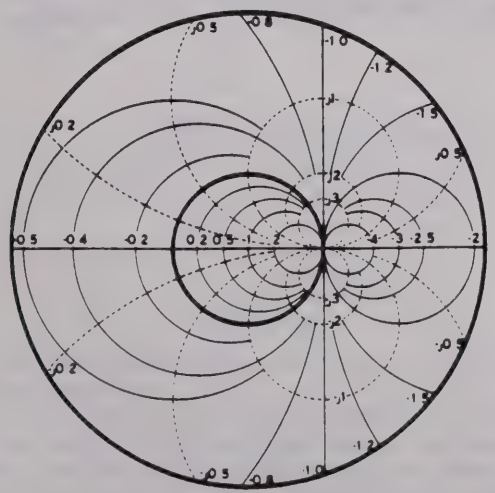

Figure 35

In the rest of this seminar, we will see how easily we can convert measured reflection coefficient data to impedance information by slipping a Smith Chart overlay over the Hewlett-Packard network analyzer polar display.

3. **Frequency response of networks:** One final point needs to be covered in this brief review of the Smith Chart and that is the frequency response for a given network. Let's look at a network having an impedance, $z = 0.4 + jx$ (Fig. 36). As we increase the frequency of the input signal, the impedance plot for the network moves clockwise along a constant resistance circle whose value is 0.4. This generally clockwise movement with increasing frequency is typical of impedance plots on the Smith Chart for passive networks. This is essentially Foster's Reactance Theorem.

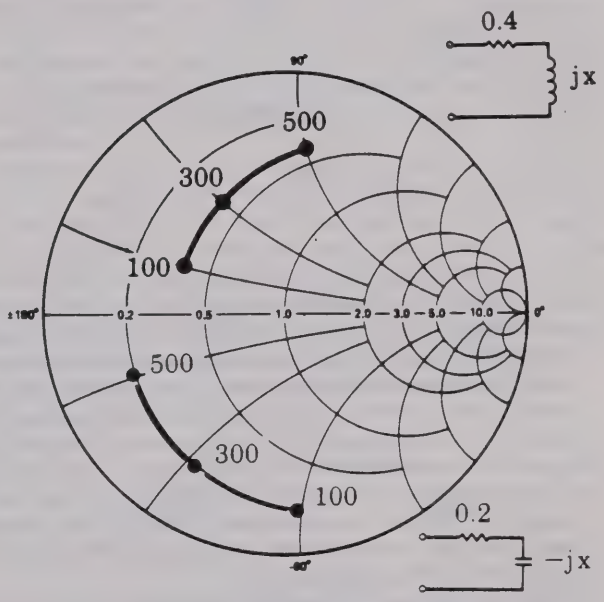

Figure 36

If we now look at another circuit having a real part of 0.2 and an imaginary part that is capacitive, the impedance plot again moves in a clockwise direction with an increase in frequency.

Another circuit that is often encountered is the tank circuit. Here again, the Smith Chart is useful for plotting the frequency response (Fig. 37). For this circuit at zero frequency, the inductor is a short circuit. We start our plot at the point, $z = 0$. As the frequency increases, the inductive reactance predominates. We move in a clockwise direction. At resonance, the impedance is purely real, having the value of the resistor. If the resistor had a higher value, the cross-over point at resonance would be farther to the right on the Smith Chart. As the frequency continues to increase, the response moves clockwise into the capacitive region of the Smith Chart until we reach infinite frequency, where the impedance is again zero.

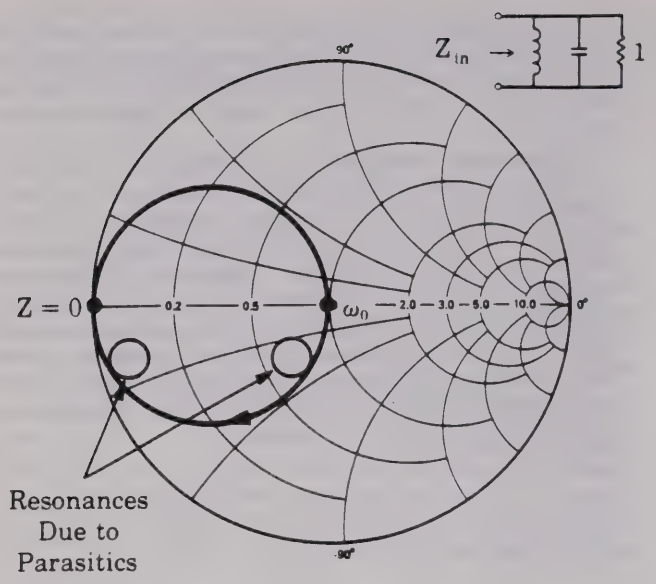

Figure 37

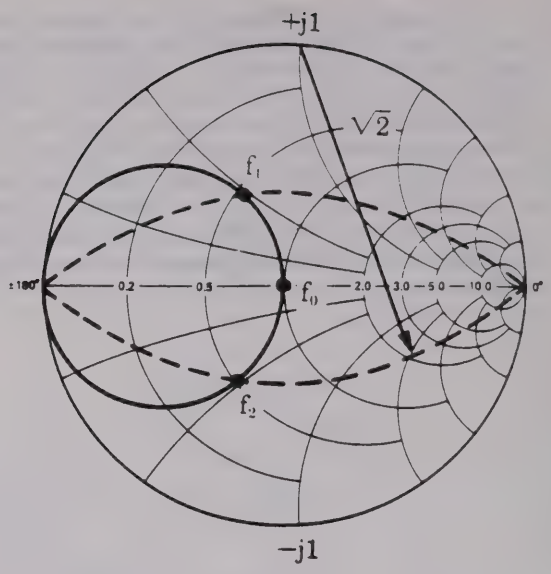

$$Q = \frac{f_0}{f_2 - f_1}$$

Figure 38

In theory, this complete response for a tank circuit would be a circle. In practice, since we do not generally have elements that are pure capacitors or pure inductors over the entire frequency range, we would see other little loops in here that indicate other resonances. These could be due to parasitic inductance in the capacitor or parasitic capacitance in the inductor. The diameter of these circles is somewhat indicative of the Q of the circuit. If we had an ideal tank circuit, the response would be the outer circle on the Smith Chart. This would indicate an infinite Q.

Hewlett-Packard Application Note 117-1 describes other possible techniques for measuring the Q of cavities and YIG spheres using the Smith Chart. One of these techniques uses the fact that with a tank circuit, the real part of the circuit equals the reactive part at the half-power points. Let's draw two arcs connecting these points on the Smith Chart (Fig. 38). The centers for these arcs are at ±j1. The radius of the arcs is $\sqrt{2}$.

We then increase the frequency and record its value where the response lies on the upper arc. Continuing to increase the frequency, we record the resonant frequency and the frequency where the response lies on the lower arc. The formula for the Q of the circuit is simply f_0, the resonant frequency, divided by the difference in frequency between the upper and lower half-power points. $Q = f_0/\Delta f$.

Summary

Let's quickly review what we've seen with the Smith Chart. It is a mapping of the impedance plane and the reflection coefficient or Γ plane. We discovered that impedances with positive real parts map inside the unit radius circle on the Smith Chart. Impedances with negative real parts map outside this unit radius circle. Impedances having positive real parts and inductive reactance map into the upper half of the Smith Chart. Those with capacitive reactance map into the lower half.

In the next part of this S-Parameter Design Seminar, we will continue our discussion of network analysis using S-parameters and flow graph techniques.

Chapter II
Basic Microwave Review -- II

This second portion of Hewlett-Packard's Basic Microwave Review will introduce some additional concepts that are used in high frequency amplifier design.

Scattering Transfer Parameters

Let's now proceed to a set of network parameters used when cascading networks. We recall that we developed the S-parameters by defining the reflected waves as dependent variables, and incident waves as independent variables (Fig. 39a). We now want to rearrange these equations such that the input waves a_1 and b_1 are the dependent variables and the output waves a_2 and b_2 the independent variables. We'll call this new parameter set scattering transfer parameters or T-parameters (Fig. 39b).

a)

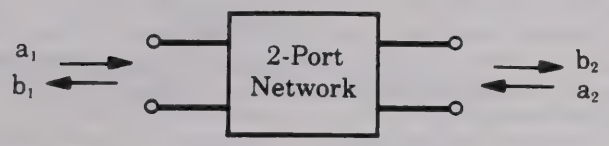

$$\begin{bmatrix} b_1 \\ b_2 \end{bmatrix} = \begin{bmatrix} S_{11} & S_{12} \\ S_{21} & S_{22} \end{bmatrix} \begin{bmatrix} a_1 \\ a_2 \end{bmatrix}$$

b)

$$\begin{bmatrix} b_1 \\ a_1 \end{bmatrix} = \begin{bmatrix} T_{11} & T_{12} \\ T_{21} & T_{22} \end{bmatrix} \begin{bmatrix} a_2 \\ b_2 \end{bmatrix}$$

Figure 39

The T-parameters can be developed by manipulating the S-parameter equations into the appropriate form. Notice that the denominator of each of these terms is S_{21} (Fig. 40).

$$\begin{bmatrix} T_{11} & T_{12} \\ T_{21} & T_{22} \end{bmatrix} = \begin{bmatrix} -\dfrac{S_{11}S_{22} - S_{12}S_{21}}{S_{21}} & \dfrac{S_{11}}{S_{21}} \\ -\dfrac{S_{22}}{S_{21}} & \dfrac{1}{S_{21}} \end{bmatrix}$$

$$\begin{bmatrix} S_{11} & S_{12} \\ S_{21} & S_{22} \end{bmatrix} = \begin{bmatrix} \dfrac{T_{12}}{T_{22}} & \dfrac{T_{11}T_{22} - T_{12}T_{21}}{T_{22}} \\ \dfrac{1}{T_{22}} & -\dfrac{T_{21}}{T_{22}} \end{bmatrix}$$

Figure 40

We can also find the S-parameters as a function of the T-parameters.

While we defined the T-parameters in a particular way, we could have defined them such that the **output** waves are the dependent variables and the **input** waves are the independent variables. This alternate definition can result in some problems when designing with active unilateral devices (Fig. 41).

$$[T_A] = \begin{bmatrix} \dfrac{S_{12}S_{21} - S_{11}S_{22}}{S_{12}} & \dfrac{S_{22}}{S_{12}} \\ -\dfrac{S_{11}}{S_{12}} & \dfrac{1}{S_{12}} \end{bmatrix}$$

Figure 41

Using the alternate definition for the transfer parameters, the denominator in each of these terms is S_{12} rather than S_{21} as we saw earlier.

Working with amplifiers, we often assume the device to be unilateral, or $S_{12} = 0$. This would cause this alternate T-parameter set to go to infinity.

Both of these definitions for T-parameters can be encountered in practice. In general, we prefer to define the T-parameters with the output waves as the dependent variables, and the input waves as the independent variables.

We use this new set of transfer parameters when we want to cascade networks—two stages of an amplifier, or an amplifier with a matching network for example (Fig. 42a). From measured S-parameter data, we can define the T-parameters for the two networks. Since the output waves of the first network are identical to the input waves of the second network, we can now simply multiply the two T-parameter matrices and arrive at a set of equations for the overall network (Fig. 42b).

a)

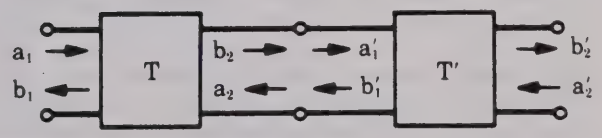

b) $\begin{bmatrix} b_1 \\ a_1 \end{bmatrix} = \begin{bmatrix} T_{11} & T_{12} \\ T_{21} & T_{22} \end{bmatrix} \begin{bmatrix} a_2 \\ b_2 \end{bmatrix}$ and $\begin{bmatrix} b'_1 \\ a'_1 \end{bmatrix} = \begin{bmatrix} T'_{11} & T'_{12} \\ T'_{21} & T'_{22} \end{bmatrix} \begin{bmatrix} a'_2 \\ b'_2 \end{bmatrix}$

but $\begin{bmatrix} a_2 \\ b_2 \end{bmatrix} = \begin{bmatrix} b'_1 \\ a'_1 \end{bmatrix}$

Therefore $\begin{bmatrix} b_1 \\ a_1 \end{bmatrix} = \begin{bmatrix} T_{11} & T_{12} \\ T_{21} & T_{22} \end{bmatrix} \begin{bmatrix} T'_{11} & T'_{12} \\ T'_{21} & T'_{22} \end{bmatrix} \begin{bmatrix} a'_2 \\ b'_2 \end{bmatrix}$

Figure 42

Since matrix multiplication is, in general, not commutative, these T-parameter matrices must be multiplied in the proper order. When cascading networks, we'll have to multiply the matrices in the same order as the networks are connected. Using the alternate definition for T-parameters, previously described, this matrix multiplication must be done in reverse order.

This transfer parameter set becomes very useful when using computer-aided design techniques where matrix multiplication is an easy task.

Signal Flow Graphs

If we design manually, however, we can use still another technique—signal flow graphs—to follow incident and reflected waves through the networks. This is a comparatively new technique for microwave network analysis.

A. Rules

We'll follow certain rules when we build up a network flow graph.

1. Each variable, a_1, a_2, b_1, and b_2 will be designated as a node.
2. Each of the S-parameters will be a branch.
3. Branches enter dependent variable nodes, and emanate from the independent variable nodes.
4. In our S-parameter equations, the reflected waves b_1 and b_2 are the dependent variables and the incident waves a_1 and a_2 are the independent variables.
5. Each node is equal to the sum of the branches entering it.

Let's now apply these rules to the two S-parameter equations (Fig. 43a). The first equation has three nodes —b_1, a_1, and a_2. B_1 is a dependent node and is connected to a_1 through the branch S_{11} and to node a_2 through the branch S_{12}. The second equation is constructed similarly. We can now overlay these to have a complete flow graph for a two-port network (Fig. 43b).

a)

$$b_1 = S_{11}\, a_1 + S_{12}\, a_2$$

$$b_2 = S_{21}\, a_1 + S_{22}\, a_2$$

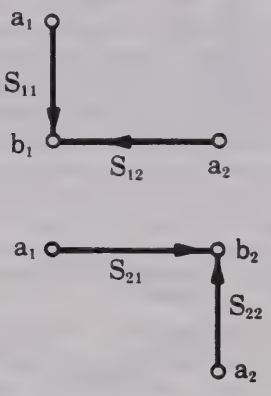

b) Complete Flow Graph for 2-Port

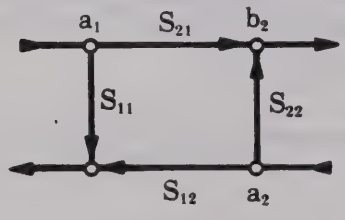

Figure 43

The relationship between the traveling waves is now easily seen. We have a_1 incident on the network. Part of it transmits through the network to become part of b_2. Part of it is reflected to become part of b_1. Meanwhile, the a_2 wave entering port two is transmitted through the network to become part of b_1 as well as being reflected from port two as part of b_2. By merely following the arrows, we can tell what's going on in the network.

This technique will be all the more useful as we cascade networks or add feedback paths.

B. Application of Flow Graphs

Let's now look at several typical networks we will encounter in amplifier designs. A **generator** with some internal voltage source and an internal impedance will have a wave emanating from it. The flow graph for the generator introduces a new term, b_s (Fig. 44). It's defined by the impedance of the generator. The units in this equation look peculiar, but we have to remember that we originally normalized the traveling waves to $\sqrt{Z_0}$. The magnitude of b_s squared then has the dimension of power.

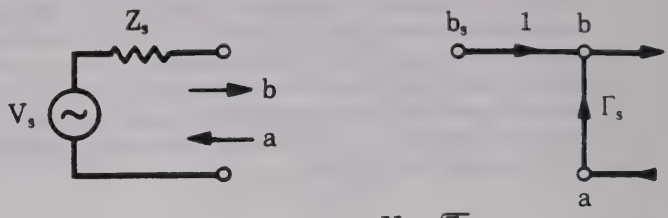

$$b_s = \frac{V_s\sqrt{Z_0}}{Z_s + Z_0}$$

Figure 44

For a **load,** the flow graph is simply Γ_L, the complex reflection coefficient of the load (Fig. 45).

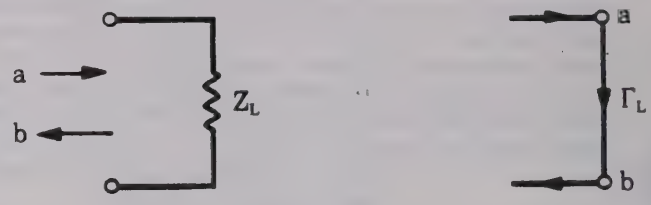

Figure 45

When the load is connected to the generator, we see a wave emanating from the generator incident on the load and a wave reflected back to the generator from the load (Fig. 46).

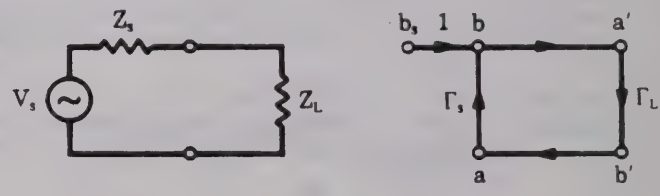

Figure 46

To demonstrate the utility of flow graphs, let's embed a two-port network between a source and a load. Combining the examples we have seen, we can now draw a flow graph for the system (Fig. 47).

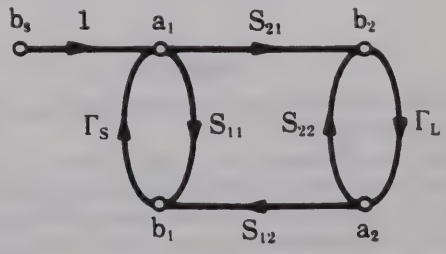

Figure 47

We can now apply the rule known as Mason's rule—or as it is often called, the non-touching loop rule—to solve for the value of any node in this network. Before applying the rule, however, we must first define several additional terms.

A **first order** loop is defined as the product of the branches encountered in a journey starting from a node and moving in the direction of the arrows back to that original node. To illustrate this, let's start at node a_1. One first order loop is $S_{11}\Gamma_s$. Another first order loop is $S_{21}\Gamma_L S_{12}\Gamma_s$. If we now start at node a_2, we find a third first order loop—$S_{22}\Gamma_L$. Any of the other loops we encounter is one of these three first order loops.

A **second order loop** is defined as the product of any two non-touching first order loops. Of the three first order loops just found, only $S_{11}\Gamma_s$ and $S_{22}\Gamma_L$ do not touch in any way. The product of these two loops establishes the second order loop for this network. More complicated networks involving feedback paths, for example, might have several second order loops.

A **third order loop** is the product of any three non-touching first order loops. This example does not have any third order loops but again more complicated networks would have third order loops and even higher order loops.

Let's now suppose that we are interested in the value of b_1. In this example, b_s is the only independent variable since its value will determine the value of each of the other variables in the network. B_1, therefore, will be a function of b_s. To determine b_1, we first have to identify the paths leading from b_s to b_1. Following the arrows, we see two paths—(1) S_{11} and (2) $S_{21}\Gamma_L S_{12}$.

The next step is to find the non-touching loops with respect to the paths just found. Here, the path S_{11} and the first order loop, $S_{22}\Gamma_L$, have no nodes or branches in common. With this condition met, we can call $S_{22}\Gamma_L$ a non-touching loop with respect to the path S_{11}.

The other path, $S_{21}\Gamma_L S_{12}$, touches all of the network's first order loops, hence there are no non-touching loops with respect to this path. Again, in more complex networks, there would be higher order non-touching loops.

Let's now look at the non-touching loop rule itself (Fig. 48). This equation appears to be rather ominous at first glance, but once we go through it term by term, it will be less awesome. This rule determines the ratio of two variables, a dependent to an independent variable. (In our example, we are interested in the ratio b_1 to b_s.)

$$T = \frac{P_1[1 - \Sigma L(1)^{(1)} + \Sigma L(2)^{(1)} - \ldots] + P_2[1 - \Sigma L(1)^{(2)} \ldots}{1 - \Sigma L(1) + \Sigma L(2) - \Sigma L(3) + \ldots}$$

$$T = \frac{b_1}{b_s}$$

Figure 48

P_1, P_2, etc., are the various paths connecting these variables.

This term, $\Sigma L(1)^{(1)}$, is the sum of all first order loops that do not touch the first path between the variables.

This term, $\Sigma L(2)^{(1)}$, is the sum of all second order loops that do not touch that path, and so on down the line.

Now, this term, $\Sigma L(1)^{(2)}$, is the sum of all first order loops that do not touch the second path.

The denominator in this expression is a function of the network geometry. It is simply one minus the sum of all first order loops, plus the sum of all second order loops, minus the third order loops, and so on.

Let's now apply this non-touching loop rule to our network (Fig. 49). The ratio of b_1, the dependent variable, to b_s, the independent variable, is equal to the first path, S_{11}, multiplied by one minus the non-touching first order loop with respect to this path, $\Gamma_L S_{22}$.

$$\frac{b_1}{b_s} = \frac{S_{11}(1 - \Gamma_L S_{22}) + S_{21}\Gamma_L S_{12}(1)}{1 - (S_{11}\Gamma_s + S_{22}\Gamma_L + S_{21}\Gamma_L S_{12}\Gamma_s) + S_{11}\Gamma_s S_{22}\Gamma_L}$$

Figure 49

The second path, $S_{21}\Gamma_L S_{12}$, is simply multiplied by one since there are no non-touching loops with respect to this path.

The denominator is one minus the sum of first order loops plus the second order loop.

This concludes our example. With a little experience drawing flow graphs of complex networks, you can see how this technique will facilitate your network analysis. In fact, using the flow graph technique, we can now derive several expressions for power and gain that are of interest to the circuit designer.

First of all, we need to know the **power delivered to a load.** We remember that the square of the magnitudes of the incident and reflected waves has the dimension of power. The power delivered to a load is then the difference between the incident power and the reflected power, $P_{del} = |a|^2 - |b|^2$.

The **power available from a source** is **that** power delivered to a conjugately matched load. This implies that the reflection coefficient of the load is the conjugate of the source reflection coefficient—$\Gamma_s^* = \Gamma_L$.

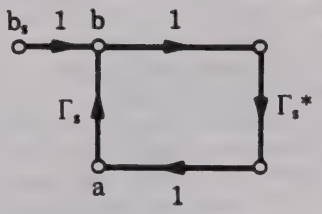

Figure 50

Looking at the flow graph describing these conditions (Fig. 50), we see that the power available from the source is:

$$P_{avs} = |b|^2 - |a|^2$$

Using the flow graph techniques previously described, we see that:

$$b = \frac{b_s}{1 - \Gamma_s\Gamma_s^*} \quad \text{and} \quad a = \frac{b_s\Gamma_s^*}{1 - \Gamma_s\Gamma_s^*} .$$

The power available from the source reduces to (Fig. 51):

$$P_{avs} = \frac{|b_s|^2}{1 - |\Gamma_s|^2}$$

Figure 51

We can also develop voltage and power gain equations that will be useful in our amplifier designs using these flow graph techniques. For a two-port network, the **voltage gain** is equal to the total voltage at the output divided by the total voltage at the input,

$$A_v = \frac{a_2 + b_2}{a_1 + b_1}$$

If we divide the numerator and denominator by b_s, we can relate each of the dependent variables of the system to the one independent variable (Fig. 52a). Now we have four expressions or four ratios that we can determine from the non-touching loop rule.

a)
$$A_v = \frac{\frac{a_2}{b_s} + \frac{b_2}{b_s}}{\frac{a_1}{b_s} + \frac{b_1}{b_s}} = \frac{S_{21}\Gamma_L + S_{21}}{1(1 - S_{22}\Gamma_L) + S_{11}(1 - S_{22}\Gamma_L) + S_{21}\Gamma_L S_{12}}$$

b)

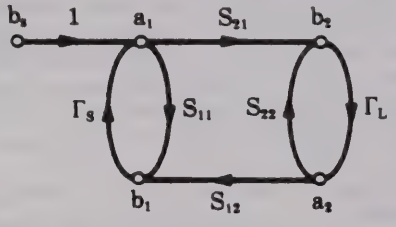

Figure 52

We can simplify this derivation by remembering that the denominator in the expression for the non-touching loop rule is a function of the network geometry. It will be the same for each of these ratios, and will cancel out in the end. So we only need to be concerned with the numerators of these ratios.

Let's trace through a couple of these expressions to firm up our understanding of the process (Fig. 52b). A_2 is connected to b_s through the path $S_{21}\Gamma_L$. All first order loops touch this path, so this path is simply multiplied by one. B_2 is connected to b_s through the path S_{21}. All first order loops also touch this path. A_1 is connected to b_s directly, and there is one non-touching loop, $S_{22}\Gamma_L$. We have already determined the ratio of b_1 to b_s, so we can simply write down the numerator of that expression. We have now derived the voltage gain of the two-port network.

The last expression we wish to develop is that for **transducer power gain.** This will be very important in the amplifier design examples contained in the final section of this seminar. Transducer power gain is defined as the power delivered to a load divided by the power available from a source.

$$G_t = \frac{P_{del}}{P_{avs}}$$

We have already derived these two expressions.

$$G_t = \frac{b_2{}^2(1 - \Gamma_L{}^2)}{b_s{}^2(1 - \Gamma_s{}^2)}$$

What remains is to solve the ratio b_2 to b_s (Fig. 53a). The only path connecting b_s and b_2 is S_{21}. There are no non-touching loops with respect to this path. The denominator is the same as in the previous example: one minus the first order loops plus the second order loop. Taking the magnitude of this ratio, squaring and substituting the result yields the expression for transducer power gain of a two-port network (Fig. 53b).

a)
$$\frac{b_2}{b_s} = \frac{S_{21}}{1 - S_{11}\Gamma_s - S_{22}\Gamma_L - S_{21}S_{12}\Gamma_L\Gamma_s + S_{11}\Gamma_s S_{22}\Gamma_L}$$

b)
$$G_T = \frac{|S_{21}|^2(1 - |\Gamma_s|^2)(1 - |\Gamma_L|^2)}{|(1 - S_{11}\Gamma_s)(1 - S_{22}\Gamma_L) - S_{21}S_{12}\Gamma_L\Gamma_s|^2}$$

Figure 53

Needless to say, this is not a simple relationship since the terms are generally complex quantities. Calculator or computer routines will greatly facilitate the circuit designer's task.

Later, when designing amplifiers, we will see that we can simplify this expression by assuming that the amplifier is a unilateral device or $S_{12} = 0$. In general, however, this assumption cannot be made and we will be forced to deal with this expression.

One of the things you might want to do is to optimize or maximize the transducer gain of the network. Since the S-parameters at one frequency are constants depending on the device selected and the bias conditions, we have to turn our attention to the source and load reflection coefficients.

Stability Considerations

To maximize the transducer gain, we must conjugately match the input and the output. Before we do this, we will have to look at what might happen to the network in terms of stability—will the amplifier oscillate with certain values of impedance used in the matching process?

There are two traditional expressions used when speaking of stability: conditional and unconditional stability.

A network is **conditionally stable** if the real part of Z_{in} and Z_{out} is greater than zero for **some** positive real source and load impedances at a specific frequency.

A network is **unconditionally stable** if the real part of Z_{in} and Z_{out} is greater than zero for **all** positive real source and load impedances at a specific frequency.

It is important to note that these two conditions apply only at **one** specific frequency. The conditions we will now discuss will have to be investigated at many frequencies to ensure broadband stability. Going back to our Smith Chart discussion, we recall that positive real source and load impedances implies:

$$|\Gamma_s| \text{ and } |\Gamma_L| \leq 1$$

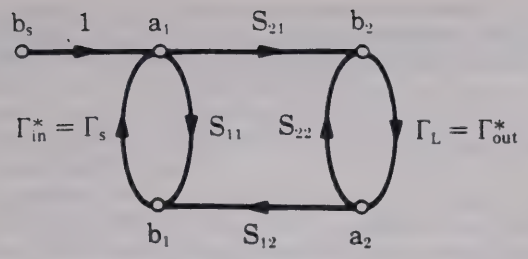

Figure 54

Let's look first at the condition where we want to conjugately match the network to the load and source to achieve maximum transducer gain (Fig. 54). Under these conditions, we can say that the network will be stable if this factor, K, is greater than one (Fig. 55). Conjugately matched conditions mean that the reflection coefficient of the source, Γ_s, is equal to the conjugate of the input reflection coefficient, Γ_{in}

$$\Gamma_s = \Gamma_{in}^*$$

Γ_L is equal to the conjugate of the output reflection coefficient, Γ_{out}

$$\Gamma_L = \Gamma_{out}^*$$

$$K = \frac{1 + |S_{11}S_{22} - S_{12}S_{21}|^2 - |S_{11}|^2 - |S_{22}|^2}{2|S_{12}||S_{21}|} > 1$$

Figure 55

A **precaution** must be mentioned here. The K factor must not be considered alone. If we were operating under matched conditions in order to achieve maximum gain, we have to ask ourselves: (1) What effect would temperature changes or drifting S-parameters of the transistor have on the stability of the amplifier? (2) We would also have to be concerned with the effect on stability as we substitute transistors into the circuit. (3) Would these changing conditions affect the conjugate match or the stability of the amplifier? Therefore, we really need to consider these other conditions in addition to the K factor.

Looking at the input and output reflection coefficient equations, we see a similarity of form (Fig. 56). The only difference is that S_{11} replaces S_{22} and Γ_L replaces Γ_s.

$$\Gamma_{in} = \frac{b_1}{a_1} = S_{11} + \frac{S_{21}S_{12}\Gamma_L}{1 - S_{22}\Gamma_L}$$

$$\Gamma_{out} = \frac{b_2}{a_2} = S_{22} + \frac{S_{21}S_{12}\Gamma_s}{1 - S_{11}\Gamma_s}$$

Figure 56

If we set this equation, Γ_{in}, equal to one, a boundary would be established. On one side of the boundary, we would expect

$$\Gamma_{in} < 1$$

On the other side, we would expect

$$\Gamma_{in} > 1$$

Let's first find the boundary by solving this expression (Fig. 57). We insert the real and imaginary values for the S-parameters and solve for Γ_L.

$$|\Gamma_{in}| = \left| S_{11} + \frac{S_{21}S_{12}\Gamma_L}{1 - S_{22}\Gamma_L} \right| = 1$$

Figure 57

The solutions for Γ_L will lie on a circle. The radius of the circle will be given by this expression as a function of S-parameters (Fig. 58a).

a) $$\text{radius} = r_L = \left| \frac{S_{12}S_{21}}{|S_{22}|^2 - |\Delta|^2} \right|$$

b) $$\text{center} = C_L = \frac{(S_{22} - \Delta S_{11}^*)^*}{|S_{22}|^2 - |\Delta|^2}$$

$$\text{where: } \Delta = S_{11}S_{22} - S_{12}S_{21}$$

Figure 58

The center of the circle will have this form (Fig. 58b). Having measured the S-parameters of a two-port device at one frequency, we can calculate these quantities.

If we now plot these values on a Smith Chart, we can determine the locus of all values of Γ_L that make

$$|\Gamma_{in}| = 1$$

This circle then represents the boundary (Fig. 59). The area either inside or outside the circle will represent a stable operating condition.

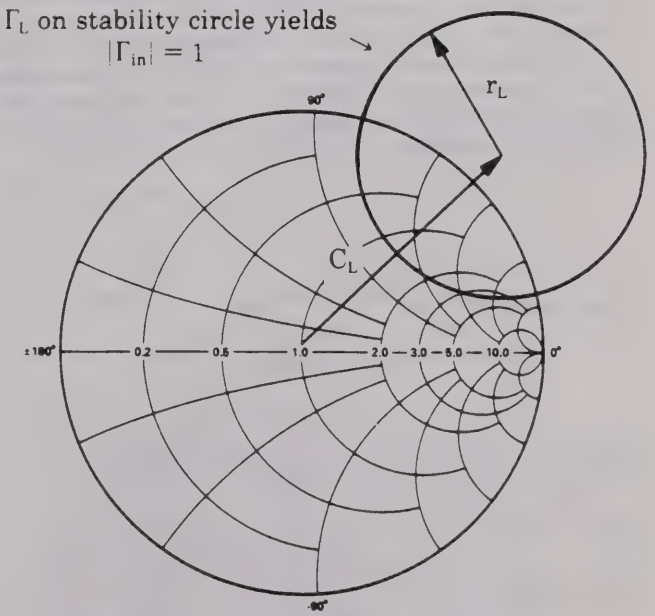

Figure 59

To determine which area represents this stable operating condition, let's make $Z_L = 50$ ohms, or $\Gamma_L = 0$. This represents the point at the center of the Smith Chart. Under these conditions,

$$|\Gamma_{in}| = |S_{11}$$

Let's now assume that S_{11} has been measured and its magnitude is less than one. Γ_{in}'s magnitude is also less than one. This means that this point, $\Gamma_L = 0$, represents a stable operating condition. This region (Fig. 60) then represents the stable operating condition for the entire network.

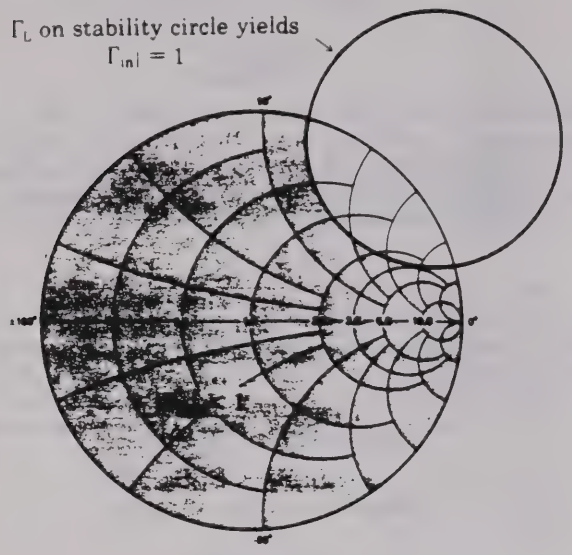

Figure 60

If we select another value of Γ_L that falls **inside** the stability circle, we would have an input reflection coefficient that would be greater than one and the network would be potentially unstable.

If we only deal with passive loads, that is, loads having a reflection coefficient less than or equal to one, then we only have to stay away from those Γ_L's that are in this region (Fig. 61) to ensure stable operation for the amplifier we are designing. Chances are, we should also stay away from impedances in the border region, since the other factors like changing temperature, the aging of the transistors, or the replacement of transistors might cause the center or radius of the stability circle to shift. The impedance of the load could then fall in the expanded unstable region, and we would again be in trouble.

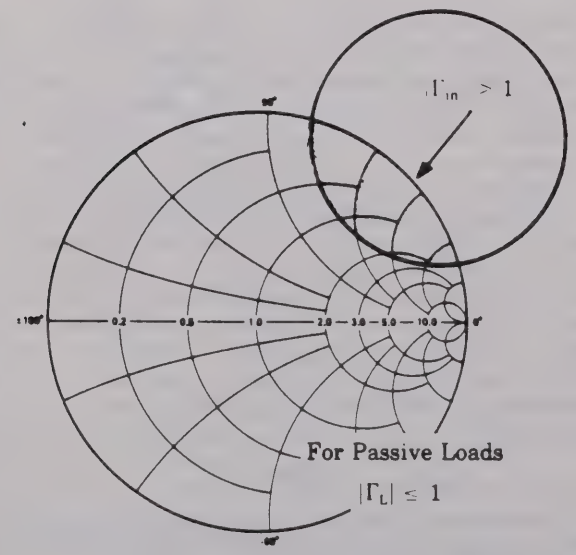

Figure 61

If, on the other hand, $S_{11} > 1$, with $Z_L = 50\ \Omega$, then this area would be the stable region and this region the unstable area (Fig. 62).

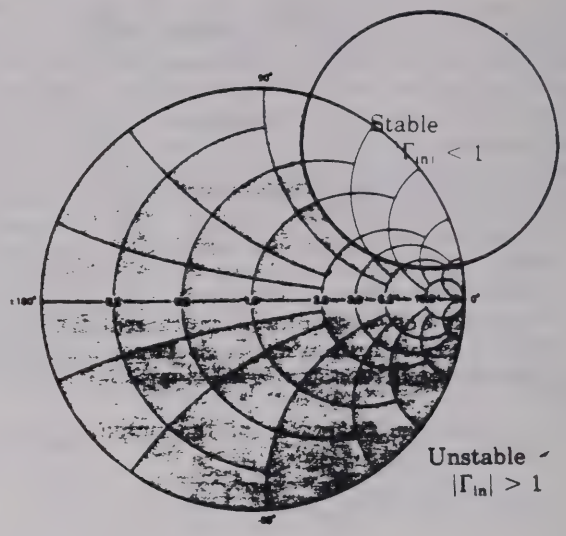

Figure 62

To ensure that we have an **unconditionally stable** condition at a given frequency in our amplifier design, we must be able to place any passive load on the network and drive it with any source impedance without moving into an unstable condition.

From a graphical point of view, we want to be sure that the stability circle falls completely outside the Smith Chart, and we want to make sure that the inside of the stability circle represents the unstable region (Fig. 63). The area outside the stability circle, including the Smith Chart, would then represent the stable operating region.

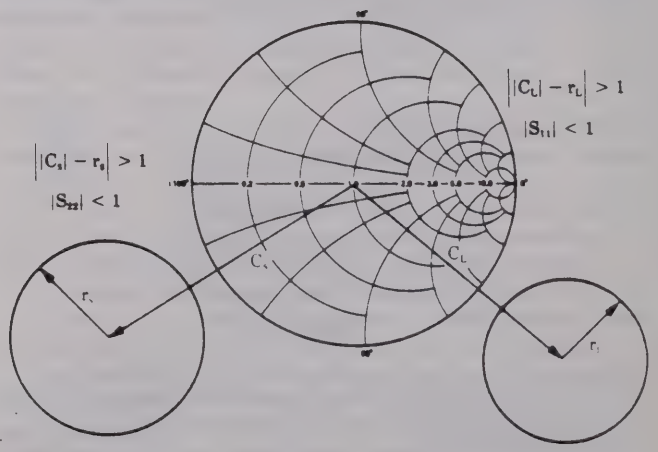

Figure 63

To satisfy this requirement, we must ensure that the magnitude of the vector, C_L, the distance from the center of the Smith Chart to the center of the stability circle, minus the radius of the stability circle, r_L, is greater than one. This means that the closest point on the stability circle would be outside the unit radius circle or Smith Chart.

To ensure that the region inside the Smith Chart represents the stable operating condition, the input **or** output impedance of the network must have a real part greater than zero when the network is terminated in 50 ohms. For completeness, we must also add the output stability circle to gain a better understanding of this concept. This means that the magnitude of S_{11} **and** S_{22} must be less than one.

One word of **caution** about stability.

S-parameters are typically measured at some particular frequency. The stability circles are drawn for **that** frequency. We can be sure that the amplifier will be stable at that frequency, but will it oscillate at some other frequency either inside or outside the frequency range of the amplifier?

Typically, we want to investigate stability over a broad range of frequencies and construct stability circles wherever we might suspect a problem. Shown here are the stability circles drawn for three different frequencies (Fig. 64). To ensure stability between f_1 and f_3, we stay away from impedances in this (shaded) area. While this process may sound tedious, we do have some notion based on experience where something may get us into trouble.

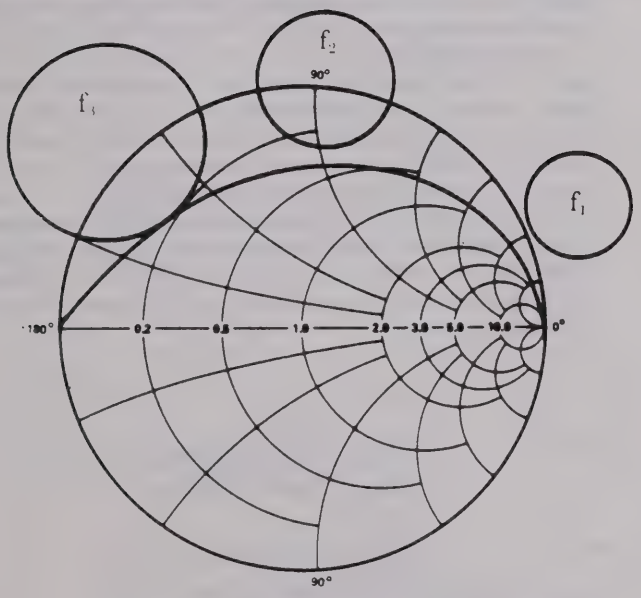

Figure 64

Stability is strongly dependent on the $|S_{12}|\,|S_{21}|$ product (Fig. 65). S_{21} is a generally decreasing function of frequency from f_β on.

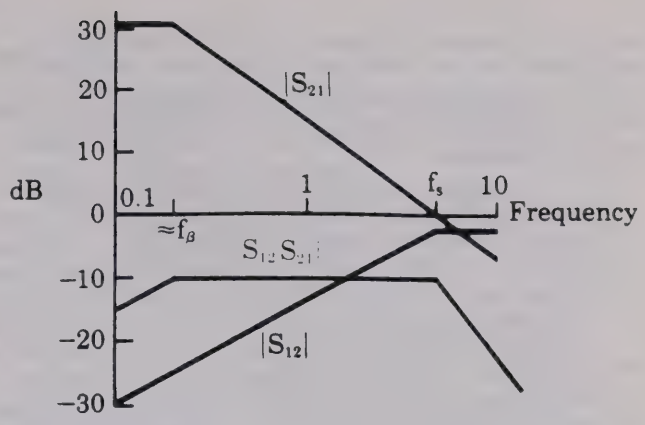

Figure 65

$|S_{12}|$ is an increasing function.

Looking at the $|S_{12}|\,|S_{21}|$ product, we see that it increases below f_β, flattens out, then decreases at higher frequencies.

It is in this flat region that we must worry about instability.

On the other hand, if we synthesize elements such as inductors by using high impedance transmission lines, we might have capacitance rather than inductance at higher frequencies, as seen here on the Impedance Phase plot (Fig. 66). If we suspect that this might cause oscillation, we would investigate stability in the region where the inductor is capacitive. Using tunnel diodes having negative impedance all the way down to dc, we would have to investigate stability right on down in frequency to make sure that oscillations did not occur outside the band in which we are working.

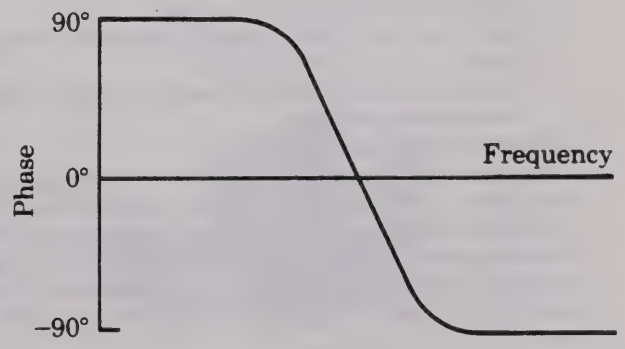

Figure 66

Summary

This program, intended as a review of concepts used by the microwave engineer, has covered a wide range of topics.

Hewlett-Packard has also developed a series of application notes on these subjects.

Circuit design programs are also available for the Hewlett-Packard 9100 Calculator System.

In addition, there are now available a series of tutorial video tape programs that cover some of the topics reviewed in this program in greater detail.

This entire package of S-parameter equipment and support material has been developed to make your microwave circuits easier to design while ensuring excellent performance.

Chapter III
S-Parameter Measurements

The material presented in this program is a continuation of Hewlett-Packard's video tape S-Parameter Design Seminar.

It is recommended that the first video tape on the 8410 Network Analyzer System as well as the first tape (S-Parameter Design Techniques—I) in this seminar be reviewed prior to viewing this presentation. There are also other video tapes on specific subjects of microwave theory and network analysis that have been developed and are available from the Hewlett-Packard video tape library. In addition, three application notes —numbers 95, 117-1, and 117-2—present material on S-parameters and the network analyzer system used to measure S-parameters.

All of this background material will help you understand more completely the material presented in this tape and the other tapes in this S-Parameter Design Seminar.

S-Parameters

A. Their Importance

Microwave transistor technology is continually pushing maximum operating frequencies ever upward. As a result, manufacturers of transistors are specifying their transistors in terms of S-parameters. This affects two groups of design engineers—the transistor circuit designer must now switch his thinking from the well-known H, Y, and Z-parameters in his circuit design to the S or scattering parameters.

The microwave engineer, since transistor technology is moving into his frequency domain, must now become conversant with transistor terminology and begin to think of applying transistors to the circuits he works with.

In this tape we will:

1. Review the S-parameter concept.
2. Show the results of typical S-parameter measurements of a 12 GHz transistor.
3. Demonstrate the network analyzer system used in these measurements.

B. Review of S-Parameters

The function of network analysis is to completely characterize or describe a network so we'll know how it will behave when stimulated by some signal. For a two-port device, such as transistors, we can completely describe or characterize it by establishing a set of equations that relate the voltages and currents at the two ports (Fig. 67).

$$V_1 = h_{11}I_1 + h_{12}V_2$$
$$I_2 = h_{21}I_1 + h_{22}V_2$$

Figure 67

In low frequency transistor work, one such set of equations relates total voltages across the ports and total current into or out of these ports in terms of H-parameters. For example,

$$h_{11} = \frac{V_1}{I_1}\Big|_{V_2 = 0}$$

These parameters are obtained under either open or short circuit conditions.

At higher frequencies, especially in the microwave domain, these operating conditions present a problem since a short circuit looks like an inductor and an open circuit has some leakage capacitance. Often, if the network is an active device such as a transistor, it will oscillate when terminated with a reactive load.

It is imperative that some new method for characterizing these devices at high frequencies has to be used.

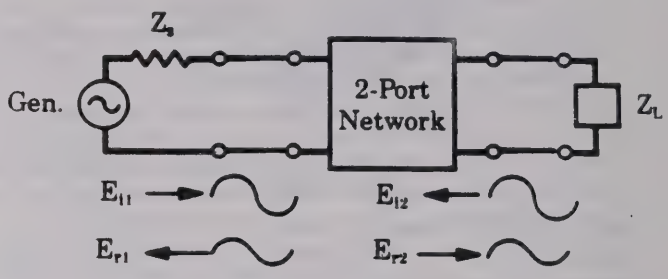

Figure 68

If we embed our two-port device into a transmission line, and terminate the transmission line in its characteristic impedance, we can think of the stimulus signal as a traveling wave incident on the device, and the response signal as a wave reflecting from the device or being transmitted through the device (Fig. 68). We can then establish this new set of equations relating these incident and "scattered" waves (Fig. 69a): E_{1r} and E_{2r} are the voltages reflected from the 1st and 2nd ports, E_{1i} and E_{2i} are the voltages incident upon the 1st and 2nd ports. By dividing through by $\sqrt{Z_o}$, where Z_o is the characteristic impedance of the transmission line, we can alter these equations to a more recognizable form (Fig. 69b). Where, for example, $|b_1|^2$ = Power reflected from the 1st port and $|a_1|^2$ = Power incident on the 1st port.

a)
$$E_{1r} = S_{11}E_{1i} + S_{12}E_{2i}$$
$$E_{2r} = S_{21}E_{1i} + S_{22}E_{2i}$$

b)
$$b_1 = S_{11}a_1 + S_{12}a_2$$
$$b_2 = S_{21}a_1 + S_{22}a_2$$

where $b_N = \frac{E_{Nr}}{\sqrt{Z_0}}$ and $a_N = \frac{E_{Ni}}{\sqrt{Z_0}}$

Figure 69

S_{11} is then equal to b_1/a_1 with $a_2 = 0$ or no incident wave on port 2. This is accomplished by terminating the output of the two-port in an impedance equal to Z_o.

C. Summary

S_{11} = input reflection coefficient with the output matched.

S_{21} = forward transmission coefficient with the output matched.

This is the gain or attenuation of the network.

S_{22} = output reflection coefficient with the input matched.

S_{12} = reverse transmission coefficient with the input matched.

To the question "Why are S-parameters important?" you can now give several answers:

1. S-parameters are determined with resistive terminations. This obviates the difficulties involved in obtaining the broadband open and short circuit conditions required for the H, Y, and Z-parameters.
2. Parasitic oscillations in active devices are minimized when these devices are terminated in resistive loads.
3. Equipment is available for determining S-parameters since only incident and reflected voltages need to be measured.

Characterization of Microwave Transistors

Now that we've briefly reviewed S-parameter theory, let's look at some typical transistor parameters. There are three terms often used by transistor circuit designers (Fig. 70):

1. f_t or the frequency at which the short circuit current gain is equal to one;
2. f_s or the frequency where $|S_{21}| = 1$ or the power gain of the device, $|S_{21}|^2$, expressed in dB is zero;
3. f_{max} or the frequency where the maximum available power gain, G_{amax}, of the device is equal to one. F_{max} is also referred to as the maximum frequency of oscillation.

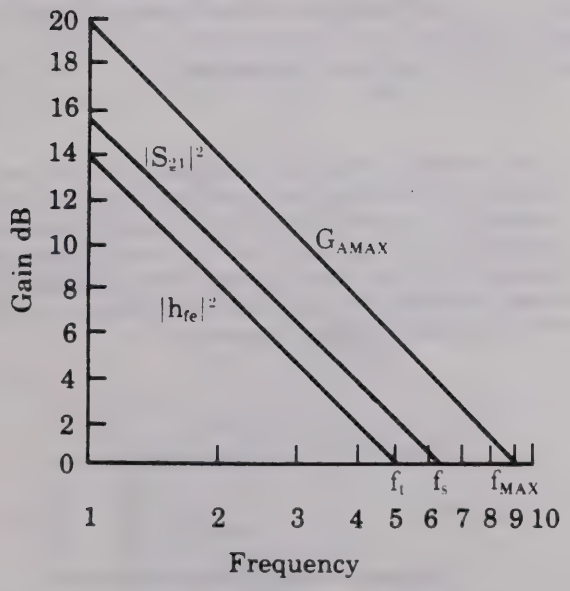

Figure 70

To determine f_s of a transistor connected in a common emitter configuration, we drive the base with a 50-ohm voltage source and terminate the collector in the 50-ohm characteristic impedance. This results in a gain versus frequency plot that decays at about 6 dB per octave at higher frequencies.

Due to the problems involved in obtaining true short circuits at high frequencies, the short circuit current gain $|h_{fe}|$ cannot be measured directly, but can be derived from measured S-parameter data. The shape of this gain versus frequency curve is similar to that of $|S_{21}|^2$ and, for this example, f_t is slightly less than f_s.

F_{max} is determined after conjugately matching the voltage source to the transistor input, and the transistor output to the characteristic impedance of the line. The resulting gain is the maximum available power gain as a function of frequency. It is higher than $|S_{21}|^2$ because of impedance matching at the input and output. With proper impedance matching techniques, the transistor is usable above f_s in actual circuit design.

S-Parameters of Transistors

A. Introduction

Let's now shift our attention to the actual S-parameters of a transistor. We'll look at transistors in chip form and after the chips have been packaged. The advantage of characterizing the chip is that you will get a better qualitative understanding of the transistor. However, fixtures to hold these chips are not readily available. Most engineers will be using packaged transistors in their R&D work. There are fixtures available for characterizing packaged transistors, and we will demonstrate these later on (Fig. 71). The bias conditions used when obtaining these transistors' parameters connected as common emitter: $V_{cb} = 15$ V and $I_c = 15$ mA.

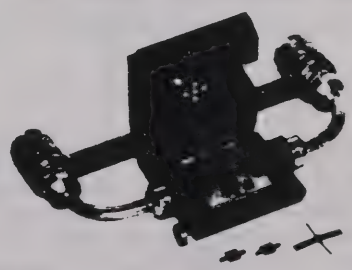

Figure 71

B. S_{11} of Common Emitter

The input reflection characteristic, S_{11}, of the chip transistor seems to be following a constant resistance circle on the Smith Chart (Fig. 72). At lower frequencies, the capacitive reactance is clearly visible and, as the frequency increases, this reactance decreases and the resistance becomes more evident. A small inductance is also evident which, for this example, resonates with the capacitance at 10 GHz.

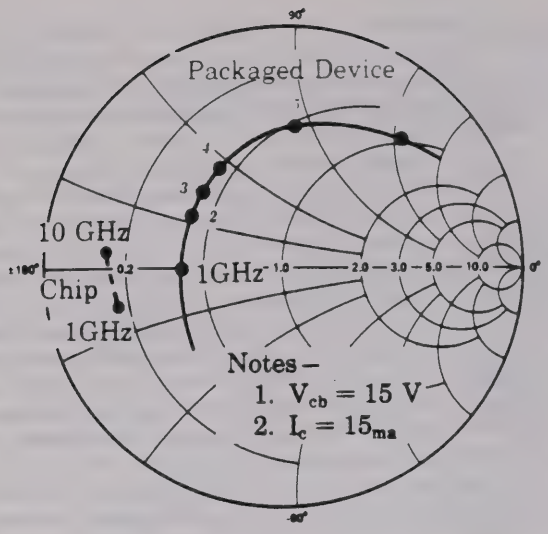

Figure 72

An equivalent circuit can be drawn that exhibits such characteristics (Fig. 73). The resistance comes from the bulk resistivities in the transistor's base region plus any contact resistance resulting from making connections to the device. The capacitance is due mainly to the base-emitter junction. The inductance results from the emitter resistance being referred back to the input by a complex β at these high frequencies.

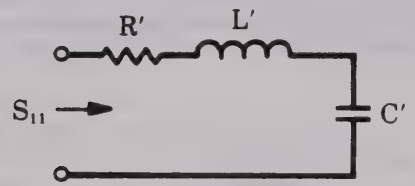

Input Equivalent Circuit (Chip)

Figure 73

If you characterize the same chip transistor after packaging, the input reflection characteristic again starts in the capacitive reactance region at lower frequencies and then moves into the inductive reactance region at higher frequencies (Fig. 72). Another equivalent circuit explaining this characteristic can be drawn (Fig. 74). Package inductance and capacitance contribute to the radial shift inward as well as to the extension of the S_{11} characteristic into the upper portion of the Smith Chart.

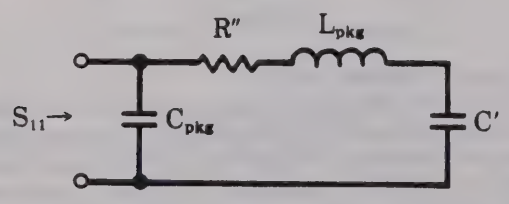

Input Equivalent Circuit (Package)

Figure 74

C. S_{22} of Common Emitter

The output reflection coefficient, S_{22}, is again in the capacitive reactance portion of the Smith Chart (Fig. 75). If you overlay an admittance Smith Chart, you can see that this characteristic roughly follows a constant conductance circle. This type of characteristic represents a shunt RC type of equivalent circuit where the angle spanned would be controlled by capacitive elements, and the radial distance from the center of the Smith Chart would be a function of the real parts (Fig. 76).

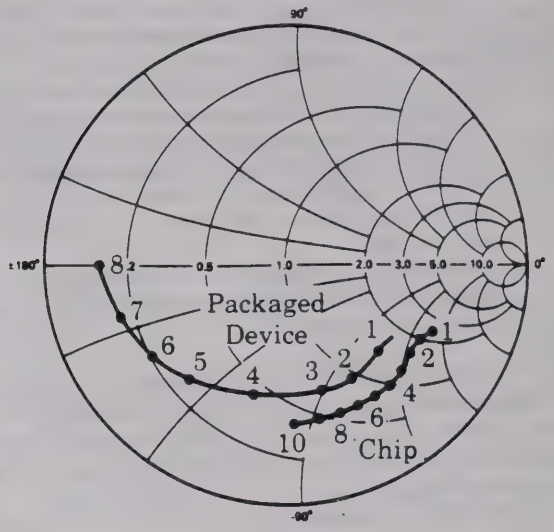

Figure 75

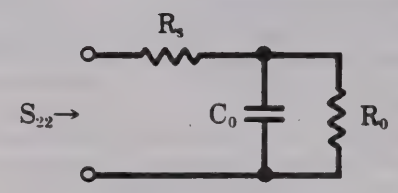

Output Equivalent Circuit (Chip)

Figure 76

The output reflection coefficient of the packaged transistor is again shifted radially inward and the angle spanned is extended. From an equivalent circuit standpoint (Fig. 77), you can see that we have added the package inductance and changed the capacitance. This added inductance causes this parameter to shift away from a constant conductance circle.

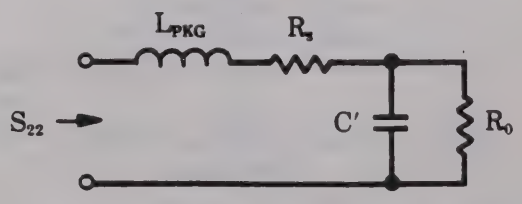

Output Equivalent Circuit (Package)

Figure 77

D. S_{21} of Common Emitter

The forward transmission coefficient, S_{21}, that we have seen before when discussing f_s, exhibits a voltage gain value slightly greater than 4 or 12 dB at 1 GHz and crosses the unity gain circle between 4 and 5 GHz (Fig. 78). The packaged transistor exhibits slightly less gain and a unity gain crossover at around 4 GHz.

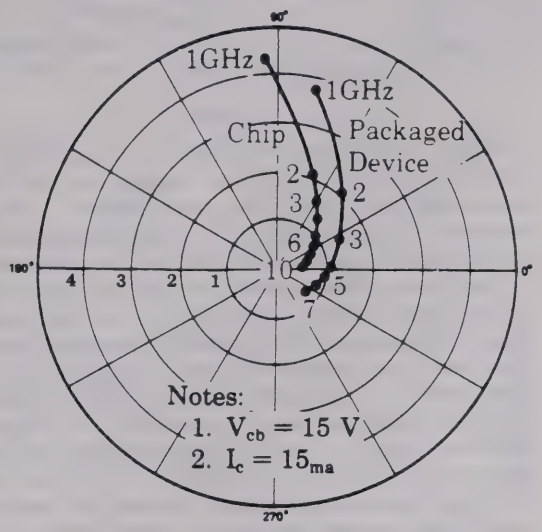

Figure 78

In an equivalent circuit, we could add a current source as the element giving gain to the transistor (Fig. 79).

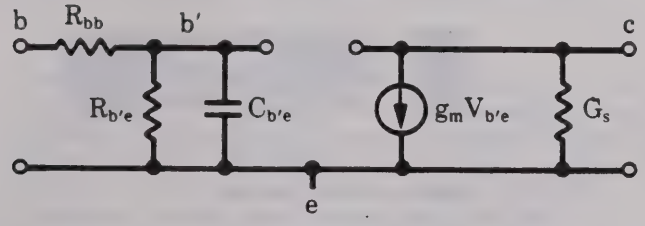

Figure 79

E. S_{12} of Common Emitter

Since a transistor is not a unilateral device, the reverse transmission characteristic, S_{12}, will have some finite value in chip form. On a polar plot, the S_{12} characteristic approximates a circular path (Fig. 80).

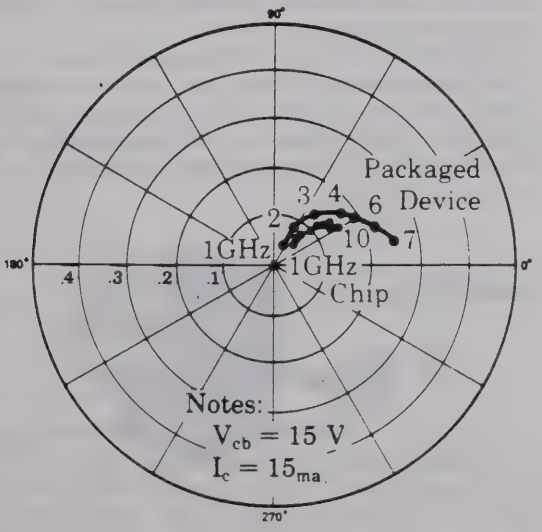

Figure 80

If you were to plot $|S_{12}|$ on a Bode Diagram, you would see a gradual buildup at about 6 dB/octave at low frequencies, a leveling off and then ultimately a decay at the higher frequencies. Let's now superimpose a Bode Plot of $|S_{21}|$. It is constant at frequencies below f_β and then decays at about 6 dB/octave. Therefore, the product of these two characteristics would increase up to f_β, around 100 to 200 MHz, and remain relatively flat until a break point at around the f_s of the transistor (Fig. 81).

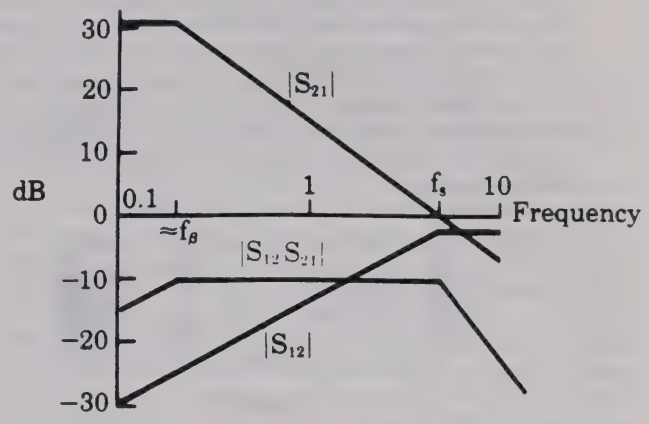

Figure 81

This $|S_{12}|\,|S_{21}|$ product is significant since it both represents a figure of merit of the feedback or stability term of the device and it also appears in the complete equations for input and output reflection coefficients.

F. Combined Equivalent Circuit

If you were to now combine the equivalent circuits drawn up to this point, you could arrive at a **qualitative** model that describes the transistor's operation (Fig. 82).

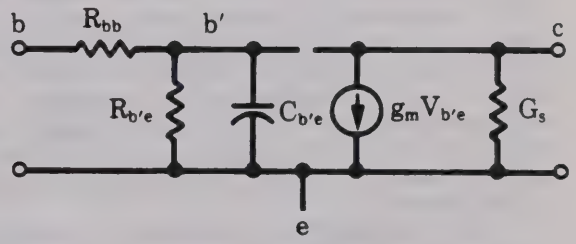

Figure 82

S-Parameter Measurement System

A. System Description

The system used to measure the characteristics we have seen is the Hewlett-Packard 8410 Network Analyzer System.

This system consists of: (1) . . . an RF source, such as the Hewlett-Packard 8620 Solid State Sweep Oscillator (Fig. 83); (2) . . . a transducer or signal conditioner that splits the incoming RF signal into two channels and provides a calibrated line stretcher for equalizing the electrical lengths between the channels; (3) . . . a harmonic frequency converter and mainframe that down converts the RF signal to a constant intermediate frequency; and (4) . . . a display unit that displays the ratio of the signals in the two channels.

Figure 83

Let's focus our attention on the transducer unit. There are two S-Parameter Test Sets available for complete network characterization: the 8745A Test Set (Fig. 84) operates in the 110 MHz to 2 GHz range, and the 8746B (Fig. 85) operates from 500 MHz to 12.4 GHz, but can be operated down to 110 MHz. Both of these units have front panel S-parameter pushbuttons that control internal switching circuits, enabling you to measure all four S-parameters with pushbutton ease. These units also contain internal biasing networks used to bias the device under test.

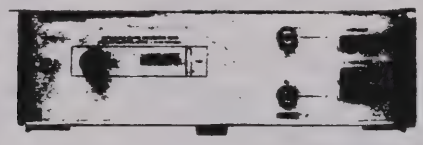

Figure 84

Figure 85

In the 8746B, the incoming RF signal goes through a 0 - 70 dB programmable attenuator that is used to ensure small signal S-parameter characterization. This feature is important since S-parameters are a small signal representation for the two-port under test.

For semiconductor measurements, some kind of fixture is required for holding the device in a way that closely approximates the manner in which it will be used in an actual circuit. Since transistors come in either chip form or in some package format, these fixtures must provide the capability of holding the device and for getting the 50-ohm lines as close to the transistor as possible.

If you are testing can type transistor packages, the Models 11600B or 11602B fixtures can be used (Fig. 86).

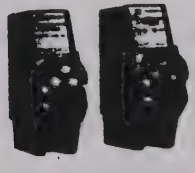

Figure 86

Stripline transistors are now being used at the higher microwave frequencies. The Model 11608A fixture provides the capability for holding TI-line or K-disc package styles. In addition, the fixture can be modified to hold many of the other package styles that are currently being manufactured and used (Fig. 87).

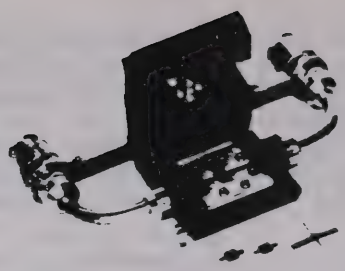

Figure 87

Many manufacturers measure transistors in chip form. To do this, they have constructed a fixture that will enable the probes to be attached to the various segments of the transistor. These fixtures are usually so specialized, however, that they must be custom built.

One other instrument is necessary for any semiconductor measurement, and this is the bias supply. The Hewlett-Packard Model 8717B Transistor Bias Supply (Fig. 88) is convenient to use in characterizing transistors with the 8745A or 8746B transducer units. Front panel switches on the 8717B enable the user to set up the bias supply for stable bias conditions for all bipolar or FET transistor configurations. This eliminates the need for external wiring changes for each new configuration. The two meters independently measure one of the voltages and one of the currents on any of the three leads of the transistor under test. The transistors are protected by an emitter current limit shutdown circuit which removes the bias when the preset limit is exceeded.

Figure 88

B. Demonstration of the System

Now that you've seen some typical transistor characteristics and the system used to measure the transistors, let's actually make several measurements to see how simply and accurately you can make the measurements that will provide you with the necessary data for designing your circuits.

The S-parameter characteristics we have seen are those of a Model 35821E Transistor. In these measurements we will measure the transistor in a K-disc common emitter package.

The 11608's rubber pads clamp the base and collector leads down over the stripline, and the emitter leads down over the ground at these points (Fig. 89). After calibrating the system, you simply insert the transistor, close the fixture lid, turn on the bias supply and depress S_{11} pushbutton.

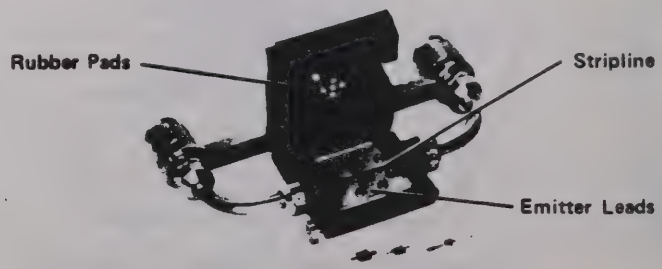

Figure 89

The standard bias conditions are: $V_{cb} = 15$ volts
$I_c = 15$ mA

On the polar display with the Smith Chart overlay inserted, the input impedance can be read off directly. To ensure that we are in the linear region of the transistor, we can measure S_{11} at two input power levels to the transistor. If these readings do not change, we know that we are driving the transistor at an optimum power level and the S-parameters are truly the small signal characteristics. If we now vary the collector current bias level, we note very little difference (Fig. 90).

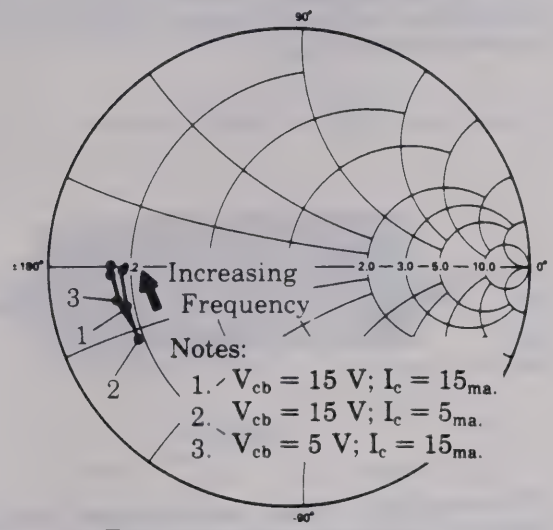

Frequency Range: 1 to 10 GHz

Figure 90

Returning the current level to the original value, we now decrease V_{cb} and note a shift of the original characteristic. Decreasing V_{cb} causes the epitaxial layer to be less depleted so you would expect less capacitive reactance in the input equivalent circuit.

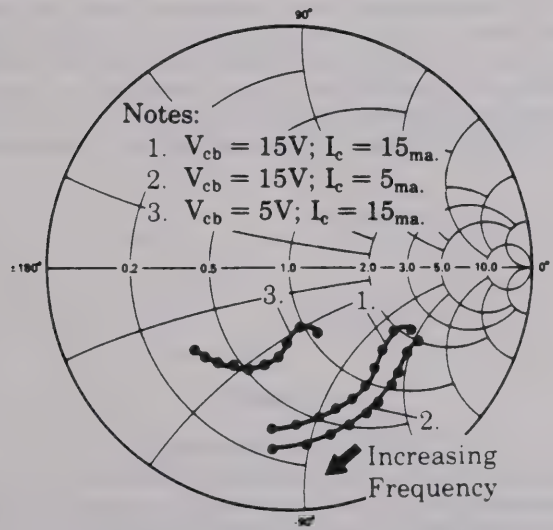

Frequency Range: 1 to 10 GHz

Figure 91

By now simply depressing 8746B's S_{22} pushbutton, you can measure the output reflection coefficient (Fig. 91). Let's now reduce the collector current and note the effect on this characteristic. The radial shift outward indicates an increase in the real part of the output impedance. This shift is due to the real part being inversely proportional to the g_m of the transistor, while the collector current is directly proportional to g_m (Fig. 92).

$$\mathrm{Re}[Z_{out}] \propto \frac{1}{g_m}$$

$$I_c \propto g_m$$

Figure 92

Let's now return I_c to 15 mA and decrease V_{cb}. You note a radial shift inward. This shift is again related to the depletion of the epitaxial layer.

Let's now turn our attention to the gain of the transistor and depress S_{21} with the bias conditions back at their original values. Since the system was initially calibrated so that the outer circle on the polar display represented a voltage gain of one, we will now have to reduce the system gain to bring this trace back on the screen. We can introduce 14 dB of attenuation into the test channel by using the IF attenuator so that the outer circle now represents a voltage gain of 5. The forward gain of the device, S_{21}, is now visible. This characteristic is also affected by varying the bias conditions (Fig. 93).

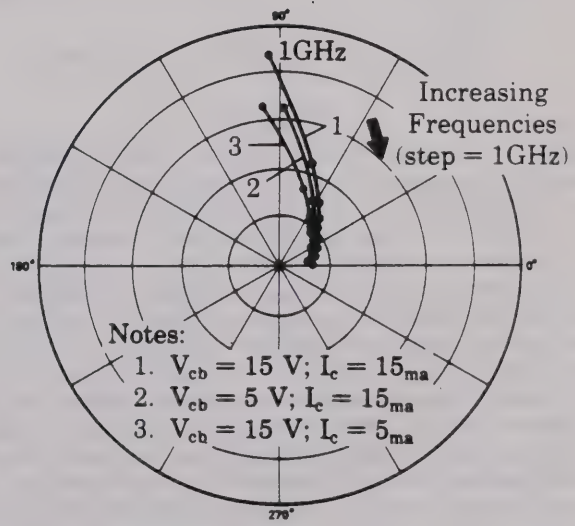

Frequency Range: 1 to 10 GHz

Figure 93

Let's look now at the reverse transmission characteristic, S_{12}. This value is much smaller than the forward gain, so we will have to introduce more test channel gain into the system to enable us to have a reasonable display. This characteristic is relatively invariant to bias changes.

One characteristic that often appears on transistor data sheets is the relation of power gain $|S_{21}|^2$ versus collector current at one frequency. This characteristic curve was determined at 1 GHz (Fig. 94).

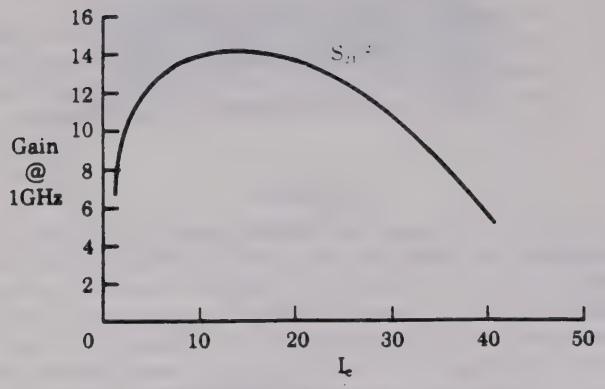

Figure 94

At low current levels, there is a gradual increase, then the power gain characteristic flattens out and decreases at higher current levels. The base-collector transit time determines the flat plateau. The high current roll-off is due to two effects: (1) thermal effects on the transistor; (2) if we try to pump more current into the device than it can handle, the base of the transistor stretches electrically. Since the electrons move across the base-collector junction at a finite rate, the current density increases as we try to pump more current in, until, at the limit, the base has stretched to the width of the epitaxial layer and this will account for the gain going toward zero.

Summary

This tape has presented an overview of S-parameter theory and has related this theory to actual transistor characterization.

The remaining tapes in this S-Parameter Design Seminar are devoted to high frequency circuit design techniques using S-parameters. Constant gain and noise figure circles will be discussed and then used in designing unilateral narrow and broadband amplifiers.

This amplifier (Fig. 95), for example, was designed with S-parameter data, and operates from 100 MHz to 2 GHz with a typical gain of 40 dB and flat to within 3 dB across the band. A similar amplifier will be designed in the next tape.

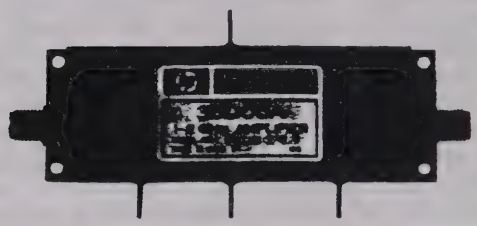

Figure 95

The use of these design techniques and measurement equipment will also prove valuable to you in your device development.

Chapter IV
High Frequency Amplifier Design

Introduction

In this tape, the practical application of S-parameters will be discussed. They will specifically be applied to unilateral amplifier design. This tape is a continuation of the Hewlett-Packard Microwave Division's S-Parameter Design Seminar. We will discuss: Transducer Power Gain, Constant Gain and Constant Noise Figure Circles, and then **use** these concepts with S-parameter data in the design of amplifiers for the case where the transistor can be assumed to be unilateral, or $S_{12} = 0$.

S-Parameter Review

Before introducing these concepts, let's briefly review S-parameters.

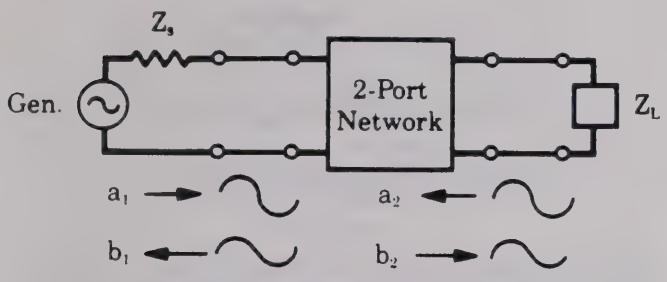

If: $Z_L = Z_0$, $a_2 = 0$

Figure 96

As opposed to the more conventional parameter sets which relate total voltages and total currents at the network ports, S-parameters relate **traveling waves** (Fig. 96). The **incident** waves, a_1 and a_2, are the independent variables and the **reflected** waves, b_1 and b_2, are the dependent variables. The network is assumed to be embedded in a transmission line system of known characteristic impedance which shall be designated Z_0. The S-parameters are then measured with Z_0 terminations on each of the ports of the network. Under these conditions, S_{11} and S_{22}, the input and output reflection coefficients, and S_{21} and S_{12}, the forward and reverse transmission coefficients, can be measured (Fig. 97).

$$S_{11} = \left.\frac{b_1}{a_1}\right|_{a_2 = 0} \qquad S_{12} = \left.\frac{b_1}{a_2}\right|_{a_1 = 0}$$

$$S_{21} = \left.\frac{b_2}{a_1}\right|_{a_2 = 0} \qquad S_{22} = \left.\frac{b_2}{a_2}\right|_{a_1 = 0}$$

Figure 97

Transducer Power Gain

In the design of amplifiers, we are most interested in the transducer power gain. An expression can be derived for transducer power gain if we first redraw the two-port network using flow graph techniques (Fig. 98).

The transducer power gain is defined as the power delivered to the load divided by the power available from the source. The ratio of b_2 to b_s can be found by applying the non-touching loop rule for flow graphs resulting in this expression for transducer power gain. (Fig. 99).

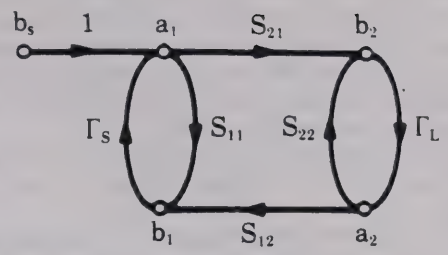

Figure 98

$$G_T = \frac{P_{del}}{P_{avs}}$$

$$= \frac{|b_2|^2(1 - |\Gamma_L|^2)}{|b_s|^2/(1 - |\Gamma_s|^2)}$$

$$= \frac{|S_{21}|^2(1 - |\Gamma_s|^2)(1 - |\Gamma_L|^2)}{|(1 - S_{11}\Gamma_s)(1 - S_{22}\Gamma_L) - S_{21}S_{12}\Gamma_L\Gamma_s|^2}$$

Figure 99

If we now assume the network to be unilateral, that is, S_{12} is equal to zero, this term ($S_{21}S_{12}\Gamma_L\Gamma_s$) drops out and the resulting expression can be separated into three distinct parts. This expression will be referred to as the **unilateral** transducer power gain (Fig. 100).

$$G_{Tu} = |S_{21}|^2 \cdot \frac{(1 - |\Gamma_s|^2)}{|1 - S_{11}\Gamma_s|^2} \cdot \frac{(1 - |\Gamma_L|^2)}{|1 - S_{22}\Gamma_L|^2}$$

Figure 100

The first term is related to the transistor or other active device being used. Once the device and its bias conditions are established, S_{21} is determined and remains invariant throughout the design.

The other two terms, however, are not only related to the remaining S-parameters of the two-port device, S_{11} and S_{22}, but also to the source and load reflection coefficients. It is these latter two quantities which we will be able to control in the design of the amplifier. We will employ lossless impedance transforming networks at the input and output ports of the network. We can then think of the unilateral transducer power gain as being made up of three distinct and independent gain terms and the amplifier as three distinct gain blocks (Fig. 101).

$$G_{tu} = \frac{(1 - |\Gamma_s|^2)}{|1 - S_{11}\Gamma_s|^2} \cdot |S_{21}|^2 \cdot \frac{(1 - |\Gamma_L|^2)}{|1 - S_{22}\Gamma_L|^2}$$

$$= G_s \cdot G_o \cdot G_L$$

$$= G_{sDB} + G_{oDB} + G_{LDB}$$

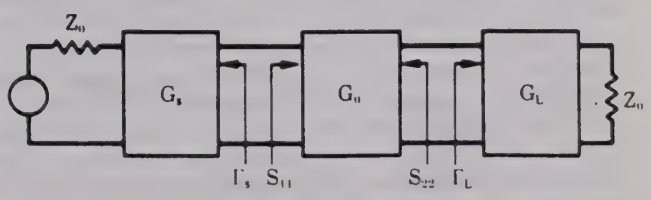

Figure 101

The G_s term affects the degree of mismatch between the characteristic impedance of the source and the input reflection coefficient of the two-port device. Even though the G_s block is made up of passive components, it can have a gain contribution greater than unity. This is true because an intrinsic mismatch loss exists between Z_o and S_{11} and the impedance transforming elements can be employed to improve this match, thus decreasing the mismatch loss, and can, therefore, be thought of as providing gain.

The G_o term is, as we said before, related to the device and its bias conditions and is simply equal to $|S_{21}|^2$.

The third term in the expression, G_L, serves the same function as the G_s term, but affects the matching at the output rather than the input.

Maximum unilateral transducer gain can be accomplished by choosing impedance matching networks such that $\Gamma_s = S_{11}^*$ and $\Gamma_L = S_{22}^*$ (Fig. 102).

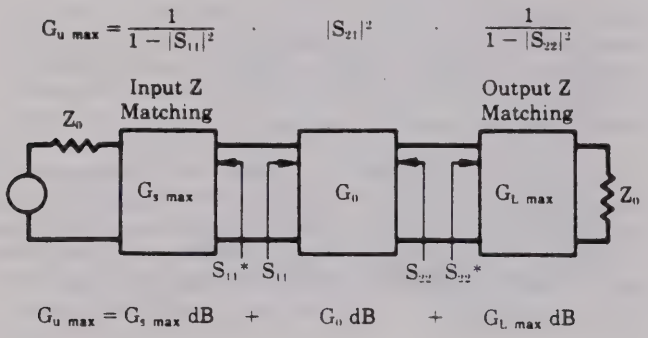

Figure 102

Constant Gain Circles

Let's look at the G_s term now in a little more detail. We have just seen that for $\Gamma_s = S_{11}^*$, G_s is equal to a maximum. It is also clear that for $|\Gamma_s| = 1$, G_s has a value of zero. For any arbitrary value of G_s between these extremes of zero and G_s max, solutions for Γ_s lie on a circle (Fig. 103).

$$\text{For} \quad G_s = 0 < g < G_{SMAX}$$

$$g = \frac{1-|\Gamma_s|^2}{|1-\Gamma_s S_{11}|^2}$$

Figure 103

It is convenient to plot these circles on a Smith Chart. The circles have their centers located on the vector drawn from the center of the Smith Chart to the point S_{11}^* (Fig. 104).

These circles are interpreted as follows:

Any Γ_s along a 2 dB circle would result in a $G_s = 2$ dB.

Any Γ_s along the 0 dB circle would result in a $G_s = 0$ dB, and so on.

For points in this region (within the 0 dB circle), the impedance transforming network is such as to improve the input impedance match and for points in this region (area outside the 0 dB circle), the device is further mismatched. These circles are called **constant gain circles.**

Since the expression for the output gain term, G_L, has the same form as that of G_s, a similar set of constant gain circles can be drawn for this term. These circles can be located precisely on the Smith Chart by applying these formulas (Fig. 105):

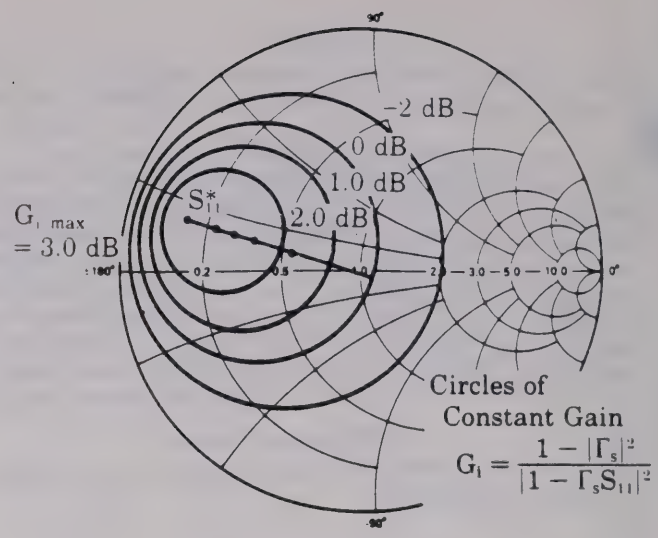

Figure 104

$$d_1 = \frac{g_1 |S_{11}|}{1-|S_{11}|^2(1-g_1)}$$

$$R_1 = \frac{\sqrt{1-g_1}\,(1-|S_{11}|^2)}{1-|S_{11}|^2(1-g_1)}$$

$$g_1 = G_1(1-|S_{11}|^2) = \frac{G_1}{G_{1\ max}}$$

G_1 = Gain represented by the circle.

Figure 105

1. d_1 being the distance from the center of the Smith Chart to the center of the constant gain circle along the vector S_{11}^*
2. R_1 is the radius of the circle and
3. g_1 is the normalized gain value for the gain circle G_1.

Constant Noise-Figure Circuits

Another important aspect of amplifier design is noise figure, which is defined as the ratio of the S/N ratio at the input to the S/N ratio at the output. $NF = \frac{S/N \text{ in}}{S/N \text{ out}}$

In general, the noise figure for a linear two-port has this form (Fig. 106a), where r_n is the equivalent input noise resistance of the two-port. G_s and b_s represent the real and imaginary parts of the source admittance, and g_o and b_o represent the real and imaginary parts of **that** source admittance which results in the minimum noise figure, F_{min}.

If we now express Y_s and Y_o in terms of reflection coefficients and substitute these equations in the noise figure expression, we see once again that the resulting equation has the form of a circle (Fig. 106B). For a given noise figure, F, the solutions for Γ_s will lie on a circle. The equations for these circles can be found given the parameters Γ_o, F_{min}, and r_n. Unless accurately specified on the data sheet for the device being used, these quantities must be found experimentally.

Generally, the source reflection coefficient would be varied by means of a slide screw tuner or stub tuners to obtain a minimum noise figure as read on a noise figure meter. F_{min} can then be read off the meter and the

source reflection coefficient can be determined on a network analyzer.

a)

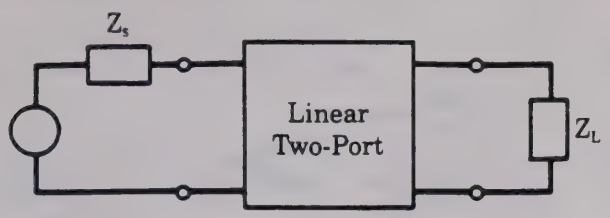

$$F = F_{min} + \frac{r_n}{g_s}[(g_s - g_0)^2 + (b_s - b_0)^2]$$

b)

$$F - F_{min} = \frac{r_n}{g_s}[(g_s - g_0)^2 + (b_s - b_0)^2]$$

Substitute $Y_s = \frac{1-\Gamma_s}{1+\Gamma_s}$; $Y_0 = \frac{1-\Gamma_0}{1+\Gamma_0}$

$$F - F_{min} = 4r_n \frac{|\Gamma_s - \Gamma_0|^2}{(1-|\Gamma_s|^2)|1+\Gamma_0|^2}$$

To Find r_n, Measure F for $\Gamma_s = 0$

$$4r_n = [F_{\Gamma_s=0} - F_{min}] \frac{|1+\Gamma_0|^2}{|\Gamma_0|^2}$$

Figure 106

The equivalent noise resistance, r_n, can be found by making one additional noise figure reading with a known source reflection coefficient. If a 50-ohm source were used, for example, $\Gamma_s = 0$ and this expression could be used to calculate r_n (Fig. 107).

For $\Gamma_s = 0$

$$r_N = [F_{\Gamma s=0} - F_{min}] \frac{|1+\Gamma_0|^2}{4|\Gamma_0|^2}$$

Figure 107

To determine a family of noise figure circles, let's first define a noise figure parameter, N_i:

$$N_i = \frac{F_i - F_{min}}{4\,r_n} \cdot \left|1 + \Gamma_o\right|^2$$

Here, F_i is the value of the desired noise figure circle and Γ_o, F_{min}, and r_n are as previously defined. With a value for N_i determined, the center and radius of the circle can be found by these expressions (Fig. 108).

$$C_{F_i} = \frac{\Gamma_0}{1+N_i}$$

$$R_{F_i} = \frac{1}{1+N_i}\sqrt{N_i^2 + N_i(1-|\Gamma_0|^2)}$$

Figure 108

From these equations, we see that $N_i = 0$ where $F_i = F_{min}$, and the center of the F_{min} circle with zero radius is located at Γ_o on the Smith Chart. The centers of the other noise figure circles lie along the Γ_o vector.

This plot then gives the noise figure for a particular device for any arbitrary source impedance at a particular frequency (Fig. 109). For example, given a source impedance of 40 + j 50 ohms, the noise figure would be 5 dB. Likewise, a source of 50 ohms would result in a noise figure of approximately 3.5 dB.

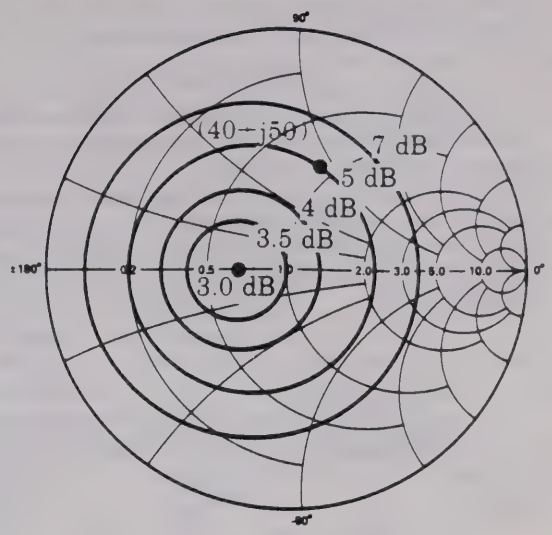

Figure 109

Constant gain circles can now be overlaid on these noise figure circles (Fig. 110). The resulting plot clearly indicates the tradeoffs between gain and noise figure that have to be made in the design of low noise stages. In general, maximum gain and minimum noise figure cannot be obtained simultaneously. In this example, designing for maximum gain results in a noise figure of about 6 dB, while designing for minimum noise figure results in approximately 2 dB less than maximum gain.

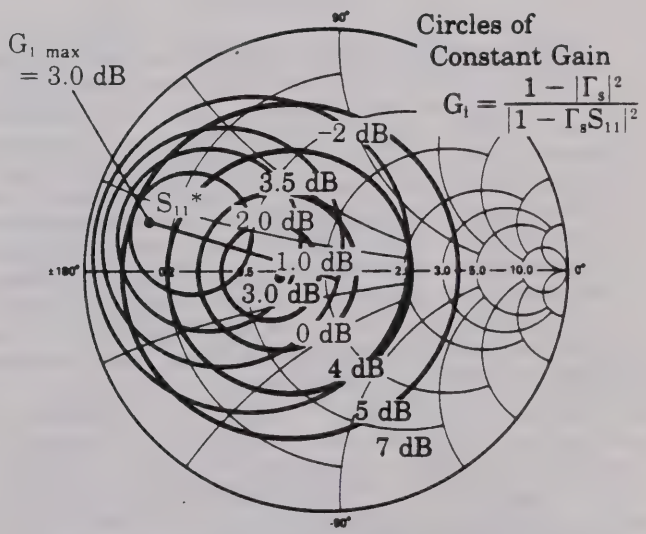

Figure 110

The relative importance of the two design objectives, gain and noise figure, will dictate the compromise that must be made in the design.

It is also important to remember that the contributions of the second stage to the overall amplifier noise figure can be significant, especially if the first stage gain is low (Fig. 111). It is, therefore, not always wise to minimize first stage noise figure if the cost in gain is

$$F_{overall} = F_1 + \frac{F_2 - 1}{G_1}$$

Figure 111

too great. Very often there is a better compromise between first stage gain and noise figure which results in a lower overall amplifier noise figure.

Design Examples

With the concepts of constant gain and constant noise figure circles well in hand, let's now embark on some actual design examples.

Shown here is a typical single stage amplifier with the device enmeshed between the input and output matching networks (Fig. 112). The device we will be using for the design examples is a HP-21, 12 GHz transistor.

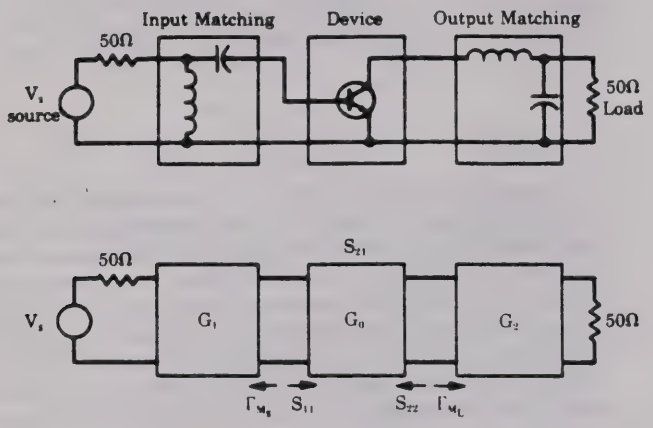

Figure 112

The forward gain characteristic, S_{21}, of this particular transistor was measured in the previous video tape of this seminar, and we noted that $|S_{21}|^2$ is a decreasing function with frequency having a slope of approximately 6 dB per octave. G_{umax}, which is the maximum unilateral transducer gain, is essentially parallel to the forward gain curve (Fig. 113). This is not necessarily true in general, but in this case, as we can see on this Smith Chart plot, the magnitudes of S_{11} and S_{22} for this device are essentially constant over the frequency band in question (Fig. 114). Thus, the maximum values of the input and output matching terms are also relatively constant over this frequency range.

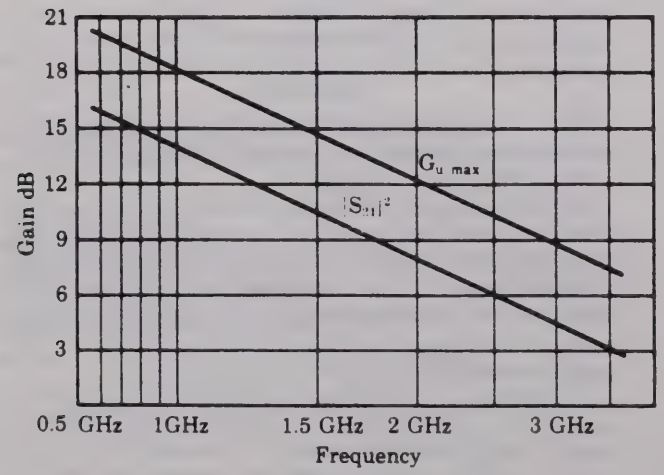

Figure 113

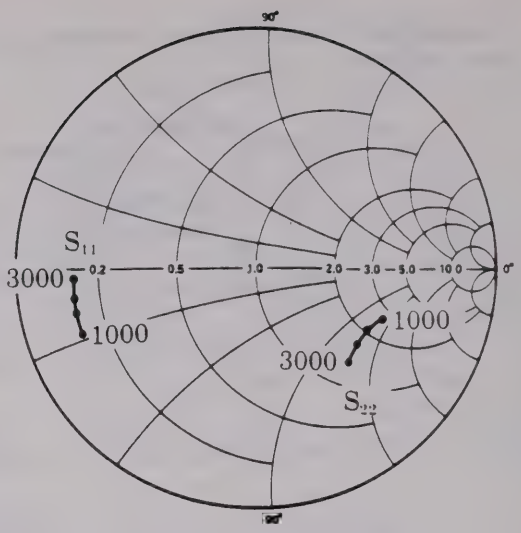

Figure 114

To illustrate the various considerations in the design of unilateral amplifier stages, let's select three design examples (Fig. 115). In the first example, we want to design an amplifier stage at 1 GHz having a gain equal to G_{umax}, which in this case is 18.3 dB. No consideration will be given in this design to noise figure. In the second example, we will aim for minimum noise figure with a gain of 16 dB. The third example will be the design of an amplifier covering the frequency band from 1 to 2 GHz with a minimum gain of 10 dB and a noise figure less than 4.5 dB.

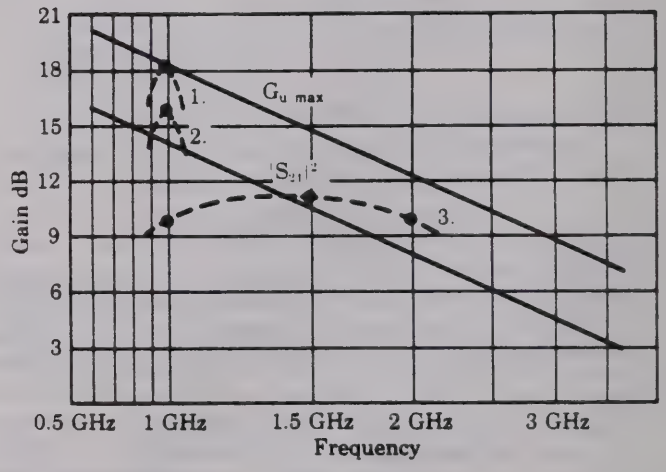

Figure 115

In these examples, we will assume a source impedance and a load impedance of 50 ohms. In general, however, the source impedance could be complex such as the output impedance of the previous stage. Likewise, the output load is quite often the input impedance of a following stage.

A. Design for G_{umax}

Now in this first example since we will be designing for G_{umax} at 1 GHz, the input matching network will be designed to conjugate match the input impedance of the transistor. This will provide a net gain contribution of 3 dB (Fig. 116).

$$G_{u\,max} = G_{1\,max} + G_0 + G_{2\,max}$$

$$= 10\ \text{Log}\left(\frac{1}{1-|S_{11}|^2}\right) + 10\ \log\left(|S_{21}|^2\right) + 10\ \log\left(\frac{1}{1-|S_{22}|^2}\right)$$

$$= 3.0 + 14.0 + 1.3 = 18.3\ \text{dB}$$

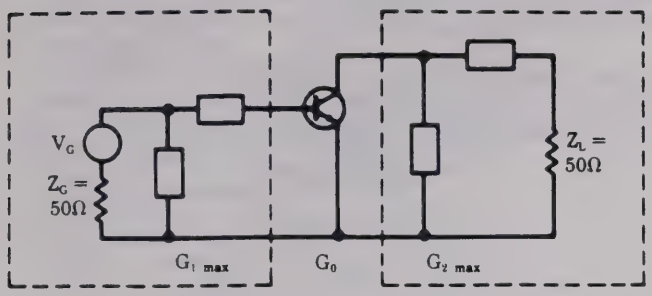

Figure 116

The output matching network will be used to conjugately match the 50-ohm load impedance to the output impedance of the transistor. From the measured data for S_{22} at 1 GHz, we find that this matching network will provide a gain contribution of 1.3 dB at the output.

Since the gain of the transistor at 1 GHz with 50-ohm source and load termination is 14 dB, the overall gain of this single stage amplifier will be 18.3 dB. The matching elements used can be any routine element—this includes inductors, capacitors, and transmission lines.

In general, to transform one impedance to any other impedance at one frequency requires two variable elements. A transmission line does, by itself, comprise two variables in that both its impedance and its length can be varied. In our example, however, we will use only inductors and capacitors for the matching elements.

The next step in the design process is to plot, on a Smith Chart, the input and output constant gain circles. If noise figure was a design consideration, it would be necessary to plot the noise figure circles as well. In most cases, it is not necessary to plot an entire family of constant gain circles. For this example, only the two circles representing maximum gain are needed. These circles have zero radius and are located at S_{11}^* and S_{22}^* (Fig. 117).

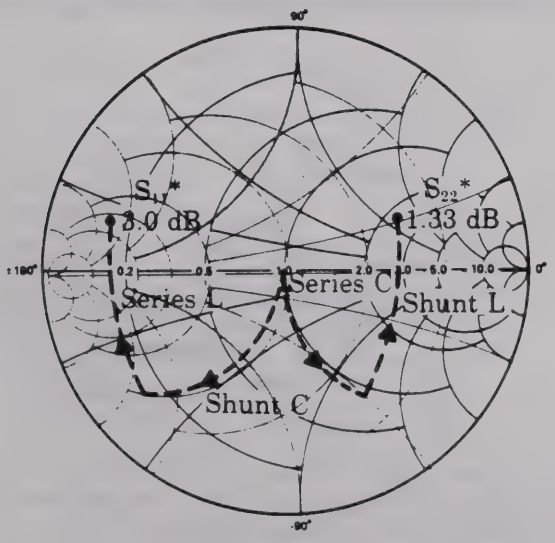

Figure 117

To facilitate the design of the matching networks, let's first overlay another Smith Chart on the one we now have. This added Smith Chart is oriented at 180° angle with respect to the original chart. The original chart can then be used to read impedances and the overlaid chart to read admittances.

To determine the matching network for the output, we start from our load impedance of 50 ohms at the center of the chart and proceed along a constant resistance circle until we arrive at the constant conductance circle which intersects the point representing S_{22}.* This represents a negative reactance of 75 ohms. Hence, the first element is a series capacitor.

We now add an inductive susceptance along the constant conductance circle so that the impedance looking into the matching network will be equal to S_{22}.*

The same procedure can now be applied at the input, resulting in a shunt capacitor and a series inductor (Fig. 118).

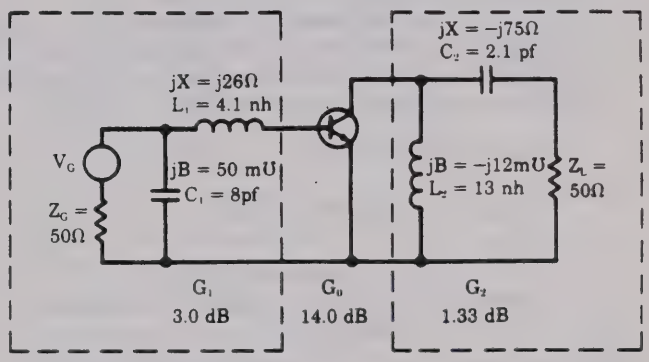

Figure 118

There are, of course, other networks which would accomplish the purpose of matching the device to the 50-ohm load and source. We could, for example, have added an inductive reactance and then a shunt capacitor for the output matching.

The choice of which matching network to use is generally a practical one. Notice, in this example, the first choice we made provides us with a convenient means of biasing the transistor without adding additional parasitics to the network other than the bypass capacitor. Another consideration might be the realizability of the elements. One configuration might give element values that are more realizable than the other.

Along these same lines, if the element values obtained in this process are too large, smaller values can generally be obtained by adding more circuit elements. But, as you can see, at the cost of added complexity.

In any case, our design example is essentially complete with the final circuit looking like this.

So far we have not considered noise figure in this design example. By plotting the noise figure circles for the device being used, we can readily determine the noise figure of the final circuit, which in this case is approximately 6 dB (Fig. 119).

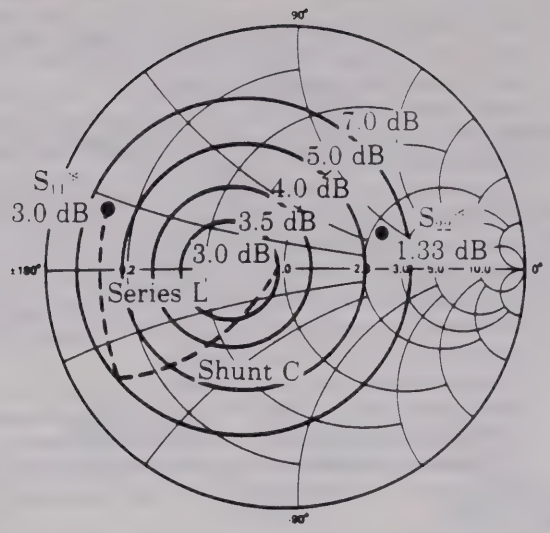

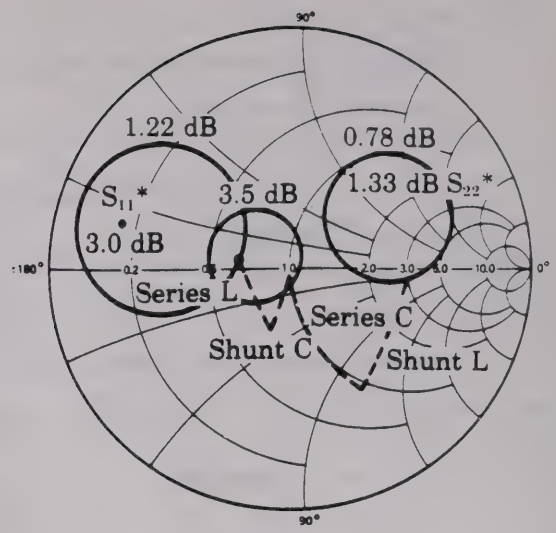

Figure 121

B. Design for Minimum Noise Figure

Let's now proceed with the second design example in which low noise figure is the design objective. This single stage amplifier will be designed to have minimum noise figure and 16 dB gain at 1 GHz (Fig. 120).

$$G_{Tu} = G_1 + G_0 + G_2$$
$$G_t + 14 + G_2$$

G_1 and G_2 are determined after input matching for minimum noise figure is accomplished

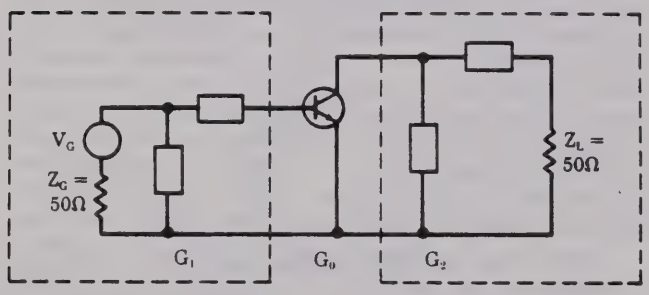

Figure 120

To accomplish the design, we first determine the input matching necessary to achieve minimum noise figure. Then using the constant gain circles, G_1, the gain contribution at the input can be determined. Knowing the gain of the device at 1 GHz, the desired value of G_2, the gain contribution of the output matching network, can then be found. The appropriate output matching network can be determined by using the constant gain circles for the output.

In this example a shunt capacitor and series inductor can be used to achieve the desired impedance for minimum noise figure. Referring once again to the Smith Chart and the mapping techniques used previously, we follow the constant conductance circle from the center of the Smith Chart and then proceed along a constant resistance circle (Fig. 121). Sometimes this requires several trials until the exact constant resistance circle that intersects the minimum noise figure point is found.

Since we now know that the minimum noise figure circle on the Smith Chart represents a specific source reflection coefficient, we can insert this value of Γ_s into the formula for G_1 to determine the value of the input constant gain circle passing through this point. In this case, it is the 1.22 dB gain circle. This is 1.8 dB less than the maximum gain attainable by matching the input.

We can now calculate the output gain circle as follows. The desired gain is 16 dB. The gain due to the input matching networks is 1.22 dB and the forward gain of the device with 50-ohm source and load terminations is 14 dB. The gain desired from the matching network at the output is, therefore, 0.78 dB.

The output matching can again be accomplished by using a series capacitor with a shunt inductor. Notice that for the output matching there are an infinite number of points which would result in a gain of 0.78 dB. Essentially, any point on the 0.78 dB circle would give us the desired amount of gain.

There is, however, a unique feature about the combination of matching elements just selected. The value of capacitance was chosen such that this point fell on the constant conductance circle which passes through the maximum gain circle represented by S_{22}^* (Fig. 122).

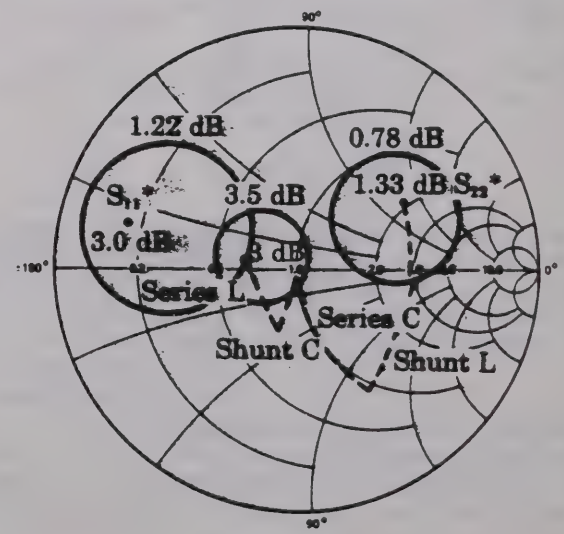

Figure 122

This combination of elements would assure an output gain-frequency response that would be symmetric with frequency.

If, for example, the frequency were increased slightly, the capacitive reactance and the inductive susceptance would both decrease and the resulting impedance would be at **this** point.

Similarly, decreasing the frequency would result in **this** impedance. Both of these points fall on a constant gain circle of larger radius and, hence, lower gain (Fig. 123).

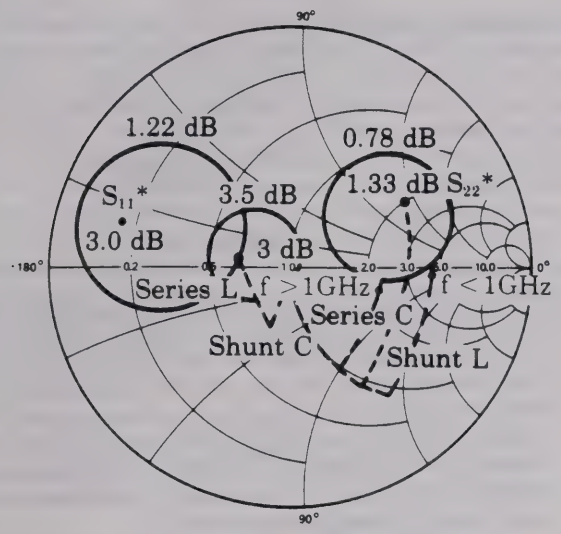

Figure 123

The gain response for the output matching, therefore, is more or less symmetric around the center frequency (Fig. 124).

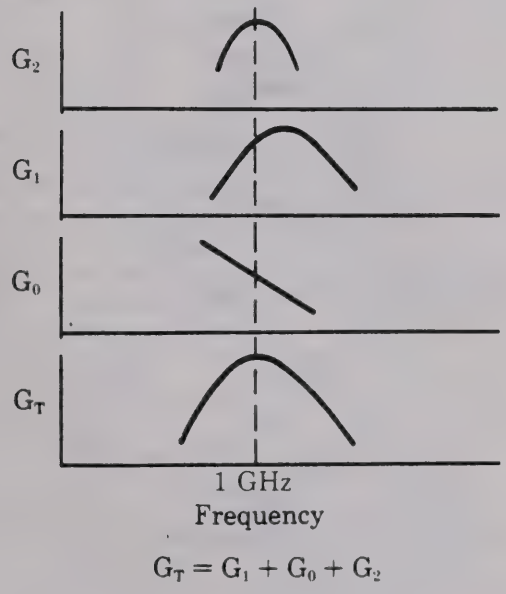

$$G_T = G_1 + G_0 + G_2$$

Figure 124

If we look at the input side, however, we have a far different situation. With an increase in frequency, both the capacitive susceptance and inductive reactance increase, resulting in an increase in gain. When the frequency is reduced, these quantities decrease, resulting in a lower value of gain. The gain contribution at the input is, therefore, unsymmetric with respect to frequency.

Since the overall gain as a function of frequency is the combination of the G_1, G_0, and G_2 terms, the resulting gain would be reasonably symmetric about the center frequency. (If another point on the 0.78 dB gain circle at the output were chosen, the final overall gain characteristic would be **asymmetric** with frequency.)

The important point is that the selection of the matching elements for the output, in this case, is not as arbitrary as it first appears. The final selection must be based not only on the gain at a specific frequency but also on the desired frequency response. The element values can now be calculated resulting in the circuit shown (Fig. 125).

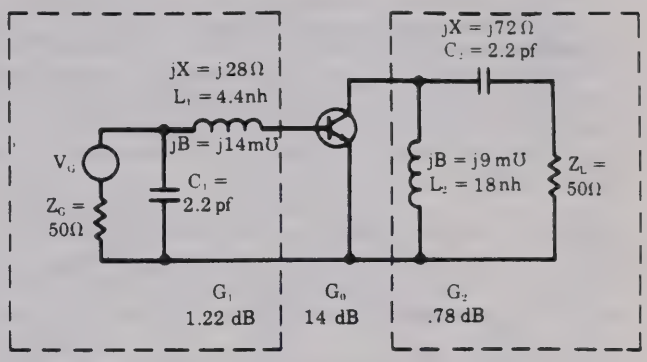

Figure 125

From a practical standpoint, one would not achieve the noise figure design objective for a number of reasons. For one thing, the circuit elements used for matching purposes would have a certain loss associated with them. This resistive loss would add directly to the noise figure. To keep this loss to a minimum, it is desirable to use high-Q circuit elements and to use the minimum number of elements necessary to obtain the desired source impedance. Second, there will be some contribution to the overall noise figure from the second stage. Third, additional degradation in noise figure would occur because of device and element variations from unit to unit.

In practice, typically ½ to 1 dB would be added from these sources to the predicted theoretical noise figure for a narrow band design. As much as 2 dB could be added in the case of an octave band design such as in our next example.

C. Broadband Design for Specific Gain and Noise Figure

Here, the design objective will be 10 dB unilateral transducer gain from 1 to 2 GHz with a noise figure less than 4.5 dB (Fig. 126).

In this example, the input and output matching networks will be designed to have a gain of 10 dB at the band edges only. The gain at 1.5 GHz will then be calculated. The response will be found to look similar to this curve. If a greater degree of flatness were necessary, additional matching elements would have to be added. We could then design for 10 dB gain at three different frequencies, or more if necessary. Three frequencies would generally be the practical limit to the graphical design approach we have been using.

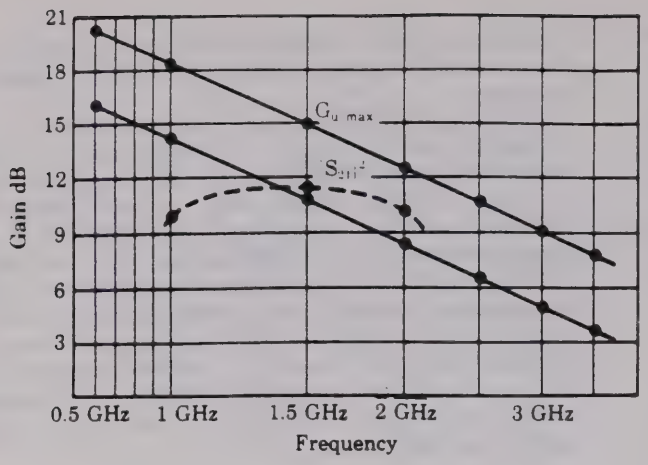

Figure 126

When matching is required at more than three frequencies, computer-aided design techniques are generally employed.

The schematic again looks similar to that which we had in the previous two examples (Fig. 127).

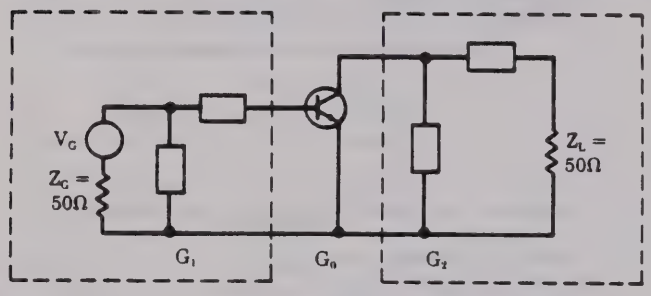

Figure 127

The design approach is to:

1. Match the input for the best compromise between low and high frequency noise figure. In this case, it is important to keep the number of matching elements to a minimum for the reasons cited earlier. It might be possible to get an additional 0.2 dB improvement in noise figure with one additional element, but the extra element might, in turn, add an additional insertion loss at 0.2 dB or more.
2. The next step is to determine the gain contribution at the input as a result of the noise figure matching. This then allows us to calculate the desired gain at the output from the design objective.
3. The output matching elements are then selected, completing the design.

Let's first plot S_{11}* for 1 and 2 GHz and then plot the points resulting in minimum noise figure for these frequencies (Fig. 128).

[1] For the particular transistor measured. We want to emphasize that the methodology followed in these design examples is more important than the specific numbers.

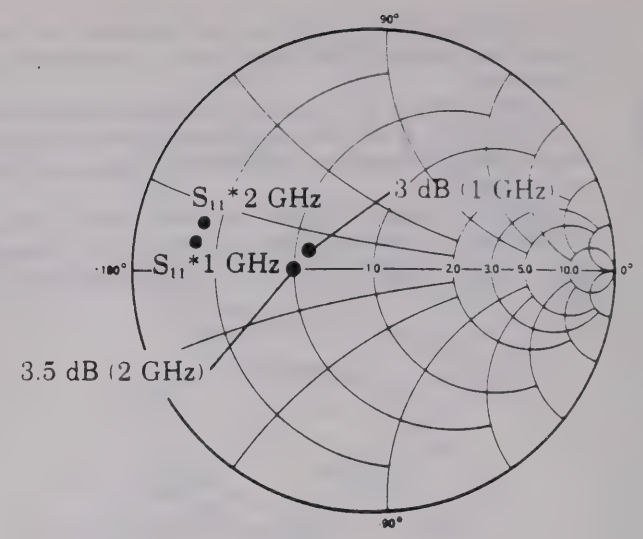

Figure 128

To match the input for minimum noise figure we must first choose a combination of elements which gives the best compromise at the two design frequencies. On the plot we see that a shunt capacitor followed by a series inductor will provide a source impedance such that the noise figure will be less than 3.5 dB at 1 GHz and less than 4.5 dB at 2 GHz[1] (Fig. 129). At both frequencies we are about as close as is practical to the theoretical minimum noise figure for the device.

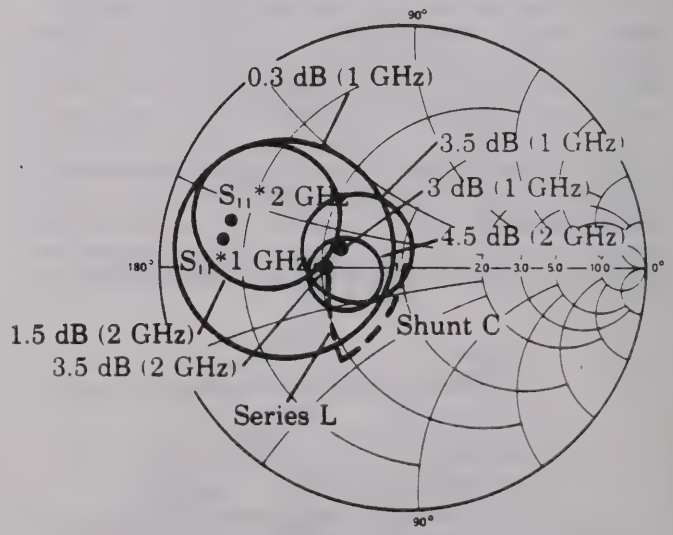

Figure 129

The constant gain circles, which intersect the points established by the input matching network, are calculated and found to have the values 0.3 dB at 1 GHz and 1.5 dB at 2 GHz.

The desired gain due to output matching can now be calculated and found to be −4.3 dB at 1 GHz and +0.5 dB at 2 GHz (Fig. 130).

AT 1 GHz

$$G_{Tu} = G_1 + G_0 + G_2 = 10 \text{ dB}$$
$$.3 + 14 + G_2 = 10 \text{ dB}$$
$$G_2 = -4.3 \text{ dB}$$

AT 2 GH_z

$$G_{Tu} = G_1 + G_0 + G_2 = 10 \text{ dB}$$
$$1.5 + 8 + G_2 = 10 \text{ dB}$$
$$G_2 = +.5 \text{ dB}$$

Figure 130

The constant gain circles having these gain values are then plotted as shown (Fig. 131). A trial-and-error process is followed to find the proper matching elements to provide the required output match at the two frequencies. Let's start from the 50-ohm point on the Smith Chart and add an **arbitrary** negative series reactance and the appropriate negative shunt susceptance to land on the 0.5 dB gain circle at 2 GHz. We then determine where these matching elements will bring us at 1 GHz and, in this case, we fall short of reaching the proper gain circle (Fig. 132). By increasing the capacitive reactance we find a combination that lands on both circles and the design is complete (Fig. 133).

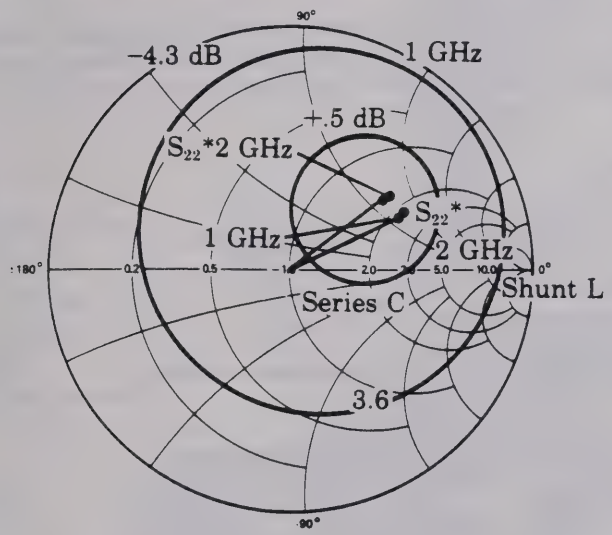

Figure 131

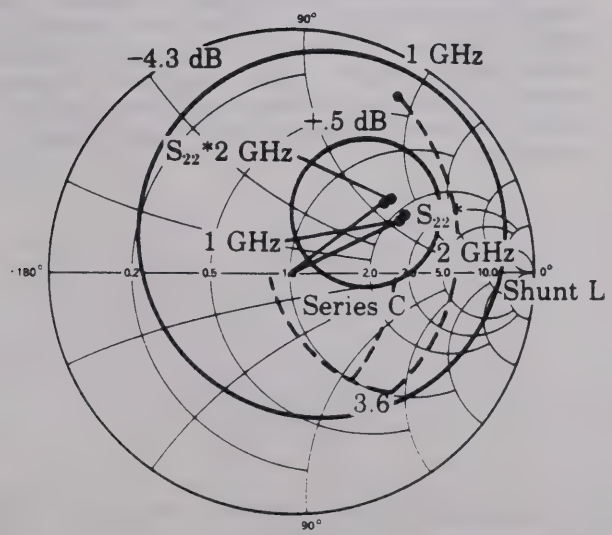

Figure 132

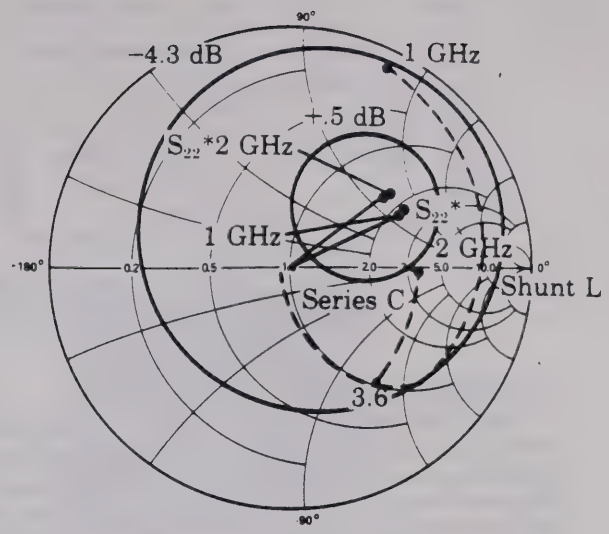

Figure 133

So far, by our design procedure we have forced the gain to be 10 dB at 1 and 2 GHz. The question naturally arises, what happens between these two frequencies? From the matching element values already determined, we can calculate the matching network impedances at **1.5** GHz and then determine the constant gain circles which intersect those points.

For this case, we find that the output gain circle has a value of −0.25 dB and the input gain circle, a value of +1 dB. The gain of the device at 1.5 GHz is 10.5 dB. Hence the overall gain of the amplifier at 1.5 GHz is 11.25 dB.

In summary form, the contribution of the three amplifier gain blocks at the three frequencies can be seen (Fig. 134). If the resulting gain characteristic was not sufficiently flat, we would add an additional matching element at the output and select values for this added element such that we landed on the original gain circles for 1 and 2 GHz, but on the −1.5 dB rather than −0.25 dB circle at 1.5 GHz. This would give us a gain for the amplifier of 10 dB at 1, 1.5, and 2 GHz with some ripple in between.

AT 1.0 GHz

$$G_1 + G_0 + G_2 = .3 + 14 - 4.3 = 10 \text{ dB}$$

AT 1.5 GHz

$$G_1 + G_0 + G_2 = 1.0 + 10.5 - .25 = 11.25 \text{ dB}$$

AT 2.0 GHz

$$G_1 + G_0 + G_2 = 1.5 + 8.0 + .5 = 10 \text{ dB}$$

Figure 134

If, however, we were satisfied with the first gain-frequency characteristic, our final schematic would look like this (Fig. 135).

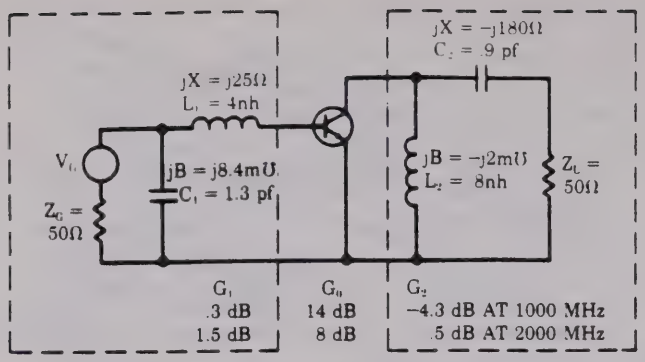

Figure 135

D. Multistage Design

While the examples we have just completed are single stage amplifiers, the techniques presented are equally applicable to multistage amplifier design. The difference in a multistage design is that the source and load impedances for a given stage of the amplifier are, in general, not 50 ohms but are rather an arbitrary complex impedance. In certain cases, this impedance might even have a negative real part.

Multistage design can be handled by simply shifting the reference impedance to the appropriate point on the Smith Chart. This is illustrated in the following example.

Let's now concentrate on the matching network design between two identical stages (Fig. 136). For the first stage, as we have seen, there is a gain of 1.3 dB attainable by matching the output to 50 ohms. Similarly, there is a gain of 3 dB attainable by matching 50 ohms to the input of the second stage. We can then think of a gain of 4.3 dB being attainable by matching the output impedance of the first stage to the input impedance of the second stage.

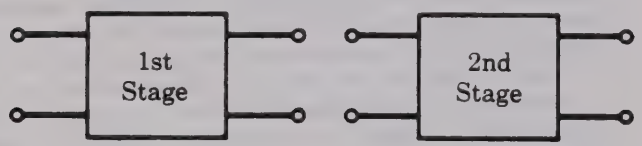

G_{11}	G_{01}	G_{21}	G_{12}	G_{02}	G_{22}
3.0 dB	14 dB	1.3 dB	3.0 dB	14 dB	1.3 dB
3.0 dB	14 dB	4.3 dB		14.dB	1.3 dB

Figure 136

The constant gain circles for the first stage output would then be plotted on the Smith Chart (Fig. 137). The maximum gain is now 4.3 dB. The gain circle that intersects the point represented by the second stage's S_{11} has a value of 0 dB.

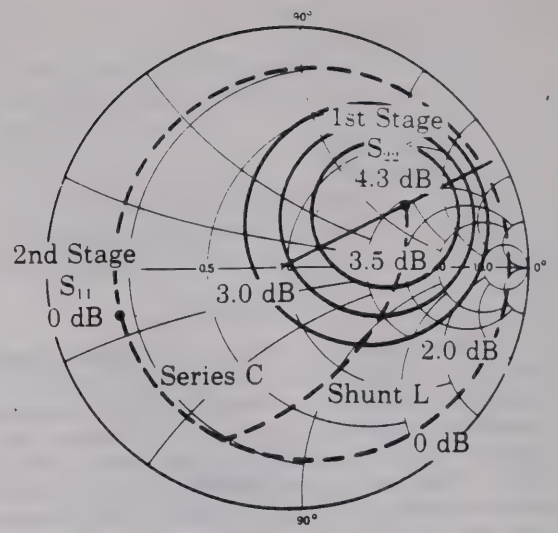

Figure 137

To design for a specific interstage gain, we could, as before, add a series capacitor followed by a shunt inductor—except in this case we start from the input impedance of the second stage, S_{11}, rather than the 50-ohm point.

The resulting interstage matching network looks like this. As you can see, the design of multistage amplifiers is as easily handled as single stage designs (Fig. 138).

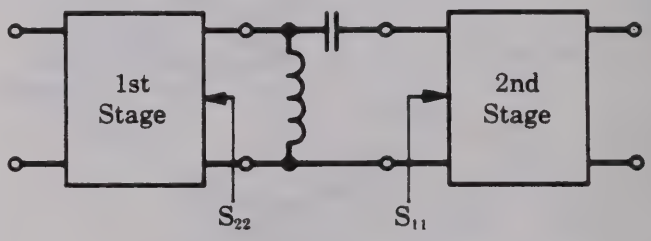

Figure 138

Summary

The measurement and design techniques demonstrated in this video-tape seminar are presently being used by engineers in advanced R&D labs throughout the world. When coupled with design and optimization computer programs, engineers will have at their disposal the most powerful and rapid design tools available.

HP 8410S Network Analyzer System

HEWLETT hp PACKARD

For more information, call your local HP sales office or East (301) 258-2000 • Midwest (312) 255-9800 • South (404) 955-1500 • West (213) 877-1282; Or write, Hewlett-Packard, 1501 Page Mill Rd., Palo Alto, California 94304
In Europe, Hewlett-Packard S.A., 7, rue du Bois-du-lan, PO Box, CH-1217 Meyrin 2-Geneva, Switzerland. **In Japan,** Yokogawa-Hewlett-Packard Ltd., 29-21, Takaido-Higashi 3-chome, Suginami-ku, Tokyo 168.

5952-1087

PRINTED IN U.S.A.

S-Parameters....

circuit analysis and design

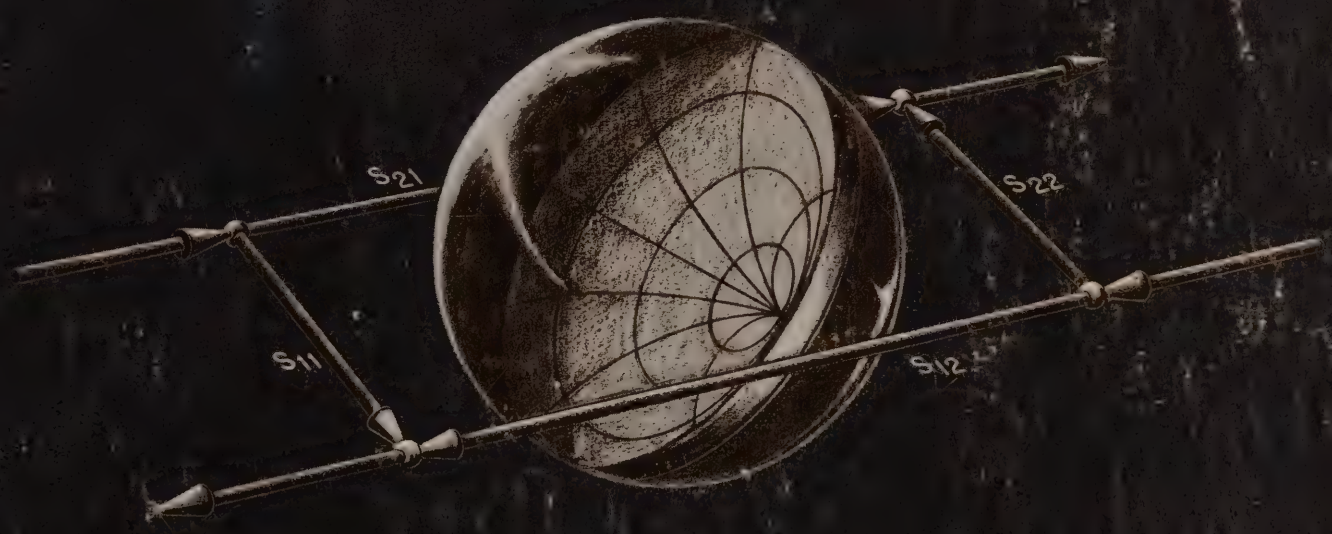

HEWLETT hp PACKARD

application note 95

WHAT ARE "S" PARAMETERS?

"S" parameters are reflection and transmission coefficients, familiar concepts to RF and microwave designers. Transmission coefficients are commonly called gains or attenuations; reflection coefficients are directly related to VSWR's and impedances.

Conceptually they are like "h," "y," or "z" parameters because they describe the inputs and outputs of a black box. The inputs and outputs are in terms of power for "s" parameters, while they are voltages and currents for "h," "y," and "z" parameters. Using the convention that "a" is a signal into a port and "b" is a signal out of a port, the figure below will help to explain "s" parameters.

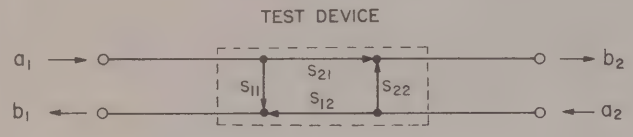

In this figure, "a" and "b" are the square roots of power; $(a_1)^2$ is the power incident at port 1, and $(b_2)^2$ is the power leaving port 2. The diagram shows the relationship between the "s" parameters and the "a's" and "b's." For example, a signal a_1 is partially reflected at port 1 and the rest of the signal is transmitted through the device and out of port 2. The fraction of a_1 that is reflected at port 1 is s_{11}, and the fraction of a_1 that is transmitted is s_{21}. Similarly, the fraction of a_2 that is reflected at port 2 is s_{22}, and the fraction s_{12} is transmitted.

The signal b_1 leaving port 1 is the sum of the fraction of a_1 that was reflected at port 1 and the fraction of a_2 that was transmitted from port 2.

Thus, the outputs can be related to the inputs by the equations:

$$b_1 = s_{11}\, a_1 + s_{12}\, a_2$$
$$b_2 = s_{21}\, a_1 + s_{22}\, a_2$$

When $a_2 = 0$, and when $a_1 = 0$,

$$s_{11} = \frac{b_1}{a_1}, \quad s_{21} = \frac{b_2}{a_1} \qquad s_{12} = \frac{b_1}{a_2}, \quad s_{22} = \frac{b_2}{a_2}$$

The setup below shows how s_{11} and s_{21} are measured.

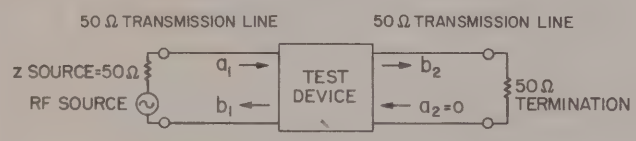

Port 1 is driven and a_2 is made zero by terminating the 50 Ω transmission line coming out of port 2 in its characteristic 50 Ω impedance. This termination ensures that none of the transmitted signal, b_2, will be reflected toward the test device.

Similarly, the setup for measuring s_{12} and s_{22} is:

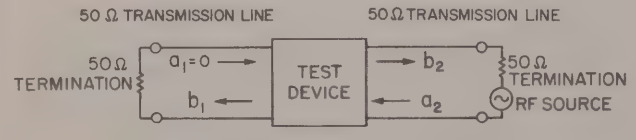

If the usual "h," "y," or "z" parameters are desired, they can be calculated readily from the "s" parameters. Electronic computers and calculators make these conversions especially easy.

WHY "S" PARAMETERS

Total Information

"S" parameters are vector quantities; they give magnitude and phase information. Most measurements of microwave components, like attenuation, gain, and VSWR, have historically been measured only in terms of magnitude. Why? Mainly because it was too difficult to obtain both phase and magnitude information.

"S" parameters are measured so easily that obtaining accurate phase information is no longer a problem. Measurements like electrical length or dielectric coefficient can be determined readily from the phase of a transmission coefficient. Phase is the difference between only knowing a VSWR and knowing the exact impedance. VSWR's have been useful in calculating mismatch uncertainty, but when components are characterized with "s" parameters there is no mismatch uncertainty. The mismatch error can be precisely calculated.

Easy To Measure

Two-port "s" parameters are easy to measure at high frequencies because the device under test is terminated in the characteristic impedance of the measuring system. The characteristic impedance termination has the following advantages:

1. The termination is accurate at high frequencies . . . it is possible to build an accurate characteristic impedance load. "Open" or "short" terminations are required to determine "h," "y," or "z" parameters, but lead inductance and capacitance make these terminations unrealistic at high frequencies.

2. No tuning is required to terminate a device in the characteristic impedance . . . positioning an "open" or "short" at the terminals of a test device requires precision tuning. A "short" is placed at the end of a transmission line, and the line length is precisely varied until an "open" or "short" is reflected to the device terminals. On the other hand, if a characteristic impedance load is placed at the end of the line, the device will see the characteristic impedance regardless of line length.

3. Broadband swept frequency measurements are possible . . . because the device will remain terminated in the characteristic impedance as frequency changes. However, a carefully reflected "open" or "short" will move away from the device terminals as frequency is changed, and will need to be "tuned-in" at each frequency.

4. The termination enhances stability . . . it provides a resistive termination that stabilizes many negative resistance devices, which might otherwise tend to oscillate.

An advantage due to the inherent nature of "s" parameters is:

5. Different devices can be measured with one setup . . . probes do not have to be located right at the test device. Requiring probes to be located at the test device imposes severe limitations on the setup's ability to adapt to different types of devices.

Easy To Use

Quicker, more accurate microwave design is possible with "s" parameters. When a Smith Chart is laid over a polar display of s_{11} or s_{22}, the input or output impedance is read directly. If a swept-frequency source is used, the display becomes a graph of input or output impedance versus frequency. Likewise, CW or swept-frequency displays of gain or attenuation can be made.

"S" parameter design techniques have been used for some time. The Smith Chart and "s" parameters are used to optimize matching networks and to design transistor amplifiers. Amplifiers can be designed for maximum gain, or for a specific gain over a given frequency range. Amplifier stability can be investigated, and oscillators can be designed.

These techniques are explained in the literature listed at the bottom of this page. Free copies can be obtained from your local Hewlett-Packard Sales Representative.

References:

1. "Transistor Parameter Measurements," Application Note 77-1, February 1, 1967.
2. "Scattering Parameters Speed Design of High Frequency Transistor Circuits," by Fritz Weinert, Electronics, September 5, 1966.
3. "S" Parameter Techniques for Faster, More Accurate Network Design," by Dick Anderson, Hewlett-Packard Journal, February 1967.
4. "Two Port Power Flow Analysis Using Generalized Scattering Parameters," by George Bodway, Microwave Journal, May 1967.
5. "Quick Amplifier Design with Scattering Parameters," by William H. Froehner, Electronics, October 16, 1967.

S-Parameters .... Circuit Analysis and Design

APPLICATION NOTE 95

A Collection of Articles Describing
S-Parameter Circuit Design and Analysis

SEPTEMBER 1968

INTRODUCTION

THE STATE OF HIGH-FREQUENCY CIRCUIT DESIGN

The designer of high-frequency circuits can now do in hours what formerly took weeks or months. For a long time there has been no simple, accurate way to characterize high-frequency circuit components. Now, in a matter of minutes, the frequency response of the inputs and outputs of a device can be measured as s parameters.

As shown in some of the articles in this application note, an amplifier circuit can be completely designed on a Smith Chart with s-parameter data. Circuit design is greatly accelerated by using small computers or calculators to solve lengthy vector design equations. This leads to some creative man-machine interactions where the designer can "tweek" his circuit via the computer and see how its response is affected The computer can search through hundreds of thousands of possible designs and select the best one. An even more powerful approach that makes one's imagination run away with itself is to combine the measuring equipment and the computer as in the HP 8541A. Theoretically, one could plug in a transistor, specify the type of circuit to be designed, and get a readout of the optimal design.

This note consists primarily of a collection of recent articles describing the s-parameter design of high-frequency circuits. Following the articles is a brief section describing the rather straightforward technique of measuring s parameters. Many useful design equations and techniques are contained in this literature, and amplifier design, stability, and high-frequency transistor characterization are fully discussed.

TABLE OF CONTENTS

SECTION I

MICROWAVE TRANSISTOR CHARACTERIZATION

Julius Lange describes the parameters he feels are most important for characterizing microwave transistors. These include the two-port s parameters, MSG (maximum stable gain), G_{max} (maximum tuned or maximum available gain), K (Rollett's stability factor), and U (unilateral gain). The test setups used for measuring these parameters are described and a transistor fixture for TI-line transistors plus a slide screw tuner designed by Lange are shown. The article concludes with equations relating y parameters, h parameters, MSG, G_{max}, K, and U to the two-port s parameters.

TEXAS INSTRUMENTS
INCORPORATED
13500 NORTH CENTRAL EXPRESSWAY • DALLAS, TEXAS
COMPONENTS GROUP

MICROWAVE TRANSISTOR CHARACTERIZATION INCLUDING S-PARAMETERS*

by

Julius Lange

A. INTRODUCTION

Since introduction of transistors with much improved high frequency capabilities, new techniques and hardware for transistor characterization have been developed. Older methods, such as characterization by H or Y parameters, are not suitable above 1 GHz since at these frequencies the package parasitics affect the response significantly. Also, test equipment for measuring those parameters directly is not available.

When measurements above 1 GHz are made on discrete components such as transistors or diodes the following basic difficulties arise:

1) Terminals of the intrinsic device (semiconductor chip) are not directly accessible; that is, between the device and the measurement apparatus there is interposed a network consisting of package parasitics, transmission lines, etc. Thus, the device properties have to be measured with respect to some convenient external terminals, and then referred back to the intrinsic device via a mathematical transformation. This makes characterization in terms of invariant parameters such as maximum available gain (maximum tuned gain), maximum stable gain, and unilateral gain very attractive.

2) Special care must be taken to ensure that the tuning and dc bias networks do not present reactive, that is non-dissipative, impedances to the transistor at low frequencies causing insufficient loading, which can easily result in oscillations. The use of slide-screw tuners and

---

* The majority of the data presented in this paper was developed by Texas Instruments Incorporated under Contract No. DA 28-043 AMC-01371(E) for the United States Army Electronics Command, Fort Monmouth, New Jersey.

characterization in terms of S-parameters greatly alleviates this problem.

3) If open or short circuit terminations are desired, as is necessary for H, Y, or Z parameter measurements, resonant lines must be used. This causes a high degree of frequency sensitivity which makes broadband swept frequency measurements impossible and may allow the transistor to oscillate. Since broadband 50 Ω terminations are easily obtainable using standard components, S-parameter measurements are more practical.

4) The sources of error are multiplied and special attention must be paid to consistency and accurate calibration. A consistent set of reference planes must be established and losses and discontinuities must be held to a minimum.

B. S-PARAMETER MEASUREMENTS

The small signal response of a discrete two-port device is defined in terms of four variables v_1, i_1, v_2, and i_2, the voltages, and currents at the input and output terminals respectively as shown in Figure 1. Any two of the variables can be chosen as the independent variables making the other two dependent variables. This gives rise to the familiar Z, Y, and H parameters. In the S-parameter representation linear combinations of the currents and voltages are used as the independent and dependent variables. The independent variables are defined as:

$$a_1 = \frac{1}{2\sqrt{Z_o}} (v_1 + Z_o i_1)$$

$$a_2 = \frac{1}{2\sqrt{Z_o}} (v_2 + Z_o i_2)$$

the dependent variables as:

$$b_1 = \frac{1}{2\sqrt{Z_o}} (v_1 - Z_o i_1)$$

$$b_2 = \frac{1}{2\sqrt{Z_o}} (v_2 - Z_o i_2)$$

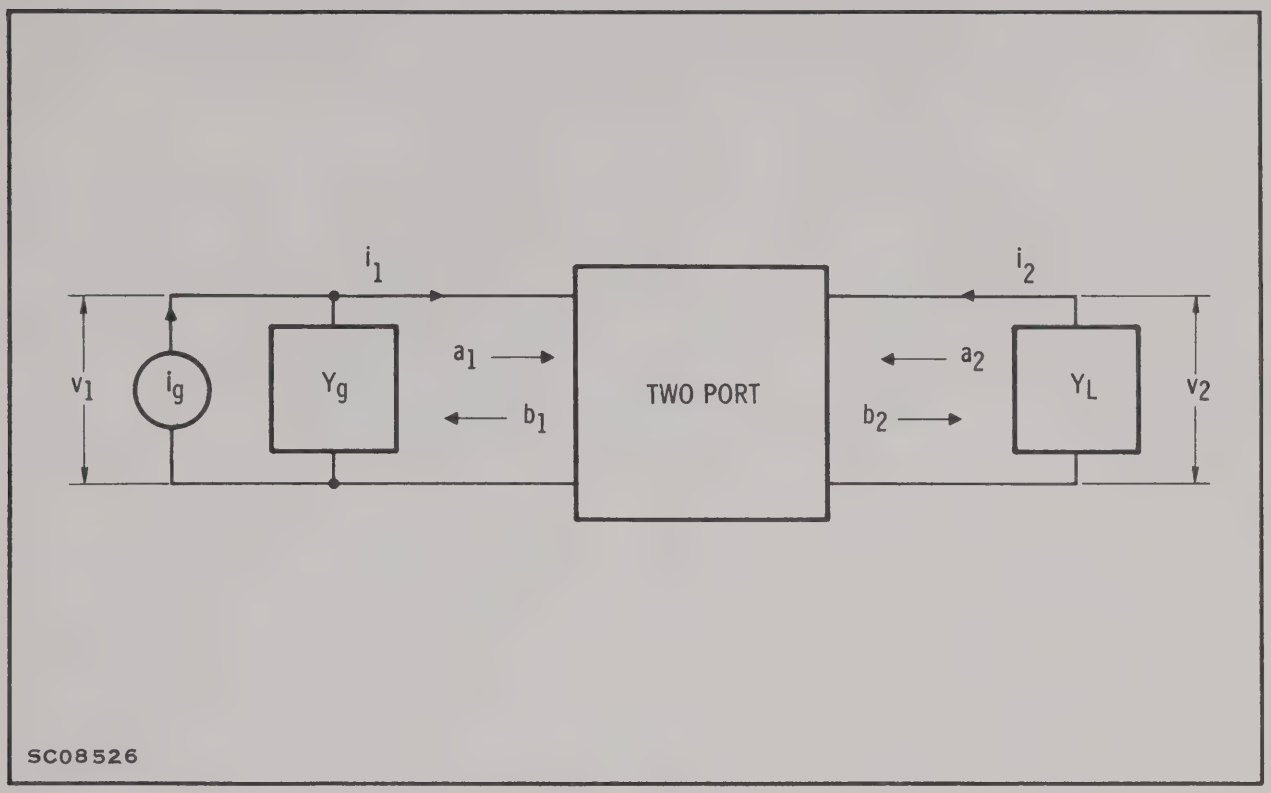

Figure 1. Two-Port Relations

Here Z_o is a real impedance called the characteristic impedance. Thus, the S-parameter matrix is defined by:

$$b_1 = S_{11}\, a_1 + S_{12}\, a_2$$

$$b_2 = S_{21}\, a_1 + S_{22}\, a_2$$

By slightly changing the definitions, complex values of Z_o different for the two ports can be used. But these have theoretical significance only and are impractical for measurements. Since 50 Ω coaxial transmission line components such as slotted lines and directional couplers are readily available, Z_o is generally taken to be 50 Ω.

At times a_1 and a_2 are referred to as the "incident voltage waves" and b_1 and b_2 as the "reflected voltage waves". If the device is terminated in Z_o at the input and output, S_{11} and S_{22} are the input and output reflection coefficients, $|S_{21}|^2$ and $|S_{12}|^2$ are the forward and reverse insertion gains, and $\angle S_{21}$ and $\angle S_{12}$ are the insertion phase shifts. Also $|a_1|^2$ is the power available from the generator (internal impedance $=Z_o$) and $|b_2|^2$ is the power dissipated in the load (load$=Z_o$). A derivation of these relationships is given in the appendix.

The S-parameters completely determine the small signal behavior of a device. Formulas for deriving the Y and H parameters and various gain and stability relationships from the S-parameters are given in the appendix.

The S-parameters can be measured using commercial test sets such as the -hp- 8410A network analyzer. A block diagram of the measurement setups is shown in Figures 2 and 3. Figure 2 illustrates the measurement of the transmission coefficients S_{12} and S_{21}. A swept-frequency source feeds a power divider which has two outputs, a reference channel and a test channel. The device to be measured is inserted into the text channel and a line stretcher is inserted into the reference channel. The line stretcher compensates for excess electrical length in the device. Both channels are then fed to the test set which measures the complex ratio between the two signals. This ratio is the desired parameter.

The reflection coefficients S_{11} and S_{22} are measured using the setup shown in Figure 3. There the swept-frequency source is fed into a dual-directional coupler. One port of the device is connected to the measurement port of the coupler the other port is terminated in a 50 Ω load. The reference output of the coupler which samples the incident wave is fed to the complex ratio test set via a line stretcher. The test output which samples the wave reflected from the device is fed directly to the test set. The line stretcher allows the plane at which the measurement is made to be extended past the connector to the unknown device.

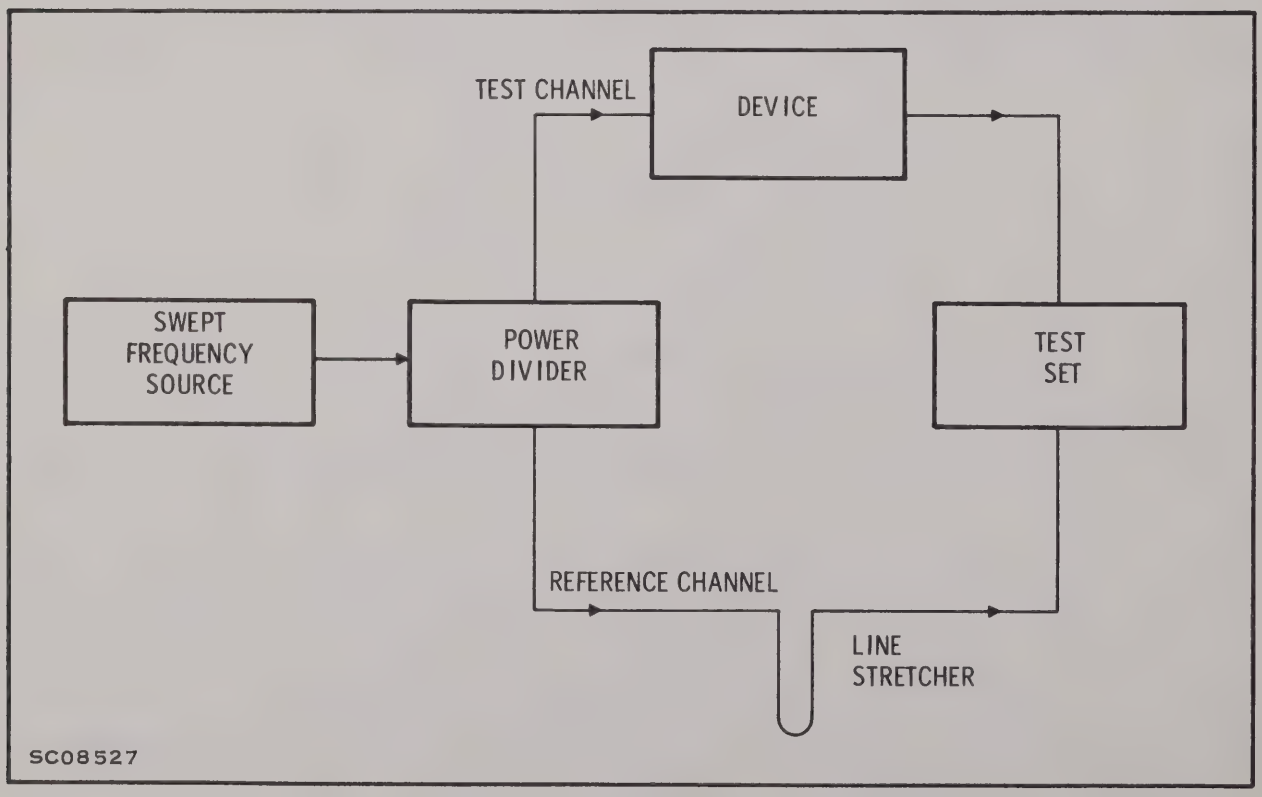

Figure 2. Setup for Measuring S_{12} and S_{21}

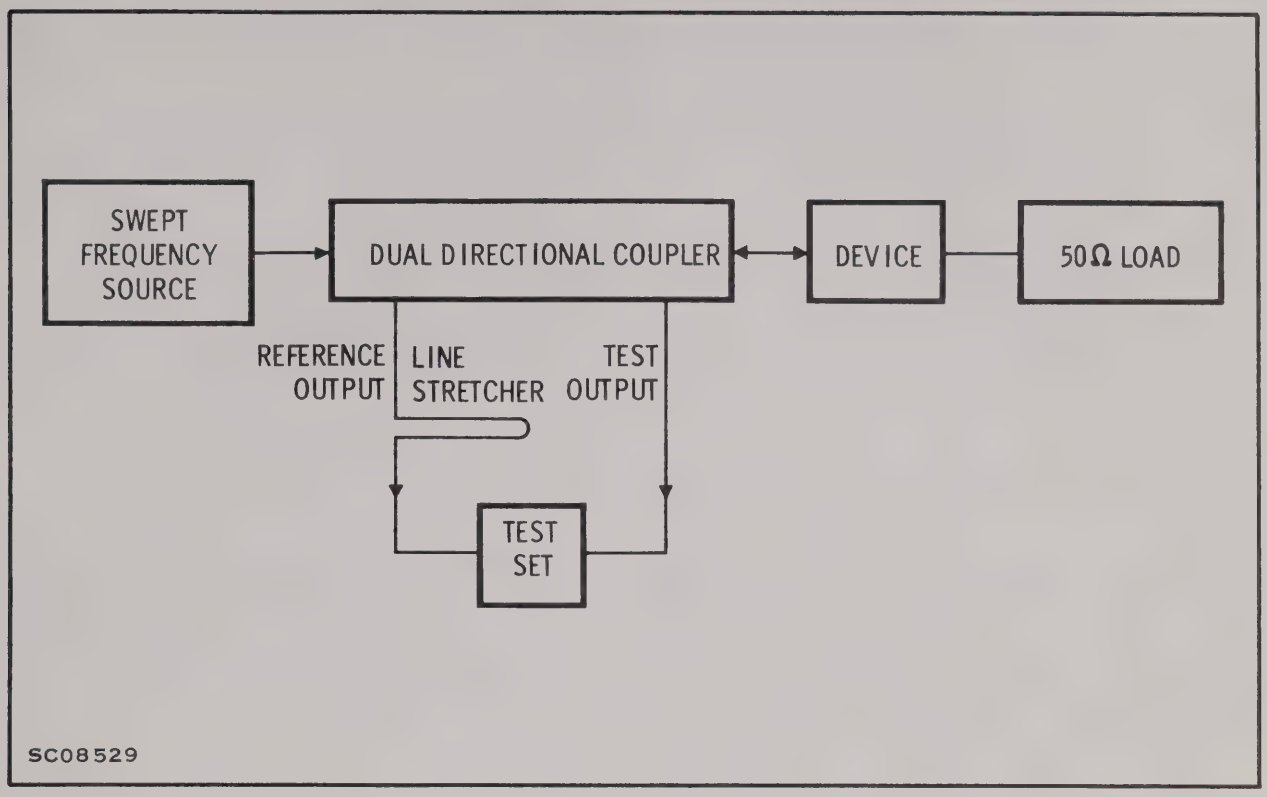

Figure 3. Setup for Measuring S_{11} and S_{22}

The stretchable lines in the measurement setups, Figures 2 and 3, allow the input and output measurement planes to be placed anywhere. Care must be taken to ensure that all four S-parameters are measured with reference to the same planes. Sexless connectors such as GR900 or APC-7 are used to establish the reference planes. These connectors allow precision shorts to be placed exactly at the mating planes of the connectors.

Since S_{11} and S_{22} are reflection coefficients. They can be measured with a slotted line. This is the most accurate method; it is, however, cumbersome and unsuited for swept frequency measurements. The reflectometer method described above is much more convenient. The transmission coeficients, S_{12} and S_{21} cannot be measured with a slotted line.

Test fixtures and dc bias injection networks used for S-parameter measurements must have low loss and very low VSWR. Design principles will be discussed below in the section on test fixtures.

C. GAIN AND STABILITY MEASUREMENTS

While it is true that the S-parameters of transistor completely and uniquely characterize it for the small signal condition several gain and stability parameters (MSG, GMAX, K, and U) are measured for the following reasons:

The S-parameters do not give any direct indication of the level of performance of the device as an amplifier.

Even though these parameters can be calculated from the S-parameters, direct measurement is preferable to calculation by formula because of round-off errors.

These parameters are invariant under various transformations. This makes them insensitive to header parasitics and reference plane location. Thus the parameters are the same for the bare chip as for the packaged device. This allows one to evaluate the intrinsic capabilities of the chip itself.

Gain and stability parameters are defined below:

1. MSG (Maximum Stable Gain)-- is the square root of the ratio of the forward to the reverse power gain. The only requirement is that the device terminations be the same for both measurements. MSG is uneffected by input or output parasitics but it is sensitive to feedback parasitics such as common lead inductance or feedthrough capacitance.

2. GMAX (Maximum Tuned Gain-Maximum Available Gain) -- is the forward power gain when the input and the output are simultaneously conjugately matched. GMAX is only defined for an unconditionally stable device ($K > 1$, see below). It is uneffected by lossless input or output parasitics but it is sensitive to loss or feedback.

3. K (Rollett's Stability Factor [1]) is a measure of oscillatory tendency. For $K < 1$ the device is potentially unstable and can be induced into oscillation by the application of some combination of passive load and source admittances. For $K > 1$ the transistor is unconditionally stable, that is in the absence of an external feedback path, no passive load or source admittance will induce oscillations. K is the inverse of Linvill's C factor and plays an important part in amplifier design.

For $K > 1$, K can be computed from the MSG and GMAX by the formula:

$$K = \frac{1}{2}\left(\frac{MSG}{GMAX} + \frac{GMAX}{MSG}\right)$$

For $K < 1$, K must be computed from the S-parameters as shown in the appendix.

4. U (Unilateral Gain-Mason Invariant[2]) is the most unique figure of merit for a device. It is defined as the forward power gain in a feedback amplifier whose reverse gain has been adjusted to zero by a lossless reciprical feedback network. Because of the feedback loop employed in the measurement of UG, the transistor may be imbedded in any lossless-reciprocal network without changing its unilateral gain. This makes unilateral gain invariant with respect to any lossless header parasitics or changes in common lead configuration.

Alternately U can be derived from MSG, K, and θ, the difference between forward and reverse phase shift. This difference, being the "phase of MSG" is invariant under input and output transformations like the MSG itself. The formula for U is[4]:

$$U = \frac{MSG - 2\cos\theta + MSG^{-1}}{2(K - \cos\theta)} \simeq \frac{MSG}{2(K - \cos\theta)}$$

Figure 4 shows a setup for measuring MSG, GMAX, K, and U in one simple procedure as follows:

Tune for maximum forward gain and record gain (which is GMAX) and phase.

Turn device and tuners around and record gain and phase.

Get gain ratio and phase difference, as described above, and calculate MSG, K, and U.

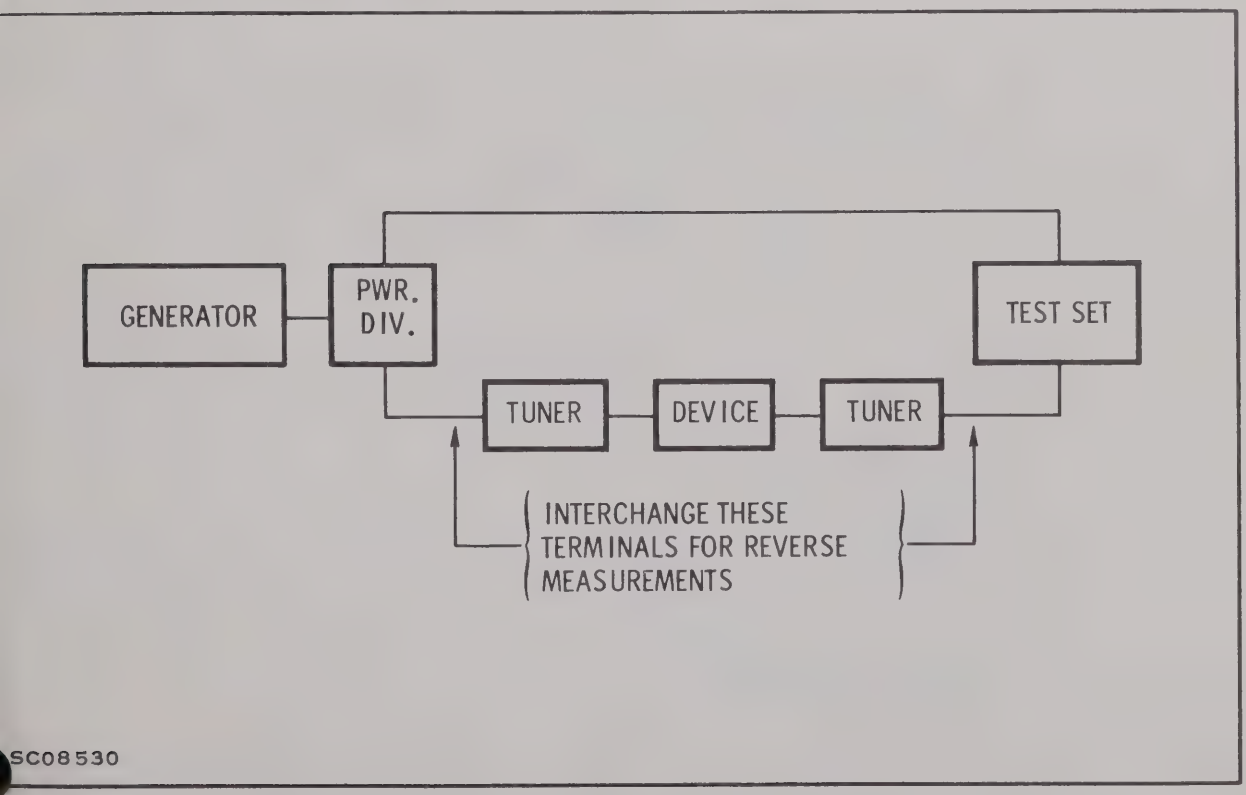

Figure 4. Setup for Measuring MSG, GMAX, K, U

D. TEST FIXTURES

Measurements at frequencies above 1 GHz require test fixtures which have low loss and VSWR. An example which fulfills these requirements is the improved mount for TI-Line ® packages shown in Figure 5. This mount contains two low VSWR coax to stripline adaptors which feed the input and output 50 Ω tri-plate strip transmission lines. These lines are carried to the very edge of the package. Contact to the input and output leads is made by clamping the flat leads between the striplines and the upper dielectric.

Another important feature of the mount is the grounding scheme. For a three-terminal device in a tri-plate structure, it is very important to ground the device to both ground planes at the same point. Therefore, the flange of the transistor package is clamped between the two ground planes. The ground lead of the package serves no purpose other than mechanical alignment.

When designing tuning and bias insertion networks for use above 1 GHz the low frequency response must be taken into account, since most devices have high gain at low frequencies and will break into oscillations when insufficiently loaded. For S-parameter measurements the device terminations should present 50 Ω at least down to 10 MHz. This can best be accomplished by inserting high capacitance dc blocks into the outer conductors of the transmission lines leadings to the device and providing dc returns through T-pad attenuators. High quality wide-band bias tees can also be used.

For making tuned power gain measurements, such as MAG and U, the special slide-screw tuner shown in Figure 6 has been built. It consists of a coaxial 50-Ω characteristic impedance slab line (round center conductor; two slabs as outer conductor ground return) provided with an anodized aluminum tuning slug whose position and penetration are adjustable. This tuner has the following advantages over the conventional multiple-stub tuners.

The distance between the device terminals and the tuning elements (movable slugs) can be made very small. This discourages parasitic oscillations and extends the usable frequency range to 9 GHz, the limiting frequency of the connectors.

The tuning elements are "transparent" at dc and low frequencies. Thus the dc bias elements can be placed outside of the tuning elements in a low VSWR portion of the system. Consequently losses are reduced and made independent of the VSWR of the transistor, making it easy to account for them.

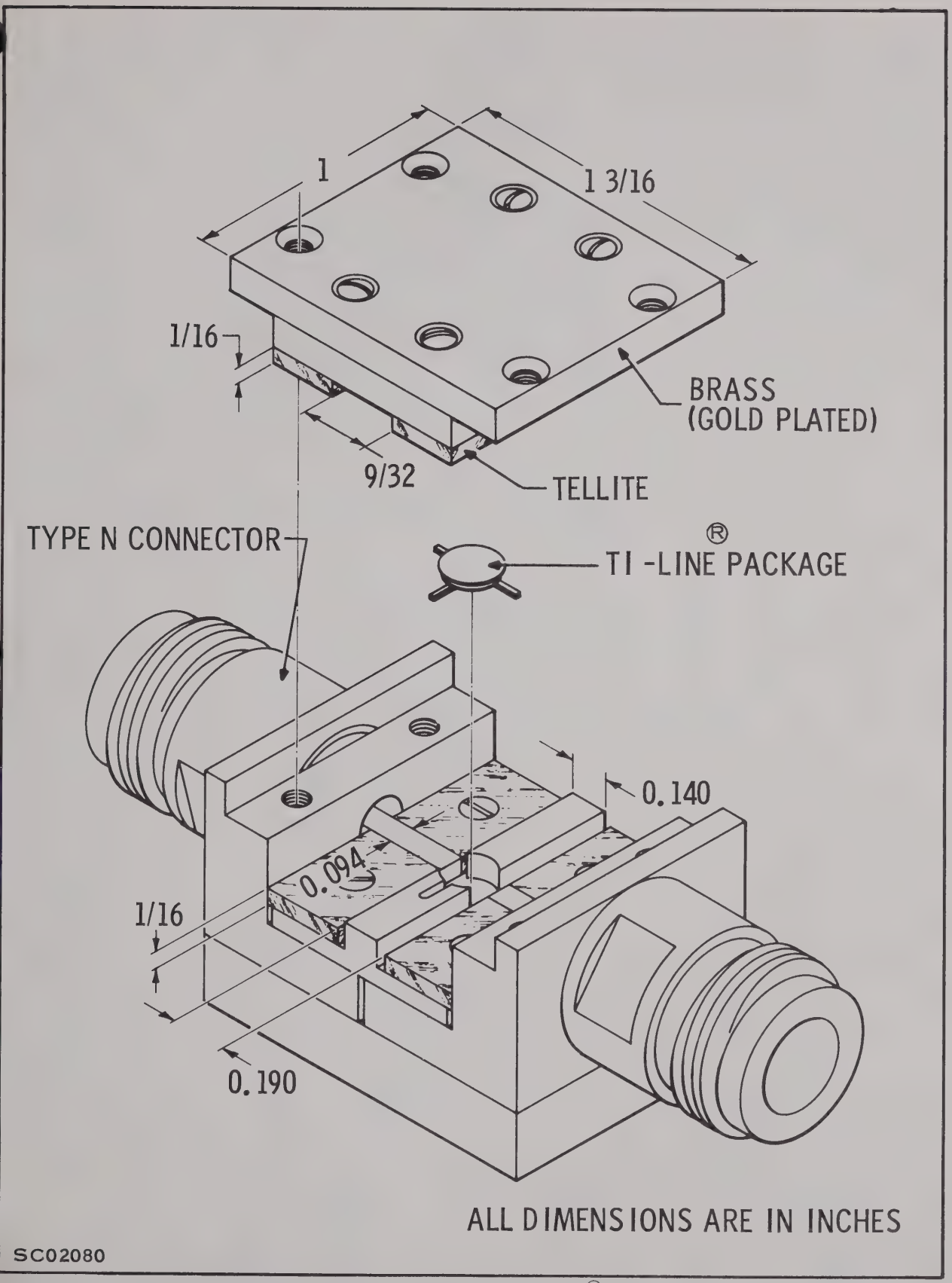

Figure 5. Improved TI-Line® Mount

SC03408

If high-capacitance outer blocks and T-pad attenuators are used for biasing the transistor sees 50 Ω at both input and output at low frequencies, resulting in heavy loading which very effectively suppresses oscillatory tendencies.

VSWRs as high as 30 have been achieved at 1 GHz while still maintaining low loss.

LITERATURE CITED

1. J. M. Rollett, "Stability and Power-Gain Invariants of Linear Twoports," IRE Transactions on Circuit Theory, Vol. CT-9, pp. 29-32; March, 1962.

2. S. J. Mason, "Power Gain in Feedback Amplifiers," MIT Research Lab of Electronics, Tech. Rep. 257; August 25, 1953. Also IRE Trans., Vol. CT-1, pp. 20-25; June 1954.

3. J. Lange, "A Much Improved Apparatus for Measuring the Gain of Transistors at GHz Frequencies", IEEE Transactions on Circuit Theory, Vol. CT-13, December, 1966.

4. A. Singhakowinta and A. R. Boothroyd, IEEE Transon Circuit Theory, Vol. CT-11 p. 169, March 1964.

APPENDIX

SPECIAL S-PARAMETER RELATIONSHIPS

Let $= Y_g = Y_L = Z_0^{-1}$

S_{11} = input reflection coefficient

S_{22} = output reflection coefficient

$|a_1|^2 = \frac{i_g^2}{4 Y_g}$ = power available from generator

$|b_2|^2 = Y_L |v_2|^2$ = output power

therefore

$|S_{21}|^2$ = forward transducer (insertion) gain

$|S_{12}|^2$ = reverse transducer gain

Derivations:

Let Z_1 = input impedance with $Y_L = Z_0^{-1}$

Then

$$S_{11} = \frac{b_1}{a_1} = \frac{v_1 - Z_0 i_1}{v_1 + Z_0 i_1} = \frac{Z_1 - Z_0}{Z_1 + Z_0}$$

$$i_2 = -Y_L v_2$$

$$b_2 = \frac{1}{2\sqrt{Z_0}} \left[v_2 - Z_0 (-Y_L v_2) \right] = v_2 \sqrt{Y_L}$$

$$i_1 = i_g - Y_g v_1$$

$$a_1 = \frac{1}{2\sqrt{Z_0}} (v_1 + Z_0 i_g - Z_0 Y_g v_1) = \frac{1}{2} i_g \sqrt{Z_0} = \frac{i_g}{2\sqrt{Y_g}}$$

Conversion Formulas

$$Y_{11} = \frac{S_{12} S_{21} + (1 - S_{11})(1 + S_{22})}{-S_{12} S_{21} + (1 + S_{11})(1 + S_{22})} Z_0^{-1}$$

$$Y_{12(21)} = \frac{-2S_{12(21)}}{-S_{12} S_{21} + (1 + S_{11})(1 + S_{22})} Z_0^{-1}$$

$$Y_{22} = \frac{S_{12} S_{21} + (1 + S_{11})(1 - S_{22})}{-S_{12} S_{21} + (1 + S_{11})(1 + S_{22})} Z_0^{-1}$$

$$H_{11} = \frac{-S_{12} S_{21} + (1 + S_{11})(1 + S_{22})}{S_{12} S_{21} + (1 - S_{11})(1 + S_{22})} Z_0$$

$$H_{12} = \frac{2S_{12}}{S_{12} S_{21} + (1 - S_{11})(1 + S_{22})}$$

$$H_{21} = \frac{-2S_{21}}{S_{12} S_{21} + (1 - S_{11})(1 + S_{22})}$$

$$H_{22} = \frac{-S_{12} S_{21} + (1 - S_{11})(1 - S_{22})}{S_{12} S_{21} + (1 - S_{11})(1 + S_{22})} Z_0^{-1}$$

$$MSG = \left| \frac{S_{21}}{S_{12}} \right|$$

$$K = \frac{1 + \left| S_{11} S_{22} - S_{12} S_{21} \right|^2 - \left| S_{11} \right|^2 - \left| S_{22} \right|^2}{2 \left| S_{12} \right| \left| S_{21} \right|}$$

$$MAG = \left| \frac{S_{21}}{S_{12}} \right| \left(K - \sqrt{K^2 - 1} \right)$$

$$U = \frac{1/2 \left| (S_{21} / S_{12}) - 1 \right|^2}{K \left| S_{21} / S_{12} \right| - \mathrm{Re} (S_{21} / S_{12})}$$

SECTION II

SCATTERING PARAMETERS SPEED DESIGN OF HIGH-FREQUENCY TRANSISTOR CIRCUITS

Fritz Weinert's article gives the neophyte a particularly good understanding of s parameters and how they relate to transistors and transistor circuit design. Weinert lucidly explains how to design a stable amplifier for a given gain over a specified bandwidth. He concludes by discussing the accuracy and limitations of his measuring system.

Electronics

Scattering parameters speed design of high-frequency transistor circuits

At frequencies above 100 Mhz scattering parameters are easily measured and provide information difficult to obtain with conventional techniques that use h, y or z parameters

By Fritz Weinert

Hewlett-Packard Co., Palo Alto, Calif.

Performance of transistors at high frequencies has so improved that they are now found in all solid-state microwave equipment. But operating transistors at high frequencies has meant design problems:

- Manufacturers' high-frequency performance data is frequently incomplete or not in proper form.
- Values of h, y or z parameters, ordinarily used in circuit design at lower frequencies, can't be measured accurately above 100 megahertz because establishing the required short and open circuit conditions is difficult. Also, a short circuit frequently causes the transistor to oscillate under test.

These problems are yielding to a technique that uses scattering or s parameters to characterize the high-frequency performance of transistors. Scattering parameters can make the designer's job easier.

- They are derived from power ratios, and consequently provide a convenient method for measuring circuit losses.
- They provide a physical basis for understanding what is happening in the transistor, without need for an understanding of device physics.
- They are easy to measure because they are based on reflection characteristics rather than short- or open-circuit parameters.

The author

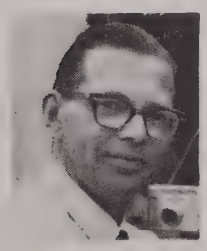

Fritz K. Weinert, who joined the technical staff of Hewlett-Packard in 1964, is project leader in the network analysis section of the microwave laboratory. He holds patents and has published papers on pulse circuits, tapered-line transformers, digital-tuned circuits and shielding systems.

Like other methods that use h, y or z parameters, the scattering-parameter technique does not require a suitable equivalent circuit to represent the transistor device. It is based on the assumption that the transistor is a two-port network—and its terminal behavior is defined in terms of four parameters, s_{11}, s_{12}, s_{21} and s_{22}, called s or scattering parameters.

Since four independent parameters completely define any two-port at any one frequency, it is possible to convert from one known set of parameters to another. At frequencies above 100 Mhz, however, it becomes increasingly difficult to measure the h, y or z parameters. At these frequencies it is difficult to obtain well defined short and open circuits and short circuits frequently cause the device to oscillate. However, s parameters may be measured directly up to a frequency of 1 gigahertz. Once obtained, it is easy to convert the s parameters into any of the h, y or z terms by means of tables.

Suggested measuring systems

To measure scattering parameters, the unknown transistor is terminated at both ports by pure resistances. Several measuring systems of this kind have been proposed. They have these advantages:

- Parasitic oscillations are minimized because of the broadband nature of the transistor terminations.
- Transistor measurements can be taken remotely whenever transmission lines connect the semiconductor to the source and load—especially when the line has the same characteristic impedance as the source and load respectively.
- Swept-frequency measurements are possible instead of point-by-point methods. Theoretical work shows scattering parameters can simplify design.

Scattering-parameter definitions

To measure and define scattering parameters the two-port device, or transistor, is terminated at both ports by a pure resistance of value Z_0, called the reference impedance. Then the scattering parameters are defined by s_{11}, s_{12}, s_{21} and s_{22}. Their physical meaning is derived from the two-port network shown in first figure below.

Two sets of parameters, (a_1, b_1) and (a_2, b_2), represent the incident and reflected waves for the two-port network at terminals 1-1′ and 2-2′ respectively. Equations 1a through 1d define them.

$$a_1 = \frac{1}{2}\left(\frac{V_1}{\sqrt{Z_0}} + \sqrt{Z_0}\, I_1\right) \tag{1a}$$

$$b_1 = \frac{1}{2}\left(\frac{V_1}{\sqrt{Z_0}} - \sqrt{Z_0}\, I_1\right) \tag{1b}$$

$$a_2 = \frac{1}{2}\left(\frac{V_2}{\sqrt{Z_0}} + \sqrt{Z_0}\, I_2\right) \tag{1c}$$

$$b_2 = \frac{1}{2}\left(\frac{V_2}{\sqrt{Z_0}} - \sqrt{Z_0}\, I_2\right) \tag{1d}$$

The scattering parameters for the two-port network are given by equation 2.

$$\begin{aligned} b_1 &= s_{11}\, a_1 + s_{12}\, a_2 \\ b_2 &= s_{21}\, a_1 + s_{22}\, a_2 \end{aligned} \tag{2}$$

In matrix form the set of equations of 2 becomes

$$\begin{bmatrix} b_1 \\ b_2 \end{bmatrix} = \begin{bmatrix} s_{11} & s_{12} \\ s_{21} & s_{22} \end{bmatrix} \begin{bmatrix} a_1 \\ a_2 \end{bmatrix} \tag{3}$$

where the matrix

$$[s] = \begin{bmatrix} s_{11} & s_{12} \\ s_{21} & s_{22} \end{bmatrix} \tag{4}$$

is called the scattering matrix of the two-port network. Therefore the scattering parameters of the two-port network can be expressed in terms of the incident and reflected parameters as:

$$\begin{aligned} s_{11} &= \left.\frac{b_1}{a_1}\right|_{a_2 = 0} & s_{12} &= \left.\frac{b_1}{a_2}\right|_{a_1 = 0} \\ s_{21} &= \left.\frac{b_2}{a_1}\right|_{a_2 = 0} & s_{22} &= \left.\frac{b_2}{a_2}\right|_{a_1 = 0} \end{aligned} \tag{5}$$

In equation 5, the parameter s_{11} is called the input reflection coefficient; s_{21} is the forward transmission coefficient; s_{12} is the reverse transmission coefficient; and s_{22} is the output reflection coefficient. All four scattering parameters are expressed as ratios of reflected to incident parameters.

Physical meaning of parameters

The implications of setting the incident parameters a_1 and a_2 at zero help explain the physical

Scattering parameters are defined by this representation of a two-port network. Two sets of incident and reflected parameters (a_1, b_1) and (a_2, b_2) appear at terminals 1-1′ and 2-2′ respectively.

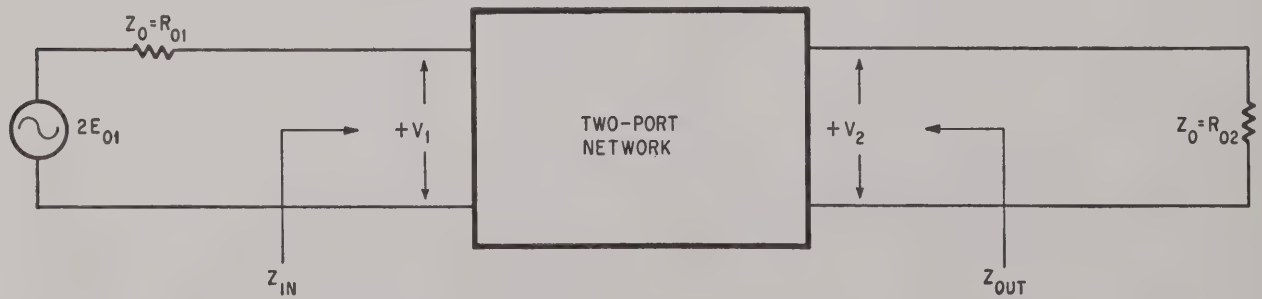

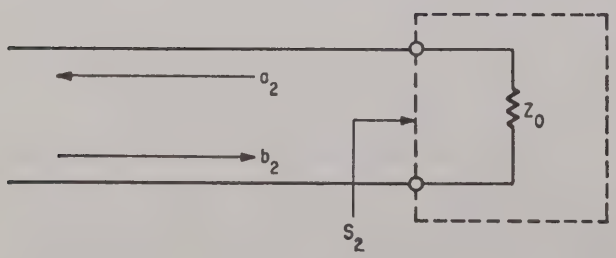

By setting a_2 equal to zero the s_{11} parameter can be found. The Z_0 resistor is thought of as a one-port network. The condition $a_2 = 0$ implies that the reference impedance R_{02} is set equal to the load impedance Z_0. By connecting a voltage source, 2 E_{01}, with the source impedance, Z_0, parameter s_{21} can be found using equation 5

meaning of these scattering parameters.

By setting $a_2 = 0$, expressions for s_{11} and s_{22} can be found. The terminating section of the two-port network is at bottom of page 79 with the parameters a_2 and b_2 of the 2-2′ port. If the load resistor Z_0 is thought of as a one-port network with a scattering parameter

$$s_2 = \frac{Z_0 - R_{02}}{Z_0 + R_{02}} \tag{6}$$

where R_{02} is the reference impedance of port 2, then a_2 and b_2 are related by

$$a_2 = s_2\, b_2 \tag{7}$$

When the reference impedance R_{02} is set equal to the local impedance Z_0, then s_2 becomes

$$s_2 = \frac{Z_0 - Z_0}{Z_0 + Z_0} = 0 \tag{8}$$

so that $a_2 = 0$ under this condition. Similarly, when $a_1 = 0$, the reference impedance of port 1 is equal to the terminating impedance; that is, $R_{01} = Z_0$. The conditions $a_1 = 0$ and $a_2 = 0$ merely imply that the reference impedances R_{01} and R_{02} are chosen to be equal to the terminating resistors Z_0.

In the relationship between the driving-point impedances at ports 1 and 2 and the reflection coefficients s_{11} and s_{22}, the driving-point impedances can be denoted by:

$$Z_{in} = \frac{V_1}{I_1}; \qquad Z_{out} = \frac{V_2}{I_2} \tag{9}$$

From the relationship

$$s_{11} = \left.\frac{b_1}{a_1}\right|_{a_2 = 0}$$

$$s_{11} = \frac{\frac{1}{2}\left[(V_1/\sqrt{Z_0}) - \sqrt{Z_0}\, I_1\right]}{\frac{1}{2}\left[(V_1/\sqrt{Z_0}) + \sqrt{Z_0}\, I_1\right]} \tag{10}$$

which reduces to

$$s_{11} = \frac{Z_{in} - Z_0}{Z_{in} + Z_0} \tag{11}$$

Similarly,

$$s_{22} = \frac{Z_{out} - Z_0}{Z_{out} + Z_0} \tag{12}$$

These expressions show that if the reference impedance at a given port is chosen to equal the ports driving-point impedance, the reflection coefficient will be zero, provided the other port is terminated in its reference impedance.

In the equation

$$s_{21} = \left.\frac{b_2}{a_1}\right|_{a_2 = 0}$$

the condition $a_2 = 0$ implies that the reference impedance R_{02} is set equal to the load impedance R_2, center figure page 79. If a voltage source 2 E_{01} is connected with a source impedance $R_{01} = Z_0$, a_1 can be expressed as:

$$a_1 = \frac{E_{01}}{\sqrt{Z_0}} \tag{13}$$

Since $a_2 = 0$, then

$$a_2 = 0 = \frac{1}{2}\left(\frac{V_2}{\sqrt{Z_0}} + \sqrt{Z_0}\, I_2\right)$$

from which

$$\frac{V_2}{\sqrt{Z_0}} = -\sqrt{Z_0}\, I_2$$

Consequently,

$$b_2 = \frac{1}{2}\left(\frac{V_2}{\sqrt{Z_0}} - \sqrt{Z_0}\, I_2\right) = \frac{V_2}{\sqrt{Z_0}}$$

Finally, the forward transmission coefficient is expressed as:

$$s_{21} = \frac{V_2}{E_{01}} \tag{14}$$

Similarly, when port 1 is terminated in $R_{01} = Z_0$ and when a voltage source 2 E_{02} with source impedance Z_0 is connected to port 2,

$$s_{12} = \frac{V_1}{E_{02}} \tag{15}$$

Both s_{12} and s_{21} have the dimensions of a voltage-ratio transfer function. And if $R_{01} = R_{02}$, then s_{12} and s_{21} are simple voltage ratios. For a passive reciprocal network, $s_{21} = s_{12}$.

Scattering parameters s_{11} and s_{22} are reflection coefficients. They can be measured directly by means of slotted lines, directional couplers, voltage-standing-wave ratios and impedance bridges. Scattering parameters s_{12} and s_{21} are voltage transducer gains. All the parameters are frequency-dependent, dimensionless complex numbers. At any one frequency all four parameters must be known to describe the two-port device completely.

There are several advantages for letting $R_{01} = R_{02} = Z_0$.

- The s_{11} and s_{22} parameters are power reflection coefficients that are difficult to measure under normal loading. However, if $R_{01} = R_{02} = Z_0$, the parameters become equal to voltage reflection coefficients and can be measured directly with available test equipment.
- The s_{12} and s_{21} are square roots of the transducer power gain, the ratio of power absorbed in the load over the source power available. But for $R_{01} = R_{02} = Z_0$, they become a voltage ratio and can be measured with a vector voltmeter.
- The actual measurement can be taken at a distance from the input or output ports. The measured scattering parameter is the same as the parameter existing at the actual location of the particular port. Measurement is achieved by connecting input and output ports to source and load by means of transmission lines having the same impedance, Z_0,

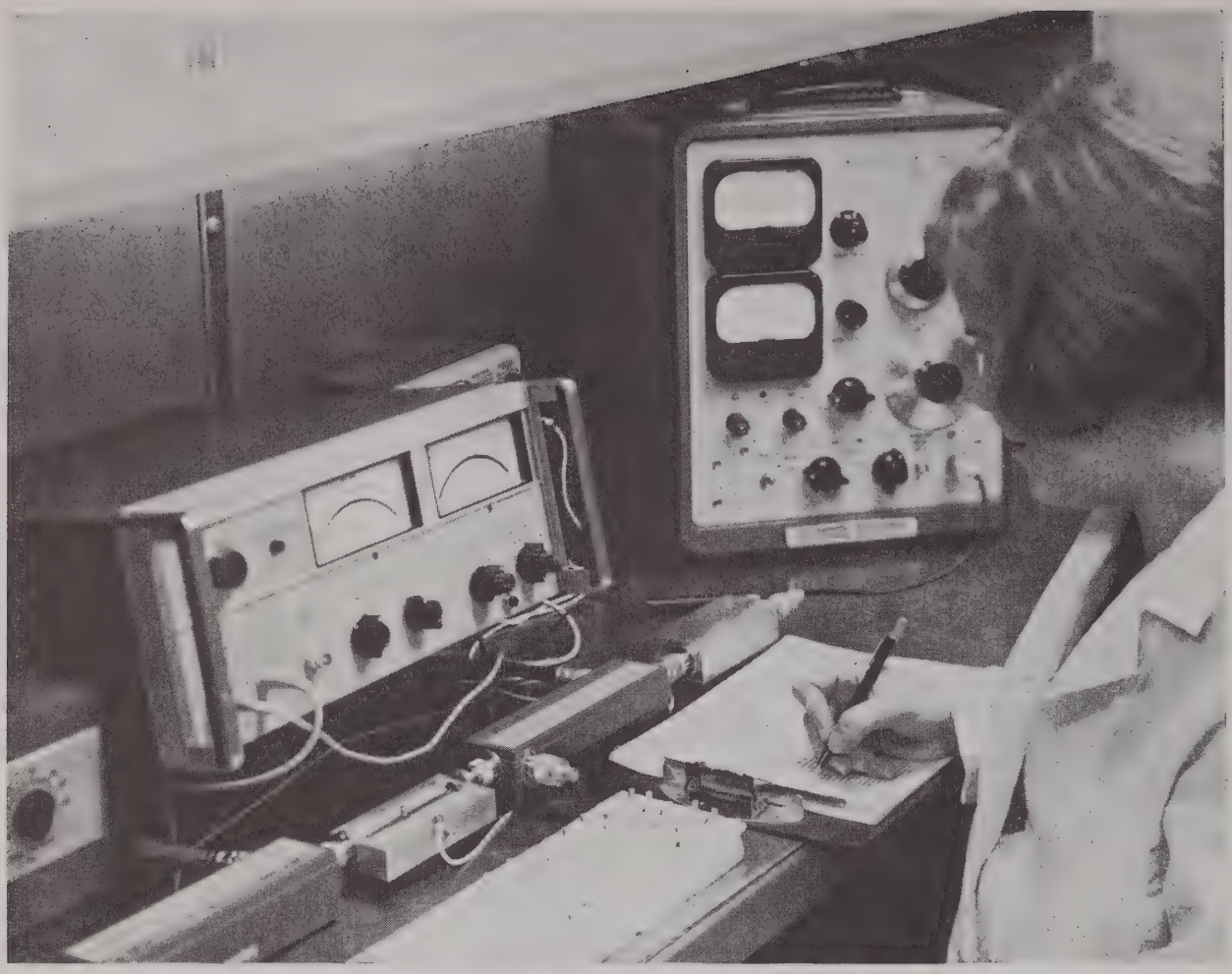

25°C	100 Mhz	300 Mhz	100°C	100 Mhz	300 Mhz
s_{11}	0.62 < −44.0°	0.305 < −81.0°	s_{11}	0.690 < −40°	0.372 < −71°
s_{12}	0.0115 < +75.0°	0.024 < +93.0°	s_{12}	0.0125 < +76.0°	0.0254 < +89.5°
s_{21}	9.0 < +130°	3.85 < +91.0°	s_{21}	8.30 < +133.0°	3.82 < +94.0°
s_{22}	0.955 < −6.0°	0.860 < −14.0°	s_{22}	0.955 < −6.0°	0.880 < −15.0°

25°C	590 Mhz	1,000 Mhz	100°C	500 Mhz	1,000 Mhz
s_{11}	0.238 < −119.0°	0.207 < +175.0°	s_{11}	0.260 < −96.0°	0.196 < +175.0°
s_{12}	0.0385 < +110.0°	0.178 < +110.0°	s_{12}	0.0435 < +100.0°	0.165 < +103.0°
s_{21}	2.19 < +66.0°	1.30 < +33.0°	s_{21}	2.36 < +69.5°	1.36 < +35.0°
s_{22}	0.830 < −26.0°	0.838 < −49.5°	s_{22}	0.820 < −28.0°	0.850 < −53.0°

Scattering parameters can be measured directly using the Hewlett-Packard 8405A vector voltmeter. It covers the frequency range of 1 to 1,000 megahertz and determines s_{21} and s_{12} by measuring ratios of voltages and phase difference between the input and output ports. Operator at Texas Instruments Incorporated measures s-parameter data for TI's 2N3571 transistor series. Values for $V_{CE} = 10$ volts; $I_C = 5$ milliamperes.

as the source and load. In this way compensation can be made for added cable length.

▪ Transistors can be placed in reversible fixtures to measure the reverse parameters s_{22} and s_{12} with the equipment used to measure s_{11} and s_{21}.

The Hewlett-Packard Co.'s 8405A vector voltmeter measures s parameters. It covers the frequency range of 1 to 1,000 megahertz and determines s_{21} and s_{12} by measuring voltage ratios and phase differences between the input and output ports directly on two meters, as shown above. A dual-directional coupler samples incident and reflected voltages to measure the magnitude and phase of the reflection coefficient.

To perform measurements at a distance, the setup on page 86 is convenient. The generator and the load are the only points accessible for measurement. Any suitable test equipment, such as a vector voltmeter, directional coupler or slotted line can be connected. In measuring the s_{21} parameter as shown in the schematic, the measured vector quantity V_2/E_o is the voltage transducer gain or forward gain scattering parameter of the two-port and cables of length L_1 and L_2. The scattering parameter s_{21} of the two-port itself is the same vector V_2/E_o but turned by an angle of $360° (L_1 + L_2)/\lambda$ in a counterclockwise direction.

Plotting s_{11} in the complex plane shows the conditions for measuring s_{11}. Measured vector r_1 is the reflection coefficient of the two-port plus

Amplifier design with unilateral s parameters

Step 1

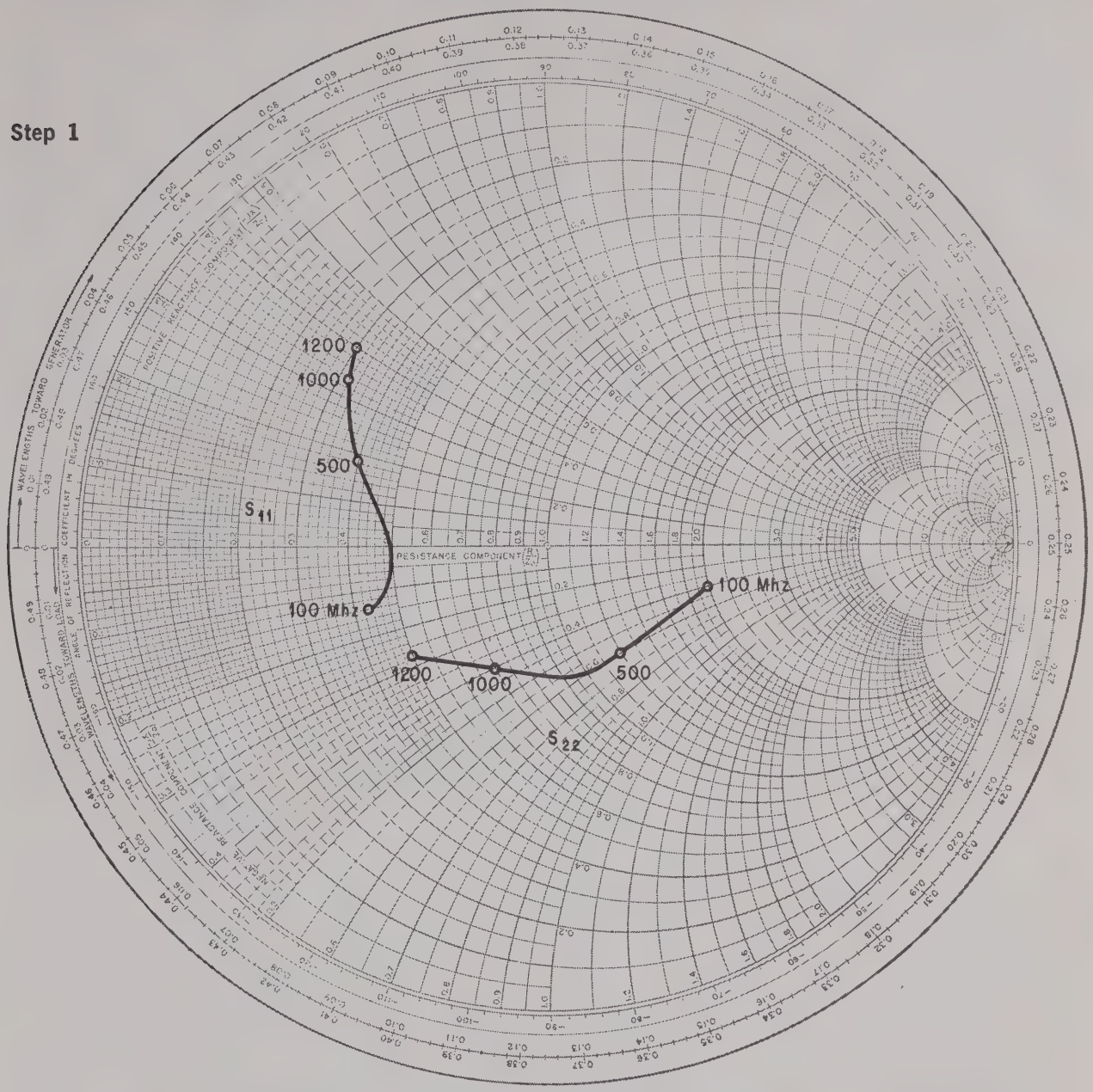

Step 2

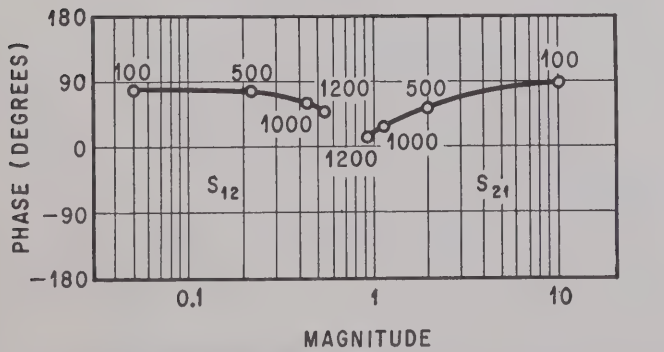

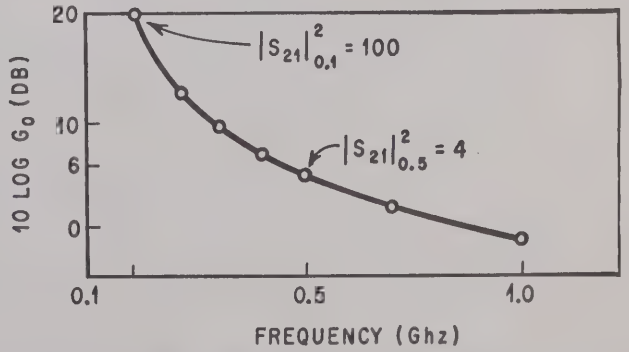

From the measured data transducer power gain is plotted as decibels versus frequency. From the plot an amplifier of constant gain is designed. Smith chart is used to plot the scattering parameters.

To design an amplifier stage, a source and load impedance combination must be found that gives the gain desired. Synthesis can be accomplished in three stages.

Step 1

The vector voltmeter measures the scattering parameters over the frequency range desired.

Step 2

Transducer power gain is plotted versus frequency using equation 19 and the measured data from step 1. This determines the frequency response of the uncompensated transistor network so that a constant-gain amplifier can be designed.

Step 3

Source and load impedances must be selected to provide the proper compensation of a constant power gain from 100 to 500 Mhz. Such a constant-gain amplifier is designed according to the following:

▪ Plot s_{11}^* on the Smith chart. The magnitude of s_{11}^* is the linear distance measured from the center of the Smith chart. Radius from the center of the chart to any point on the locus of s_{11} represents a reflection coefficient r. The value of r can therefore be determined at any frequency by drawing a line from the origin of the chart to a value of s_{11}^* at the frequency of

Step 3

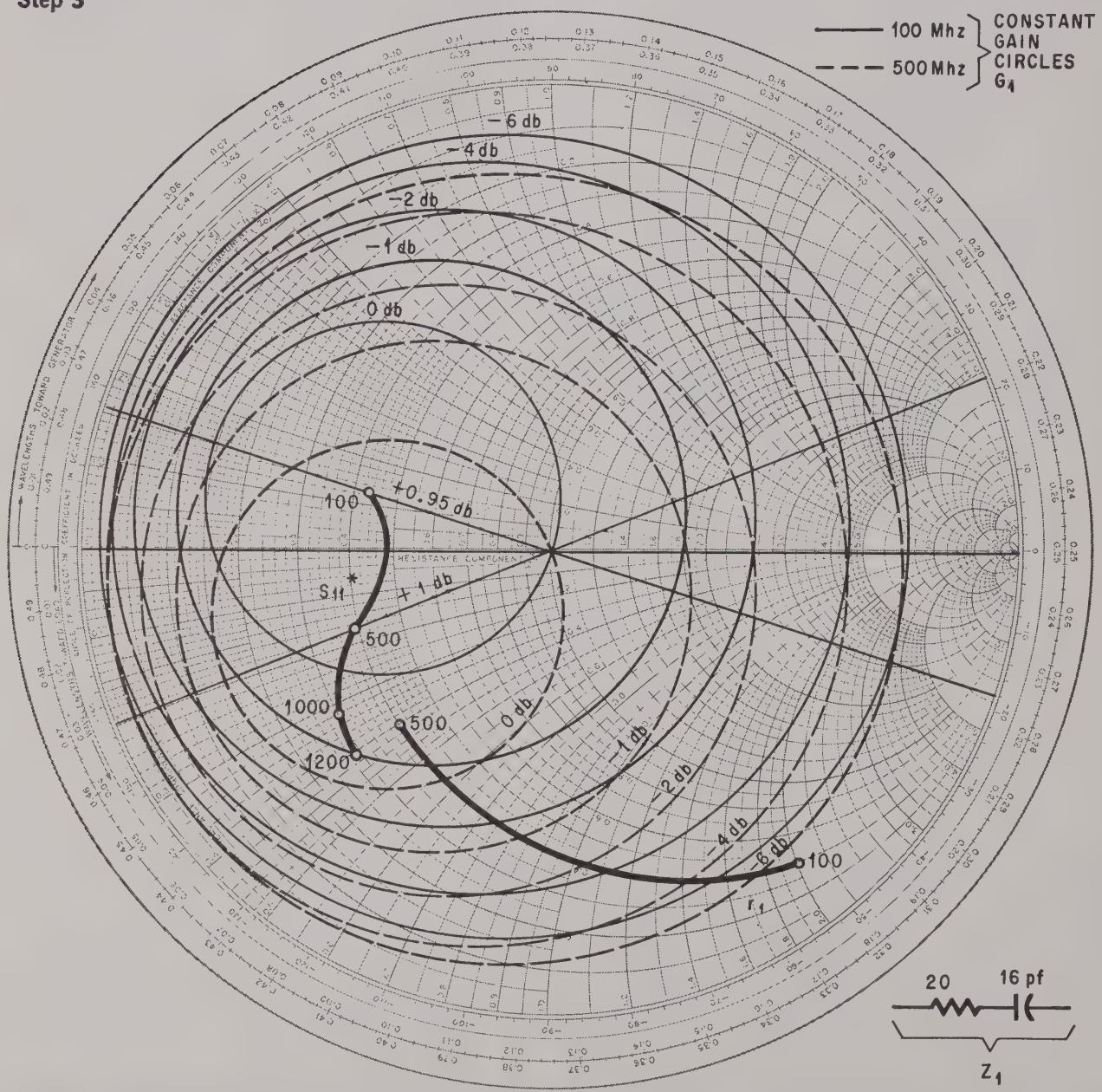

Source impedance is found by inspecting the input plane for realizable source loci that give proper gain. Phase angle is read on the peripheral scale "angle of reflection coefficient in degrees."

interest. The value of r is scaled proportionately with a maximum value of 1.0 at the periphery of the chart. The phase angle is read on the peripheral scale "angle of reflection coefficient in degrees." Constant-gain circles are plotted using equations 24 and 25 for G_1. These correspond to values of 0, −1, −2, −4 and −6 decibels for s_{11}^* at 100 and 500 Mhz. Construction procedure is shown on page 83.

▪ Constant-gain circles for s_{22}^* at 100 and 500 Mhz are constructed similarly to that below.

▪ The gain G_0 drops from 20 db at 100 Mhz to 6 db at 500 Mhz, a net reduction of 14 db. It is desirable to find source and load impedances that will flatten this slope over this frequency range. For this case it is accomplished by choosing a value of r_1 and r_2 on the constant-gain circle at 100 Mhz, each corresponding to a loss of −7 db. If this value of r_1 and r_2 falls on circles of 0-db gain at 500 Mhz, the over-all gain will be:

At 100 Mhz,

$$G_T(\text{db}) = G_0 + G_1 + G_2 = 20 - 7 - 7 = +6 \text{ db}$$

At 500 Mhz,

$$G_T(\text{db}) = 6 + 0 + 0 = +6 \text{ db}$$

▪ A source impedance of 20 ohms resistance in series with 16 picofarads of capacitance is chosen. Its value is equal to 50 (0.4 − j2) ohms at 100 Mhz. This point crosses the r_1 locus at about the −7 db constant-gain circle of G_1 as illustrated on page 83. At 500 Mhz this impedance combination equals 50 (0.4 − j0.4) ohms and is located at approximately the +0.5 db constant-gain circle. The selection of source impedance is an iterative process of inspection of

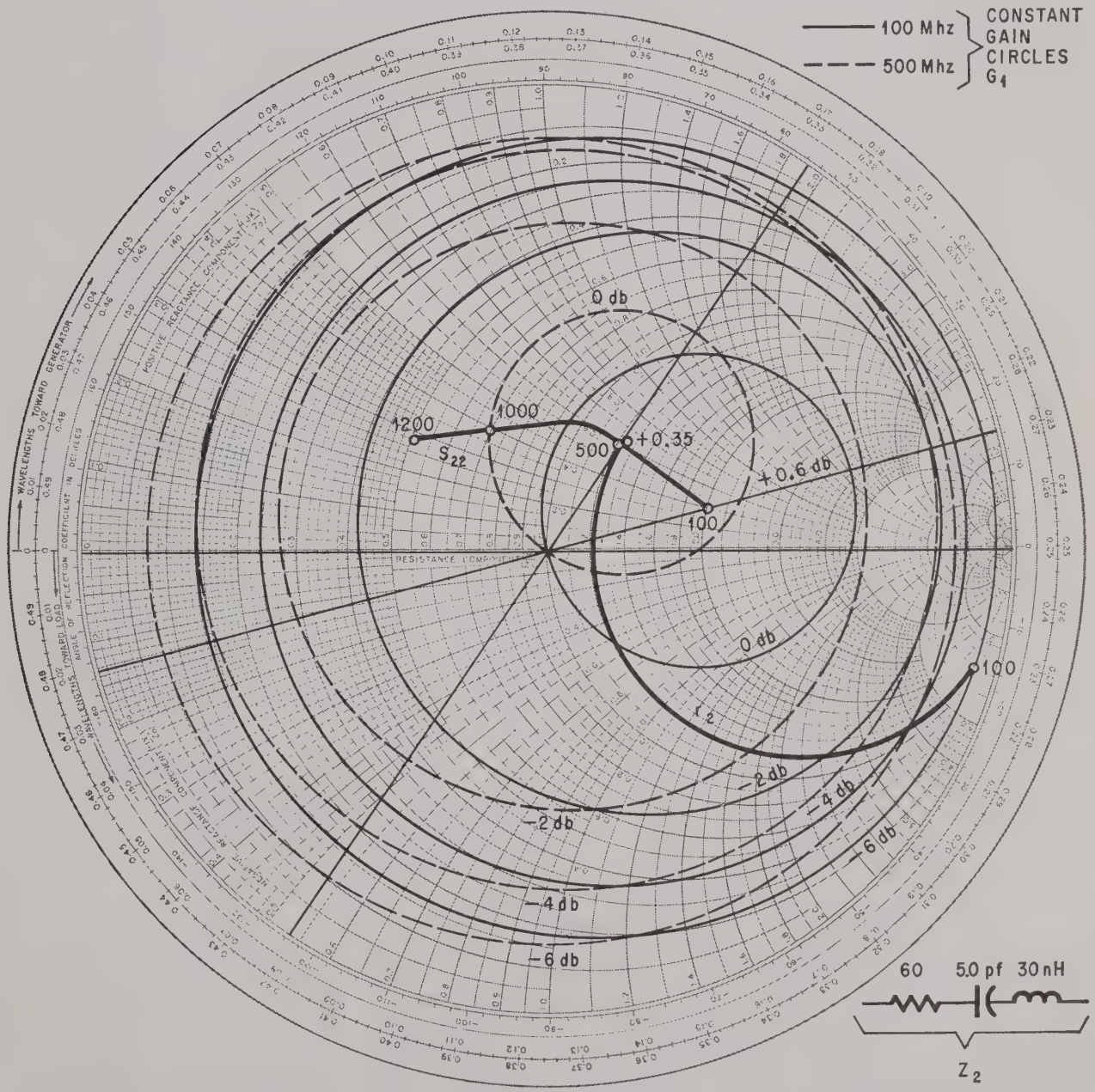

Load impedance is found by inspecting the output plane for loci that give proper gain.

the input r_1 plane on the Smith chart. The impedance values at various frequencies between 100 and 500 Mhz are tried until an impedance that corresponds to an approximate constant—gain circle necessary for constant power gain across the band is found.

▪ At the output port a G_2 of −6 db at 100 Mhz and +0.35 db at 500 Mhz is obtained by selecting a load impedance of 60 ohms in series with 5 pf and 30 nanohenries.

▪ The gain is:

At 100 Mhz,

$$G_T(\text{db}) = G_0 + G_1 + G_2 = 20 - 7 - 6 = +7 \text{ db}$$

At 500 Mhz,

$$6 + 0.5 + 0.35 = +6.85 \text{ db}$$

Thus the 14-db variation from 100 to 500 Mhz is reduced to 0.15 db by selecting the proper source and load impedances.

Stability criterion. Important in the design of amplifiers is stability, or resistance to oscillation. Stability is determined for the unilateral case from the measured s parameters and the synthesized source and load impedances. Oscillations are only possible if either the input or the output port, or both, have negative resistances. This occurs if s_{11} or s_{22} are greater than unity. However, even with negative resistances the amplifier might be stable. The condition for stability is that the locus of the sum of input plus source impedance, or output plus load impedance, does not include zero impedance from frequencies zero to infinity [shown in figure below]. The technique is similar to Nyquist's feedback stability criterion and has been derived directly from it.

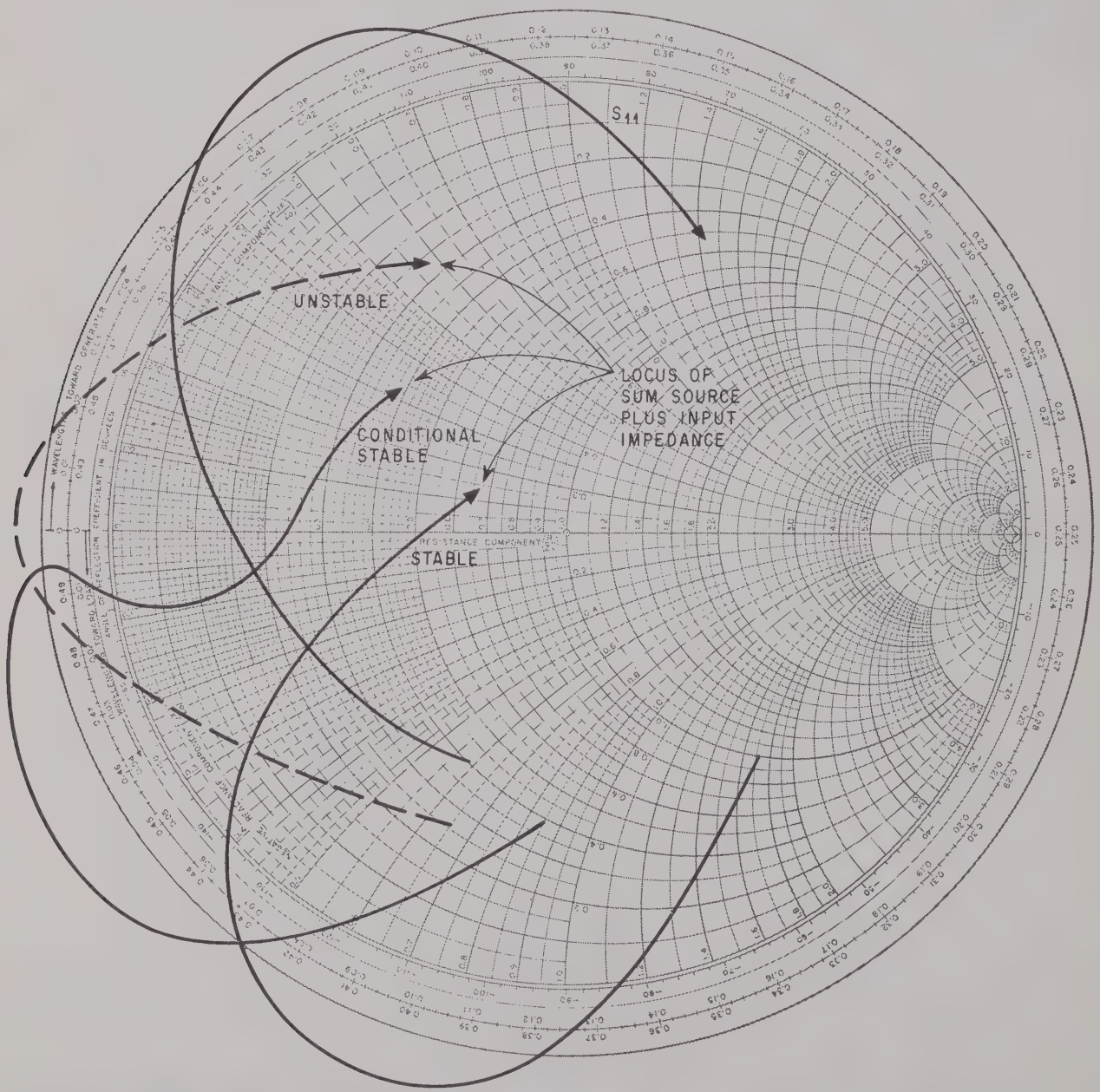

Amplifier stability is determined from scattering parameters and synthesized source and load impedances.

input cable L_1 (the length of the output cable has no influence). The scattering parameter s_{11} of the two-port is the same vector r_1 but turned at an angle 720° L_1/λ in a counterclockwise direction.

Using the Smith chart

Many circuit designs require that the impedance of the port characterized by s_{11} or the reflection coefficient r be known. Since the s parameters are in units of reflection coefficient, they can be plotted directly on a Smith chart and easily manipulated to establish optimum gain with matching networks. The relationship between reflection coefficient r and the impedance R is

$$r = \frac{R - Z_0}{R + Z_0} \qquad (16)$$

The Smith chart plots rectangular impedance coordinates in the reflection coefficient plane. When the s_{11} or s_{22} parameter is plotted on a Smith chart, the real and imaginary part of the impedance may be read directly.

It is also possible to chart equation 1 on polar coordinates showing the magnitude and phase of the impedance R in the complex reflection coefficient plane. Such a plot is termed the Charter chart. Both charts are limited to impedances having positive resistances, $|r_1| < 1$. When measuring transistor parameters, impedances with negative resistances are sometimes found. Then, extended charts can be used.

Measurement of a device's s parameters provides data on input and output impedance and forward and reverse gain. In measuring, a device is inserted between known impedances, usually 50 ohms. In practice it may be desirable to achieve higher gain by changing source or load impedances or both.

An amplifier stage may now be designed in two steps. First, source and load impedances must be found that give the desired gain. Then the impedances must be synthesized, usually as matching networks between a fixed impedance source or between the load and the device [see block diagram top of p. 87].

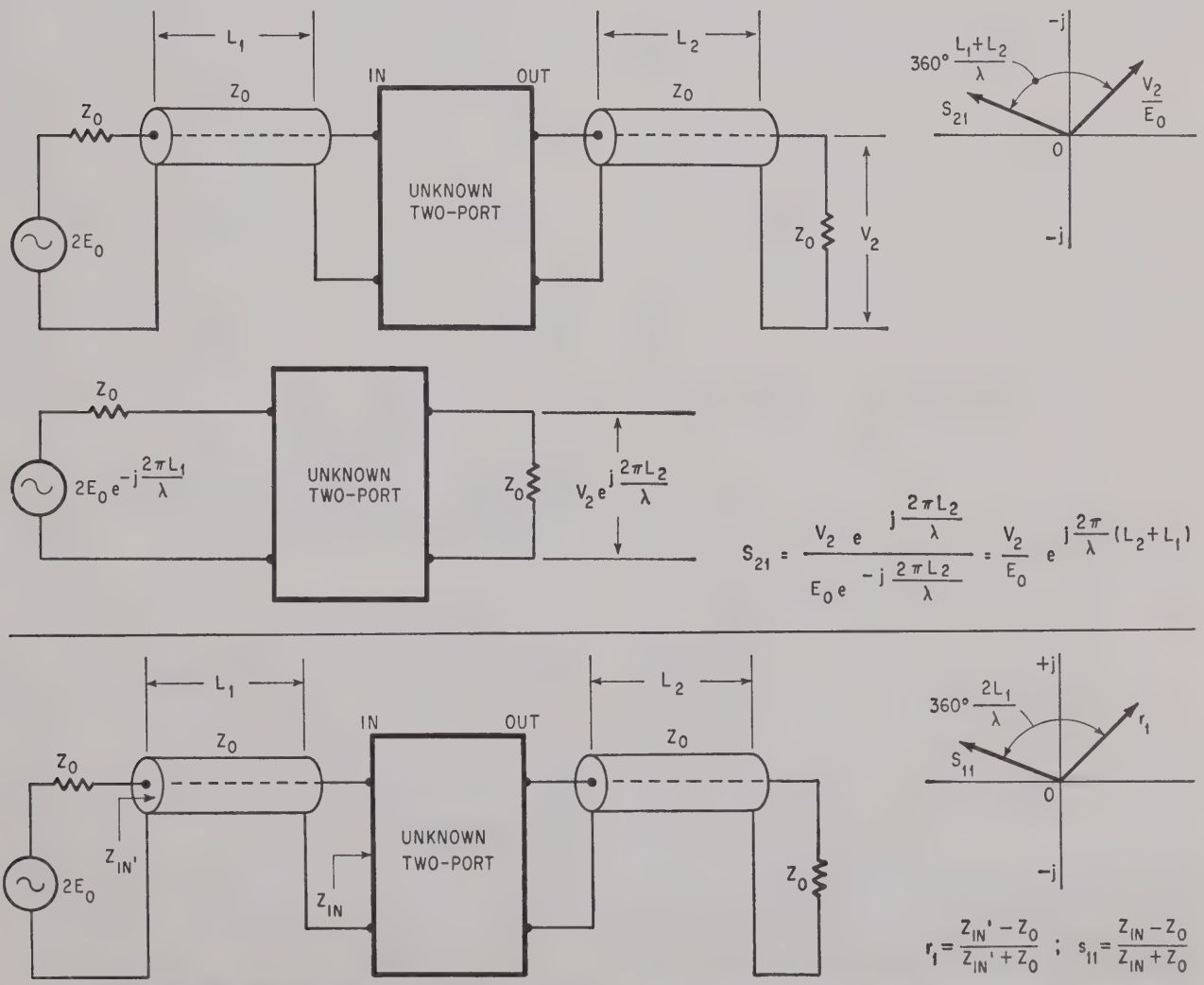

S parameters can be measured remotely. Top test setup is for measuring s_{21}; bottom, for s_{11}. Measured vector V_2/E_0 is the voltage transducer gain of the two-port and cables L_1 and L_2. The measured vector r_1 is the reflection coefficient of the two-port plus input cable $L_1 + L_2$. Appropriate vectors for r_1 and s parameters are plotted.

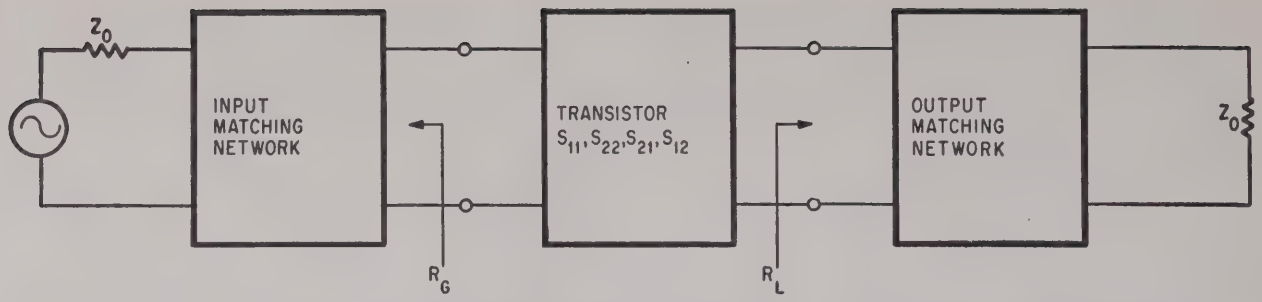

To design an amplifier stage, source and load impedances are found to give the gain desired. Then impedances are synthesized, usually as matching networks between a fixed impedance source or the load and the device. When using s parameters to design a transistor amplifier, it is advantageous to distinguish between a simplified or unilateral design for times when s_{12} can be neglected and when it must be used.

When designing a transistor amplifier with the aid of s parameters, it is advantageous to distinguish between a simplified or unilateral design for instances where the reverse-transmission parameter s_{12} can be neglected and the more general case in which s_{21} must be shown. The unilateral design is much simpler and is, for many applications, sufficient.

Unilateral-circuit definitions

Transducer power gain is defined as the ratio of amplifier output power to available source power.

$$G_T = \frac{I_2^2 . R_{e2}}{\frac{E_0^2}{4R_{e1}}} \tag{17}$$

For the unilateral circuit G_T is expressed in terms of the scattering parameters s_{11}, s_{21} and s_{12} with $s_{12} = 0$.

$$G_T = G_0 . G_1 . G_2 \tag{18}$$

where:

$$G_0 = |s_{21}|^2 = \text{transducer power gain for } R_1 = Z_0 = R_2 \tag{19}$$

$$G_1 = \frac{\left|1 - |r_1|^2\right|}{|1 - r_1 s_{11}|^2} \tag{20}$$

= power gain contribution from change of source impedance from Z_0 to R_1

$$r_1 = \frac{R_1 - Z_0}{R_1 + Z_0} \tag{21}$$

= reflection coefficient of source impedance with respect to Z_0

$$G_2 = \frac{\left|1 - |r_2|^2\right|}{|1 - r_2 s_{22}|^2} \tag{22}$$

= power gain contribution from change of load impedance from Z_0 to R_2

$$r_2 = \frac{R_2 - Z_0}{R_2 + Z_0} \tag{23}$$

= reflection coefficient of load impedance with respect to Z_0

In designing an amplifier stage the graphical procedure shown at the bottom is helpful. The measured values of parameter s_{11} and its complex conjugate s_{11}^* are plotted on the Smith chart together with radius distances. Center of the constant-gain circles located on the line through s_{11}^* and the origin at a distance

$$r_{01} = \frac{G_1}{G_{1\,max}} \left[\frac{|s_{11}|}{1 - |s_{11}|^2 (1 - G_1/G_{1\,max})} \right] \tag{24}$$

The radius of circles on which G_1 is constant is

$$\rho_{01} = \frac{\sqrt{1 - G_1/G_{1\,max}}\,(1 - |s_{11}|^2)}{1 - |s_{11}|^2 (1 - G_1/G_{1\,max})} \tag{25}$$

If the source reflection coefficient r_1 is made equal

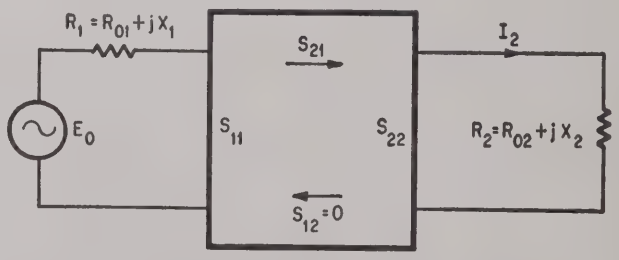

The two-port network is terminated at the ports by impedances containing resistance and reactance. Expressions for the transducer power gain can then be derived in terms of the scattering parameters.

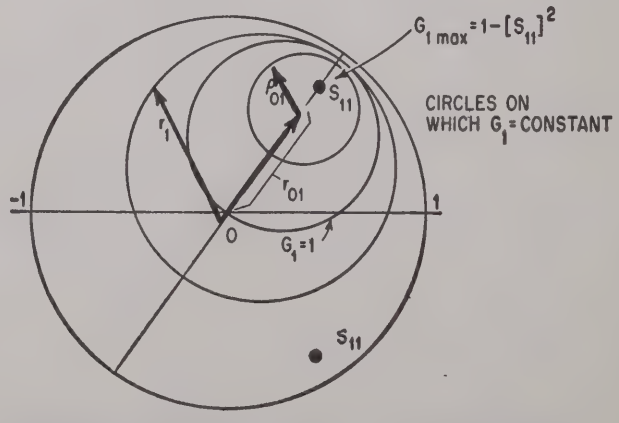

A graphical plot helps in design of an amplifier stage. Here the measured parameters s_{11} and s_{11}^* are plotted on a Smith chart. The upper point is s_{11}^*.

to s_{11}^*, then the generator is matched to the load and the gain becomes maximum (G_{1max}). Constant-gain circles can be constructed, as shown, in 1- or 2-decibel increments or whatever is practical using equations 9 and 10.

If the source impedance R_1 or its reflection coefficient is plotted, the gain contribution G_1 is read directly from the gain circles. The same method is used to determine G_2 by plotting s_{22}, s_{22}^*, constant-gain circles and r_2.

Examples for the design procedure are given in greater detail in Transistor Parameter Measurements, Hewlett-Packard Application Note 77-1. The procedure is outlined in "Amplifier design with unilateral s parameters," beginning on page 82.

Measuring s parameters

S-parameter measurements of small-signal transistors require fairly sensitive measuring equipment. The input signal often cannot exceed 10 millivolts root mean square. On the other hand, wide frequency ranges are required as well as fast and easy operation. Recent advantages in measuring equipment have provided a fast and accurate measuring system. It is based on the use of a newly developed instrument, the H-P sampling vector voltmeter 8405A [see photo p. 81], and couplers.

The vector voltmeter covers a frequency range of 1 to 1,000 Mhz, a voltage measurement range of 100 microvolts full scale and a phase range of $\pm 180°$ with 0.1° resolution. It is tuned automatically by means of a phase-locked loop.

Directional couplers are used to measure reflection coefficients and impedances. A directional coupler consists of a pair of parallel transmission lines that exhibit a magnetic and electric coupling between them. One, called the main line, is connected to the generator and load to be measured. Measurement is taken at the output of the other, called the auxiliary line. Both lines are built to have a well defined characteristic impedance; 50 ohms is usual. The voltage coupled into the auxiliary line consists of components proportional to the voltage and current in the main line. The coupling is arranged so that both components are equal in magnitude when the load impedance equals the characteristic impedance of the line.

Directional couplers using two auxiliary lines in reverse orientation are called dual-directional couplers. A feature of the unit is a movable reference plane; the point where the physical measurement is taken can be moved along the line connecting the coupler with the unknown load. A line stretcher is connected to the output of the first auxiliary line.

The reference plane is set closer to the transistor package than the minimum lead length used with the transistor. Additional lead length is then considered part of the matching networks. The influence of lead length is also measured by changing the location of the reference plane.

Measurement of s_{11} parameter is made when the instrument is switched to one of two positions. The quotient V_B/V_A equals the magnitude of s_{11}. Its phase is read directly on the 8405A meter. When switched to the alternate position, the s_{21} parameter is read directly from the same ratio.

Accuracy and limitations

When measuring small-signal scattering parameters, a-c levels beyond which the device is considered linear must not be exceeded. In a grounded-emitter or grounded-base configuration, input voltage is limited to about 10 millivolts rms maximum (when measuring s_{11} and s_{21}). Much higher voltages can be applied when measuring s_{22} and s_{12} parameters. In uncertain cases linearity is checked by taking the same measurements at a sampling of several different levels.

The system shown is inherently broadband. Frequency is not necessarily limited by the published range of the dual directional couplers. The coupling factor K falls off inversely with frequency below the low-frequency limit of a coupler. The factor K does not appear in the result as long as it is the same for each auxiliary port. Since construction of couplers guarantees this to a high degree, measurements can be made at lower frequencies than are specified for the coupler.

The system's measurement accuracy depends on the accuracy of the vector voltmeter and the couplers. Although it is possible to short circuit the reference planes of the transistors at each frequency, it is not desirable for fast measurements. Hence, broadband tracking of all auxiliary arms of the couplers and tracking of both channels of the vector voltmeter are important. Tracking errors are within about 0.5 db of magnitude and $\pm 3°$ of phase over wide frequency bands. Accuracy of measuring impedances expressed by s_{11} and s_{22} degrade for resistances and impedances having a high reactive component. This is because s_{11} or s_{22} are very close to unity. These cases are usually confined to lower frequencies.

Bibliography

Charter, P.S., "Charts for Transmission-Line Measurements and Computations," Radio Corp. of America Review, Vol. III, No. 3, January, 1939, pp. 355-368.

Smith, P.H., "An Improved Transmission Line Calculator," Electronics, January, 1944, pp. 130-325.

Alsbert, D.A., "A Precise Sweep-Frequency Method of Vector Impedance Measurement," Proceedings of the IRE, November, 1951, pp. 1393-1400.

Follingstad, H.G., "Complete Linear Characterization of Transistors from Low through Very High Frequencies," IRE Transactions on Instruments, March, 1957, pp. 49-63.

General Radio Experimenter, "Type 1607-A Transfer-Function and Immitance Bridge," May, 1959, pp. 3-11. General Radio Experimenter, "Mounts for Transistor Measurements with the Transfer-Function Bridge," February-March, 1965, pp. 16-19.

Mathis, H.F., "Extended Transmission-line Charts," Electronics, Sept. 23, 1960, pp. 76-78.

Leed, D., and O. Kummer, "A Loss and Phase Set for Measuring Transistor Parameters and Two-Port Networks Between 5 and 250 Mc," Bell System Technical Journal, May, 1961, pp. 841-884.

Kurokawa, K., "Power Waves and the Scattering Matrix," Institute of Electronic and Electrical Engineers Transactions Microwave Theory and Techniques, March, 1965, pp. 194-202.

Leed, D., "An Insertion Loss, Phase and Delay Measuring Set for Characterizing Transistors and Two-Port Networks between 0.25 and 4.2 Gc," Bell System Technical Journal, March, 1966, pp. 340-397.

Hewlett-Packard Journal, "The RF Vector Voltmeter," Vol. 17, No. 9, May, 1966, pp. 2-12.

SECTION III

S-PARAMETER TECHNIQUES FOR FASTER, MORE ACCURATE NETWORK DESIGN

Richard W. Anderson describes s parameters and flowgraphs and then relates them to more familiar concepts such as transducer power gain and voltage gain. He takes swept-frequency data obtained with a network analyzer and uses it to design amplifiers. He shows how to calculate the error caused by assuming the transistor is unilateral. Both narrow band and broad band amplifier designs are discussed. Stability criteria are also considered.

HEWLETT-PACKARD JOURNAL
FEBRUARY 1967 *Volume 18 • Number 6*

S-Parameter Techniques for Faster, More Accurate Network Design

LINEAR NETWORKS, OR NONLINEAR NETWORKS operating with signals sufficiently small to cause the networks to respond in a linear manner, can be completely characterized by parameters measured at the network terminals (ports) without regard to the contents of the networks. Once the parameters of a network have been determined, its behavior in any external environment can be predicted, again without regard to the specific contents of the network. The new microwave network analyzer described in the article beginning on p. 2 characterizes networks by measuring one kind of parameters, the scattering parameters, or s-parameters.

S-parameters are being used more and more in microwave design because they are easier to measure and work with at high frequencies than other kinds of parameters. They are conceptually simple, analytically convenient, and capable of providing a surprising degree of insight into a measurement or design problem. For these reasons, manufacturers of high-frequency transistors and other solid-state devices are finding it more meaningful to specify their products in terms of s-parameters than in any other way. How s-parameters can simplify microwave design problems, and how a designer can best take advantage of their abilities, are described in this article.

Two-Port Network Theory

Although a network may have any number of ports, network parameters can be explained most easily by considering a network with only two ports, an input port and an output port, like the network shown in Fig. 1. To characterize the performance of such a network, any of several parameter sets can be used, each of which has certain advantages.

Each parameter set is related to a set of four variables associated with the two-port model. Two of these variables represent the excitation of the network (independent variables), and the remaining two represent the response of the network to the excitation (dependent variables). If the network of Fig. 1 is excited by voltage sources V_1 and V_2, the network currents I_1 and I_2 will be related by the following equations (assuming the network behaves linearly):

$$I_1 = y_{11}V_1 + y_{12}V_2 \quad (1)$$

$$I_2 = y_{21}V_1 + y_{22}V_2 \quad (2)$$

In this case, with port voltages selected as independent variables and port currents taken as dependent variables, the relating parameters are called short-circuit admittance parameters, or y-parameters. In the absence of additional information, four measurements are required to determine the four parameters y_{11}, y_{21}, y_{12}, and y_{22}. Each measurement is made with one port of the network excited by a voltage source while the other port is short circuited. For example, y_{21}, the forward transadmittance, is the ratio of the current at port 2 to the voltage at port 1 with port 2 short circuited as shown in equation 3.

$$y_{21} = \left.\frac{I_2}{V_1}\right|_{V_2 = 0 \text{ (output short circuited)}} \quad (3)$$

If other independent and dependent variables had been chosen, the network would have been described, as before, by two linear equations similar to equations 1 and 2, except that the variables and the parameters describing their relationships would be different. However, all parameter sets contain the same information about a network, and it is always possible to calculate any set in terms of any other set.

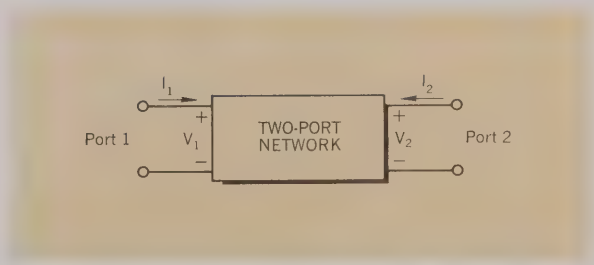

Fig. 1. *General two-port network.*

S-Parameters

The ease with which scattering parameters can be measured makes them especially well suited for describing transistors and other active devices. Measuring most other parameters calls for the input and output of the device to be successively opened and short circuited. This is difficult to do even at RF frequencies where lead inductance and capacitance make short and open circuits difficult to obtain. At higher frequencies these measurements typically require tuning stubs, separately adjusted at each measurement frequency, to reflect short or open circuit conditions to the device terminals. Not only is this inconvenient and tedious, but a tuning stub shunting the input or output may cause a transistor to oscillate, making the measurement difficult and invalid. S-parameters, on the other hand, are usually measured with the device imbedded between a 50Ω load and source, and there is very little chance for oscillations to occur.

Another important advantage of s-parameters stems from the fact that traveling waves, unlike terminal voltages and currents, do not vary in magnitude at points along a lossless transmission line. This means that scattering parameters can be measured on a device located at some distance from the measurement transducers, provided that the measuring device and the transducers are connected by low-loss transmission lines.

Generalized scattering parameters have been defined by K. Kurokawa.[1] These parameters describe the interrelationships of a new set of variables (a_i, b_i). The variables a_i and b_i are normalized complex voltage waves incident on and reflected from the i^{th} port of the network. They are defined in terms of the terminal voltage V_i, the terminal current I_i, and an arbitrary reference impedance Z_i, as follows

[1] K. Kurokawa, 'Power Waves and the Scattering Matrix,' IEEE Transactions on Microwave Theory and Techniques, Vol. MTT-13, No. 2, March, 1965.

$$a_i = \frac{V_i + Z_i I_i}{2\sqrt{|\text{Re } Z_i|}} \tag{4}$$

$$b_i = \frac{V_i - Z_i^* I_i}{2\sqrt{|\text{Re } Z_i|}} \tag{5}$$

where the asterisk denotes the complex conjugate.

For most measurements and calculations it is convenient to assume that the reference impedance Z_i is positive and real. For the remainder of this article, then, all variables and parameters will be referenced to a single positive real impedance Z_o.

The wave functions used to define s-parameters for a two-port network are shown in Fig. 2. The independent variables a_1 and a_2 are normalized incident voltages, as follows:

$$a_1 = \frac{V_1 + I_1 Z_o}{2\sqrt{Z_o}} = \frac{\text{voltage wave incident on port 1}}{\sqrt{Z_o}} = \frac{V_{i1}}{\sqrt{Z_o}} \tag{6}$$

$$a_2 = \frac{V_2 + I_2 Z_o}{2\sqrt{Z_o}} = \frac{\text{voltage wave incident on port 2}}{\sqrt{Z_o}} = \frac{V_{i2}}{\sqrt{Z_o}} \tag{7}$$

Dependent variables b_1 and b_2 are normalized reflected voltages:

$$b_1 = \frac{V_1 - I_1 Z_o}{2\sqrt{Z_o}} = \frac{\text{voltage wave reflected (or emanating) from port 1}}{\sqrt{Z_o}} = \frac{V_{r1}}{\sqrt{Z_o}} \tag{8}$$

$$b_2 = \frac{V_2 - I_2 Z_o}{2\sqrt{Z_o}} = \frac{\text{voltage wave reflected (or emanating) from port 2}}{\sqrt{Z_o}} = \frac{V_{r2}}{\sqrt{Z_o}} \tag{9}$$

The linear equations describing the two-port network are then:

$$b_1 = s_{11}a_1 + s_{12}a_2 \tag{10}$$

$$b_2 = s_{21}a_1 + s_{22}a_2 \tag{11}$$

The s-parameters s_{11}, s_{22}, s_{21}, and s_{12} are:

$$s_{11} = \left.\frac{b_1}{a_1}\right|_{a_2 = 0} = \text{Input reflection coefficient with the output port terminated by a matched load } (Z_L = Z_o \text{ sets } a_2 = 0). \tag{12}$$

$$s_{22} = \left.\frac{b_2}{a_2}\right|_{a_1 = 0} = \text{Output reflection coefficient with the input terminated by a matched load } (Z_S = Z_o \text{ and } V_S = 0). \tag{13}$$

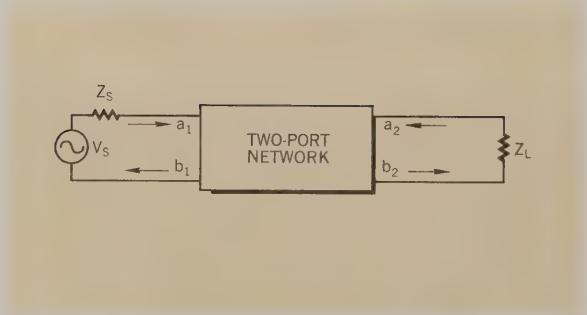

Fig. 2. *Two-port network showing incident* (a_1, a_2) *and reflected* (b_1, b_2) *waves used in s-parameter definitions.*

$$s_{21} = \left.\frac{b_2}{a_1}\right|_{a_2 = 0} = \text{Forward transmission (insertion) gain with the output port terminated in a matched load.} \quad (14)$$

$$s_{12} = \left.\frac{b_1}{a_2}\right|_{a_1 = 0} = \text{Reverse transmission (insertion) gain with the input port terminated in a matched load.} \quad (15)$$

Notice that

$$s_{11} = \frac{b_1}{a_1} = \frac{\frac{V_1}{I_1} - Z_o}{\frac{V_1}{I_1} + Z_o} = \frac{Z_1 - Z_o}{Z_1 + Z_o} \quad (16)$$

and

$$Z_1 = Z_o \frac{(1 + s_{11})}{(1 - s_{11})} \quad (17)$$

where $Z_1 = \frac{V_1}{I_1}$ is the input impedance at port 1.

This relationship between reflection coefficient and impedance is the basis of the Smith Chart transmission-line calculator. Consequently, the reflection coefficients s_{11} and s_{22} can be plotted on Smith charts, converted directly to impedance, and easily manipulated to determine matching networks for optimizing a circuit design.

The above equations show one of the important advantages of s-parameters, namely that they are simply gains and reflection coefficients, both familiar quantities to engineers. By comparison, some of the y-parameters described earlier in this article are not so familiar. For example, the y-parameter corresponding to insertion gain s_{21} is the 'forward transadmittance' y_{21} given by equation 3. Clearly, insertion gain gives by far the greater insight into the operation of the network.

Another advantage of s-parameters springs from the simple relationships between the variables a_1, a_2, b_1, and b_2, and various power waves:

$|a_1|^2$ = Power incident on the input of the network.
= Power available from a source of impedance Z_o.

$|a_2|^2$ = Power incident on the output of the network.
= Power reflected from the load.

$|b_1|^2$ = Power reflected from the input port of the network.
= Power available from a Z_o source minus the power delivered to the input of the network.

$|b_2|^2$ = Power reflected or emanating from the output of the network.
= Power incident on the load.
= Power that would be delivered to a Z_o load.

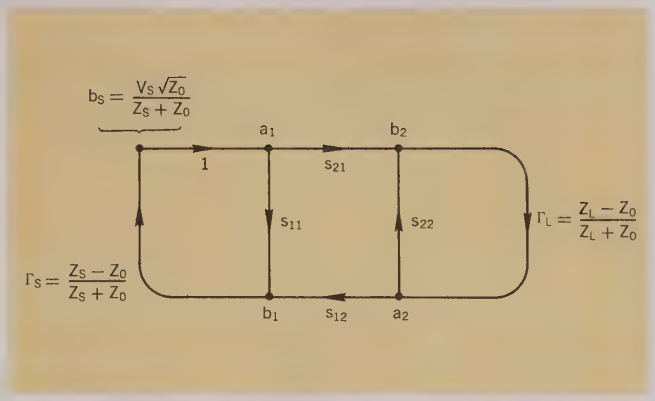

Fig. 3. *Flow graph of network of Fig. 2.*

Hence s-parameters are simply related to power gain and mismatch loss, quantities which are often of more interest than the corresponding voltage functions:

$$|s_{11}|^2 = \frac{\text{Power reflected from the network input}}{\text{Power incident on the network input}}$$

$$|s_{22}|^2 = \frac{\text{Power reflected from the network output}}{\text{Power incident on the network output}}$$

$$|s_{21}|^2 = \frac{\text{Power delivered to a } Z_o \text{ load}}{\text{Power available from } Z_o \text{ source}}$$
= Transducer power gain with Z_o load and source

$|s_{12}|^2$ = Reverse transducer power gain with Z_o load and source.

Network Calculations with Scattering Parameters

Scattering parameters turn out to be particularly convenient in many network calculations. This is especially true for power and power gain calculations. The transfer parameters s_{12} and s_{21} are a measure of the complex insertion gain, and the driving point parameters s_{11} and s_{22} are a measure of the input and output mismatch loss. As dimensionless expressions of gain and reflection, the parameters not only give a clear and meaningful physical interpretation of the network

performance but also form a natural set of parameters for use with signal flow graphs[2,3]. Of course, it is not necessary to use signal flow graphs in order to use s-parameters, but flow graphs make s-parameter calculations extremely simple, and I recommend them very strongly. Flow graphs will be used in the examples that follow.

In a signal flow graph each port is represented by two nodes. Node a_n represents the wave coming into the device from another device at port n and node b_n represents the wave leaving the device at port n. The complex scattering coefficients are then represented as multipliers on branches connecting the nodes within the network and in adjacent networks. Fig. 3 is the flow graph representation of the system of Fig. 2.

Fig. 3 shows that if the load reflection coefficient Γ_L is zero ($Z_L = Z_o$) there is only one path connecting b_1 to a_1 (flow graph rules prohibit signal flow against the forward direction of a branch arrow). This confirms the definition of s_{11}:

$$s_{11} = \left.\frac{b_1}{a_1}\right|_{a_2 = \Gamma_L b_2 = 0}$$

The simplification of network analysis by flow graphs results from the application of the "non-touching loop rule." This rule applies a generalized formula to determine the transfer function between any two nodes within a complex system. The non-touching loop rule is explained in footnote 4.

[2] J. K. Hunton, 'Analysis of Microwave Measurement Techniques by Means of Signal Flow Graphs,' IRE Transactions on Microwave Theory and Techniques, Vol. MTT-8, No. 2, March, 1960.

[3] N. Kuhn, 'Simplified Signal Flow Graph Analysis,' Microwave Journal, Vol. 6, No. 11, Nov., 1963.

[4] The nontouching loop rule provides a simple method for writing the solution of any flow graph by inspection. The solution T (the ratio of the output variable to the input variable) is

$$T = \frac{\sum_k T_k \Delta_k}{\Delta}$$

where T_k = path gain of the k^{th} forward path

Δ = 1 − (sum of all individual loop gains) + (sum of the loop gain products of all possible combinations of two nontouching loops) − (sum of the loop gain products of all possible combinations of three nontouching loops) + ...

Δ_k = The value of Δ not touching the k_{th} forward path.

A path is a continuous succession of branches, and a forward path is a path connecting the input node to the output node, where no node is encountered more than once. Path gain is the product of all the branch multipliers along the path. A loop is a path which originates and terminates on the same node, no node being encountered more than once. Loop gain is the product of the branch multipliers around the loop.

For example, in Fig. 3 there is only one forward path from b_S to b_2 and its gain is s_{21}. There are two paths from b_S to b_1; their path gains are $s_{21}s_{12}\Gamma_L$ and s_{11} respectively. There are three individual loops, only one combination of two nontouching loops, and no combinations of three or more nontouching loops; therefore, the value of Δ for this network is

$$\Delta = 1 - (s_{11}\Gamma_S + s_{21}s_{12}\Gamma_L\Gamma_S + s_{22}\Gamma_L) + (s_{11}s_{22}\Gamma_L\Gamma_S).$$

The transfer function from b_S to b_2 is therefore

$$\frac{b_2}{b_S} = \frac{s_{21}}{\Delta}$$

Using scattering parameter flow-graphs and the non-touching loop rule, it is easy to calculate the transducer power gain with arbitrary load and source. In the following equations the load and source are described by their reflection coefficients Γ_L and Γ_S, respectively, referenced to the real characteristic impedance Z_o.

Transducer power gain

$$G_T = \frac{\text{Power delivered to the load}}{\text{Power available from the source}} = \frac{P_L}{P_{avS}}$$

$$P_L = P(\text{incident on load}) - P(\text{reflected from load})$$
$$= |b_2|^2 (1 - |\Gamma_L|^2)$$

$$P_{avS} = \frac{|b_S|^2}{(1 - |\Gamma_S|^2)}$$

$$G_T = \left|\frac{b_2}{b_s}\right|^2 (1 - |\Gamma_S|^2)(1 - |\Gamma_L|^2)$$

Using the non-touching loop rule,

$$\frac{b_2}{b_S} = \frac{s_{21}}{1 - s_{11}\Gamma_S - s_{22}\Gamma_L - s_{21}s_{12}\Gamma_L\Gamma_S + s_{11}\Gamma_S s_{22}\Gamma_L}$$
$$= \frac{s_{21}}{(1 - s_{11}\Gamma_S)(1 - s_{22}\Gamma_L) - s_{21}s_{12}\Gamma_L\Gamma_S}$$

$$G_T = \frac{|s_{21}|^2 (1 - |\Gamma_S|^2)(1 - |\Gamma_L|^2)}{|(1 - s_{11}\Gamma_S)(1 - s_{22}\Gamma_L) - s_{21}s_{12}\Gamma_L\Gamma_S|^2} \qquad (18)$$

Two other parameters of interest are:

1) Input reflection coefficient with the output termination arbitrary and $Z_S = Z_o$.

$$s'_{11} = \frac{b_1}{a_1} = \frac{s_{11}(1 - s_{22}\Gamma_L) + s_{21}s_{12}\Gamma_L}{1 - s_{22}\Gamma_L}$$
$$= s_{11} + \frac{s_{21}s_{12}\Gamma_L}{1 - s_{22}\Gamma_L} \qquad (19)$$

2) Voltage gain with arbitrary source and load impedances

$$A_V = \frac{V_2}{V_1} \qquad V_1 = (a_1 + b_1)\sqrt{Z_o} = V_{i1} + V_{r1}$$
$$V_2 = (a_2 + b_2)\sqrt{Z_o} = V_{i2} + V_{r2}$$
$$a_2 = \Gamma_L b_2$$
$$b_1 = s'_{11} a_1$$

$$A_V = \frac{b_2(1 + \Gamma_L)}{a_1(1 + s'_{11})} = \frac{s_{21}(1 + \Gamma_L)}{(1 - s_{22}\Gamma_L)(1 + s'_{11})} \qquad (20)$$

On p. 23 is a table of formulas for calculating many often-used network functions (power gains, driving point characteristics, etc.) in terms of scattering parameters. Also included in the table are conversion formulas between s-parameters and h-, y-, and z-parameters, which are other parameter sets used very often for specifying transistors at

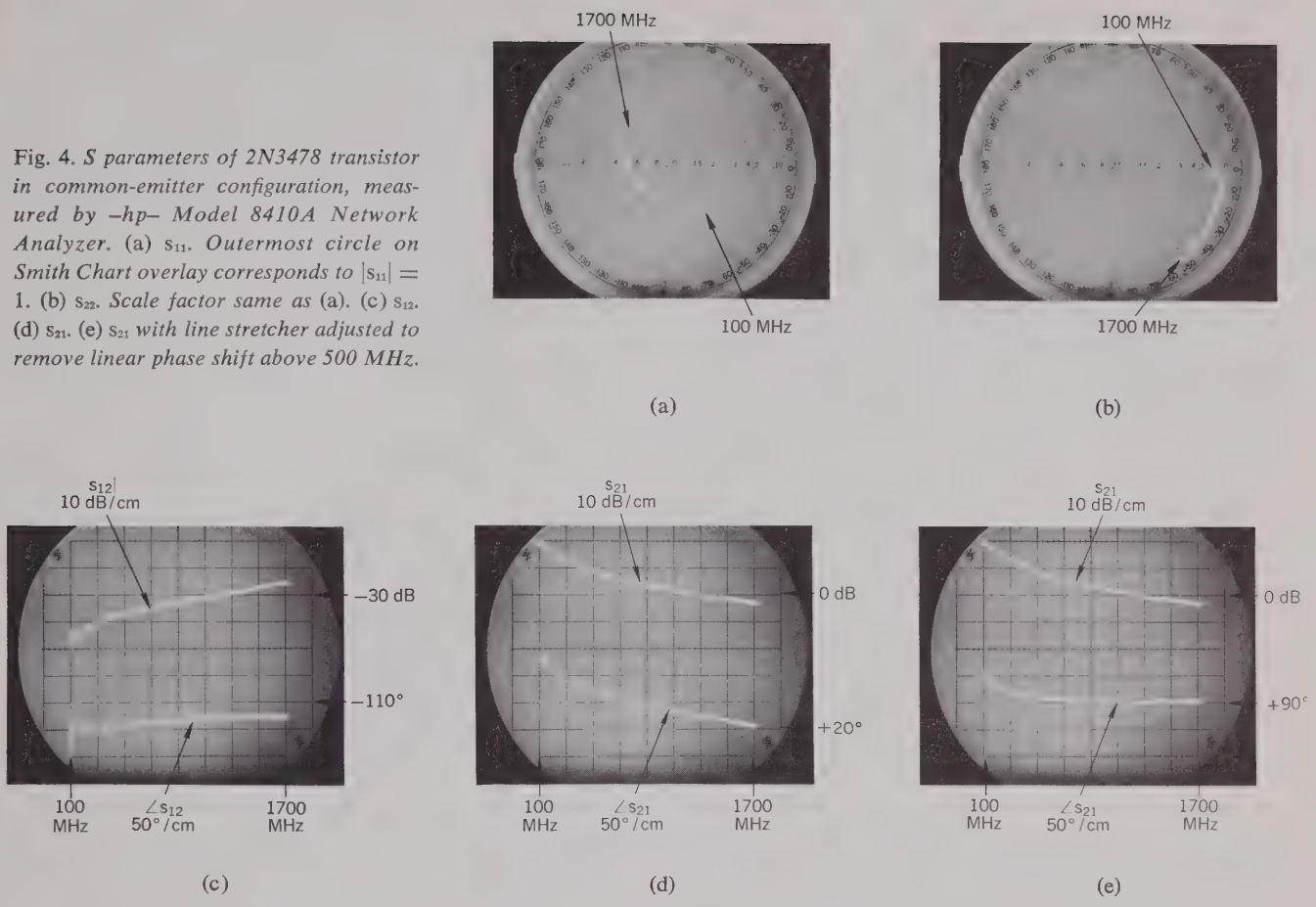

Fig. 4. *S parameters of 2N3478 transistor in common-emitter configuration, measured by –hp– Model 8410A Network Analyzer.* (a) s_{11}. *Outermost circle on Smith Chart overlay corresponds to* $|s_{11}| = 1$. (b) s_{22}. *Scale factor same as* (a). (c) s_{12}. (d) s_{21}. (e) s_{21} *with line stretcher adjusted to remove linear phase shift above 500 MHz.*

lower frequencies. Two important figures of merit used for comparing transistors, f_t and f_{max}, are also given, and their relationship to s-parameters is indicated.

Amplifier Design Using Scattering Parameters

The remainder of this article will show by several examples how s-parameters are used in the design of transistor amplifiers and oscillators. To keep the discussion from becoming bogged down in extraneous details, the emphasis in these examples will be on s-parameter design *methods,* and mathematical manipulations will be omitted wherever possible.

Measurement of S-Parameters

Most design problems will begin with a tentative selection of a device and the measurement of its s-parameters. Fig. 4 is a set of oscillograms containing complete s-parameter data for a 2N3478 transistor in the common-emitter configuration. These oscillograms are the results of swept-frequency measurements made with the new microwave network analyzer described elsewhere in this issue. They represent the actual s-parameters of this transistor between 100 MHz and 1700 MHz.

In Fig. 5, the magnitude of s_{21} from Fig. 4(d) is replotted on a logarithmic frequency scale, along with additional data on s_{21} below 100 MHz, measured with a vector voltmeter. The magnitude of s_{21} is essentially constant to 125 MHz, and then rolls off at a slope of 6 dB/octave. The phase angle of s_{21}, as seen in Fig. 4(d), varies linearly with frequency above about 500 MHz. By adjusting a calibrated line stretcher in the network analyzer, a compensating linear phase shift was introduced, and the phase curve of Fig. 4(e) resulted. To go from the phase curve of Fig. 4(d) to that of Fig. 4(e) required 3.35 cm of line, equivalent to a pure time delay of 112 picoseconds.

After removal of the constant-delay, or linear-phase, component, the phase angle of s_{21} for this transistor [Fig. 4(e)] varies from 180° at dc to +90° at high frequencies, passing through +135° at 125 MHz, the −3 dB point of the magnitude curve. In other words, s_{21} behaves like a single pole in the frequency domain, and it is possible to write a closed expression for it. This expression is

$$s_{21} = \frac{-s_{21o}e^{-j\omega T_o}}{1 + j\frac{\omega}{\omega_o}} \qquad (21)$$

where

$$T_o = 112 \text{ ps}$$

$$\omega = 2\pi f$$

$$\omega_o = 2\pi \times 125 \text{ MHz}$$

$$s_{21o} = 11.2 = 21 \text{ dB}$$

The time delay $T_o = 112$ ps is due primarily to the transit time of minority carriers (electrons) across the base of this npn transistor.

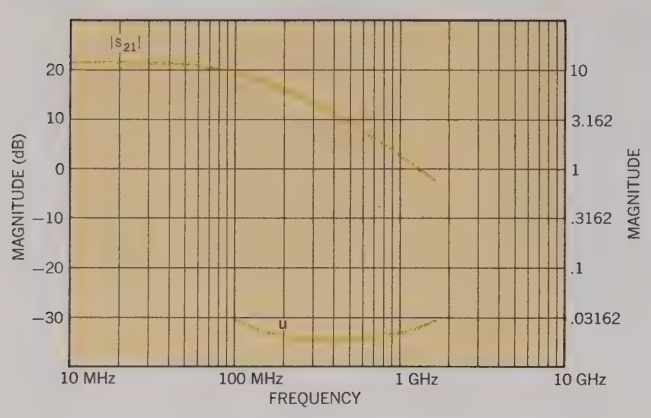

Fig. 5. *Top curve:* $|s_{21}|$ *from Fig. 4 replotted on logarithmic frequency scale. Data below 100 MHz measured with –hp– 8405A Vector Voltmeter. Bottom curve: unilateral figure of merit, calculated from s parameters (see text).*

Narrow-Band Amplifier Design

Suppose now that this 2N3478 transistor is to be used in a simple amplifier, operating between a 50Ω source and a 50Ω load, and optimized for power gain at 300 MHz by means of lossless input and output matching networks. Since reverse gain s_{12} for this transistor is quite small — 50 dB smaller than forward gain s_{21}, according to Fig. 4 — there is a possibility that it can be neglected. If this is so, the design problem will be much simpler, because setting s_{12} equal to zero will make the design equations much less complicated.

In determining how much error will be introduced by assuming $s_{12} = 0$, the first step is to calculate the unilateral figure of merit u, using the formula given in the table on p. 23, i.e.

$$u = \frac{|s_{11}s_{12}s_{21}s_{22}|}{|(1 - |s_{11}|^2)(1 - |s_{22}|^2)|} \quad . \qquad (22)$$

A plot of u as a function of frequency, calculated from the measured parameters, appears in Fig. 5. Now if G_{Tu} is the transducer power gain with $s_{12} = 0$ and G_T is the actual transducer power gain, the maximum error introduced by using G_{Tu} instead of G_T is given by the following relationship:

$$\frac{1}{(1 + u)^2} < \frac{G_T}{G_{Tu}} < \frac{1}{(1 - u)^2} \quad . \qquad (23)$$

From Fig. 5, the maximum value of u is about 0.03, so the maximum error in this case turns out to be about ±0.25 dB at 100 MHz. This is small enough to justify the assumption that $s_{12} = 0$.

Incidentally, a small reverse gain, or feedback factor, s_{12}, is an important and desirable property for a transistor to have, for reasons other than that it simplifies amplifier design. A small feedback factor means that the input characteristics of the completed amplifier will be independent of the load, and the output will be independent of the source impedance. In most amplifiers, isolation of source and load is an important consideration.

Returning now to the amplifier design, the unilateral expression for transducer power gain, obtained either by setting $s_{12} = 0$ in equation 18 or by looking in the table on p. 23, is

$$G_{Tu} = \frac{|s_{21}|^2(1 - |\Gamma_s|^2)(1 - |\Gamma_L|^2)}{|1 - s_{11}\Gamma_s|^2|1 - s_{22}\Gamma_L|^2} \quad . \qquad (24)$$

When $|s_{11}|$ and $|s_{22}|$ are both less than one, as they are in this case, maximum G_{Tu} occurs for $\Gamma_S = s^*_{11}$ and $\Gamma_L = s^*_{22}$ (table, p. 23).

The next step in the design is to synthesize matching networks which will transform the 50Ω load and source impedances to the impedances corresponding to reflection coefficients of s^*_{11} and s^*_{22}, respectively. Since this is to be a single-frequency amplifier, the matching networks need not be complicated. Simple series-capacitor, shunt-inductor networks will not only do the job, but will also provide a handy means of biasing the transistor — via the inductor — and of isolating the dc bias from the load and source.

Values of L and C to be used in the matching networks are determined using the Smith Chart of Fig. 6. First, points corresponding to s_{11}, s^*_{11}, s_{22}, and s^*_{22} at 300 MHz are plotted. Each point represents the tip of a vector leading away from the center of the chart, its length equal to the magnitude of the reflection coefficient being plotted, and its angle equal to the phase of the coefficient. Next, a combination of constant-resistance and constant-conductance circles is found, leading from the center of the chart, representing 50Ω, to s^*_{11} and s^*_{22}. The circles on the Smith Chart are constant-resistance circles; increasing series capacitive reactance moves an impedance point counter-clockwise along these circles. In this case, the circle to be used for finding series C is the one passing through the center of the chart, as shown by the solid line in Fig. 6.

Increasing shunt inductive susceptance moves impedance points clockwise along constant-conductance circles. These circles are like the constant-resistance circles, but they are on another Smith Chart, this one being just the reverse of the one in Fig. 6. The constant-conductance circles for shunt L all pass through the leftmost point of the chart rather than the rightmost point. The circles to be used are those passing through s^*_{11} and s^*_{22}, as shown by the dashed lines in Fig. 6.

Once these circles have been located, the normalized values of L and C needed for the matching networks are calculated from readings taken from the reactance and susceptance scales of the Smith Charts. Each element's reactance or susceptance is the difference between the scale readings at the two end points of a circular arc. Which arc corresponds to which element is indicated in Fig. 6. The final network and the element values, normalized and unnormalized, are shown in Fig. 7.

Broadband Amplifier Design

Designing a broadband amplifier, that is, one which has nearly constant gain over a prescribed frequency range, is a matter of surrounding a transistor with external elements in order to compensate for the variation of forward gain $|s_{21}|$ with frequency. This can be done in either of two ways — first, negative feedback, or second, selective mismatching of the input and output circuitry. We will use the second method. When feedback is used, it is usually convenient to convert to y- or z-parameters (for shunt or series feedback respectively) using the conversion equations given in the table, p. 24, and a digital computer.

Equation 24 for the unilateral transducer power gain can be factored into three parts:

$$G_{Tu} = G_o G_1 G_2$$

where

$$G_o = |s_{21}|^2$$

$$G_1 = \frac{1 - |\Gamma_s|^2}{|1 - s_{11}\Gamma_s|^2}$$

$$G_2 = \frac{1 - |\Gamma_L|^2}{|1 - s_{22}\Gamma_L|^2} .$$

When a broadband amplifier is designed by selective mismatching, the gain contributions of G_1 and G_2 are varied to compensate for the variations of $G_o = |s_{21}|^2$ with frequency.

Suppose that the 2N3478 transistor whose s-parameters are given in Fig. 4 is to be used in a broadband amplifier which has a constant gain of 10 dB over a frequency range of 300 MHz to 700 MHz. The amplifier is to be driven from a 50Ω source and is to drive a 50Ω load. According to Fig. 5,

$$|s_{21}|^2 = 13 \text{ dB at } 300 \text{ MHz}$$
$$= 10 \text{ dB at } 450 \text{ MHz}$$
$$= 6 \text{ dB at } 700 \text{ MHz}.$$

To realize an amplifier with a constant gain of 10 dB, source and load matching networks must be found which will decrease the gain by 3 dB at 300 MHz, leave the gain the same at 450 MHz, and increase the gain by 4 dB at 700 MHz.

Although in the general case both a source matching network and a load matching network would be designed, $G_{1\,max}$ (i.e., G_1 for $\Gamma_S = s^*_{11}$) for this transistor is less than 1 dB over the frequencies of interest, which means there is little to be gained by matching the source. Consequently, for this example, only a load-matching network will be designed. Procedures for designing source-matching networks are identical to those used for designing load-matching networks.

The first step in the design is to plot s^*_{22} over the required frequency range on the Smith Chart, Fig. 8. Next, a set of constant-gain circles is drawn. Each circle is drawn for a single frequency; its center is on a line between the center of the Smith Chart and the point representing s^*_{22} at that frequency. The distance from the center of the Smith Chart to the center of the constant gain circle is given by (these equations also appear in the table, p. 23):

$$r_2 = \frac{g_2|s_{22}|}{1 - |s_{22}|^2(1 - g_2)}$$

where

$$g_2 = \frac{G_2}{G_{2\,max}} = G_2(1 - |s_{22}|^2).$$

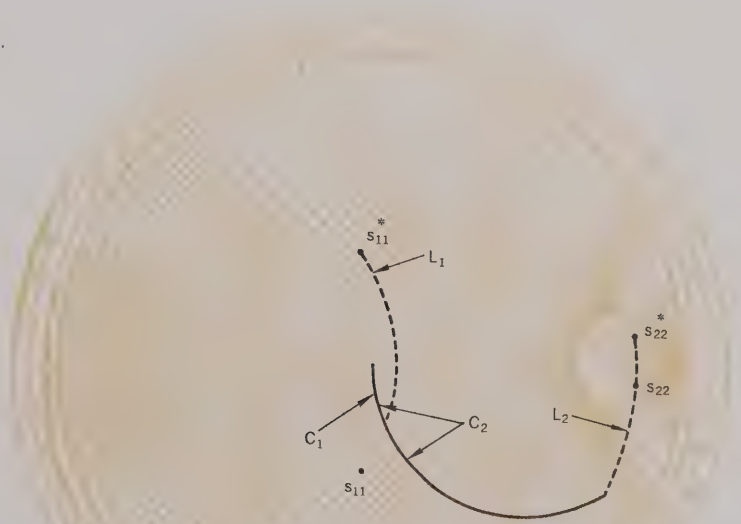

Fig. 6. *Smith Chart for 300-MHz amplifier design example.*

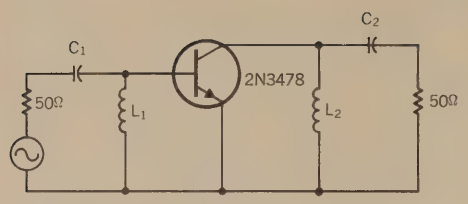

Calculations:

$$X_{L2} = \frac{50}{0.32} = 156\ \Omega$$

$$L_2 = \frac{156}{2\pi\ (0.3 \times 10^9)} = 83\ \text{nH}$$

$$C_2 = \frac{1}{2\pi\ (0.3 \times 10^9)\ (3.5)\ (50)} = 3\ \text{pF}$$

$$C_1 = \frac{3\ (3.5)}{0.42}\ \text{pF} = 25\ \text{pF}$$

$$L_1 = \frac{50}{1.01}\ \text{nH} = 26\ \text{nH}$$

Fig. 7. *300-MHz amplifier with matching networks for maximum power gain.*

The radius of the constant-gain circle is

$$\rho_2 = \frac{\sqrt{1 - g_2}\,(1 - |s_{22}|^2)}{1 - |s_{22}|^2\,(1 - g_2)}.$$

For this example, three circles will be drawn, one for $G_2 = -3$ dB at 300 MHz, one for $G_2 = 0$ dB at 450 MHz, and one for $G_2 = +4$ dB at 700 MHz. Since $|s_{22}|$ for this transistor is constant at 0.85 over the frequency range [see Fig. 4(b)], $G_{2\,max}$ for all three circles is $(0.278)^{-1}$, or 5.6 dB. The three constant-gain circles are indicated in Fig. 8.

The required matching network must transform the center of the Smith Chart, representing 50Ω, to some point on the −3 dB circle at 300 MHz, to some point on the 0 dB circle at 450 MHz, and to some point on the +4 dB circle at 700 MHz. There are undoubtedly many networks that will do this. One which is satisfactory is a combination of two inductors, one in shunt and one in series, as shown in Fig. 9.

Shunt and series elements move impedance points on the Smith Chart along constant-conductance and constant-resistance circles, as I explained in the narrow-band design example which preceded this broadband example. The shunt inductance transforms the 50Ω load along a circle of constant conductance and varying (with frequency) inductive susceptance. The series inductor transforms the combination of the 50Ω load and the shunt inductance along circles of constant resistance and varying inductive reactance.

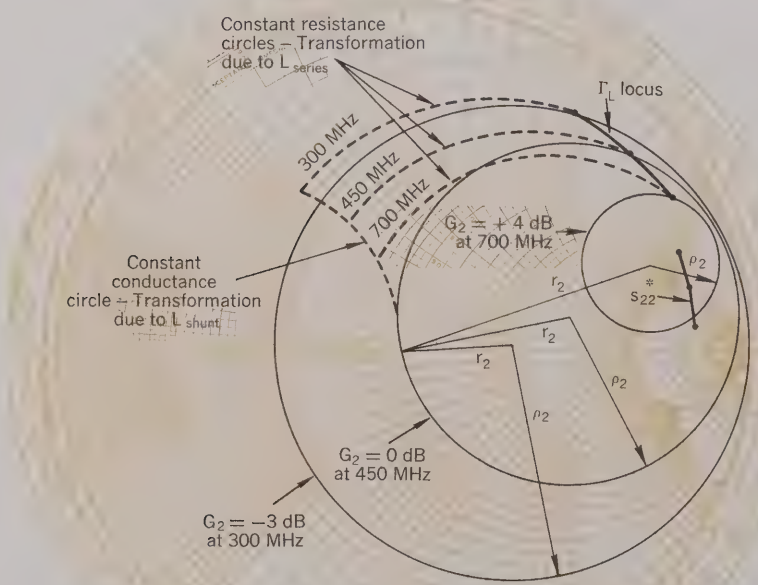

Fig. 8. *Smith Chart for broadband amplifier design example.*

Optimizing the values of shunt and series L is a cut-and-try process to adjust these elements so that

—the transformed load reflection terminates on the right gain circle at each frequency, and

—the susceptance component decreases with frequency and the reactance component increases with frequency. (This rule applies to inductors; capacitors would behave in the opposite way.)

Once appropriate constant-conductance and constant-resistance circles have been found, the reactances and susceptances of the elements can be read directly from the Smith Chart. Then the element values are calculated, the same as they were for the narrow-band design.

Fig. 10 is a schematic diagram of the completed broadband amplifier, with unnormalized element values.

Stability Considerations and the Design of Reflection Amplifiers and Oscillators

When the real part of the input impedance of a network is negative, the corresponding input reflection coefficient (equation 17) is greater than one, and the network can be used as the basis for two important types of circuits, reflection amplifiers and oscillators. A reflection amplifier (Fig. 11) can be realized with a circulator—a nonreciprocal three-port device — and a negative-resistance device. The circulator is used to separate the incident (input) wave from the larger wave reflected by the negative-resistance device. Theoretically, if the circulator is perfect and has a positive real characteristic impedance Z_o, an amplifier with infinite gain can be built by selecting a negative-resistance device whose input impedance has a real part equal to $-Z_o$ and an imaginary part equal to zero (the imaginary part can be set equal to zero by tuning, if necessary).

Amplifiers, of course, are not supposed to oscillate, whether they are reflection amplifiers or some other kind. There is a convenient criterion based upon scattering parameters for determining whether a device is stable or potentially unstable with given source and load impedances. Referring again to the flow graph of Fig. 3, the ratio of the reflected voltage wave b_1 to the input voltage wave b_S is

$$\frac{b_1}{b_S} = \frac{s'_{11}}{1 - \Gamma_S s'_{11}}$$

where s'_{11} is the input reflection coefficient with $\Gamma_S = 0$ (that is, $Z_S = Z_o$) and an arbitrary load impedance Z_L, as defined in equation 19.

If at some frequency

$$\Gamma_S s'_{11} = 1 \qquad (25)$$

the circuit is unstable and will oscillate at that frequency. On the other hand, if

$$|s'_{11}| < \left|\frac{1}{\Gamma_S}\right|$$

the device is unconditionally stable and will not oscillate, whatever the phase angle of Γ_S might be.

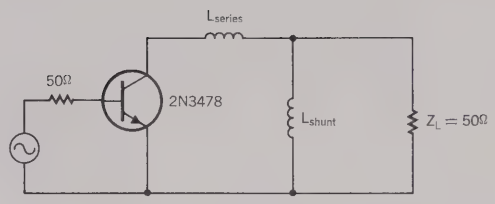

Fig. 9. *Combination of shunt and series inductances is suitable matching network for broadband amplifier.*

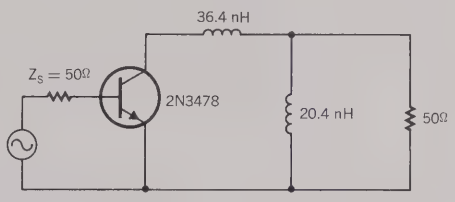

Inductance calculations:

From 700 MHz data, $\frac{j\omega L_{series}}{Z_0} = j(3.64 - 0.44) = j3.2$

$$L_{series} = \frac{(3.2)(50)}{2\pi(0.7)}\text{nH} = 36.4\text{ nH}$$

From 300 MHz data, $\frac{Z_0}{j\omega L_{shunt}} = -j1.3$

$$L_{shunt} = \frac{50}{(1.3)(2\pi)(0.3)} = 20.4\text{ nH}$$

Fig. 10. *Broadband amplifier with constant gain of 10 dB from 300 MHz to 700 MHz.*

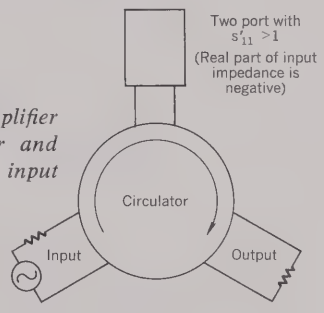

Fig. 11. *Reflection amplifier consists of circulator and transistor with negative input resistance.*

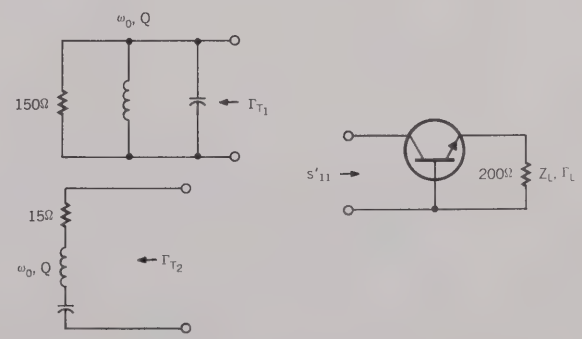

Fig. 12. *Transistor oscillator is designed by choosing tank circuit such that* $\Gamma_T s'_{11} = 1$.

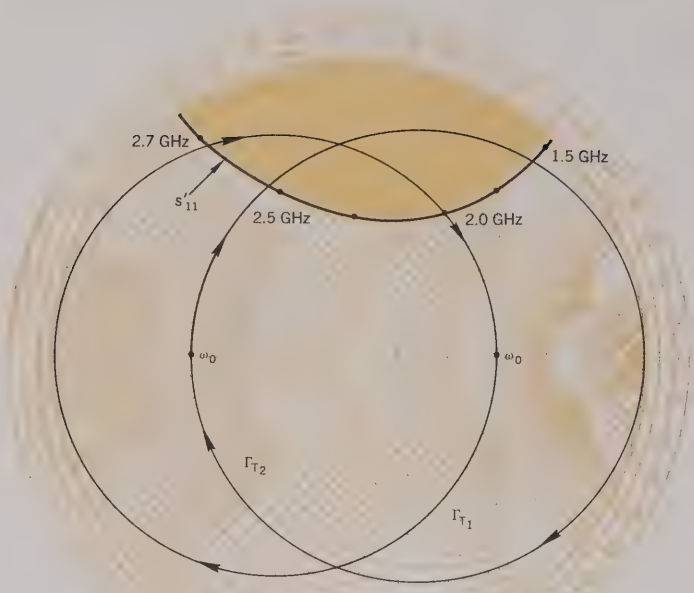

Fig. 13. *Smith Chart for transistor oscillator design example.*

As an example of how these principles of stability are applied in design problems, consider the transistor oscillator design illustrated in Fig. 12. In this case the input reflection coefficient s'_{11} is the reflection coefficient looking into the collector circuit, and the 'source' reflection coefficient Γ_S is one of the two tank-circuit reflection coefficients, Γ_{T1} or Γ_{T2}. From equation 19,

$$s'_{11} = s_{11} + \frac{s_{12}\, s_{21}\, \Gamma_L}{1 - s_{22}\, \Gamma_L}$$

To make the transistor oscillate, s'_{11} and Γ_S must be adjusted so that they satisfy equation 25. There are four steps in the design procedure:

—Measure the four scattering parameters of the transistor as functions of frequency.

—Choose a load reflection coefficient Γ_L which makes s'_{11} greater than unity. In general, it may also take an external feedback element which increases $s_{12}\, s_{21}$ to make s'_{11} greater than one.

—Plot $1/s'_{11}$ on a Smith Chart. (If the new network analyzer is being used to measure the s-parameters of the transistor, $1/s'_{11}$ can be measured directly by reversing the reference and test channel connections between the reflection test unit and the harmonic frequency converter. The polar display with a Smith Chart overlay will then give the desired plot immediately.)

—Connect either the series or the parallel tank circuit to the collector circuit and tune it so that Γ_{T1} or Γ_{T2} is large enough to satisfy equation 25 (the tank circuit reflection coefficient plays the role of Γ_S in this equation).

Fig. 13 shows a Smith Chart plot of $1/s'_{11}$ for a high-frequency transistor in the common-base configuration. Load impedance Z_L is 200Ω, which means that Γ_L referred to 50Ω is 0.6. Reflection coefficients Γ_{T1} and Γ_{T2} are also plotted as functions of the resonant frequencies of the two tank circuits. Oscillations occur when the locus of Γ_{T1} or Γ_{T2} passes through the shaded region. Thus this transistor would oscillate from 1.5 to 2.5 GHz with a series tuned circuit and from 2.0 to 2.7 GHz with a parallel tuned circuit.

—Richard W. Anderson

Additional Reading on S-Parameters

Besides the papers referenced in the footnotes of the article, the following articles and books contain information on s-parameter design procedures and flow graphs.

—F. Weinert, 'Scattering Parameters Speed Design of High-Frequency Transistor Circuits,' Electronics, Vol. 39, No. 18, Sept. 5, 1966.

—G. Fredricks, 'How to Use S-Parameters for Transistor Circuit Design,' EEE, Vol. 14, No. 12, Dec., 1966.

—D. C. Youla, 'On Scattering Matrices Normalized to Complex Port Numbers,' Proc. IRE, Vol. 49, No. 7, July, 1961.

—J. G. Linvill and J. F. Gibbons, 'Transistors and Active Circuits,' McGraw-Hill, 1961. (No s-parameters, but good treatment of Smith Chart design methods.)

Useful Scattering Parameter Relationships

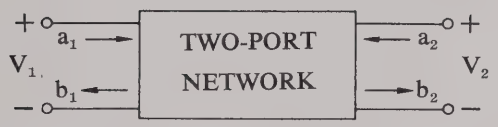

$$b_1 = s_{11}a_1 + s_{12}a_2$$

$$b_2 = s_{21}a_1 + s_{22}a_2$$

Input reflection coefficient with arbitrary Z_L

$$s'_{11} = s_{11} + \frac{s_{12}s_{21}\Gamma_L}{1 - s_{22}\Gamma_L}$$

Output reflection coefficient with arbitrary Z_S

$$s'_{22} = s_{22} + \frac{s_{12}s_{21}\Gamma_S}{1 - s_{11}\Gamma_S}$$

Voltage gain with arbitrary Z_L and Z_S

$$A_V = \frac{V_2}{V_1} = \frac{s_{21}(1 + \Gamma_L)}{(1 - s_{22}\Gamma_L)(1 + s'_{11})}$$

$$\text{Power Gain} = \frac{\text{Power delivered to load}}{\text{Power input to network}}$$

$$G = \frac{|s_{21}|^2(1 - |\Gamma_L|^2)}{(1 - |s_{11}|^2) + |\Gamma_L|^2(|s_{22}|^2 - |D|^2) - 2\,\mathrm{Re}\,(\Gamma_L N)}$$

$$\text{Available Power Gain} = \frac{\text{Power available from network}}{\text{Power available from source}}$$

$$G_A = \frac{|s_{21}|^2(1 - |\Gamma_S|^2)}{(1 - |s_{22}|^2) + |\Gamma_S|^2(|s_{11}|^2 - |D|^2) - 2\,\mathrm{Re}\,(\Gamma_S M)}$$

$$\text{Transducer Power Gain} = \frac{\text{Power delivered to load}}{\text{Power available from source}}$$

$$G_T = \frac{|s_{21}|^2(1 - |\Gamma_S|^2)(1 - |\Gamma_L|^2)}{|(1 - s_{11}\Gamma_S)(1 - s_{22}\Gamma_L) - s_{12}s_{21}\Gamma_L\Gamma_S|^2}$$

Unilateral Transducer Power Gain ($s_{12} = 0$)

$$G_{Tu} = \frac{|s_{21}|^2(1 - |\Gamma_S|^2)(1 - |\Gamma_L|^2)}{|1 - s_{11}\Gamma_S|^2\,|1 - s_{22}\Gamma_L|^2}$$

$$= G_o G_1 G_2$$

$$G_0 = |s_{21}|^2$$

$$G_1 = \frac{1 - |\Gamma_S|^2}{|1 - s_{11}\Gamma_S|^2}$$

$$G_2 = \frac{1 - |\Gamma_L|^2}{|1 - s_{22}\Gamma_L|^2}$$

Maximum Unilateral Transducer Power Gain when $|s_{11}| < 1$ and $|s_{22}| < 1$

$$G_u = \frac{|s_{21}|^2}{|(1 - |s_{11}|^2)(1 - |s_{22}|)^2|}$$

$$= G_o\, G_{1\,\max}\, G_{2\,\max}$$

$$G_{i\,\max} = \frac{1}{1 - |s_{ii}|^2} \qquad i = 1, 2$$

This maximum attained for $\Gamma_S = s^*_{11}$ and $\Gamma_L = s^*_{22}$

Constant Gain Circles (Unilateral case: $s_{12} = 0$)

—center of constant gain circle is on line between center of Smith Chart and point representing s^*_{ii}

—distance of center of circle from center of Smith Chart:

$$r_i = \frac{g_i|s_{ii}|}{1 - |s_{ii}|^2(1 - g_i)}$$

—radius of circle:

$$\rho_i = \frac{\sqrt{1 - g_i}\,(1 - |s_{ii}|^2)}{1 - |s_{ii}|^2(1 - g_i)}$$

where: $i = 1, 2$

$$\text{and } g_i = \frac{G_i}{G_{i\,\max}} = G_i(1 - |s_{ii}|^2)$$

Unilateral Figure of Merit

$$u = \frac{|s_{11}s_{22}s_{12}s_{21}|}{|(1 - |s_{11}|^2)(1 - |s_{22}|^2)|}$$

Error Limits on Unilateral Gain Calculation

$$\frac{1}{(1 + u^2)} < \frac{G_T}{G_{Tu}} < \frac{1}{(1 - u^2)}$$

HEWLETT-PACKARD JOURNAL
TECHNICAL INFORMATION FROM THE LABORATORIES OF THE HEWLETT-PACKARD COMPANY
FEBRUARY 1967 Volume 18 • Number 6
PUBLISHED AT THE CORPORATE OFFICES
1501 PAGE MILL ROAD, PALO ALTO, CALIFORNIA 94304
Staff: F. J. BURKHARD, Editor; R. P. DOLAN, L. D. SHERGALIS
R. A. ERICKSON, Art Director

Conditions for Absolute Stability

No passive source or load will cause network to oscillate if a, b, and c are all satisfied.

a. $|s_{11}| < 1, |s_{22}| < 1$

b. $\left| \dfrac{|s_{12}s_{21}| - |M^*|}{|s_{11}|^2 - |D|^2} \right| > 1$

c. $\left| \dfrac{|s_{12}s_{21}| - |N^*|}{|s_{22}|^2 - |D|^2} \right| > 1$

Condition that a two-port network can be simultaneously matched with a positive real source and load:

$K > 1$ or $C < 1$

$C =$ Linvill C factor

Linvill C Factor

$$C = K^{-1}$$

$$K = \frac{1 + |D|^2 - |s_{11}|^2 - |s_{22}|^2}{2\,|s_{12}s_{21}|}$$

Source and Load for Simultaneous Match

$$\Gamma_{mS} = M^* \left[\frac{B_1 \pm \sqrt{B_1^2 - 4\,|M|^2}}{2\,|M|^2} \right]$$

$$\Gamma_{mL} = N^* \left[\frac{B_2 \pm \sqrt{B_2^2 - 4\,|N|^2}}{2\,|N|^2} \right]$$

Where $B_1 = 1 + |s_{11}|^2 - |s_{22}|^2 - |D|^2$

$B_2 = 1 + |s_{22}|^2 - |s_{11}|^2 - |D|^2$

Maximum Available Power Gain

If $K > 1$,

$$G_{A\,max} = \left| \frac{s_{21}}{s_{12}} (K \pm \sqrt{K^2 - 1}) \right|$$

$K = C^{-1}$

$C =$ Linvill C Factor

(Use plus sign when B_1 is positive, minus sign when B_1 is negative. For definition of B_1 see 'Source and Load for Simultaneous Match,' elsewhere in this table.)

$$D = s_{11}s_{22} - s_{12}s_{21}$$

$$M = s_{11} - D\,s^*_{22}$$

$$N = s_{22} - D\,s^*_{11}$$

s-parameters in terms of h-, y-, and z-parameters	h-, y-, and z-parameters in terms of s-parameters
$s_{11} = \dfrac{(z_{11}-1)(z_{22}+1) - z_{12}z_{21}}{(z_{11}+1)(z_{22}+1) - z_{12}z_{21}}$	$z_{11} = \dfrac{(1+s_{11})(1-s_{22}) + s_{12}s_{21}}{(1-s_{11})(1-s_{22}) - s_{12}s_{21}}$
$s_{12} = \dfrac{2z_{12}}{(z_{11}+1)(z_{22}+1) - z_{12}z_{21}}$	$z_{12} = \dfrac{2s_{12}}{(1-s_{11})(1-s_{22}) - s_{12}s_{21}}$
$s_{21} = \dfrac{2z_{21}}{(z_{11}+1)(z_{22}+1) - z_{12}z_{21}}$	$z_{21} = \dfrac{2s_{21}}{(1-s_{11})(1-s_{22}) - s_{12}s_{21}}$
$s_{22} = \dfrac{(z_{11}+1)(z_{22}-1) - z_{12}z_{21}}{(z_{11}+1)(z_{22}+1) - z_{12}z_{21}}$	$z_{22} = \dfrac{(1+s_{22})(1-s_{11}) + s_{12}s_{21}}{(1-s_{11})(1-s_{22}) - s_{12}s_{21}}$
$s_{11} = \dfrac{(1-y_{11})(1+y_{22}) + y_{12}y_{21}}{(1+y_{11})(1+y_{22}) - y_{12}y_{21}}$	$y_{11} = \dfrac{(1+s_{22})(1-s_{11}) + s_{12}s_{21}}{(1+s_{11})(1+s_{22}) - s_{12}s_{21}}$
$s_{12} = \dfrac{-2y_{12}}{(1+y_{11})(1+y_{22}) - y_{12}y_{21}}$	$y_{12} = \dfrac{-2s_{12}}{(1+s_{11})(1+s_{22}) - s_{12}s_{21}}$
$s_{21} = \dfrac{-2y_{21}}{(1+y_{11})(1+y_{22}) - y_{12}y_{21}}$	$y_{21} = \dfrac{-2s_{21}}{(1+s_{11})(1+s_{22}) - s_{12}s_{21}}$
$s_{22} = \dfrac{(1+y_{11})(1-y_{22}) + y_{12}y_{21}}{(1+y_{11})(1+y_{22}) - y_{12}y_{21}}$	$y_{22} = \dfrac{(1+s_{11})(1-s_{22}) + s_{12}s_{21}}{(1+s_{22})(1+s_{11}) - s_{12}s_{21}}$
$s_{11} = \dfrac{(h_{11}-1)(h_{22}+1) - h_{12}h_{21}}{(h_{11}+1)(h_{22}+1) - h_{12}h_{21}}$	$h_{11} = \dfrac{(1+s_{11})(1+s_{22}) - s_{12}s_{21}}{(1-s_{11})(1+s_{22}) + s_{12}s_{21}}$
$s_{12} = \dfrac{2h_{12}}{(h_{11}+1)(h_{22}+1) - h_{12}h_{21}}$	$h_{12} = \dfrac{2s_{12}}{(1-s_{11})(1+s_{22}) + s_{12}s_{21}}$
$s_{21} = \dfrac{-2h_{21}}{(h_{11}+1)(h_{22}+1) - h_{12}h_{21}}$	$h_{21} = \dfrac{-2s_{21}}{(1-s_{11})(1+s_{22}) + s_{12}s_{21}}$
$s_{22} = \dfrac{(1+h_{11})(1-h_{22}) + h_{12}h_{21}}{(h_{11}+1)(h_{22}+1) - h_{12}h_{21}}$	$h_{22} = \dfrac{(1-s_{22})(1-s_{11}) - s_{12}s_{21}}{(1-s_{11})(1+s_{22}) + s_{12}s_{21}}$

The h-, y-, and z-parameters listed above are all normalized to Z_o. If h′, y′, and z′ are the actual parameters, then

$z_{11}' = z_{11}Z_o$	$y_{11}' = \dfrac{y_{11}}{Z_o}$	$h_{11}' = h_{11}Z_o$
$z_{12}' = z_{12}Z_o$	$y_{12}' = \dfrac{y_{12}}{Z_o}$	$h_{12}' = h_{12}$
$z_{21}' = z_{21}Z_o$	$y_{21}' = \dfrac{y_{21}}{Z_o}$	$h_{21}' = h_{21}$
$z_{22}' = z_{22}Z_o$	$y_{22}' = \dfrac{y_{22}}{Z_o}$	$h_{22}' = \dfrac{h_{22}}{Z_o}$

Transistor Frequency Parameters

f_t = frequency at which $|h_{fe}|$

$= |h_{21}$ for common-emitter configuration$| = 1$

f_{max} = frequency at which $G_{A\,max} = 1$

SECTION IV

COMBINE S PARAMETERS WITH TIME SHARING

This article describes how s parameters were used in conjunction with a small time-sharing computer for the design of thin-film amplifier circuits. Les Besser describes in clear detail how he approached the problem from both a circuit and a programming standpoint. He took advantage of the fact that one set of parameters can be used to calculate another set. The numerous transitions between s, y, z, and x parameters were readily done on the small computer. Finally he shows how his theoretical design utilizing s-parameter data agrees extremely well with the actual amplifier performance.

Combine s parameters with time sharing

and bring thin-film, high-frequency amplifier design closer to a science than an art.

High-frequency amplifier design traditionally has followed the route of an art rather than a science. The engineer would carry out approximate calculations and then make his amplifier circuit work by means of a tricky layout, shielding, grounding and so on.

The concept of the *s* parameters (see box) and the advent of computer time-sharing together are signaling an end to these trial and error techniques. And high time, too. Such techniques could not have helped approach, for example, the theoretical maximum performance of a transistor—a feat that required, in addition to time sharing and use of the *s* parameters, two other advances as well: thin-film hybrid circuits and lossless wideband matching networks. And even more specifically, *s* parameters and thin-film circuits have also been behind the designs of several wideband amplifiers for frequencies of from 10 kHz to 2 GHz, with 20 to 30 dB of gain. Each amplifier covers at least 4 to 5 octaves. In most cases, the first breadboard measurements were so close to the design values that only minor adjustments had to be made before turning the prototypes for production.

Why s parameters and thin-film circuits?

The conventional parameters—*y*, *z* and *h*—are hard to measure at frequencies above 100 MHz. This is because all of them require that open and short circuits be established and call for laborious and tedious measurements.

Then, commonly-used models of transistors do not truly represent the actual devices. Thus, when the inaccurate *y*, *z*, or *h* parameters are used in an inaccurate transistor model it is only natural to get inaccurate results.

S parameters, on the other hand, even in the GHz region, are measured easily and accurately by direct readout. Swept measurements of the *s* parameters can be made today with existing instruments (see photo) and the results easily observed on polar displays such as the familiar Smith chart or any other suitable graph.

Mathematically, *s* parameters lend themselves nicely to matrix manipulations. A circuit of any complexity is built by adding and cascading two-port blocks. Since these blocks contain real elements that can be measured accurately, no approximations are used.

A designer cannot normally expect an amplifier above 500 MHz to give really accurate results with discrete components, because the physical dimensions of the components are approaching the order of magnitude of the electrical wavelengths. Thus, for 500 MHz or higher, microcircuits would be his natural choice.

However, for amplifiers below 500 MHz, too, microcircuits have definite advantages. The thin-film technique reduces size, parasitic reactances and long-term costs, and at the same time improves design accuracy, reliability, heat dissipation, and repeatability.

Accordingly, rather than utilize a conventional design routine, suppose we follow the outline given below in adapting the *s*-parameter approach and the thin-film circuits to be used:

1. Use s parameters throughout. All high-frequency measurements are done with *s* parameters, from taking the parameters of the active devices to evaluating the complete amplifier. Measurement errors can be reduced to as low as 2 to 3 per cent even in the GHz region. Magnitude and phase are both measurable.[1] Swept measurements and visual polar display of the *s* parameters are possible.

Some of the leading transistor manufacturers already are supplying *s*-parameter information for their products. Vector voltmeters, network analyzers, and other test equipment permit the designer to obtain the *s* parameters from 1 MHz up to 12.4 GHz both swiftly and accurately. A typical wideband system to measure transistor (discrete or chip form) *s* parameters can be calibrated into the GHz region in a few minutes, and the *s* parameters can be read directly without any additional tuning or adjustment (see photo).

2. Work with parameter matrices. Build up the circuits step by step by adding and cascading two-port blocks.[2] Keep converting the parameters[3] (*x*, *y*, *z* and *s*) to the form that offers the

Les Besser, Project Supervisor, Hewlett-Packard Co., Palo Alto, Calif.

What are s parameters?

S parameters[1,2] are reflection and transmission coefficients. Transmission coefficients are commonly called gain or attenuation; reflection coefficients are directly related to VSWR and impedance.

Conceptually, s parameters are like h, y, or z parameters insofar as they describe the inputs and outputs of a black box. But the inputs and outputs for s parameters are expressed in terms of power, and for h, y, and z parameters as voltages and currents. Also, s parameters are measured with all circuits terminated in an actual characteristic line impedance of the system, doing away with the open- and short-circuit measurements specified for h, y or z parameters.

The figure below, which uses the convention that a is a signal into a port and b a signal out of a port, explains s parameters.

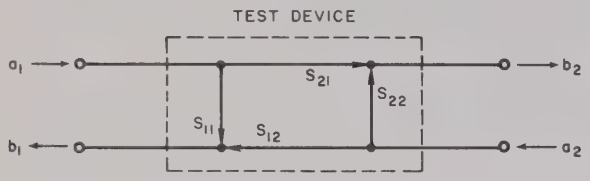

In this figure, a and b are the square roots of power; $(a_1)^2$ is the power incident at port 1, and $(b_2)^2$ is the power leaving port 2. The fraction of a_1 that is reflected at port 1 is s_{11}, and the transmitted part is s_{21}. Similarly, the fraction of a_2 that is reflected at port 2 is s_{22}, and s_{12} is transmitted in the reverse direction.

The signal b_1 leaving port 1 is the sum of the fraction of a_1 that was reflected at port 1 and what was transmitted from port 2.

The outputs related to the inputs are

$$b_1 = s_{11}\, a_1 + s_{12}\, a_2, \qquad (1)$$

$$b_2 = s_{21}\, a_1 + s_{22}\, a_2. \qquad (2)$$

When port 1 is driven by an RF source, a_2 is made zero by terminating the 50-Ω transmission line, coming out of port 2, in its characteristic impedance.

The setup for measuring s_{11} and s_{21} is this:

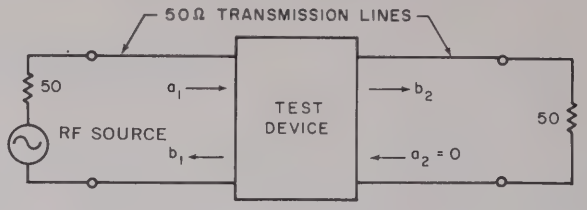

If $a_2 = 0$, then:

$$s_{11} = b_1/a_1,\ s_{21} = b_2/a_1 \qquad (3)$$

Similarly, the setup for measuring s_{12} and s_{22} is this:

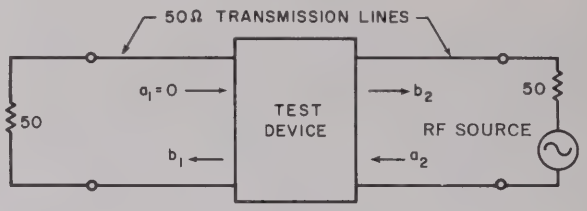

If $a_1 = 0$, then:

$$s_{12} = b_1/a_2,\ s_{22} = b_2/a_2 \qquad (4)$$

Another advantage of s parameters is that, being vector quantities, they contain both magnitude and phase information.

By definition, s_{11} and s_{22} are ratios of the reflected and incident powers, or exactly the same as the reflection coefficient, Γ, commonly used with the Smith chart. The input and output parameters of a two-port device can be presented on a polar display without any transformation (see photos in text) and the corresponding normalized impedances can be readily obtained on the same chart. Impedance transformation and matching can be done either graphically or analytically. Mismatch losses that occur between any port and a 50-Ω termination can be calculated. For example,

$$P_{\text{Mismatch}} = 10 \log_{10} (1 - |\Gamma|^2),$$

where P_M is the mismatch loss in dB at any given port having a reflection coefficient Γ. When the s parameters are known, s_{11} or s_{22} can be substituted for Γ.

The transducer power gain of the two-port network can be computed by

$$G_T = |s_{21}|^2 \qquad (5)$$

or in dB

$$G_T = 10 \log_{10} (|s_{21}|^2) \qquad (6)$$

simplest operation at every step. Since there are no approximations, the calculations will not introduce any additional error. This approach also eliminates the need for conventional transistor models, which not only do not truly represent the device, but require h parameters that can be accurately measured at frequencies above 100 MHz only with great difficulty.

3. Use on-line time sharing, and let the computer do all the work. With the help of a few simple "do-loops" the optimum values of the circuit elements can be readily determined. Time sharing offers extraordinary flexibility. The designer need not wait until his program is returned from the computer center; and program changes can be done by teletypewriter and the results seen within seconds.

A completely automated network analyzer system was recently developed.[4] Here a small computer controls all calibrations and measurements and also solves the circuit program. Its automatic calibration eliminates practically all uncertainties and human-factor errors to bring an unprecedented accuracy into microwave-circuit design. The maximum

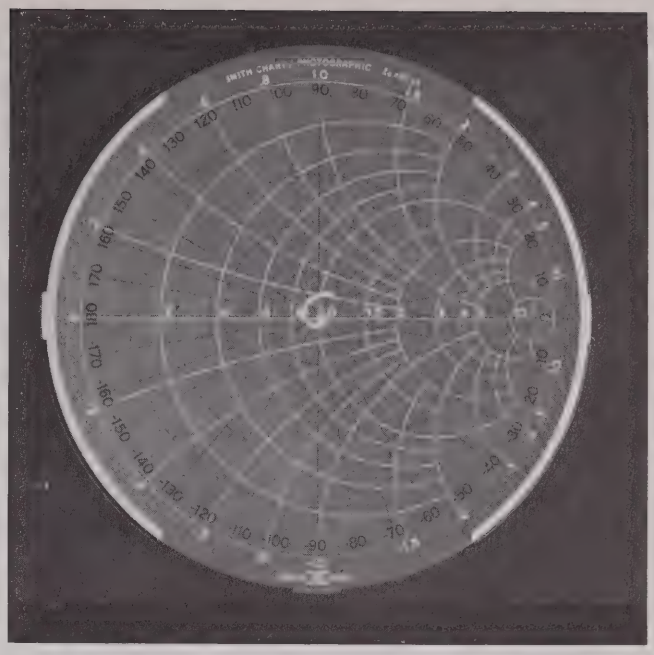

A complete s-parameter test setup good for frequencies up to 12 GHz includes an HP 8410A/ 8411A Network Analyzer ($4300) and an HP 8414A Polar Display ($1100), both housed in the top frame. In the center is an HP 8745A S-Parameter Test Set ($3000) and under it an HP 8690A Sweeper ($1600). If you are willing to sacrifice the convenience of polar display and swept measurement, you can get by with just the Vector Voltmeter (HP 8405, $2750), top of the shelf to the left. It will work up to 1 GHz. A photo of a Smith chart overlay (white grid) of S_{22} over a 100 to 400 MHz range obtained by the author, Les Besser, is shown on the right.

magnitude of errors can be as low as 0.1%—and this is almost entirely due to the standard shorts and terminations that are used to calibrate the system.

Selecting the circuitry

The amplifier we are designing must meet the following specifications (all measurements are made in a 50-Ω system, i.e., 50-Ω load and a 50-Ω source):

- Forward gain at 10 MHz: 20 dB ±0.5 dB.
- Gain flatness 10 kHz — 400 MHz: ±0.5 dB.
- Reverse gain (isolation): < —30 dB.
- Input and output VSWR: < 1.5:1.

These specifications may be expressed in terms of the s parameters by using the following relationships for a two port network:

1. Input, output reflection parameters (s_{11} and s_{22}) are:

$$|s| = (\delta - 1)/(\delta + 1),$$

where δ is the VSWR of the port that is being specified while the other port is terminated in the characteristic line impedance, i.e., 50 Ω; and

2. Forward and reverse gain parameters (s_{21} and s_{12}) are:

$$|s| = \log_{10}^{-1}(G/20),$$

where G is the network gain in dB, when both the driving source and the terminating load have the characteristic line impedance.

Thus the above specifications become, in terms of the s parameters:

$$|s_{11}| < 0.2$$
$$|s_{12}| < 0.03$$
$$|s_{21}| = 10 \pm \frac{0.60}{0.55}$$
$$|s_{22}| < 0.2$$

The stated 20-dB wideband gain requires a voltage gain-bandwidth product of 4 GHz. This is impractical with a single stage, and may be impossible to achieve. An expensive transistor would be needed, and even with this transistor the specified isolation and stability could impose severe limitations. There are, however, several low-cost transistors (for example, HP-1, HP-2, 2N3570) on the market with the guaranteed f_T of 1.5 GHz. If mismatch losses are kept to a minimum value, two such transistors cascaded in a feedback circuit can provide 20-dB gain and meet the above gain-flatness specifications without requiring adjustment. Feedback, of course, reduces the circuit's sensitivity to component parameter variations and changes, and helps maintain flat-gain response through a wide range of frequencies. Of the various feedback arrangements the most stable consists of separate complex shunt and series feedbacks for each transistor (rather than over-all feedbacks around both). This approach also permits the designer to obtain the parameters of a single stage, and thus find a conjugate interstage match that assures maximum power transfer.

If the feedback circuit includes purely resistive elements, or if it includes reactive elements to reduce the effect of the feedback at the higher fre-

quencies, the bandwidth can be increased.

Combining two-port networks

It was mentioned earlier that the network parameter matrices should be continuously converted to the form that offers the simplest means for combining the various circuit elements. Besides the s parameters, three other parameter matrices are used (Fig. 1). The admittance Y and the impedance Z parameter matrices do not require an explanation, but the X-parameter matrice, which is used to cascade the two-port networks, does. Here is how it was derived:

The transmission parameters[5], T, are commonly used to cascade two-port networks. In terms of the s parameters:

$$T = \begin{vmatrix} s_{21} - (s_{22}\, s_{11}/s_{12}) & s_{22}/s_{12} \\ -s_{11}/s_{12} & 1/s_{12} \end{vmatrix}$$

In the case of unilateral design ($s_{12} = 0$), the value of T would go to infinity. A more meaningfull form called X matrix is obtained[6] where s_{21} rather than s_{12} is in the denominator. This matrix, which has a finite value for all active devices, is defined as:

$$X = L(LT)^{-1} ,$$

where

$$L = \begin{vmatrix} 0 & 1 \\ 1 & 0 \end{vmatrix}$$

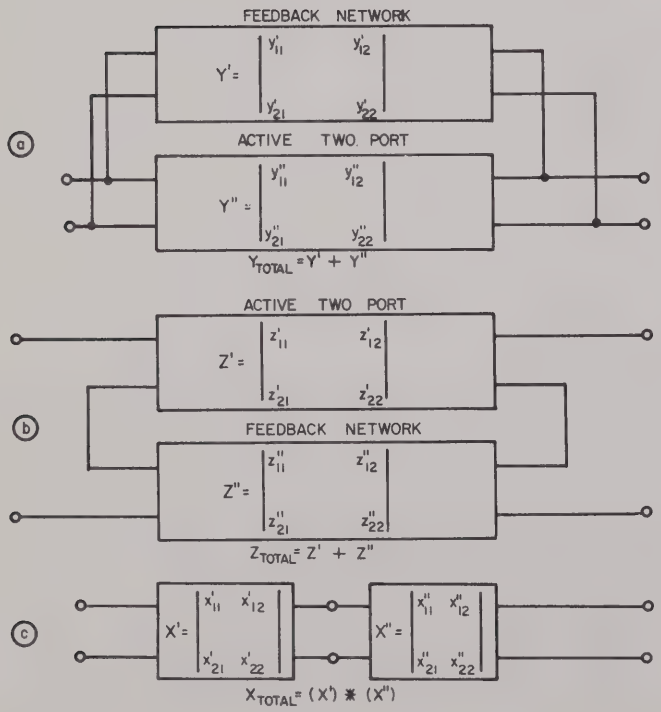

1. **Feedback is added and two-port networks** are cascaded by means of admittance (a), impedance (b) and modified transmission (c) parameters. See text for the derivation of the X-parameter matrix.

Set up the program

The computer program for this design was written for the GE time-share BASIC language through remote teletype outlets. It consists of a control section and several subroutines for the various conversions. The BASIC language handles matrices by simple (MAT READ, MAT PRINT, etc.) commands. However, at the present time it does not offer complex variable operation. A special subroutine therefore was developed in the following manner to enable the computer to operate with complex matrices:

It can be proved[7] that any complex number can be represented by a 2 × 2 matrix *for the duration* of some mathematical operations, if, at the end, the matrix is "retransformed" in a comparable manner to the initial transformation. For example:

$$z_{11} = r_{11} + jx_{11} ===> \begin{vmatrix} r_{11} & x_{11} \\ -x_{11} & r_{11} \end{vmatrix} = Z_{11} .$$

It can also be proved that the matrix operation will not change if all matrix elements are replaced by their equivalent matrices.

Now the real and imaginary parts of a complex 2 × 2 matrix form a 4 × 4 matrix. After the operations, this 4 × 4 matrix yields results in the original complex form

$$Z'_{11} = \begin{vmatrix} r'_{11} & x'_{11} \\ -x'_{11} & r'_{11} \end{vmatrix} \longrightarrow \quad r'_{11} + jx'_{11} = z'_{11}$$

Since all calculations are done in matrix form, the passive network elements should be expressed in matrix form. The method is illustrated in Fig. 2, which deals with finding the equivalent Z matrix of a resistive "T." Here, in the matrix form, we have

$$Z = \begin{vmatrix} z_{11} & z_{12} \\ z_{21} & z_{22} \end{vmatrix} = \begin{vmatrix} (r_a + r_c) & r_c \\ r_c & (r_b + r_c) \end{vmatrix}$$

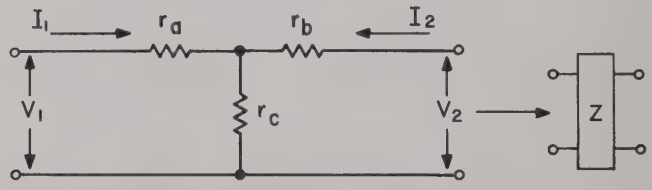

2. **An equivalent Z matrix** for a common resistive "T" is derived (in text) using the symbols defined above. All operations involve matrices; accordingly, the reader should familiarize himself with matrix algebra.

Step-by-step computerized design

We can now proceed with a description of the steps required to design an amplifier stage.

Note that since all the steps below are illustrated pictorially, the schematics sometimes will not change in converting matrices, say, S to Y.

1. Read in frequency.
2. Read in transistor s parameters in matrix form, S_{T1}.

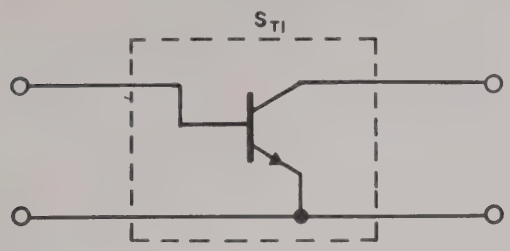

3. Convert device S matrix to Y matrix, $S_{T1} \rightarrow Y_{T1}$.
4. Set up Y matrix for complex shunt feedback element, Y_P.
5. Add shunt feedback, $Y_{T2} = Y_P + Y_{T1}$.

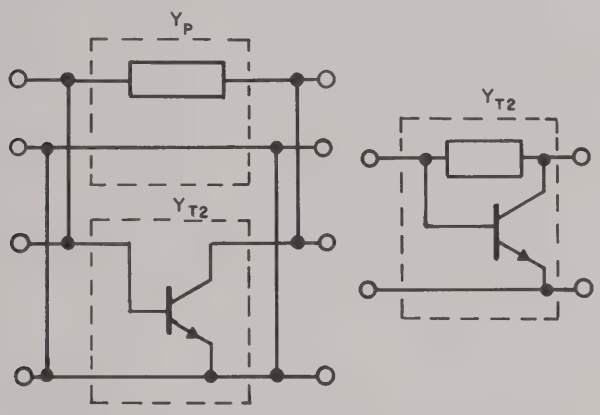

6. Convert Y matrix of device and shunt feedback to Z matrix, $Y_{T2} \rightarrow Z_{T1}$.
7. Set up Z matrix for complex emitter feedback element, Z_E.

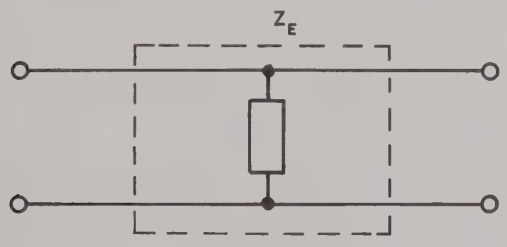

8. Add emitter feedback to device with shunt feedback, $Z_{T2} = Z_E + Z_{T1}$.

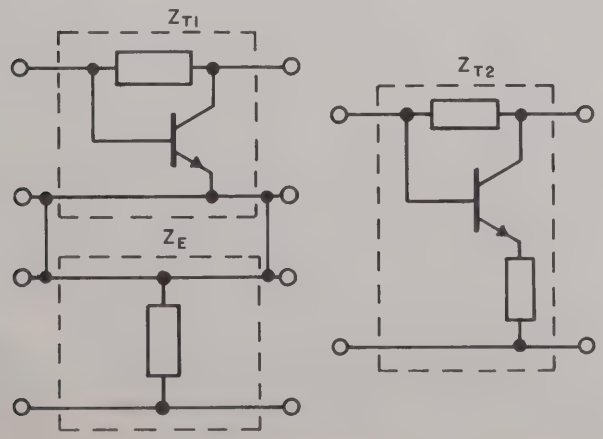

9. Convert Z matrix of device with feedbacks to X matrix, $Z_{T2} \rightarrow X_{T1}$.

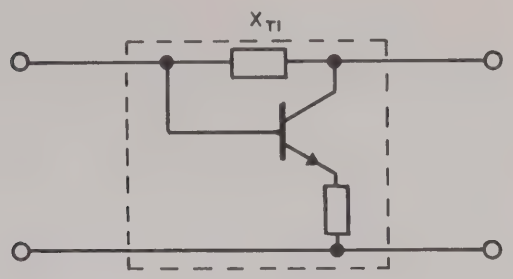

10. Set up X matrices for base and collector bias elements (may be complex), X_B, X_C.

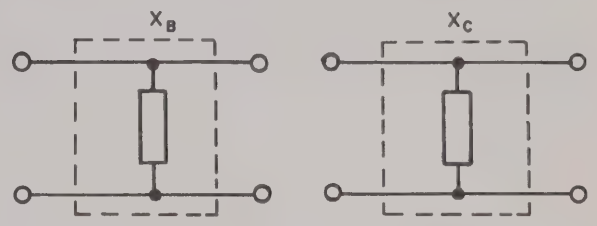

11. Multiply X matrices of bias elements by device and feedback matrices,
$X_{T2} = (X_B) * (X_{T1})$
$X_{T3} = (X_{T2}) * (X_C)$.

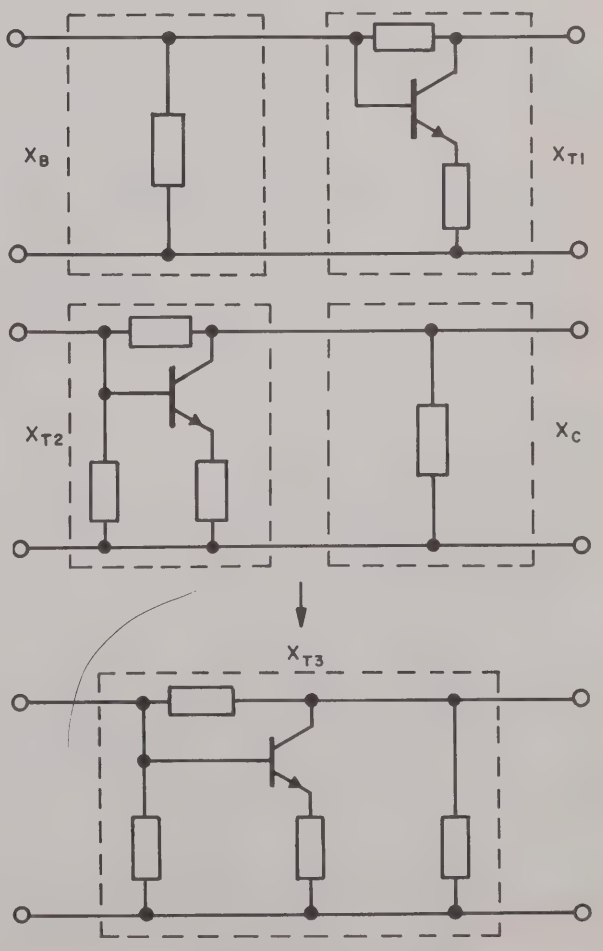

12. Set up X matrices for input and output matching elements (lumped or distributed), X_{M1}, X_{M2}.

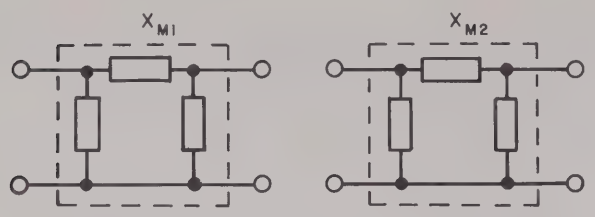

13. Multiply matching elements and device,
$X_{T4} = (X_{M1})\ *\ (X_{T3})$
$X_{T5} = (X_{T4})\ *\ (X_{M2})$.

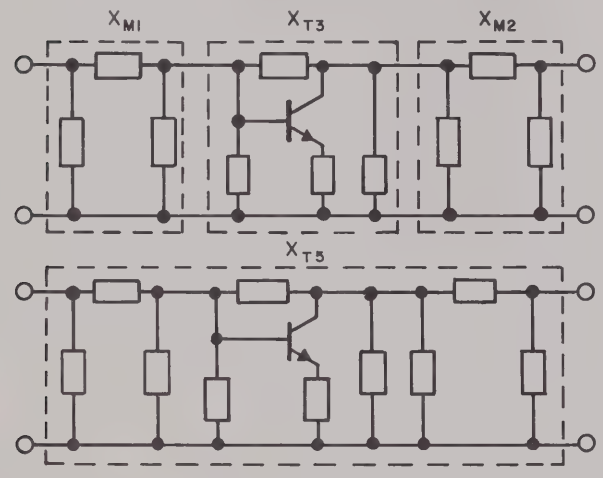

14. Convert over-all X matrix to S matrix, $X_{T5} \rightarrow S_{T2}$.

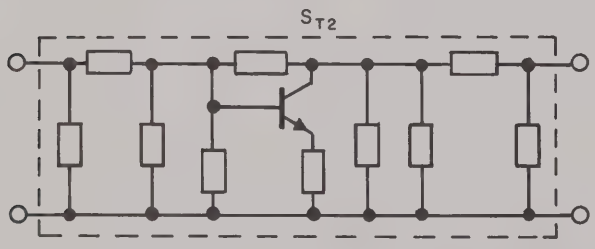

15. Print out:
- S parameters of amplifier.
- Maximum available gain.
- Transducer power gain (G_T).
- Circuit (mismatch) losses.
- Stability factor.
- Unilateral figure of merit, U.

(This outline should be followed for each stage of the amplifier. Afterward the stage should be optimized and its X matrices multiplied together to obtain the over-all parameters).

16. Go to next frequency (step 1).
17. End.

A sample printout for two cascaded stages operating at 100 MHz is shown below.

```
H P MICROW

GE·TIME-SHARING SERVICE

ON AT  19:26   SF WED 05/22/68   TTY 13

USER NUMBER--
SYSTEM--BASIC
NEW OR OLD--OLD
OLD PROBLEM NAME--LB-AMP

READY.

RUN

LB-AMP    19:27   SF WED 05/22/68

F= 100  MHZ    N= 2    STAGES

GT= 20.1109 DB
MISMATCH LOSSES
   INPUT PM= 3.02588 E-2   DB
  OUTPUT PM= 1.55601 E-2   DB
G MAX= 103.668  20.1567 DB
U= 1.15472 E-3
STABILITY FACTOR = 2.14316

OVERALL S MATRIX,S11,S12,S21,S22,  (MAGN.+ ANGLE)

 8.33249 E-2   -49.2713        2.28023 E-2   -69.5409

 10.1282       -63.5409        5.98029 E-2   -64.777
```

Note that the maximum gain is given as 20.1567 dB, while the $G_T = 20.1109$ dB. The difference is due to the mismatch losses. The input mismatch loss, for instance, is printed out as 3.02588 E-2 dB. The E-2 notation stands for 10^{-2}. Subtracting the input and output mismatch losses from the maximum gain results in the obtained G_T value.

Also note that the stability factor is well over one and that the s-parameter values are well within the specified limits.

Understand the program

The shunt and series feedback networks of the single stages should be determined first. With the help of two "do-loops" in steps 4 and 7 the feedback elements are varied and the trends of the resultant changes in s_{11}, s_{22} and the maximum available gain are printed out. The values of the feedback elements are selected to give flat response of maximum available gain, with an absolute value equal to the specified transducer gain, G_T, and the lowest possible set of values for $|s_{11}|$, $|s_{22}|$. A good flat response of maximum available gain within the frequency range of the amplifier indicates that the circuit will provide the required gain if and only if it is properly matched both at the input and the output.

It is advisable to keep the magnitudes of both s_{11} and s_{22} below 0.5 (the lower the better). Otherwise the wideband match will become rather difficult, requiring a ladder network of several sections.

After selecting the feedback networks the corresponding s_{11} and s_{22} should be plotted on a Smith chart and the matching networks deter-

mined.[8,9] S_{11} of the first stage and s_{22} of the second stage are matched to have magnitudes smaller than 0.2, as specified earlier. S_{22} of the first stage is matched to the conjugate value of s_{11} of the second stage. Again, the "do-loops" will help to arrive at the optimum values.

The importance of this technique cannot be overemphasized. Using conventional design techniques, most engineers will accept far less satisfactory matches without much hesitation rather than face the difficulties involved in trial and error. For example, consider the case in which two stages are cascaded, each having a VSWR of 2.5:1 at the input and output (magnitudes of s_{11} and s_{22} equal to 0.43). The mismatch losses can total 3.5 dB—and yet in many instances they would still be acceptable.

In our own case, however, the s_{22} of the unmatched amplifier was 0.49 at 400 MHz, which would result in a 1.2-dB mismatch loss when the amplifier is terminated by a 50-Ω load. After the three-element matching network is placed into the output circuit, $|s_{22}|$ becomes less than 0.08 over the complete frequency range of the amplifier. The maximum value of the mismatch loss is reduced to 0.04 dB.

Once the matching networks are determined, the component values should be fed into step 12 and the over-all response of the amplifier checked. At this point the transducer gain G_T is to have a flat response. If the unilateral approach is not followed ($s_{12} \neq 0$), the output match will affect the input impedance and the input match may affect the output impedance. However, even here only minor changes of the component values will be needed, which the computer will do simultaneously. The circuit is ready to be built.

Stability and final measurements

Stability is of vital importance; the designer should be certain that the amplifier will be unconditionally stable. Although the Linvill stability factor,[10] C, defines a necessary condition for stability, it alone does not guarantee absolute stability for all passive load and source impedances.

In terms of the s parameters, the general conditions for stability[11] require that

$$k = 1/C > 1$$

where

$$K = \frac{1 + |s_{11}\, s_{22} - s_{12}\, s_{21}|^2 - |s_{11}|^2 - |s_{22}|^2}{2\,|s_{12}|\,|s_{21}|}.$$

In addition, the quantity

$$1 + |s_{11}|^2 - |s_{22}|^2 - |s_{11}|s_{22} - s_{12}s_{21}|^2$$

must be greater than zero.

Only when both the above conditions are fulfilled can the circuit be considered to be unconditionally stable for all possible combinations of source and load impedances. If the amplifier shows tendencies toward instability, the gain-bandwidth product of the circuit may have to be reduced or the phase of the matching networks changed.

Table. S parameters at 100 MHz.

	s_{11}	s_{12}	s_{21}	s_{22}
Specified magnitudes	< 0.2	< 0.03	$(10\ ^{+0.6}_{-0.55})$	< 0.2
Design values	$0.083\ \angle -49°$	$0.023\ \angle -70°$	$10.13\ \angle -63°$	$0.060\ \angle -64°$
Measured values	$0.110\ \angle -52°$	$0.020\ \angle -60°$	$10.36\ \angle -54°$	$0.035\ \angle -60°$

The efficiency and accuracy of the design are reflected in the close correlation between the computer-predicted and measured parameter values obtained on the first prototype (see table).

The thin-film process asserted itself through the unusual repeatability of the first five laboratory prototypes. The magnitudes of all s parameters were found to be within ±2 per cent. ■■

References:

1. "Network Analysis at Microwave Frequency," HP Application Note No. 92.
2. Franklin F. Kuo, *Network Analysis and Synthesis,* 2nd ed., John Wiley & Sons, New York, 1966.
3. Seshn, Balabanian, *Linear Network Analysis,* Wiley.
4. Richard A. Hackborn, "An Automatic Network Analyzer System," *Microwave Journal,* May 1968.
5. C. G. Montgomery, R. H. Dicke, E. M. Purcell, "*Principles of Microwave Circuits,* MIT Radiation Laboratory Series, Vol. 8, Boston Technical Publishers, Inc., Lexington, Mass., 1964.
6. George E. Bodway, Hewlett-Packard Internal Publication.
7. Luis Peregrino, Russ Riley, "A Method of Operating with Complex Matrices in the Time-Sharing Computer," Hewlett-Packard Internal Publication.
8. Gerald E. Martes, "Make Impedance Matching Easier," *Electronic Design,* July 5, 1966.
9. J. Linvill and J. Gibbons, *Transistors and Active Circuits,* McGraw-Hill, MC, New York, 1961.
10. *Ibid.*
11. George E. Bodway, "Two-Port Power Flow Analysis Using Generalized S Parameters," *Microwave Journal,* May 1967.
12. "S Parameter Test Set," *Hewlett-Packard Technical Data,* March 1967.

Test your retention

Here are questions based on the main points of this article. They are to help you see if you have overlooked any important ideas. You'll find the answers in the article.

1. What is the main advantage of s parameters over h, y, or z parameters?

2. Can you define each s parameter in terms of their physical significance?

3. Why is it desirable to have s_{12} as small as possible?

4. What is unconditional stability?

SECTION V

QUICK AMPLIFIER DESIGN WITH SCATTERING PARAMETERS

William H. Froehner's article shows how to design an amplifier from scattering parameter data. He shows the s parameters can be used to reliably predict the gain, bandwidth, and stability of a given design. Two design examples are included. One is the design of an amplifier for maximum gain at a single frequency from an unconditionally stable transistor. The second is the design of an amplifier for a given gain at a single frequency when the transistor is potentially unstable.

Electronics®

Quick amplifier design with scattering parameters

By William H. Froehner
Texas Instruments Incorporated, Dallas

Reprinted for **Hewlett Packard Company** from **Electronics**, October 16, 1967.

Quick amplifier design with scattering parameters

Smith chart and s parameters are combined in a fast, reliable method of designing stable transistor amplifiers that operate above 100 megahertz

By William H. Froehner

Texas Instruments Incorporated, Dallas

Bandwidth, gain, and stability are the most important parameters in any amplifier design. Designing for one without considering the other two can mean a mediocre amplifier instead of one with high performance. A reliable technique for predicting bandwidth, determining gain, and assuring stability uses scattering or s parameters.

Scattering parameters make it easy to characterize the high-frequency performance of transistors. As with h, y, or z parameter methods, no equivalent circuit is needed to represent the transistor device. A transistor is represented as a two-port network whose terminal behavior is defined by four s parameters, s_{11}, s_{12}, s_{21}, and s_{22}.

For designs that operate under 100 megahertz the problem of accurately representing the transistor is not acute, because transistor manufacturers provide relatively complete data in a form other than s parameters. However, at frequencies above 100 Mhz the performance data is frequently incomplete or in an inconvenient form. In addition, h, y, or z parameters, ordinarily used in circuit design at lower frequencies, cannot be measured accurately. But s parameters may be measured directly up to a frequency of 12.4 gigahertz. Once the four s parameters are obtained, it is possible to convert them to h, y, or z terms with conventional tables.

Looking back

This is the second major article on scattering parameters to appear in Electronics. In the first, "Scattering parameters speed design of high-frequency transistor circuits," [Sept. 5, 1966, p. 78], F.K. Weinert described how to use the technique in a special case where the input impedance is matched to the load. This condition always results in an unconditionally stable amplifier. In practice, this ideal condition is not always possible.

In this article, author W. H. Froehner describes how to use the technique more generally—when the input impedance is not matched to the load and the scattering parameter s_{12} does not equal zero.

Defining the terms

Because scattering parameters are based on reflection characteristics derived from power ratios they provide a convenient method for measuring circuit losses. Representing a network in terms of power instead of the conventional voltage-current description can help solve microwave-transmission problems where circuits can no longer be characterized using lumped R, L, and C elements.

When a network is described with power parameters, the power into the network is called incident, the power reflected back from the load is called reflected. A description of a typical two-port network based on the incident and reflected power is given by the scattering matrix. To understand the relationships, consider the typical two-port network, bottom of page 101, which is terminated at both ports by a pure resistance of value Z_o, called the reference impedance. Incident and reflected waves for the two-port network are expressed by two sets of parameters (a_1,b_1) and (a_2,b_2) at terminals 1-1′ and 2-2′ respectively. They are

$$a_1 = \tfrac{1}{2}\left[\frac{V_1}{\sqrt{Z_o}} + \sqrt{Z_o}I_1\right] = \text{input power to the load applied at port 1} \quad (1a)$$

$$b_1 = \tfrac{1}{2}\left[\frac{V_1}{\sqrt{Z_o}} - \sqrt{Z_o}I_1\right] = \text{reflected power from the load as seen from port 1} \quad (1b)$$

$$a_2 = \frac{1}{2}\left[\frac{V_2}{\sqrt{Z_o}} + \sqrt{Z_o} I_2\right] = \text{input power to the load applied at port 2} \quad (1c)$$

$$b_2 = \frac{1}{2}\left[\frac{V_2}{\sqrt{Z_o}} - \sqrt{Z_o} I_2\right] = \text{reflected power from the load as seen from port 2} \quad (1d)$$

Hence, the scattering parameters for the two-port network are given by

$$\begin{aligned} b_1 &= s_{11}a_1 + s_{12}a_2 \\ b_2 &= s_{21}a_1 + s_{22}a_2 \end{aligned} \quad (2)$$

Expressed as a matrix, equation 2 becomes

$$\begin{bmatrix} b_1 \\ b_2 \end{bmatrix} = \begin{bmatrix} s_{11} & s_{12} \\ s_{21} & s_{22} \end{bmatrix} \begin{bmatrix} a_1 \\ a_2 \end{bmatrix} \quad (3)$$

where the scattering matrix is

$$[s] = \begin{bmatrix} s_{11} & s_{12} \\ s_{21} & s_{22} \end{bmatrix} \quad (4)$$

Thus, the scattering parameters for the two-port network can be expressed as ratios of incident and reflected power waves.

$$s_{11} = \left.\frac{b_1}{a_1}\right|_{a_2=0} \qquad s_{12} = \left.\frac{b_1}{a_2}\right|_{a_1=0}$$

$$s_{21} = \left.\frac{b_2}{a_1}\right|_{a_2=0} \qquad s_{22} = \left.\frac{b_2}{a_2}\right|_{a_1=0} \quad (5)$$

The parameter s_{11} is called the input reflection coefficient; s_{21} is the forward transmission coefficient; s_{12} is the reverse transmission coefficient; and s_{22} is the output reflection coefficient.

By setting $a_2 = 0$, expressions for s_{11} and s_{21} can be found. To do this the load impedance Z_0 is set equal to the reference impedance R_{ML}. This conclusion is proven with the help of the terminating section of the two-port network shown above with the a_2 and b_2 parameters. The load resistor Z_0 is considered as a one-port network with a scattering parameter

$$s_2 = \frac{Z_o - R_{ML}}{Z_o + R_{ML}} \quad (6)$$

Hence a_2 and b_2 are related by

$$a_2 = s_2 b_2 \quad (7)$$

When the reference impedance R_{ML} is set equal to the load impedance Z_0, then s_2 becomes

$$s_2 = \frac{Z_o - Z_o}{Z_o + Z_o} = 0 \quad (8)$$

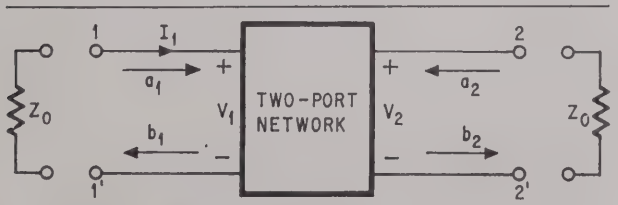

Defining the s parameters. Ratios of incident waves a_1, a_2 and reflected power waves b_1, b_2 for ports 1 and 2 define the four scattering parameters.

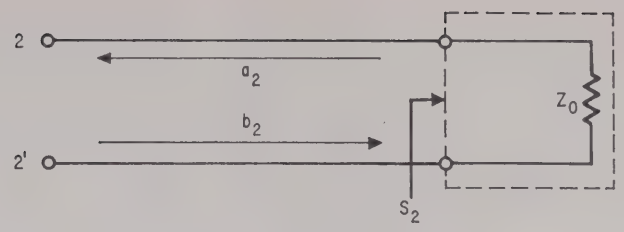

Impedance matching. By setting a_2 equal to zero the engineer can determine the s_{11} value. The condition $a_2 = 0$ implies that the reference impedance R_{MS} is set equal to the load impedance Z_0.

so that $a_2 = 0$ under this condition. Likewise, when $a_1 = 0$, the reference impedance of port 1 is equal to the terminating impedance; $R_{MS} = Z_0$.

By defining the driving-point impedances at ports 1 and 2 as

$$Z_1 = \frac{V_1}{I_1}; \qquad Z_2 = \frac{V_2}{I_2} \quad (9)$$

s_{11} and s_{22} can be written in terms of equation 9.

$$s_{11} = \left.\frac{b_1}{a_1}\right|_{a_2=0} = \frac{\frac{1}{2}[(V_1/\sqrt{Z_o}) - \sqrt{Z_o} I_1]}{\frac{1}{2}[(V_1/\sqrt{Z_o}) + \sqrt{Z_o} I_1]} = \frac{Z_1 - Z_o}{Z_1 + Z_o} \quad (10)$$

$$s_{22} = \frac{Z_2 - Z_o}{Z_2 + Z_o} \quad (11)$$

In the expression

$$s_{21} = \left.\frac{b_2}{a_1}\right|_{a_2=0}$$

The condition $a_2 = 0$ implies that the reference impedance R_{ML} is set equal to the load Z_0. If a voltage source $2E_1$ is connected with a source impedance $R_{MS} = Z_0$, as seen on page 102, a_1 can be expressed as

$$a_1 = \frac{E_1}{\sqrt{Z_o}} \quad (12)$$

Since $a_2 = 0$, then $a_2 = 0 = \frac{1}{2}\left[\frac{V_2}{\sqrt{Z_o}} + \sqrt{Z_o} I_2\right]$

from which $\frac{V_2}{\sqrt{Z_o}} = -\sqrt{Z_o} I_2$

Consequently,

$$b_2 = \frac{1}{2}\left[\frac{V_2}{\sqrt{Z_o}} - \sqrt{Z_o} I_2\right] = \frac{V_2}{\sqrt{Z_o}}$$

Hence,

$$s_{21} = \frac{V_2}{E_1} \quad (13)$$

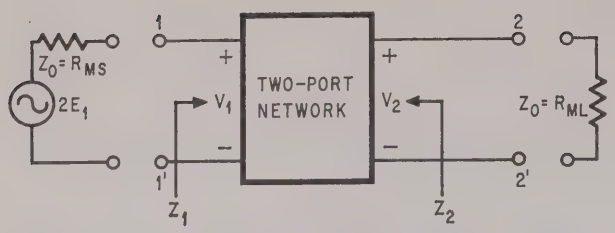

Finding s_{21}. By connecting a voltage source, $2E_1$, with the source impedance, Z_0, parameter s_{21} can be evaluated.

Similarly when port 1 is terminated in $R_{MS} = Z_0$ and a voltage source equal to $2E_2$ having an impedance of Z_0 is connected to port 2

$$s_{12} = \frac{V_1}{E_2} \tag{14}$$

Both s_{12} and s_{21} are voltage-ratios and therefore have no dimensions. For a passive network, $s_{21} = s_{12}$. Parameters s_{11} and s_{22} are reflection coefficients and are also dimensionless.

Stabilizing an amplifier

Since the s parameters are based on reflection coefficients, they can be plotted directly on a Smith chart and easily manipulated to establish optimum gain with matching networks. To design an amplifier the engineer first plots the s-parameter values for the transistor on a Smith chart and then, using the plot, synthesizes matching impedances between a source and load impedance.

Stability or resistance to oscillation is most important in amplifier design and is determined from the s parameters and the synthesized source and load impedances. The oscillations are only possible if either the input or the output port, or both, have negative resistance. This occurs if s_{11} or s_{22} are greater than unity. However, even with negative resistances the amplifier might still be stable.

For a device to be unconditionally stable s_{11} and s_{22} must be smaller than unity and the transistor's inherent stability factor, K, must be greater than unity and positive. K is computed from

$$K = \frac{1 + |\Delta|^2 - |s_{11}|^2 - |s_{22}|^2}{2|s_{21}s_{12}|} \tag{15}$$

Plotting circles

Stability circles can be plotted directly on a Smith chart. These separate the output or input planes into stable and potentially unstable regions. A stability circle plotted on the output plane indicates the values of all loads that provide negative real input impedance, thereby causing the circuit to oscillate. A similar circle can be plotted on the input plane which indicates the values of all loads that provide negative real output impedance and again cause oscillation. A negative real impedance is defined as a reflection coefficient which has a magnitude that is greater than unity.

The regions of instability occur within the circles whose centers and radii are expressed by

$$\text{center on the input plane} = r_{s1} = \frac{C_1^*}{|s_{11}|^2 - |\Delta|^2} \tag{16}$$

$$\text{radius on the input plane} = R_{s1} = \frac{|s_{12}s_{21}|}{|s_{11}|^2 - |\Delta|^2} \tag{17}$$

$$\text{center on the output plane} = r_{s2} = \frac{C_2^*}{|s_{22}|^2 - |\Delta|^2} \tag{18}$$

$$\text{radius on the output plane} = Rs_2 = \frac{|s_{12}s_{21}|}{|s_{22}|^2 - |\Delta|^2} \tag{19}$$

where

$$C_1 = s_{11} - \Delta s_{22}^* \tag{20}$$

$$C_2 = s_{22} - \Delta s_{11}^* \tag{21}$$

$$\Delta = s_{11}s_{22} - s_{12}s_{21} \tag{22}$$

In these equations the asterisk represents the complex conjugate value. Six examples of stable and potentially unstable regions plotted on the output plane are on the opposite page. In all cases the gray areas indicate the loads that make the circuit stable.

The first two drawings, A, and B, show the possible locations for stability, when the value of K is less than unity; C and D are for K greater than unity. When the stability circle does not enclose the origin of the Smith chart, its area provides negative real input impedance. But when the stability circle does enclose the origin, then the area bounded by the stability circle provides positive real input impedance.

Drawings E and F indicate the possible locations for stability when the value of K is greater than unity and positive. If the stability circle falls completely outside the unity circle, the area bounded by this circle provides negative real input impedance. But if the stability circle completely surrounds the unity circle then the area of the stability circle provides positive real input impedance.

When K is positive

The design of an amplifier where K is positive and greater than unity is relatively simple since these conditions indicate that the device is unconditionally stable under any load conditions. All the designer need do is compute the values of R_{MS} and R_{ML} that will simultaneously match both the input and output ports and give the maximum power gain of the device.

$$\text{Reflection coefficient of the generator impedance required to conjugately match the input of the transistor} = R_{MS} = C_1^* \left[\frac{B_1 \pm \sqrt{B_1^2 - 4|C_1|^2}}{2|C_1|^2} \right] \tag{23}$$

Stability examples

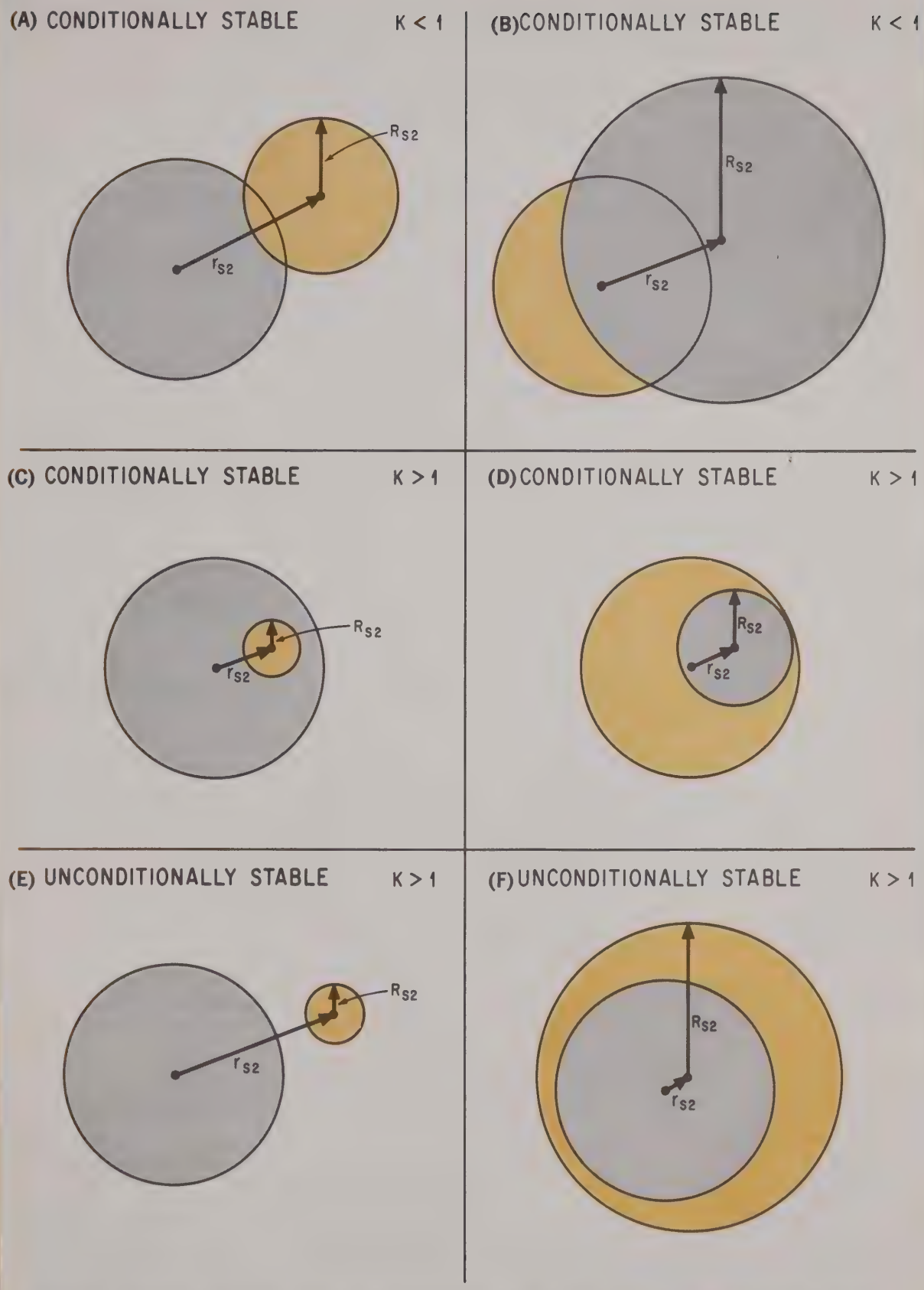

Controlling oscillation. Stability circles are superimposed on the output plane. Load impedances chosen from gray areas will not cause oscillation. Colored areas represent unstable loads.

where

$$B_1 = 1 + |s_{11}|^2 - |s_{22}|^2 - |\Delta|^2 \quad (24)$$

and

Reflection coefficient of that load impedance required to conjugately match the output of the transistor = R_{ML}

$$= C_2^* \left[\frac{B_2 \pm \sqrt{B_2^2 - 4|C_2|^2}}{2|C_2|^2} \right] \quad (25)$$

where

$$B_2 = 1 + |s_{22}|^2 - |s_{11}|^2 - |\Delta|^2 \quad (26)$$

and C_1 and C_2 are as previously defined.

If the computed value of B_1 is negative, then the plus sign should be used in front of the radical in equation 23. Conversely, if B_1 is positive, then the negative sign should be used. This also applies in equation 25 for B_2. By using the appropriate sign only one answer will be possible in either equation and a value of less than unity will be computed.

The maximum power gain possible is found from the relationship

$$G_{MAX} = \frac{|s_{21}|}{|s_{12}|} |K \pm \sqrt{K^2 - 1}| \quad (27)$$

Once again the plus sign is used if B_1 is negative and the minus sign if B_1 is positive. This maximum power gain is obtained only if the device is loaded with R_{MS} and R_{ML} expressed as reflection coefficients. These values are plotted directly on a Smith chart that has been normalized to the reference impedance, ($Z_0 = 50$ ohms, in this case). The actual values of R_{MS} and R_{ML} are read from the Smith chart coordinates and multiplied by Z_0. A lossless transforming network can then be placed between the transistor and the source and load terminations to obtain the maximum gain.

If a power gain other than G_{MAX} is desired, constant gain circles must be constructed. The solution for contours of constant gain is given by the equation of a circle whose center and radius are

The center of the constant gain circle on the output plane = r_{02}

$$= \left[\frac{G}{1 + D_2 G} \right] C_2^* \quad (28)$$

The radius of the constant gain circle on the output plane = R_{02}

$$= \frac{(1 - 2K|s_{12}s_{21}|G + |s_{12}s_{21}|^2 G^2)^{1/2}}{1 + D_2 G} \quad (29)$$

where

$$D_2 = |s_{22}|^2 - |\Delta|^2 \quad (30)$$

$$G = \frac{G_p}{G_o} = \text{power gain} \quad (31)$$

$$G_o = |s_{21}|^2 \quad (32)$$

and G_p = desired total amplifier gain (numeric)

After a load that falls on the desired constant gain circle has been selected, a generator impedance is selected to achieve the desired gain. The value for the generator impedance that simultaneously matches the input load is given by

$$r_1 = \left[\frac{s_{11} - r_2\Delta}{1 - r_2 s_{22}} \right]^* \quad (33)$$

where

r_2 = the reflection coefficient of the load picked.

To prove stability

With the following example it can be demonstrated that when a positive K is greater than unity, the amplifier will always be stable.

Objective: Design an amplifier to operate at 750 Mhz with a maximum gain using a 2N3570 transistor. The bias conditions are $V_{CE} = 10$ volts and $I_C = 4$ milliamperes. Scattering parameters for this transistor were measured and found to be

$s_{11} = 0.277 \angle -59.0°$
$s_{12} = 0.078 \angle 93.0°$
$s_{21} = 1.920 \angle 64.0°$
$s_{22} = 0.848 \angle -31.0°$

Solution: Compute the values for the maximum gain, and the load impedances R_{MS} and R_{ML}.

$\Delta = s_{11}s_{22} - s_{12}s_{21} = 0.324 \angle -64.8°$
$C_1 = s_{11} - \Delta s_{22}^* = 0.120 \angle -135.4°$
$B_1 = 1 + |s_{11}|^2 - |s_{22}|^2 - |\Delta|^2 = 0.253$
$C_2 = s_{22} - \Delta s_{11}^* = 0.768 \angle -33.8°$
$B_2 = 1 + |s_{22}|^2 - |s_{11}|^2 - |\Delta|^2 = 1.537$

$$K = \frac{1 + |\Delta|^2 - |s_{11}|^2 - |s_{22}|^2}{2|s_{12}s_{21}|} = 1.033$$

$$D_2 = |s_{22}|^2 - |\Delta|^2 = 0.614$$

Since B_1 and B_2 are both positive, the negative sign is used in the following:

$$G_{MAX} = |s_{21}|K - \sqrt{K^2 - 1}|$$
$$= 19.087 = 12.807 \text{ db}$$

$$R_{MS} = C_1^* \left[\frac{B_1 - \sqrt{B_1^2 - 4|C_1|^2}}{2|C_1|^2} \right]$$
$$= 0.730 \angle 135.4°$$

$$R_{ML} = C_2^* \left[\frac{B_2 - \sqrt{B_2^2 - 4|C_2|^2}}{2|C_2|^2} \right]$$
$$= 0.951 \angle 33.8°$$

R_{MS} and R_{ML} are plotted on the Smith chart on the opposite page. The actual values of R_{MS} and R_{ML} can now be read from the Smith chart coordinates as Z_s and Z_L.

$R_{MS} = Z_s = 9.083 + j\ 19.903$ ohms
$R_{ML} = Z_L = 14.686 + j\ 163.096$ ohms

These results were obtained with a computer and do not represent the actual reading of the coordinates on the Smith chart.

A lossless matching network can now be inserted between a 50-ohm generator and the transistor to provide a conjugate match for the input of the transistor. To conjugately match the output of the transistor a lossless matching network can be inserted between the transistor and a 50-ohm load. With the transistor's input and output conjugately

Strip-line design

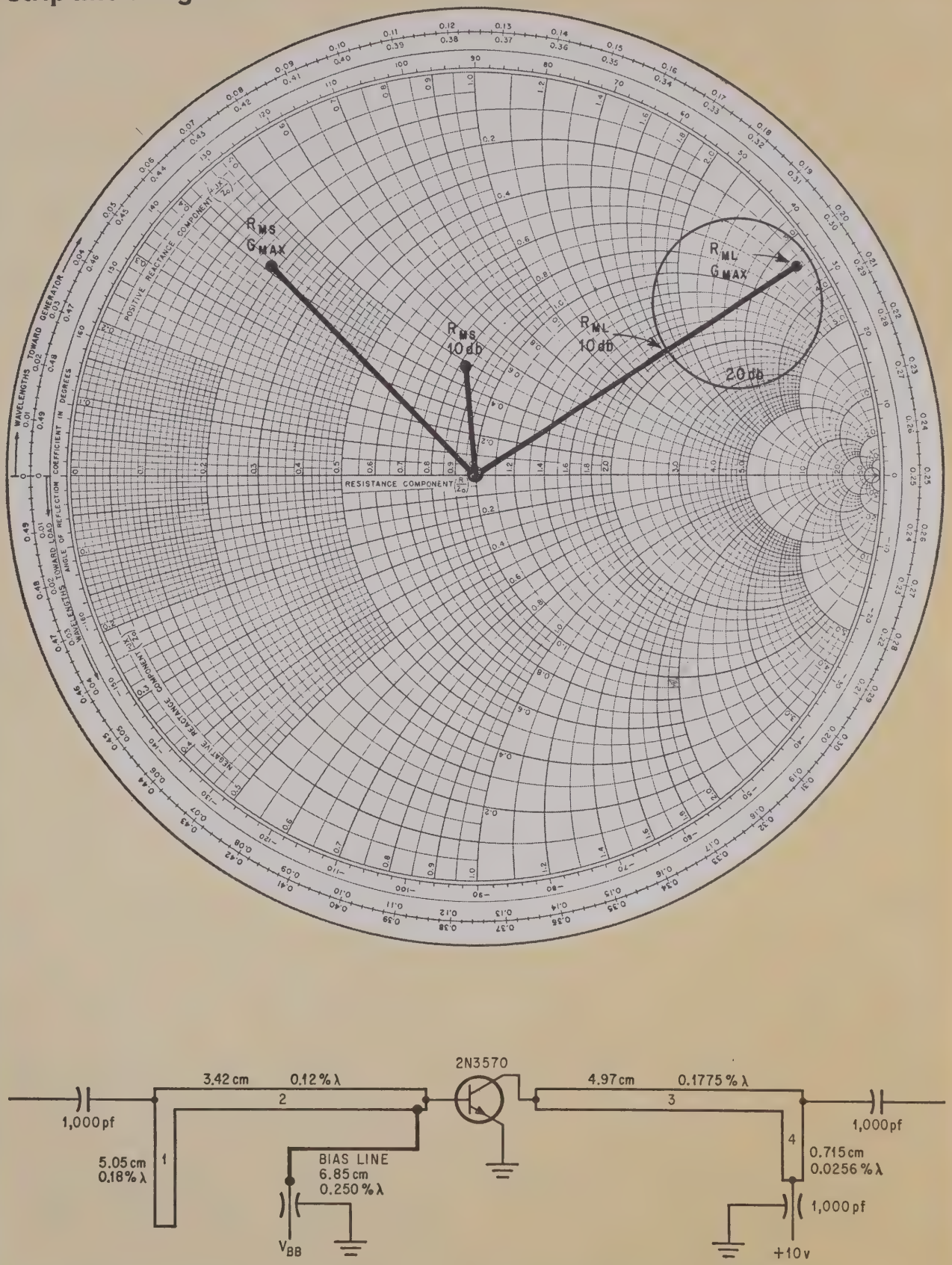

Design example. Graphical plot of a 750-Mhz amplifier design using a 2N3570 transistor. Completed circuit uses strip lines to match the input and output to the transistor.

matched, a maximum power gain is achieved.

In this example Teflon transmission lines, using $\frac{1}{16}$" Teflon Fiberglas p-c board, were chosen for matching the input and output. The values for the lines are determined as follows:

Output circuit

Step 1. Transform R_{ML} to 50± jz ohms or 20± jb mmhos using the relationship

$$jb = \pm \left[\frac{|R_{ML}|^2 (Y_o + G_L)^2 - (Y_o - G_L)^2}{1 - |R_{ML}|^2} \right]^{1/2}$$

where

jb = reactance of the parallel stub
Y_o = characteristic admittance of the transmission line
G_L = real part of load admittance

In this case Y_0 and $G_L = 20$ mmhos. Hence,

$$jb = \pm \left[\frac{(0.951)^2(20 + 20)^2 - (20 - 20)^2}{1 - (0.951)^2} \right]^{1/2}$$
$$= \pm 123.5 \text{ mmhos}$$

The negative sign was chosen for a shorted inductive stub to keep the over-all length below $\lambda/4$.

Step 2. Find the lengths for elements 3 and 4.

$$\tan \beta L = \frac{-Y_o}{jb} = \frac{20}{123.5} = 0.162$$

therefore,

$\beta L = 9.2°$

but

$$\beta = \frac{2\pi}{\lambda}$$

and

$$\lambda = \frac{\text{velocity of light}}{\text{frequency}} = \frac{300 \times 10^6 \text{ meters/sec}}{750 \times 10^6 \text{ hz/sec}}$$
$$= 40 \text{ cm/hz}$$

Hence,

$$L = \frac{9.2°}{360°} \times 40 \text{ cm} = 1.02 \text{ cm}$$

For element 4

$L_4 = (1.02)(0.7) = 0.715$ cm

where λ on Teflon Fiberglas $\frac{1}{16}" = (0.7)\ (\lambda_{\text{free air}})$

For element 3

$$\Gamma = \left[\frac{Y_o - Y_L}{Y_o + Y_L} \right]$$
$$= \left[\frac{20 - (20 - j\,123.5)}{20 + (20 - j\,123.5)} \right] = 0.953 \angle 162°$$
$$L_3 = \left[\frac{\theta_\Gamma - \theta_{R_{ML}}}{720°} \right] \lambda (0.7)$$
$$= \left[\frac{162° - 33.8°}{720°} \right] (40)(0.7) = 4.97 \text{ cm}$$

Input circuit

Step 1. Transform R_{MS} to 50 ± jz ohms or 20 ± jb mmhos using the relationship

$$jb = \pm \left[\frac{|R_{MS}|^2 (Y_o + G_s)^2 - (Y_o - G_s)^2}{1 - |R_{MS}|^2} \right]^{1/2}$$

where

G_S = real part of the source admittance which in this case is 20 mmhos. Hence,

$$jb = \pm \left[\frac{(0.730)^2(20 + 20)^2 - (20 - 20)^2}{1 - (0.730)^2} \right]^{1/2}$$
$$= \pm 42.8 \text{ mmhos}$$

The positive sign was chosen for an open capacitive stub to keep its length below $\lambda/4$.

Step 2. Find the lengths of elements 1 and 2.

$$\cot \beta L = \frac{Y_o}{jb}$$
$$= \frac{20}{42.8} = 0.467$$

therefore,

$\beta L = 65°$

and the length of element 1 is

$$L_1 = \left[\frac{65°}{360°} \right] (40)(0.7)$$
$$= 5.05 \text{ cm}$$
$$\Gamma = \left[\frac{Y_o - Y_s}{Y_o + Y_s} \right]$$
$$= \left[\frac{20 - (20 + j\,42.8)}{20 + (20 + j\,42.8)} \right]$$
$$= 0.730 \angle -137°$$

Thus the length of element 2 is

$$L = \left[\frac{\theta_\Gamma - \theta_{R_{MS}}}{720°} \right] \lambda$$
$$= \left[\frac{-137° - 135.4°}{720°} \right] (40)$$
$$= -\frac{272.4}{720°} \times 40$$

Since a positive angle is required, add 360°, then

$$L_2 = \frac{87.6°}{720°} (40)(0.7) = 3.42 \text{ cm}$$

The completed circuit is on page 105.

If a gain other than G_{MAX} had been desired, a constant gain circle would be required. For example, suppose a power gain of 10 db is desired. Thus,

$G_p = 10$ db

and

$G_o = |s_{21}|^2 = 3.686 = 5.666$ db

Discrete-component design

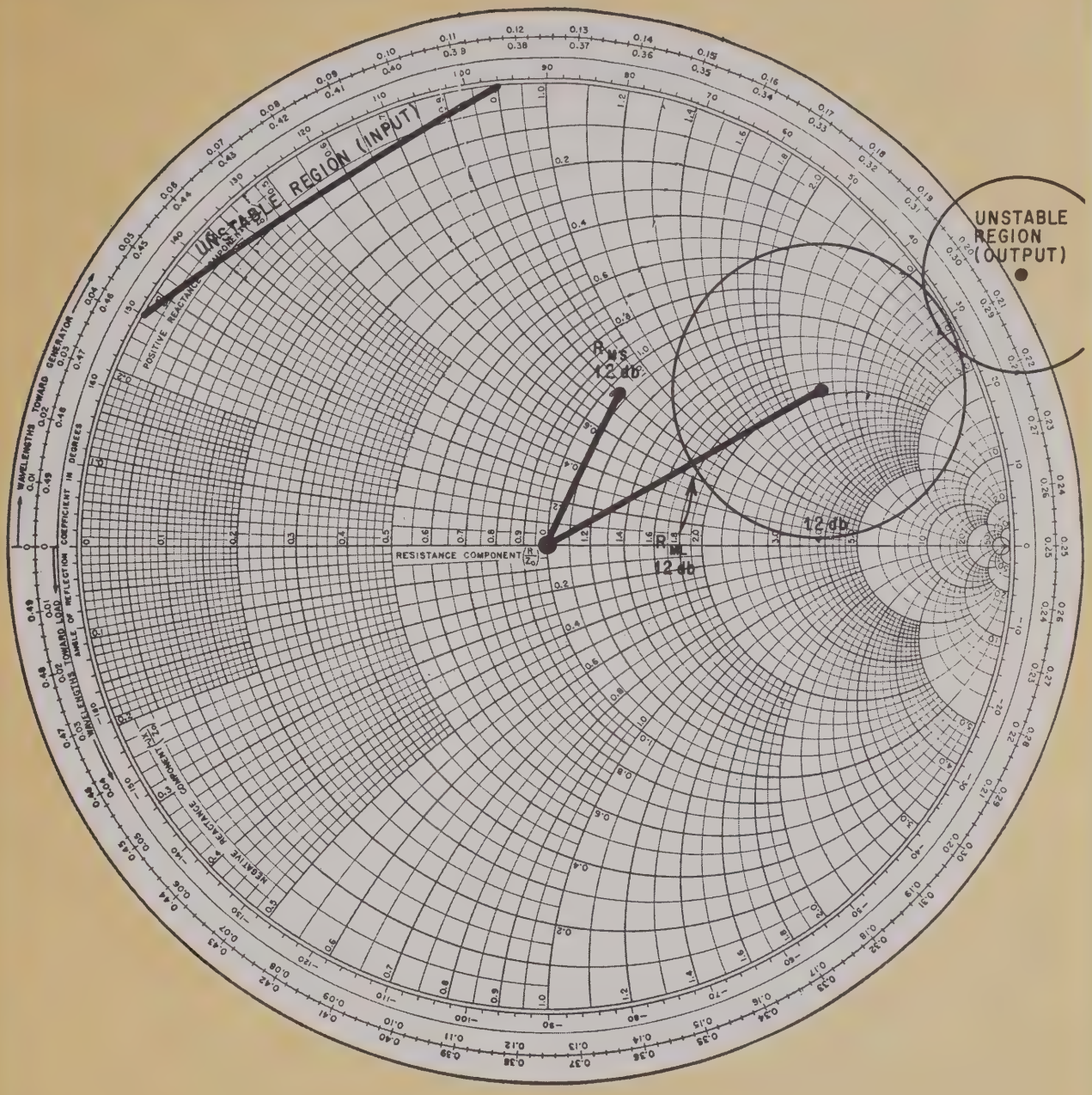

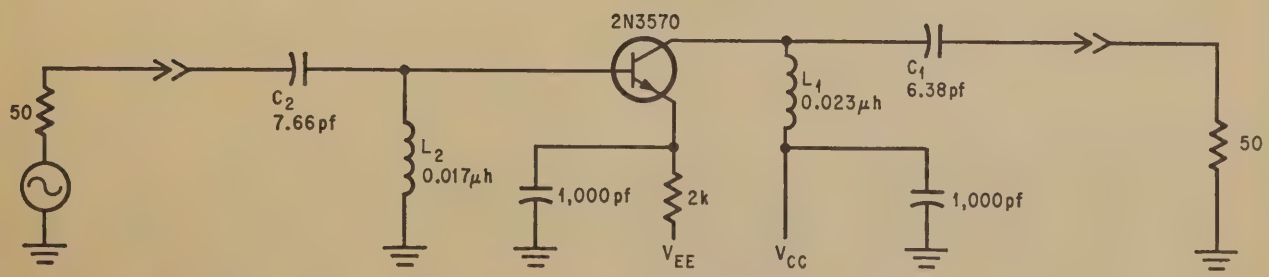

Design example. Graphical plot of a 500-Mhz amplifier design using a 2N3570 transistor. Matching is achieved with discrete components whose values are determined from the Smith chart plot.

then

$$G = \frac{G_p}{G_o} = 2.713 = 4.334 \text{ db}$$

Now by computing the center

$$r_{02} = \left[\frac{G}{1 + D_2G}\right] C_2^* = 0.781 \angle 33.851°$$

and radius

$$R_{02} = \frac{(1 - 2K|s_{12}s_{21}|G + |s_{12}s_{21}|^2G^2)^{1/2}}{1 + D_2G} = 0.136$$

where

$$D_2 = |s_{22}|^2 - |\Delta|^2 = 0.614$$

a constant gain circle, which shows all loads for the output that yield a power gain of 10 db, can be constructed directly on the Smith chart on page 107. The R_{ML} picked in this example was $0.567 \angle 33.851°$, and read off the Smith chart coordinates as 89.344 + j 83.177 ohms. The source reflection coefficient required with this load is

$$R_{MS} = \left[\frac{s_{11} - R_{ML}\Delta}{1 - R_{ML}s_{22}}\right]^* = 0.276 \angle 93.329°$$

Hence,

$Z_s = 41.682 + j\ 24.859$ ohms.

Since K is greater than unity and B_1 is positive, unconditional stability is assured for all loads.

Alternate design

When the value of K is less than unity, a load must be chosen to assure stable operation of the amplifier. To accomplish this a stability circle is plotted on the Smith chart and examined to determine those loads that may cause oscillation. As long as a load is picked that does not fall in the area of the stability circle, stable operation is assured.

When K is less than unity, the gain of a potentially unstable device approaches infinity by definition. Therefore, equations 23, 25, and 27 cannot be used. Instead, a G_p must first be chosen and then the same procedure as used for $K > 1$ is followed.

The amplifier must be protected from oscillating by careful selection of the load impedance as demonstrated in this example.

Objective: Design an amplifier using a 2N3570 transistor that has a power gain of 12 db at 500 Mhz. The bias conditions are $V_{CE} = 10$ volts and $I_C = 4$ milliamperes. The s parameters are

$s_{11} = 0.385 \angle -55.0°$
$s_{12} = 0.045 \angle 90.0°$
$s_{21} = 2.700 \angle 78.0°$
$s_{22} = 0.890 \angle -26.5°$

Solution: Compute the values of G, R_{MS}, and R_{ML}.

$\Delta = s_{11}s_{22} - s_{12}s_{21} = 0.402 \angle -65.040°$
$C_1 = s_{11} - \Delta s_{22}^* = 0.110 \angle -122.395°$
$B_1 = 1 + |s_{11}|^2 - |s_{22}|^2 - |\Delta|^2 = 0.195$
$C_2 = s_{22} - \Delta s_{11}^* = 0.743 \angle -29.881°$
$B_2 = 1 + |s_{22}|^2 - |s_{11}|^2 - |\Delta|^2 = 1.483$
$D_2 = |s_{22}|^2 - |\Delta|^2 = 0.631$

$$K = \frac{1 + |\Delta|^2 - |s_{11}|^2 - |s_{22}|^2}{2|s_{12}s_{21}|} = 0.909$$

$$G = \frac{G_p}{G_o} = 2.174 \quad \text{or} \quad 3.373 \text{ db}$$

Since K is less than unity it is necessary to pick a load that does not cause oscillation. To accomplish this, first consider a stability circle on the output plane. This circle has a center at

$$r_{s2} = \frac{C_2^*}{|s_{22}|^2 - |\Delta|^2} = 1.178 \angle 29.881°$$

and a radius of

$$R_{s2} = \frac{|s_{12}s_{21}|}{|s_{22}|^2 - |\Delta|^2} = 0.193$$

and is represented as the unstable region on the Smith chart on the previous page. As long as an output load is not picked that lies in the unstable region, stable operation is assured.

The constant gain circle that yields 12.0 db of power gain now has a center at

$$r_{02} = \left[\frac{G}{1 + D_2G}\right] C_2^* = 0.681 \angle 29.881°$$

and a radius of

$$R_{02} = \frac{(1 + 2K|s_{12}s_{21}|G + |s_{12}s_{21}|^2G^2)^{1/2}}{1 + D_2G} = 0.324$$

By constructing this constant gain circle, an output load is again chosen. The R_{ML} chosen on the circle had a reflection coefficient of $0.357 \angle 29.881°$, and was read off the Smith chart coordinates as 85.866 + j 35.063 ohms. The source reflection coefficient required for this load is

$$R_{MS} = \left[\frac{s_{11} - R_{ML}\Delta}{1 - R_{ML}s_{22}}\right]^* = 0.373 \angle 64.457°$$

Thus,

$Z_s = 52.654 + j\ 41.172$ ohms

Now a look at the stability circle plotted on the input plane is required to see if the value of R_{MS} assures stable operation. The circle on the input plane has a center at

$$r_{s1} = \frac{C_1^*}{|s_{11}|^2 - |\Delta|^2} = 8.372 \angle -57.605°$$

and a radius of

$$R_{s1} = \frac{|s_{12}s_{21}|}{|s_{11}|^2 - |\Delta|^2} = 9.271$$

Only a portion of the input stability circle is shown due to its size. The shaded area is unstable.

Since R_{MS} does not fall inside this circle and R_{ML} does not fall inside the output circle stable operation is assured.

The complete circuit, bottom of page 107, was

constructed from this data. Values for the matching components were obtained using the following procedure.

Output circuit

Step 1. Transform R_{ML} to 50 ± jz ohms or 20 ± jb mmhos. Since individual components are used for matching it is necessary to convert R_{ML} to its parallel equivalent circuit by adding −180° to a positive angle, or +180° to a negative angle.

Therefore,

$$R_{ML_1} = 0.357 \angle -150.119°$$

Using the formula

$$Y_L = \left[\frac{1 + R_{ML_1}}{1 - R_{ML_1}}\right] Y_o$$

where $Y_o = 20$ mmhos

$$Y_L = 10 - j\,4.08 \text{ mmhos}$$

Converting the Y_L admittance to an impedance yields $Z_L = 100 - j\,245$ ohms.

Step 2. Compute the value for the capacitor from the relationship

$$X_c = \sqrt{(R_p - R_s)R_s}$$

where

R_p = real part of $Z_L = 100$
R_s = load impedance = 50

therefore,

$$X_c = \sqrt{2500} = 50$$

and

$$C_1 = \frac{1}{2\pi f X_c} = 6.38 \text{ pf}$$

Step 3. Compute L_1 from

$$X_{L_1} = \frac{R_s^2 + X_c^2}{X_c} = \frac{(50)^2 + (50)^2}{50} = 100$$

The total X_L is

$$X_{LT} = \frac{(X_{L_1})(X_L)}{(X_{L_1} + X_L)} = 71$$

where

X_L = 245 ohms = imaginary part of Z_L

hence,

$$L_1 = \frac{X_{LT}}{2\pi f} = 0.023\ \mu h$$

Input circuit

Step 1. Transform R_{MS} to 50 ± jz ohms or 20 ± jb mmhos. To do so convert R_{MS} to its parallel equivalent circuit by adding −180° to a positive angle, or +180° to a negative angle.

Therefore,

$$R_{MS_1} = 0.373 \angle -115.543°$$

Using the formula

$$Y_s = \left[\frac{(1 + R_{MS})}{(1 - R_{MS})}\right] Y_o$$

where $Y_0 = 20$ mmhos

Compute Y_S. Thus,

$$Y_s = 11.8 - j\,9.4 \text{ mmhos}$$

or

$$Z_s = 84.7 - j\,106.4 \text{ ohms}$$

Step 2. Compute C_2

$$X_{C_2} = \sqrt{(R_p - R_s)R_s}$$

where

R_p = real part of Z_s = 84.7 ohms
R_s = source impedance = 50 ohms

Thus,

$$X_{C_2} = 41.6 \text{ ohms}$$

and

$$C_2 = \frac{1}{2\pi f X_c} = 7.66 \text{ pf}$$

Step 3. Compute L_2

$$X_{L2} = \frac{R_s^2 + Y_C^2}{X_C} = \frac{(50)^2 + (41.6)^2}{41.6}$$

$$= 102 \text{ ohms}$$

$$X_{LT} = \frac{(X_{L_1})(X_L)}{(X_{L_1})(X_L)} = 52.2 \text{ ohms}$$

where

X_L = imaginary part of Z_s = 106.4 ohms

hence

$$L_2 = \frac{X_{LT}}{2\pi f} = 0.017\ \mu h$$

Bandwidth, the third important design factor, is dependent on the Q of the circuit. There are no magic formulas for accurately predicting bandwidth in all cases. Many LC combinations provide the same complex impedance at the center frequency but yield different Q's and bandwidths.

If the inherent bandwidth, Q, of a transistor loaded with a particular LC combination yields a bandwidth that is greater than desired, adding LC elements narrows the bandwidth and keeps the gain constant. But if the inherent bandwidth is narrower than desired, a gain reduction or different LC combination changes the bandwidth.

The author

William H. Froehner, who started working at TI in 1964, designs high frequency measurement and test equipment. In the last 18 months he has been applying the scattering parameter technique to design high frequency amplifiers.

SECTION VI

TWO-PORT POWER FLOW ANALYSIS USING GENERALIZED SCATTERING PARAMETERS

Dr. George Bodway's article, first published as an internal HP report in April, 1966, was the first analytical treatment on the practical characterization of active semiconductor devices with s parameters.

Dr. Bodway shows the relation between generalized s parameters and those measured on a transmission line system with a real characteristic impedance. He then shows how these s parameters are related to power gain, available power gain, and transducer power gain. Stability and constant gain circles are derived from the s parameters. Bodway then shows, both mathematically and graphically, how stability and gain are considered in amplifier design.

microwave journal

Vol. 10, number 6

May 1967

TECHNICAL SECTION

TWO PORT POWER FLOW ANALYSIS USING GENERALIZED SCATTERING PARAMETERS

George E. Bodway
Hewlett-Packard
Palo Alto, California

INTRODUCTION

The difficulty of measuring the commonly accepted amplifier design parameters, such as the admittance or y parameters, increases rapidly as the frequency of interest is extended above 100 MHz. When the desired parameters must be referred either to a short or an open above 1000 MHz, a wideband measurement system becomes essentially impossible. A convenient way to overcome this problem is to refer the measurements to the characteristic impedance of a transmission line. A set of informative parameters which can readily be measured in terms of the traveling waves on a transmission line are the scattering or "s" parameters.

To illustrate the bandwidths possible, two measurement systems have been set up which measure the scattering parameters (amplitude and phase) without adjustments or calibrations of any kind (once the system is set up) over the frequency ranges 10 MHz to 3.0 GHz and 1.0 - 12.4 GHz.

There are then many advantages for having a design available in terms of the easily measured scattering parameters. One important advantage is that the matching networks are also measured in terms of scattering parameters, for reasons of simplicity at the lower frequencies, and at higher frequencies because of necessity. At microwave frequencies many of the passive elements in a design are open, shorted or coupled sections of transmission line which can be represented as a reflection coefficient on a Smith Chart. Thus, the process of design is readily served by a procedure involving reflection coefficients rather than impedance. Having measured both the active device and associated passive elements in terms of one set of parameters, much feeling for the importance of each measured parameter would be lost by converting all the parameters to another set and proceeding with the design from there. Another significant advantage is in the resulting simplicity of understanding and the intuitive insight one may thus gain from a design based on the generalized scattering parameters. Because of this, the design method is being used at frequencies far below the microwave region. The reason for this simplicity is that the parameters used for the design are inherently power flow parameters.

This paper attempts to formulate a theory which can be simply applied to the measured s parameters in order to synthesize a desired power transfer versus frequency for a linear two port. In addition to obtaining and displaying the three familiar forms of power flow, the power gain G, the available gain G_A and the transducer gain G_T versus the load and generator impedances, the potential stability, or instability as the case may be, is completely and simply specified graphically in terms of the measured quantities. A stability circle is defined for both the input and output planes (generator and load Smith Charts) which simply and completely defines the network both with respect to potential instability and with respect to the nature of constant power flow contours.

INTRODUCTION TO GENERALIZED SCATTERING PARAMETERS

The power waves and generalized scattering matrix were defined very elegantly in a paper by K. Kurakawa.[1] These parameters were introduced previously by Penfield,[2,3] and also by Youla[4] for positive real reference impedances. These parameters will be presented here in a form consistent with the rest of the paper. It is possible that the usefulness of these parameters was not realized or used previously for transistor circuit design because of the slow, tedious job of measuring them accurately with a slotted line or a bridge.

The power waves are defined by Equations [1(a), (b)] and Fig. 1.

$$a_i = \frac{V_i + Z_i I_i}{2\sqrt{|\mathrm{Re}\, Z_i|}} \qquad [1(a)]$$

$$b_i = \frac{V_i - Z_i^* I_i}{2\sqrt{|\mathrm{Re}\, Z_i|}} \qquad [1(b)]$$

Equation (1) defines a new set of variables a_i, b_i, in terms of an old set, the terminal voltages and currents V_i and I_i. This change of variables accomplishes two things: for one, the a_i and b_i have units of $(\text{power})^{1/2}$ and a very precise meaning with respect to power flow; second, the relationship between the variables a_i, b_i will now depend on the terminal impedances of the network.

The expression for the relation between the a_i's and b_i's is defined by

$$b_i = s_{ij} a_j \qquad (2)$$

where s_{ij} is an element of the generalized scattering matrix and b_i and a_i are, respectively, the components of the reflected and incident power wave vectors.

If Z_i is real and equal to the characteristic impedance of transmission lines connected to the ports of a network, then the definition of a_i, b_i reduces to that of the forward and reverse traveling waves on the transmission lines and s reduces to the microwave scattering matrix. There-

Fig. 1 — Representation of an n port network defining voltages, currents and reference impedances at each port.

fore the advantages of remote transmission line techniques can be used to measure the properties of the network and determine the generalized scattering matrix.

The physical meaning of the power waves a_i, b_i and the generalized parameters s_{ij} are demonstrated by the following equations (Fig. 2). The results follow from Equation (1) and circuit relations indicated by Fig. 2.

$$a_2 = 0 \tag{4}$$

$$\begin{aligned} |b_2|^2 &= |I_2|^2 \, |\mathrm{Re}\, Z_2| \\ &= P_L \text{ for real part } Z_2 \text{ positive} \\ &= -P_L \text{ for real part } Z_2 \text{ negative} \end{aligned} \tag{5}$$

where P_L is the power delivered to the load.

$$\begin{aligned} |a_1|^2 &= \frac{|E_0|^2}{4|\mathrm{Re}\, Z_1|} \\ &= P_a \text{ for real part } Z_1 \text{ positive} \\ &= P_e \text{ for real part } Z_1 \text{ negative} \end{aligned} \tag{6}$$

where P_a is equal to the power available from the generator and P_e is the exchangeable power of the generator,

and

$$|b_1|^2 = |a_1|^2 - \mathrm{Re}(V_1 I_1^*) \tag{7}$$

Using the relations above for $|a_1|^2$ and $|b_1|^2$ the following significant and useful physical content of the generalized scattering parameters is evident. With the real part of Z_1 and Z_2 positive, the forward scattering parameter* $|s_{21}|^2$ is identically equal to the transducer power gain of the network.

$$\begin{aligned} |s_{21}|^2 = \frac{|b_2|^2}{|a_1|^2} = \frac{P_L}{P_a} &= G_T \\ &= \text{transducer power gain} \end{aligned} \tag{8}$$

Fig. 2 — Two port model showing voltages, currents, load and generator impedances and power waves.

When either the load or generator impedance consists of negative real parts, appropriate negative signs must be used. In the remainder of this paper (unless stated otherwise) we will assume that the real parts of Z_1 and Z_2 are positive, in order to keep the repetitions in bounds. Nevertheless negative real loads and generator impedances come up quite often such as when cascading potentially unstable stages and are treated in the same way.

Similarly we have

$$|s_{11}|^2 = \frac{\text{Power reflected from the input of the network}}{\text{Power available from a generator at the input port}} \tag{9}$$

for the real part of Z_1 positive.

Placing the generator at the output port, we observe that

$$|s_{12}|^2 = \text{reverse transducer power gain} \tag{10}$$

and

$$|s_{22}|^2 = \frac{\text{Power reflected from the output of the device}}{\text{Power available from a generator at the output port}} \tag{11}$$

where

$$P_{\text{reflected}} = P_a - P_{\text{delivered to the network}} \tag{12}$$

To repeat, for "positive real" load and generator impedances, $|s_{21}|^2$ and $|s_{12}|^2$ are the forward and reverse transducer power gains, while $|s_{11}|^2$ and $|s_{22}|^2$ express the difference between power available from a generator and that which is delivered to the network normalized to the power available from the generator.

In addition to the transducer power gain $|s_{21}|^2$, there are two other useful measures of power flow for a two port network; these are given by

$$\begin{aligned} G &= \frac{\text{Power delivered to load}}{\text{Power into two port}} \\ &= \frac{|s_{21}|^2}{1-|s_{11}|^2} \end{aligned} \tag{13}$$

$$G_A = \frac{\text{Power available at the output}}{\text{Power available from the generator}} = \frac{|s_{21}|^2}{1-|s_{22}|^2} \tag{14}$$

Fig. 3 — Circle defined by r_{s2} and ρ_{s2} divides r_2 plane into a stable and potentially unstable region of operation. If $|s_{11}| < 1$, the inside of the circle indicates those loads which provide negative real input impedance ($|s_{11}'| > 1$). The heavier weight circle defines the unit circle on the Smith Chart.

Because of the close relationship between power flow and the generalized scattering parameters we might expect that transistor amplifier design, which is intimately concerned with power flow, could be intuitively clear and straightforward in terms of these parameters.

The generalized scattering parameters are defined in terms of specific load and generator impedance. To make broadband measurements, the parameters are usually referred to 50 ohms. Then, to proceed with the design or to utilize the measured parameters, we must have an expression for the generalized scattering parameters in terms of the measured parameters and arbitrary generator and load impedances. The new scattering parameters for arbitrary load and generator are given by

* *The word "generalized" will be deleted, but is to be understood throughout the remainder of the paper.*

$$s_{11}' = \frac{A_1^*}{A_1} \frac{[(1-r_2 s_{22})(s_{11}-r_1^*)+r_2 s_{12} s_{21}]}{[(1-r_1 s_{11})(1-r_2 s_{22})-r_1 r_2 s_{12} s_{21}]} \quad (15)$$

$$s_{12}' = \frac{A_2^*}{A_1} \frac{s_{12}[1-|r_1|^2]}{[(1-r_1 s_{11})(1-r_2 s_{22})-r_1 r_2 s_{12} s_{21}]} \quad (16)$$

$$s_{21}' = \frac{A_1^*}{A_2} \frac{s_{21}[1-|r_2|^2]}{[(1-r_1 s_{11})(1-r_2 s_{22})-r_1 r_2 s_{12} s_{21}]} \quad (17)$$

$$s_{22}' = \frac{A_2^*}{A_2} \frac{[(1-r_1 s_{11})(s_{22}-r_2^*)+r_1 s_{12} s_{21}]}{[(1-r_1 s_{11})(1-r_2 s_{22})-r_1 r_2 s_{12} s_{21}]} \quad (18)$$

where

$$A_i = \frac{(1-r_i^*)}{|1-r_i|}(1-|r_i|^2)^{1/2} \quad (19)$$

and

$$r_i = \frac{Z_i'-Z_i}{Z_i'+Z_i^*} \quad (20)$$

The three forms of power gain can now be expressed in terms of a given set of scattering parameters (s) and arbitrary load and generator impedances.*

$$G_T = |s_{21}'|^2 = \frac{|s_{21}|^2(1-|r_1|^2)(1-|r_2|^2)}{|1-r_1 s_{11}-r_2 s_{22}-r_1 r_2 \triangle|^2} \quad (21)$$

$$G = \frac{|s_{21}'|^2}{(1-|s_{11}'|^2)} = \frac{|s_{21}|^2(1-|r_2|^2)}{(1-|s_{11}|^2)+|r_2|^2(|s_{22}|^2-|\triangle|^2)-2\,\mathrm{Re}(r_2 C_2)} \quad (22)$$

$$G_A = \frac{|s_{21}'|^2}{(1-|s_{22}'|^2)} = \frac{|s_{21}|^2(1-|r_1|^2)}{(1-|s_{22}|^2)+|r_1|^2(|s_{11}|^2-|\triangle|^2)-2\,\mathrm{Re}(r_1 C_1)} \quad (23)$$

where

$$\triangle = s_{11} s_{22}-s_{12} s_{21} \quad (24)$$

$$C_1 = s_{11}-\triangle s_{22}^* \quad (25)$$

$$C_2 = s_{22}-\triangle s_{11}^* \quad (26)$$

STABILITY OF TWO PORT NETWORK

An important consideration in designing transistor amplifiers is to insure that the circuit does not oscillate. A two port network can be classed as either being absolutely stable or potentially unstable, it is desirable to consider two types of loading and by this means two degrees of potential instability; one in which the input and output impedances of the device are insured of having a positive real part and stability thereby guaranteed, and a second which allows the input and output impedance to have negative real parts, but only to the extent that the total circuity is still stable.[6]

The question of stability must be investigated at all frequencies of course, but design for a specific gain or amplifier response versus frequency is usually required over some more restricted frequency range. If this specific range is restricted to absolute stability, then the design is simplified considerably. However, this in turn severely restricts the potential usefulness of the device. The two alternative considerations, for potentially unstable frequency ranges, offer increased potential use for a given device. They also necessitate a corresponding increase in the complexity of the design. The information we desire concerning stability can then be summarized as follows. It is necessary to know over what frequency ranges the two port is potentially unstable; and in those frequency ranges where the device is potentially unstable, we desire information about which loads and generator impedances provide stable operation. The answers to these questions are approached by considering Equations (15) and (18) with $r_1=0$ and r_2 as a variable.

Consideration of Equation (18) shows that if $|s_{22}|>1$, then any passive r_2 still gives $|s_{22}'|>1$ and the network is potentially unstable for all loads r_2 and the given r_1. Stability with respect to the output port will be attained by insuring that the positive real part of r_2 is greater than the negative real part of the output impedance. For the condition $|s_{22}|<1$, the magnitude of $|s_{22}'|$ is less than one for a passive r_2.

Consideration of Equation (15) shows that the whole r_2 plane can be separated into two regions, one for which the input impedance is positive real and a second for which the input is negative real. The regions can be located by requiring $|s_{11}'|$ to be less than one. The solution for r_2, separating the two regions, is given by the equation of a circle in the r_2 plane where the center and radius of the circle are

$$r_{s2} = \frac{C_2^*}{|s_{22}|^2-|\triangle|^2} \quad (27)$$

$$\rho_{s2} = \left| \frac{s_{12} s_{21}}{|s_{22}|^2-|\triangle|^2} \right| \quad (28)$$

respectively, and $C_2 = s_{22}-\triangle s_{11}^*$.

An example of the stable and potentially unstable regions is indicated in Fig. 3 where the shaded part or inside of the circle corresponds to those loads which provide a negative real input impedance.

The region of the r_2 plane which provides a positive real input impedance is obtained as follows: if the input impedance is positive real with $r_2=0$, and if the circle includes the origin, then the inside of the circle indicates a positive real input impedance; whereas if the circle excludes the origin, then the inside of the circle indicates a negative real input. If the input is negative real with $r_2=0$, then the converse is true.

In the same manner the load can be assumed fixed and the stability investigated as a function of r_1. The same results are obtained with a corresponding stability circle defined by Equations (27) and (28) with twos replaced with ones.

GEORGE E. BODWAY received a BS in 1960, an MS in 1964 and a PhD in Engineering Physics in 1967 from the University of California at Berkeley. He is presently Project Supervisor of the thin film microcircuit research, development and processing in the Microwave Division of Hewlett Packard. Before this position Dr. Bodway was a research engineer working with solid state microwave circuit design.

* *The generator r_1 and load r_2 are assumed positive real in Equations (21) through (23). For negative real loads or generators appropriate negative signs are required.*

The circles defined by Equations (27), (28) and corresponding equation for the input plane (r_1) were obtained by setting $r_1=0$ and $r_2=0$ respectively. A simple intuitive argument can show that the circle in the r_2 plane is invariant to r_1 and the circle in the r_1 plane is invariant to changes in r_2. In particular, if the input impedance is positive real, then the input reflection coefficient has a magnitude less than one; if the input impedance is negative real, the input reflection coefficient will have a magnitude greater than one; both statements are obviously independent of the generator impedance, as long as it is positive real. The converse is true if the generator impedance is negative real.

The condition for a two port to be absolutely stable can now be obtained. A two port network is absolutely stable if there exists no passive load or generator impedance which will cause the circuit to oscillate. This is equivalent to requiring the two stable regions to lie outside the unit circles in the r_1 and r_2 planes when the origins are stable. This is satisfied if

$$|\rho_{s1}-|r_{s1}|| > 1 \qquad (29)$$

$$|\rho_{s2}-|r_{s2}|| > 1 \qquad (30)$$

$$|s_{11}| < 1$$

and

$$|s_{22}| < 1$$

The stability circles would normally be superimposed on the generator (r_1) and load (r_2) planes, upon which the constant gain circles have already been constructed. The three different degrees of stability are then easily distinguished: first, if the two unstable regions lie outside the unit circles, the device is unconditionally stable; second, if the unstable regions lie inside the unit circles, but all load and generator impedances are chosen to lie outside these two regions, the network is assured of having positive real input and output impedances, and stability is assured. The third situation arises when r_1 or r_2 are allowed to be in one or both unstable regions. Then negative real input or output impedances exist, and it is necessary to make sure the positive real generator or load is sufficiently positive real to insure a stable system.

It is also appropriate to point out at this time that the section on stability can quite readily be used to design oscillators.

CONJUGATE MATCHED TWO PORT

The load and generator impedance which simultaneously conjugate match-

Fig. 4 — Contours of constant gain G_i and constant $|s_{11}'|$ indicating gain and match obtained for various generators r_1. $|s_{11}|$ was taken as 0.867 at −45°.

es a two port can be expressed in terms of the s parameters by solving the pair of equations which result when $|s_{11}'|$ and $|s_{22}'|$ are both set equal to zero.*

The solution of this pair of equations for r_1 and r_2 provides the load and generator impedances (r_{m1} and r_{m2}) which will simultaneously match both the input and output ports.

$$r_{m1} = C_1^* \left[\frac{B_1 \pm \sqrt{B_1^2 - 4|C_1|^2}}{2|C_1|^2} \right] \qquad (42)$$

$$r_{m2} = C_2^* \left[\frac{B_2 \pm \sqrt{B_2^2 - 4|C_2|^2}}{2|C_2|^2} \right] \qquad (43)$$

where

$$B_1 = 1+|s_{11}|^2-|s_{22}|^2-|\triangle|^2$$

$$C_1 = s_{11}-\triangle\, s_{22}^*$$

$$B_2 = 1+|s_{22}|^2-|s_{11}|^2-|\triangle|^2$$

$$C_2 = s_{22}-\triangle\, s_{11}^*$$

Equations (42) and (43) give two solutions for r_{m1} and two for r_{m2}. Considering the i^{th} load if $\left|\frac{B_i}{2C_i}\right|$ is larger than unity, then one solution will have a magnitude less than unity and the other will have a magnitude larger than unity. The r_{m1} which has a magnitude less than one is obtained from Equations (42) and (43) using the plus sign for B_i negative and the minus sign for B_i positive. On the other hand if $\left|\frac{B_i}{2C_i}\right|$ is less than unity, then both solutions will have a magnitude equal to unity.

The condition $\left|\frac{B_i}{2C_i}\right| >$ can be expressed as

$$|K| > 1 \qquad (44)$$

where

$$K = \frac{1+|\triangle|^2-|s_{11}|^2-|s_{22}|^2}{2\,|s_{12}|\,|s_{21}|} \qquad (45)$$

The two solutions for r_{m1} and the two for r_{m2} result in two pairs of solutions for a load and generator which simultaneously match the two port network.

The simultaneously matching pairs can be summarized as follows: for $|K| < 1$ both generator and load for each pair have a magnitude equal to one; for $|K| > 1$ and K positive then one solution has both r_{m1} and r_{m2} less

* *The matched generator and load can also be obtained readily from $G_A'(r_{m1}) = 0$, and $G'(r_{m2}) = 0$.*

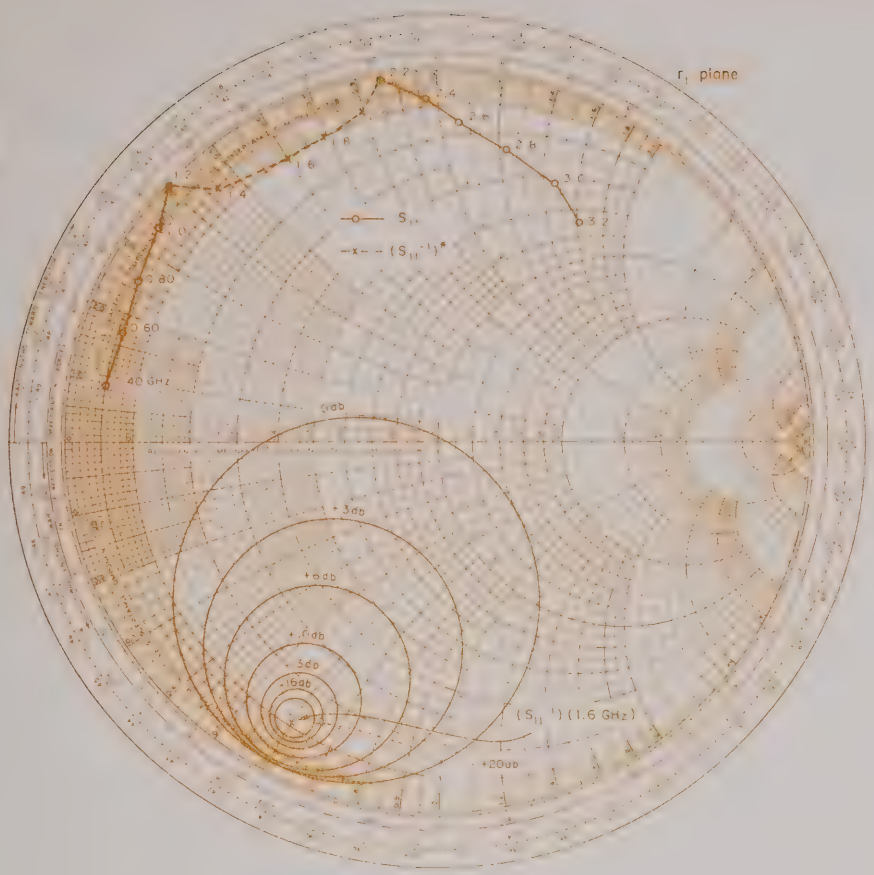

Fig. 5 — Plot of s_{11} vs. frequency for a transistor in common base showing frequency ranges over which the input is positive and negative real with 50 Ω on the output. Where the curve is dashed, the real part is read off as negative. Any generator placed on the device which lies outside the shaded region provides a total positive resistance at all frequencies. The circles indicate contours of constant gain at 1.6 GHz.

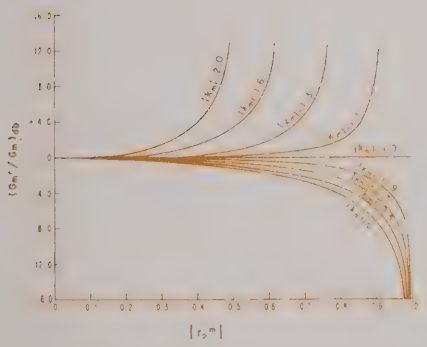

Fig. 6(a) — Set of curves giving the radii of constant power gain circles as a function of the load $|r_2^m|$ with $|k_m|$ as a parameter. This set of curves provides circles of positive power gain for $K > 1$.

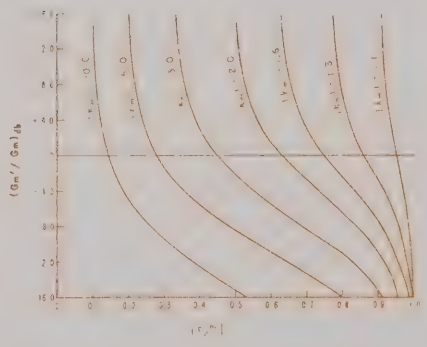

Fig. 6(b) — The curves shown for various values of $|K_m| > 1$ can be used to obtain constant power gain circles on the r_2^m plane. This graph gives the radii of stable power gain for the case $|K| > 1$ and K negative.

than one and the other solution has both greater than unity. For $|K| > 1$ and K negative then, both solutions consist of one $|r_1| > 1$ and the other $|r_1| < 1$.

The condition that a two port network can be simultaneously matched with a positive real generator and load* is therefore given by

$$K > 1 \qquad (46)$$

Equation (45) for K is invariant to changes in load and generator impedance, and is given in terms of the h parameters by

$$K = \frac{2(\mathrm{Re}h_{11})\,\mathrm{Re}(h_{22}) - \mathrm{Re}(h_{12}h_{21})}{|h_{12}h_{21}|} = k^7 = C^{-1}\ (\text{Linville factor}) \qquad (47)$$

If $|K| > 1$ then

$$|s_{21}^m|^2 = \left|\frac{s_{21}}{s_{12}}\right| |(K \pm \sqrt{K^2-1})| \qquad (48)$$

$$|s_{12}^m|^2 = \left|\frac{s_{12}}{s_{21}}\right| |(K \pm \sqrt{K^2-1})| \qquad (49)$$

where the plus sign applies when B_1 is negative and the minus sign occurs when B_1 is positive.

The physical significance of K is stressed by repeating that $(C^{-1} = k = K) > 1$ is the condition that a two port can be simultaneously matched by a positive real generator and load. This is only a necessary condition for absolute stability. A necessary and sufficient condition for absolute stability is $K > 1$ and B_1 positive.

POWER FLOW

Unilateral Case

In this section the feedback term s_{12} is assumed to be sufficiently small in some sense so that we can set it equal to zero. The sense of being small is defined later in terms of a transducer power gain error which results when using the unilateral design.

For $s_{12}=0$ we obtain the following equation for G_T

$$|s_{21}'|_u^2 = |s_{21}|^2 \frac{|1-|r_1|^2|}{|1-r_1 s_{11}|^2} \frac{|1-|r_2|^2|}{|1-r_2 s_{22}|^2} = G_0 G_1 G_2 \qquad (31)$$

G_0 is the transducer power gain given by the original s_{21} parameters (for example the measured G_T). G_1 and G_2 are contributions to the transducer power gain due to changes in generator and loads respectively.

If $|s_{11}|$ and $|s_{22}|$ are less than one, then Equation (31) attains a finite maximum at $r_1 = s_{11}^*$ and $r_2 = s_{22}^*$ which is given by

$$|s_{21}'|_u^2{}_{max} = \frac{|s_{21}|^2}{|1-|s_{11}|^2|\ |1-|s_{22}|^2|} = \text{M.A.G.} = G_u \qquad (32)$$

Equation (32) can be expressed in

* *The conditions under which a two port can be simultaneously matched were given previously in Reference 1.*

terms of the h parameters. The equivalent expression is

$$|s_{21}'|_u^2{}_{max} = \frac{|h_{21}|^2}{4\,(\mathrm{Re}\,h_{11})\quad(\mathrm{Re}\,h_{22})} \tag{33}$$

In addition to Equation (32) for G_u, we also desire the gain for conditions other than that of conjugate match. The behavior of G_i versus r_i can be obtained by letting

$$G_i = \frac{|1-|r_i|^2|}{|1-r_i\ S_{ii}|^2} = \text{constant} \tag{34}$$

and solving for r_i. At this point it is convenient to break the discussion into two sections, Case 1, in which $|s_{ii}|<1$ and Case 2, in which $|s_{ii}|>1$.

Case 1

In this case the resulting expression for r_i, the reflection coefficient of the generator impedance with respect to the complex conjugate of the reference impedance,* is an equation of a circle on a Smith Chart. The centers of the circles for different gains are located on a line through the origin and s_{ii}.* The circle at $r_i = s_{ii}^*$ of course reduces to a single point. The location of the center of the circle and the radius of the circle are given by r_{oi} and ρ_{oi} respectively. A circle of constant gain also corresponds to an input reflection coefficient s_{ii}' of constant magnitude.

Defining a normalized gain

$$g_i = \frac{G_i}{G_{i\,max}} = G_i(1-|s_{ii}|^2) \tag{35}$$

the center and radius of each circle and the magnitude of the corresponding reflection coefficient $|s_{ii}'|$ for a constant g_i is given by

$$r_{oi} = \frac{g_i\,|s_{ii}|}{1-|s_{ii}|^2\,(1-g_i)} = \text{center} \tag{36}$$

$$\rho_{oi} = \frac{(1-g_i)^{1/2}\,(1-|s_{ii}|^2)}{1-|s_{ii}|^2\,(1-g_i)} = \text{radius}$$

$$|s_{ii}'| = (1-g_i)^{1/2}$$

where $0 < g_i = \dfrac{G_i}{G_{i\,max}} < 1$

Circles of constant g_i are illustrated in Fig. 4. The circle which goes through the origin is always the zero decibel circle for G_i. In other words, inside this circle $G_i>1$, and outside $G_i<1$.

Case 2

If values of $|s_{ii}|>1$ are encountered when measuring a transistor it is convenient to place $(s_{ii}^{-1})^*$ on a Smith Chart with a dotted line where $|s_{ii}|>1$, and s_{ii} with a solid line for the ranges where $|s_{ii}|<1$. Where the dotted line occurs the resistance is now read off as negative resistance. In both cases the reactive part is read off as given on the Smith Chart. As we shall see this achieves two objectives. For one, it makes the curves for the device continuous on the inside of the Smith Chart; second, it makes the design for Case 2 correspond very closely to that of Case 1. A Smith Chart plot for $s_{ii}>1$ is given in Fig. 5 for a microwave transistor.

Fig. 7 — Return loss circles indicating constant gains G_{1m} or G_{2m} as a function of r_1^m or r_2^m respectively.

The contribution to the total transducer power gain provided by G_i is again given by Equation (34).

The location and radii of constant gain circles, as well as the corresponding $|s_{ii}'|$, are given again by Equation (36) except that now

$$-\infty < g < 0 \tag{37}$$

and the maximum gain $G_{i\,max}$ is now infinite at

$$r_i = [(s_{ii}^{-1})^*]^* = s_{ii}^{-1} \tag{38}$$

As mentioned earlier, it is desirable to know in what sense s_{12} is small, or how adequate the unilateral design is. The actual transducer power gain $|s_{21}'|^2_{true}$ is given by

$$|s_{21}'|^2_{true} = |s_{21}'|_u^2 \frac{1}{|1-x|^2} \tag{39}$$

where

$$x = \frac{r_1\,r_2\,s_{12}\,s_{21}}{(1-r_1\,s_{11})\,(1-r_2\,s_{22})}$$

The ratio of the true gain to the unilateral gain is bounded by

$$\frac{1}{|1+|x|\,|^2} < \frac{|s_{21}'|^2_{true}}{|s_{21}'|_u^2} < \frac{1}{|1-|x|\,|^2} \tag{40}$$

We can define a unilateral figure of merit u where

$$u = \frac{|s_{11}|\,|s_{22}|\,|s_{12}\,s_{21}|}{|1-|s_{11}|^2|\ \ |1-|s_{22}|^2|} \tag{41}$$

u has the following physical significance for $|s_{11}|$ and $|s_{22}|$ less than one. The ratio of the actual transducer power gain to the transducer power gain obtained by the unilateral design

---

* *From now on r_i will simply be called the generator and the load. The actual load and generator impedance are given by Equation (20).*

is bounded by $\frac{1}{|1-u|^2}$ and $\frac{1}{|1+u|^2}$

for any generator and load impedance which have a magnitude equal to or less than $|s_{11}|$ and $|s_{22}|$ respectively.

Transducer Power Gain, Power Gain and Available Power Gain Referred to Matched Generator and Load

If $|K|$ is greater than one, *a particularly simple design procedure will evolve* because the number of scattering parameters which occur in Equations (15) through (18) is reduced from four to two by definition. With matched load and generator impedances on the network, the matched scattering parameters s^m are given by $s_{11}{}^m = s_{22}{}^m = 0$ and

$$s_{12}{}^m = \frac{(A_2{}^m)^*}{A_1{}^m} \frac{s_{12}\,[1-|r_{m1}|^2]}{[(1-r_{m1}\,s_{11})(1-r_{m2}\,s_{22})-r_{m1}\,r_{m2}\,s_{12}\,s_{21}]} \quad (50)$$

$$s_{21}{}^m = \frac{(A_1{}^m)^*}{A_2} \frac{s_{21}\,[1-|r_{m2}|^2]}{[(1-r_{m1}\,s_{11})(1-r_{m2}\,s_{22})-r_{m1}\,r_{m2}\,s_{12}\,s_{21}]} \quad (51)$$

where r_{m1} and r_{m2} were given previously by Equations (42) and (43).

The scattering parameters s′ can now be expressed as a function of arbitrary load and generator impedances $r_1{}^m$ and $r_2{}^m$ which are referred to the matched impedances r_{m1} and r_{m2}.

$$r_1{}^m = \frac{Z_1{}^m - Z_{m1}}{Z_1{}^m + Z_{m1}{}^*} \quad (52)$$

$$r_2{}^m = \frac{Z_2{}^m - Z_{m2}}{Z_2{}^m + Z_{m2}{}^*} \quad (53)$$

Z_{m1} is equal to the matched generator impedance, and Z_{m2} is the matched load impedance. On a Smith Chart $Z_1{}^m$ is obtained from $r_1{}^m$ by reading off the coordinates, multiplying by the real part of Z_{m1}, and adding the imaginary part of Z_{m1}, in particular.

$$Z_1{}^m = R_{m1}r + i(R_{m1}x + X_{m1}) \quad (54)$$

where r and x are the Smith Chart coordinates. The constant conductance and reactance coordinates of the Smith Chart are still preserved in $Z_1{}^m$.

The new s′ parameters for arbitrary load and generator are now given by

$$s_{11}{}' = \frac{(A_1{}^m)^*}{A_1{}^m} \frac{[-(r_1{}^m)^* + r_2{}^m\,s_{12}{}^m\,s_{21}{}^m]}{(1-r_1{}^m\,r_2{}^m\,s_{12}{}^m\,s_{21}{}^m)} \quad (55)$$

$$s_{12}{}' = \frac{(A_2{}^m)^*}{A_1{}^m} \frac{s_{12}{}^m\,(1-|r_1{}^m|^2)}{(1-r_1{}^m\,r_2{}^m\,s_{12}{}^m\,s_{21}{}^m)} \quad (56)$$

$$s_{21}{}' = \frac{(A_1{}^m)^*}{A_2{}^m} \frac{s_{21}{}^m\,(1-|r_2{}^m|^2)}{(1-r_1{}^m\,r_2{}^m\,s_{12}{}^m\,s_{21}{}^m)} \quad (57)$$

$$s_{22}{}' = \frac{(A_2{}^m)^*}{A_2{}^m} \frac{[-(r_2{}^m)^* + r_1{}^m\,s_{12}{}^m\,s_{21}{}^m]}{(1-r_1{}^m\,r_2{}^m\,s_{12}{}^m\,s_{21}{}^m)} \quad (58)$$

where

$$A_1{}^m = \frac{[1-(r_1{}^m)^*]\,(1-|r_1{}^m|^2)^{1/2}}{|1-r_1{}^m|}$$

$$A_2{}^m = \frac{[1-(r_2{}^m)^*]\,(1-|r_2{}^m|^2)^{1/2}}{|1-r_2{}^m|}$$

The Linville design,[8,9] with transducer gain a function of the load but keeping the input matched ($G_t = G$) for each value of the load, is obtained simply by requiring* that $s_{11}{}' = 0$. This is satisfied if

$$r_1{}^m = (r_2{}^m\,s_{12}{}^m\,s_{21}{}^m)^* \quad (59)$$

The new set of scattering parameters for the matched input is now a function of only $r_2{}^m$, the load, and is given by

$$s_{11}{}^{im} = 0 \quad (60)$$

$$s_{12}{}^{im} = \frac{(A_2{}^m)^*\,s_{12}{}^m}{A_1{}^m} \quad (61)$$

$$s_{21}{}^{im} = \frac{(A_1{}^m)^*}{A_2{}^m} \frac{s_{21}{}^m(1-|r_2{}^m|^2)}{(1-|r_2{}^m\,K_m|^2)} \quad (62)$$

$$s_{22}{}^{im} = \frac{(1-r_2{}^m)}{[1-(r_2{}^m)^*]}\left(\frac{1-|K_m|^2}{1-|r_2{}^m\,K_m|^2}\right)\left[-(r_2{}^m)^*\right] \quad (63)$$

where

$$|K_m| = |s_{12}{}^m\,s_{21}{}^m| = |K \pm \sqrt{K^2-1}| \quad (64)$$

The transducer power gain indicated by Equation (62) can be expressed as the product of two terms; one a constant, the matched gain, G_m, and the second, G_{1m2}, a function of the load $r_2{}^m$.

If $K > 1$ and $|K_m| < 1$ (B_1 positive) the device is unconditionally stable, and constant power gain circles for G_{1m2} concentric with the origin can be constructed. Any circle other than the origin represents a gain which is less than the gain obtained under the simultaneous matched conditions. The radius of a circle for a given gain is

$$|r_2{}^m|^2 = \frac{1-g_m}{1-|K_m|^2\,g_m} \quad (65)$$

where

$$g_m = \frac{G_{1m2}}{g_m} \quad (66)$$

and $0 < g_m < 1$.

For $K > 1$ and $K_m > 1$ (B_1 negative), the device is potentially unstable and the transducer power gain under matched generator and load represents the minimum power gain obtainable under matched input conditions. Constant gain circles can again be constructed in the $r_2{}^m$ plane. The circles are again concentric with the origin. The radius of the circle in this case is also given by Equation (65) but now g_m goes to infinity at

$$|r_2{}^m| = \frac{1}{|K_m|} \quad (67)$$

and the network is potentially unstable outside of this region.

For $|K| > 1$ but K negative, stable gain is obtained only for $|K_m| > 1$ (B_1 positive) and only for $|r_2{}^m| > \frac{1}{|K_m|}$.

The gain $G_m{}'$ is a function only of the magnitude of $r_2{}^m$, the load, and it is therefore possible to display $\frac{G_m{}'}{G_m}$ as a function of $|r_2{}^m|$ with $|K_m|$ as a parameter. If on this plot the load coordinate ($r_2{}^m$) is physically equal to the radius of a standard Smith Chart, and the vertical scale is specified in decibels, then the constant gain circles for a given $|K_m|$ can be located on the r_2 plane [Fig. 6(a) $K > 1$, Fig. 6(b) $K < -1$].

With Equation (57) it is also possible now to display the transducer power gain for any load and any generator by means of two universal sets of curves. The transducer power gain Equation (57) can be expressed as the product of four terms.

* *The available power gain G_A can be treated in a manner parallel to that which follows for G by setting $|s_{22}{}'| = 0$.*

$$|s_{21}'| = G_m G_{1m} G_{2m} G_{12m} \quad (68)$$

G_m is the matched gain, G_{1m} is a function of only the generator r_1^m, G_{2m} is a function of only the load r_2^m, and G_{12m} is an interaction term between the generator and load.

$$G_m = |s_{21}^m|^2 = |K_m| \left|\frac{s_{21}}{s_{12}}\right| \quad (69)$$

$$G_{1m} = (1-|r_1^m|^2) \quad (70)$$

$$G_{2m} = (1-|r_2^m|^2) \quad (71)$$

$$G_{12m} = \frac{1}{|1-r_1^m r_2^m K_m|^2} \quad (72)$$

Equations (70) and (71) simply represent constant return loss circles on the r_1^m and r_2^m planes and are therefore universal (Fig. 7). Constant gain circles represented by Equation (72) are given in Fig. 8 where the position from the origin is given by $f = r_1^m r_2^m K_m$.

For $|K| < 1$ the transducer power gain can still be given by the universal curves of Figs. 7 and 8. To accomplish this, the scattering parameters are normalized to $r_1 = s_{11}^*$ and $r_2 = s_{22}^*$. The transducer power gain is then given by the product of four terms similar to Equation (68). The vector f to be used in Fig. 8 is now the sum of three terms.

Constant power gain and available power gain circles are given in the next section for any value of $|K|$ including $|K| < 1$.

Power Gain and Available Power Gain in General Case

A constant power gain G and available power gain G_A, Equations (22) and (23), give the equation of a circle on the r_2 and r_1 planes respectively.

Equations (22) and (23) can be expressed as

$$G = |s_{21}|^2 \, g_2 \quad (73)$$

$$G_A = |s_{21}|^2 \, g_1 \quad (74)$$

where

$$g_2 = \frac{|1-|r_2|^2|}{(1-|s_{11}|^2)+|r_2|^2\,(|s_{22}|^2-|\triangle|^2)-2\,\mathrm{Re}\,r_2 C_2}$$

and g_1 is given simply by interchanging the indices 1 and 2. A discussion of one, g_2 in this instance, then suffices for both g_2 and g_1.

The radius and location of a constant gain circle for g_2 is given by

$$\rho_g = \frac{(1-2K|s_{12}\,s_{21}|g_2+|s_{12}\,s_{21}|^2\,g_2^2)^{1/2}}{(1+D_2\,g_2)} \quad (75)$$

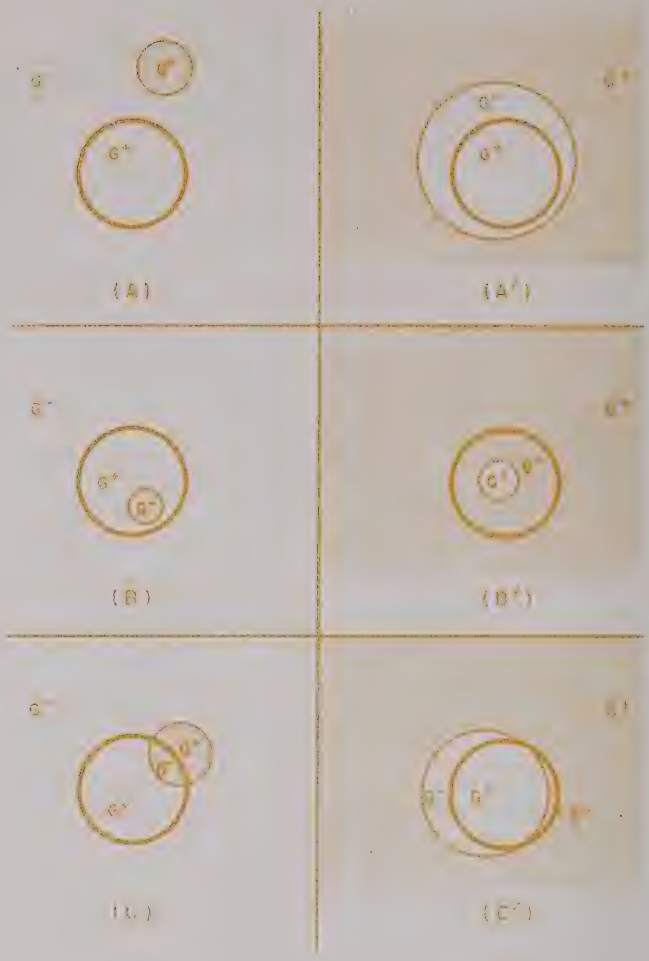

Fig. 9 — The six possible locations for the instability circle in the output plane. The shaded regions indicate the values of r_2 which provide a negative real input impedance for $|s_{11}| < 1$. Also indicated on the figures are the signs of the power gain in the various regions. The circles of equal size for all cases are the unit circles (inside the Smith chart) for r_2; outside of this circle r_2 is negative real and inside positive real.

9(A)
Input unconditionally stable; simultaneous matched load positive real. $|r_2^m| < 1$; $k > 1$; D_2 positive; $k_m < 1$.

9(A′)
Input unconditionally stable; simultaneous matched load positive real. $|r_2^m| < 1$; $k > 1$; D_2 negative; $k_m < 1$.

9(B)
Input potentially unstable; simultaneous matched loads positive real. $|r_{2m}| < 1$; $k > 1$; D_2 positive; $k_m > 1$.

9(B′)
Input potentially unstable; simultaneous matched loads positive real. $|r_{2m}| < 1$; $k > 1$; D_2 negative; $k_m > 1$.

9(C)
Input potentially unstable. $|r_{2m}| = 1$; $|k| < 1$; D_2 positive.

9(C′)
Input potentially unstable. $|r_{2m}| = 1$; $|k| < 1$; D_2 negative.

$$r_g = \left(\frac{g_2}{1+D_2\,g_2}\right) C_2^* \quad (76)$$

respectively, where

$$D_2 = |s_{22}|^2 - |\triangle|^2 \quad (77)$$

For $g_2 = \infty$ the radius ρ_g and location r_g reduce to the stability circle in the r_2 plane.

The gain at which $\rho_g = 0$ is of interest and is given by

$$g_{20} = \frac{1}{|s_{12}\,s_{21}|}\,(K \pm \sqrt{K^2-1}) \quad (78)$$

It is very informative at this time to give the six different possible locations for the stability circles, since their location indicates the general nature of the constant gain circles. Fig. 9 corresponds to an $|s_{11}| < 1$. If $|s_{11}| > 1$, then the shaded and unshaded regions simply change roles. The primed and unprimed cases are physically the same and just correspond to a positive or negative D_2. The three pairs of cases correspond to these separate physical situations: In case A the device is unconditionally stable, the matched loads

Fig. 8 — Constant gain circles giving contribution to total transducer panel gain due to interaction term G_{12m} as a function of the generator r_1^m, the load r_2^m and the device k_m.

Fig. 10 — Constant gain circles (g_2) for a set of s parameters which satisfy case C of Fig. 9. Gain g_2 is given as a numerical ratio, not in dB. Circles are plotted on the r_2 plane. $s_{11} = 0.707 \angle 0°$; $s_{22} = 0.707 \angle 0°$; $s_{12}\, s_{21} = 0.2 \angle 0°$.

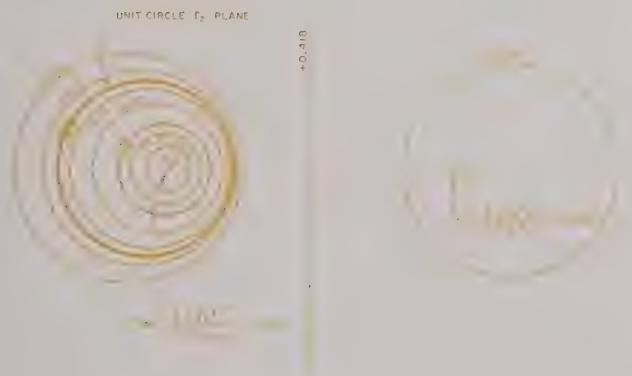

Fig. 11 — Constant gain circles for case B′ of Fig. 9. The inside of the heavily lined circle provides positive real input impedance. $s_{11} = -0.707$; $s_{22} = 0.707$; $s_{12}\, s_{21} = 1.2$; $r_{m2} = (3.53, 0.287)$.

are positive real and g_{20} is a maximum gain; for case B the loads are positive real but the device is potentially unstable and g_{20} is a minimum gain; the third case C corresponds to a potentially unstable device and also to the situation where the matched loads are pure imaginary and g_{20} is complex.

The sign of G is also given in Fig. 9 for the different regions. Equations (22) and (23) are valid for $|r_1| < 1$ and $|r_2| < 1$ only and it is necessary to return to the original definition to obtain the correct signs.

If $|K| > 1$ (case A, B) then constant power gain circles can be obtained from the previous section without having to calculate their radii and location, but if $|K| < 1$ (case C) that procedure fails and it is necessary to use Equations (75) and (76).

An example of the constant gain circles for both case B′ and C is given in Figs. 10 and 11.

As indicated previously, to realize ($G_t = G$), it is necessary to place the proper generator impedance on the input for each r_2. The proper value is given by

$$r_1^* = \frac{s_{11} - r_2 \triangle}{1 - r_2 s_{22}} \qquad (79)$$

CONCLUSION

It has been shown that a two port can be analyzed completely in terms of an easily measured set of parameters, "the generalized scattering parameters." In the first section the generalized scattering parameters were presented and fundamental power flow relations developed. In the section on power flow, an analysis of power flow was given for the case when s_{12} is sufficiently small so that it can be neglected and the unilateral design is formulated. This leads to the case in which s_{12} is not assumed zero and general power flow relations are obtained and displayed in unique and very informative graphical form. Closely tied to power flow are questions of stability which are also thoroughly discussed.

The potential use of these parameters has only been touched on; some work that is under way deals with the set of equations similar to Equations (26) - (29) for a three port network. For example, a transistor which has Z_o on all three leads can be defined by an easily measured (3 x 3) matrix. From these original 9 values all 12 s parameters for any two port configuration is given by a single equation using different sets of 4 of the original 9 matrix elements.

Possibly more important is the fact that the two port parameters for any configuration and a common lead feedback, are also then given by an equation of the same form but which includes the feedback impedance.

The practical use of the measurement system also seems unlimited.

ACKNOWLEDGMENT

The author wishes to express his appreciation to everyone who assisted in preparing and editing this manuscript. Particularly Sydney Neih, Ross Snyder and the late George Frederick for their technical assistance; also Roseanne Caldwell and Mee Chow among others for preparing the manuscript.

REFERENCES

1. Kurokawa, K., *IEEE Trans. - MTT*, March 1965, p. 194.
2. Penfield, P., Jr., "Noise in Negative Resistance Amplifiers," *IRE Trans. - CT*, Vol. CT-7, June 1960, pp. 166-170.
3. Penfield, P., Jr., "A Classification of Lossless Three Ports," *IRE Trans. - CT*, Vol. CT-9, September 1962, pp. 215-223.
4. Youla, D. C., "On Scattering Matrices Normalized to Complex Port Numbers," *Proc. IRE*, Vol. 49, July 1961, p. 122.
5. Hower, M. M., *1963 ISSCC Digest of T.P.*, p. 90.
6. Stern, A. P., "Stability and Power Gain of Tuned Transistor Amplifiers," *Proc. IRE*, Vol. 45, March 1957, pp. 335-343.
7. Rollett, J. M., "Stability and Power Gain Invariants of Linear Two Ports," *IRE Trans. - CT*, Vol. CT-9, March 1962, pp. 29-32.
8. Linville, J. G. and L. G. Schimpf, *Bell Systems Tech. Journal*, Vol. 35, July 1956, p. 818.
9. Linville and Gibbons, "Transistors and Active Circuits," McGraw-Hill Book Co., Inc., New York, 1961.

SECTION VII

CIRCUIT DESIGN AND CHARACTERIZATION OF TRANSISTORS BY MEANS OF THREE-PORT SCATTERING PARAMETERS

This article defines the three-port parameters of a transistor with or without arbitrary terminations in the transistor leads. Dr. Bodway then relates the three-port parameters to the more familiar two-port parameters for common emitter, base, and collector. He next shows that all the two-port equations have a similar form and can be mapped into constant gain circles on a Smith Chart. The variation of two-port parameters, specifically for a common emitter configuration, is analyzed with respect to series or shunt feedback. Finally, he describes the equipment used to measure three parameters of transistor chips.

CIRCUIT DESIGN AND CHARACTERIZATION OF TRANSISTORS BY MEANS OF THREE-PORT SCATTERING PARAMETERS

GEORGE E. BODWAY
Hewlett-Packard Co.
Palo Alto, California

microwave journal
Vol. 11, number 5
May 1968

INTRODUCTION

There are two requirements for the effective use of transistors, solid-state devices, and passive components. First, their characteristics must be precisely measured; second, a design capability must exist in terms of the measured quantities. Scattering (s) parameters satisfy these requirements from both a measurement and design point of view. They are particularly useful in the microwave frequency range.

Ordinarily, s-parameters of an active three-terminal device are determined by two-port measurements, connecting the common lead to ground. Unfortunately, the physical length between the device and the ground plane usually introduces a serious parisitic common-lead inductance, especially if the spacings are made large enough to obtain a very accurate 50-ohm system. The same reason that scattering parameters are measured at high frequencies (i.e. because accurate shorts and opens are difficult to achieve at these frequencies) necessitates measuring three-terminal parameters and thus, reducing considerably the errors due to this parasitic common-lead inductance.

Three-port admittance or impedance transistor parameters have been discussed before,[1] but they have never been as useful or as desirable as the three-terminal scattering parameters at microwave frequencies. When making three-port measurements, all three ports are terminated with 50 ohms. Bringing three 50-ohm transmission lines up to the device eliminates the common-lead inductance, ensures accurate reference planes, and results in a very stable measurement system. (Four-port measurements can be made in the same way for IC transistors where the substrate is the fourth terminal.) A 50-ohm termination also approximates the final circuit environment more closely at microwave frequencies than the open or short terminations required by h, y, or z parameters.

This paper discusses the theory of three-port scattering parameters and shows how previously complicated design procedures can be performed very simply in these terms. For example, all of the two-port parameters in any common configuration (CB, CE, CC) with any series feedback and any shunt feedback can be determined by using one single transformation and one matrix transformation. The two-port parameters with series feedback are related to the 9 measured quantities by 12 equations all identical in form, that is, the equations look alike. They only use different variables and consequently, only one equation has to be solved. Having only one equation to solve has been a tremendous help in tying a small desk top computer into the measurement system for instantaneous device characterizations and circuit design.

THREE-PORT SCATTERING PARAMETERS

Parameters for the three terminals of a transistor are shown schematically in Fig. 1, where the three terminals are all referred to a common ground. The incident and reflected power waves[2] can be represented by the three-port scattering matrix

$$\begin{bmatrix} b_1 \\ b_2 \\ b_3 \end{bmatrix} = \begin{bmatrix} s_{11}\, s_{12}\, s_{13} \\ s_{21}\, s_{22}\, s_{23} \\ s_{31}\, s_{32}\, s_{33} \end{bmatrix} \begin{bmatrix} a_1 \\ a_2 \\ a_3 \end{bmatrix} \qquad (1)$$

where $|s_{ij}|^2 i \neq j$ represents the transducer power gain from port j to port i, and $|s_{ii}|^2$ represents the available generator power that is reflected from the device at the i^{th} port.*

The measured parameters are referred to the characteristic impedance of the three transmission lines that terminate the device. To be of universal use, the parameters for arbitrary termination of the transistor leads are required as a function of these arbitrary terminations and the original measured parameters and arbitrary reference impedances. The expression for the new scattering parameters is given by

$$S' = A^{-1}(S - \Gamma^{\dagger})\,(I - \Gamma S)^{-1} A^{\dagger} \qquad (2)$$

where

$A_i = \dfrac{(1 - r_i^*)}{|1 - r_i|}\,(1 - |r_i|^2)\,1/2$ is the ii^{th} element in a diagonal matrix.

$$r_i = \frac{Z_i - Z_i}{Z_i' + Z_i^*} \qquad (3)$$

and

$$\Gamma_{11} = r_1,$$

$A^{\dagger}, \Gamma^{\dagger}$ = transpose of the diagonal matrices A, Γ, respectively.

The nine new scattering parameters in terms of the original parameters and arbitrary reference impedances are given by

$$s'_{11} = \frac{A_1^*}{DA_1}\Big\{ (s_{11} - r_1^*)\triangle_{23} + r_2 S_{12} s_{21}(1 - r_3 s_{33}) + r_2 r_3 [s_{23} s_{12} s_{31} + s_{21} s_{13} s_{32}] + r_3 s_{13} s_{31}(1 - r_2 s_{22}) \Big\} \qquad (4)$$

---

* *For a detailed consideration of the physical interpretation of s_{ij}, see References 2, 3 and 4.*

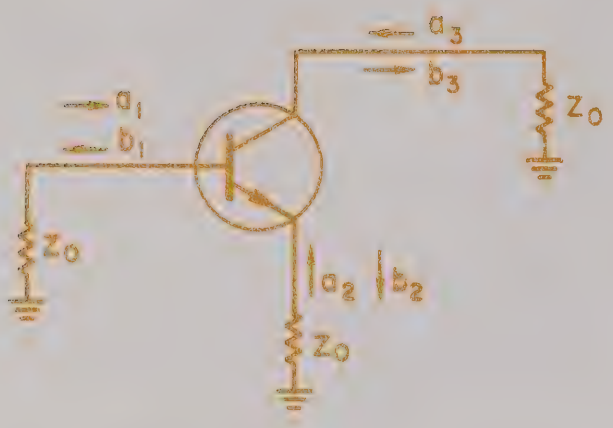

Fig. 1 — Incident and reflected waves (a, b respectively) for a transistor imbedded in a structure where all three leads are terminated by the characteristic impedance Z_0 of a transmission line.

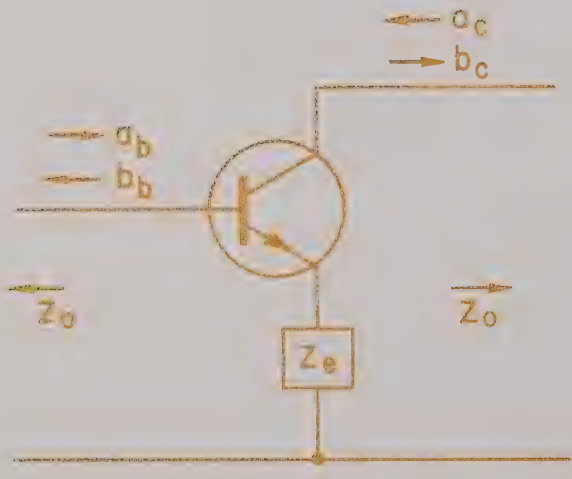

Fig. 2 — Incident and reflected waves for a transistor in common emitter configuration with an arbitrary impedance Z_e in the emitter lead.

$$s_{12}' = \frac{A_2^*}{DA_1}(1-|r_1|^2)\,[s_{12}(1-r_3s_{33})+r_3s_{13}s_{32}] \tag{5}$$

where

$$D = 1-r_1s_{11}-r_2s_{22}-r_3s_{33}+r_1r_2(s_{11}s_{22}-s_{12}s_{31}) + r_2r_3(s_{22}s_{33}-s_{23}s_{32})+r_1r_3(s_{11}s_{33}-s_{12}s_{21}) \tag{6}$$

$$\Delta_{23} = s_{22}s_{33}-s_{23}s_{32} \tag{7}$$

The other seven expressions are obtained by exchanging the indices on the above equations.

Although the set of equations represented by (4) and (5) can be used for computer analysis, it is unwieldy to manipulate and does not convey very much insight into what is taking place. A far more useful and rewarding approach has been to leave two of the ports terminated by Z_0 and allow the third port to be arbitrarily terminated. The two-port parameters are obtained in this manner by treating the common lead as arbitrarily terminated in a series impedance different than Z_0. The maximum available gain, isolation, stability and other characteristics are simply related to the two-port parameters and thus, can be evaluated as a function of this series lead impedance.

To avoid any confusion with indices, an obvious convention has been adopted for labeling the three-port scattering parameters for a transistor:

$$s = \begin{bmatrix} s_{bb} & s_{be} & s_{bc} \\ s_{eb} & s_{ee} & s_{ec} \\ s_{cb} & s_{ce} & s_{cc} \end{bmatrix} \tag{8}$$

where, for example, s_{bb} is the driving point reflection coefficient of the base with the emitter and collector both terminated by Z_0. Similarly, s_{cb} is the transducer power gain for the collector port when driving the base. s_{cb} is of particular significance for a device, being similar to h_{21} when using h-parameters and to s_{21} when considering two-port s-parameters. The frequency at which s_{cb} goes through 0 dB is defined as f_s and represents a minimum value for f_{max}. The other parameters have similar meanings.

The nine elements of matrix (8) are not all independent because we are considering a three-terminal device. In fact, there are only four independent parameters; if these are known, the others can be found, being related by the condition:

$$\sum_{j=1}^{3} s_{ij} = \sum_{i=1}^{3} s_{ij} = 1. \tag{9}$$

This relation follows from a similar relation for the y-parameters where

$$\sum_{i=1}^{3} Y_{ij} = \sum_{j=1}^{3} Y_{ij} = 0; \tag{10}$$

for example,

$$s_{cb} = 1 - s_{eb} - s_{bb}. \qquad (11)$$

From Equation (4) it is now possible to obtain the expressions for the two-port parameters, with any feedback element as a common-lead impedance. See Fig. 2.

Obtaining Two-Port Parameters From Three-Port Information

The two-port parameters for the three possible configurations are given by three sets of Equations: (12a), (12b), and (12c).

Common Emitter

$$s_{fe} = s_{cb} + \frac{s_{ce}s_{eb}}{\frac{1}{r_e} - s_{ee}} \qquad s_{1e} = s_{bb} + \frac{s_{be}s_{eb}}{\frac{1}{r_e} - s_{ee}}$$

$$s_{re} = s_{bc} + \frac{s_{be}s_{ec}}{\frac{1}{r_e} - s_{ee}} \qquad s_{2e} = s_{cc} + \frac{s_{ce}s_{ec}}{\frac{1}{r_e} - s_{ee}} \qquad (12a)$$

Common Base

$$s_{fb} = s_{ce} + \frac{s_{cb}s_{be}}{\frac{1}{r_b} - s_{bb}} \qquad s_{1b} = s_{ee} + \frac{s_{eb}s_{be}}{\frac{1}{r_b} - s_{bb}}$$

$$s_{rb} = s_{ec} + \frac{s_{eb}s_{bc}}{\frac{1}{r_b} - s_{bb}} \qquad s_{2b} = s_{cc} + \frac{s_{cb}s_{bc}}{\frac{1}{r_b} - s_{bb}} \qquad (12b)$$

Common Collector

$$s_{fc} = s_{eb} + \frac{s_{ec}s_{cb}}{\frac{1}{r_c} - s_{cc}} \qquad s_{2c} = s_{ee} + \frac{s_{ec}s_{ce}}{\frac{1}{r_c} - s_{cc}}$$

$$s_{rc} = s_{be} + \frac{s_{bc}s_{ce}}{\frac{1}{r_c} - s_{cc}} \qquad s_{1c} = s_{bb} + \frac{s_{bc}s_{cb}}{\frac{1}{r_c} - s_{cc}} \qquad (12c)$$

where

$$r_1 = \frac{Z_1 - Z_o}{Z_1 + Z_o^*}.$$

If r_1 is replaced with -1, this is the same as grounding the common lead; consequently the above series of equations give the normal two-port parameters.

Before discussing the properties of Equation (12) series, several interesting observations can be made. First, it has been recognized previously that the gain in the common emitter configuration can be increased by adding a capacitor in series with the emitter. It can be shown from typical data for s_{ee} that when Z_e is capacitive, $|(1/r_e) - s_{ee}|$ can be made a minimum, and s_{fe} attains a maximum value. The disadvantage is that the other parameters also increase; in fact, s_{1e} and s_{2e} (the input and output reflection coefficients in common emitter configuration) become greater than unity and the device is very unstable.

It can also be observed from typical data that an inductance in the common-base lead will usually cause $|1/r_b) - s_{bb}|$ to diminish and the common-base gain to increase.

Another application of the equations is to find a common-lead impedance which will minimize the reverse transducer power gain. For example, the value of r_b which makes $s_{rb} = 0$ is given by Equation (13) and a similar expression holds for the other two configurations.

$$r_b = \frac{s_{ec}}{s_{ec}s_{bb} - s_{eb}s_b}. \qquad (13)$$

If the magnitude of $r_b \leq 1$, then the element is passive and a neutralized device can be obtained.

We have touched briefly on some special applications of Equations (12). Because of the relative simplicity, a considerable amount of information can be obtained very quickly, particularly if the significance of the two-port parameters, with respect to desired circuit response, is kept in mind. The accuracy of the derived two-port parameters for a given accuracy in the original measured parameters can also be monitored easily.

Properties of Equation (12)

Equations (12a, b and c) are all of a single form which we can express as

$$s = a + \frac{b}{\frac{1}{r} - c}, \qquad (14)$$

where a, b and c are related to the measured three-port parameters. Equation (14) is a complex equation relating the variables s and r; it is a standard equation in complex variable theory. Manipulating Equation (14) shows that the relationship between r and s is a bilinear transformation:

$$s = \frac{a + r(b - ac)}{1 - rc} \qquad (15)$$

There are two ways of looking at Equation (14) for s as a function of r. One is similar to that considered for the two-port transducer power gain. In this case, we can display circles of constant magnitude of s on the r plane. For s_{fe}, those are common emitter constant-gain circles as a function of the common-lead impedance instead of the load or generator. The radius and center of the constant-gain circles are given by (16) and (17) respectively:

$$\rho = \frac{1}{k^2}\sqrt{|f|^2 - g^2k^2} \qquad (16)$$

$$r_o = \frac{f^*}{k^2} \qquad (17)$$

where

$$g^2 = |s|^2 - |a|^2$$
$$f = c\,g^2 + a^*\,b$$
$$k^2 = |s|^2|c|^2 - |b - ac|^2$$

The other way to handle Equation (14) is to map the r plane onto the s plane. It is well known that, for the bilinear transformation, circles on the r plane map into circles on the s plane. This is significant since it means that the Smith Chart for the r plane can be mapped onto the s plane, giving both the magnitude and phase of s for each complex value of r. Precision depends only on how many circles are mapped onto the s plane. This technique gives an exceedingly broad picture of what is going on.

SHUNT FEEDBACK

Not only can the effects of a common lead impedance be characterized by the set of Equation (12), but also shunt feedback can be handled in precisely the same way.

All three leads in the three-port measurement system are referred to a common ground through a characteristic impedance Z_o. The parameters measured form the three-terminal scattering matrix. It is then possible to make a simple transformation to a new 3 x 3 scattering matrix where the ports are referred to one another (Fig. 3).

The two-port parameters with any shunt element in any configuration are then given by the same transformation as the series case [Equation (12)]. The series and shunt feedback transformation can be combined resulting in the analysis of very complicated circuits.

APPLICATIONS OF THREE-PORT SCATTERING PARAMETERS

An example of the use of the preceding three-port transformation will be described in order to demonstrate the capability and usefulness of the approach. The example chosen, because of its wide applications, will show how the two-port common emitter parameters at 1 and 2 GHz vary with either series or shunt feedback elements.

Fig. 4 is used as a reference for the mapping of circles from the r plane to circles in the s plane. For example, Point 1 is a short circuit and the values of the transformed parameters that occur at Point 1 are those that exist with a short as a series or shunt element.

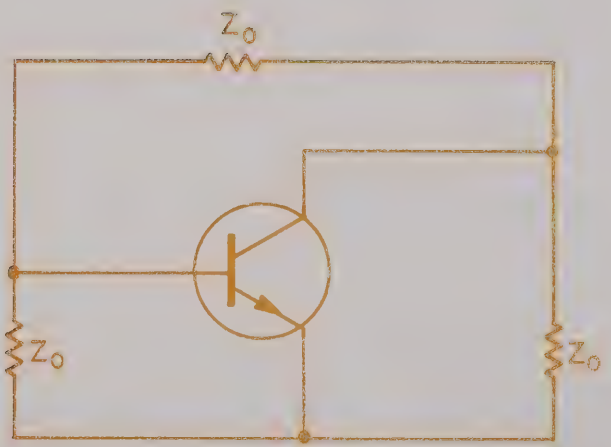

Fig. 3 — A three-terminal device imbedded in a network which can be used to readily evaluate the effects of shunt feedback.

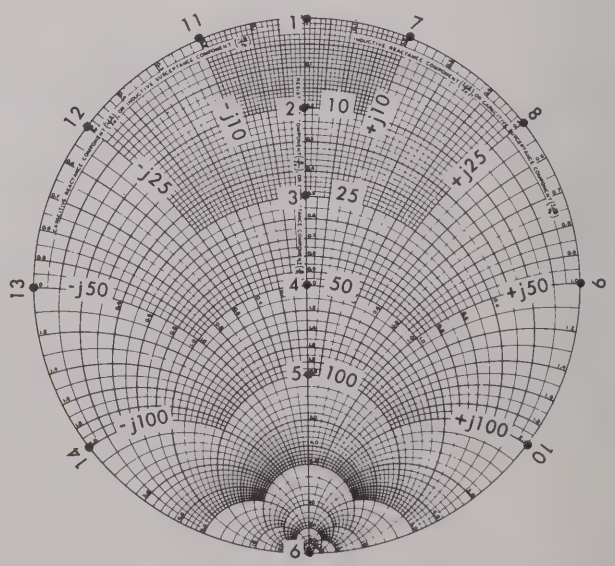

Fig. 4 — Points on the r plane (r defined by Equation 3) identified for location on the s plane for the series and shunt mapping. Note the circles which go through 1-6, 2-6, 3-6, 4-6 and 5-6 are constant r circles, while those through 7-6, 8-6, 9-6 and 10-6 are constant inductive reactance circles and the corresponding circles through 11-6, 12-6, 13-6 and 14-6 are capacitive reactance circles.

The graphs 5 through 8 display how the above theory can be applied to synthesizing the performance of transistor circuits. The example given is for a microwave small signal transistor with an f_t of about 4 GHz and an f_{max} of about 6 GHz. The transformation for 1 and 2 GHz for series feedback are given by Figs. 5 and 6 and for shunt feedback by Figs. 7 and 8.

Figs. 5 through 8 have a very general nature, in that, essentially all high frequency, small signal transistors behave similarly. Some of the information contained in Figs. 5 through 8 will be discussed in order to provide examples of the meaning and use of the graphs as well as to point out some of this general information.

Common Emitter Configuration With Series Feedback

Let us see what happens to s_{1E} or the input impedance as the common lead impedance varies (Figs. 5a and 6a). Point 1 represents a short circuit and the resulting input reflection coefficient is that of the grounded common emitter stage. As resistance is added in the emitter (moving from Points 1 through 6) s_{1E} moves essentially on a constant resistance line of a few ohms in the direction of increasing series capacitance. Similarly increasing inductance (Points 1, 6, 7, 8, 9, 10) results in essentially an increase in the real part of the input impedance; the reactance, being relatively constant.

In the case of s_{2E} (Figs. 5d and 6d) the effect is more complicated; the magnitude of s_{2E} increases with increasing L, R or C. With inductance or resistance in the emitter, the output impedance becomes more capacitive and, for values of R less than Point 4, the real part decreases while it increases for inductive loads.

The transducer power gain in a Z_o system $|s_{2E}|^2$ decreases for either a resistor or inductance in the common lead. The effect is less at higher frequencies for a given device; for example, a resistance indicated by Point 4 results in a gain which is the same at both 1 and 2 GHz. The very serious effect small inductances can have at high frequencies could be illustrated by evaluating the drop in gain if, for example, a 100 mil lead length were used with this chip. This would correspond to about 12.5 ohms of inductance, or just past Point 7 at 1 GHz (Fig. 5b), and 25 ohms on Point 8 at 2 GHz (Fig. 6b). The drop in gain is significant. The effect is, of course, much more serious as you move up in frequency to the 4-6 GHz range which is the present practical limit for useful transistor operation. A capacitive emitter impedance, in general, increases the transducer power gain, but also causes an increase in s_{11} and s_{22} resulting in instability. Notice also that there does not exist a positive real value of impedance which will neutralize the device at 1 or 2 GHz.

Common Emitter With Shunt Feedback

In this case Point 6 (Figs. 7 and 8) or an open circuit corresponds to the grounded emitter configuration. The values for the parameters obtained with an open shunt impedance (Point 6, Figs. 6 and 8) should, of course, be identical to that for a short circuit emitter series impedance (Point 1, Figs. 5 and 6).

The input impedance s_{1E} is relatively independent with either capacitive or resistive feedback (Figs. 7a and 8a). This is because of the low input impedance into the device. The value of s_{1E} is much more sensitive to inductive shunt feedback as indicated by moving from an open circuit Point 6 through Points 10, 9, 8, 7 and 1 corresponding to lower values of inductive impedance.

$|s_{21}|^2$, the transducer power gain, decreases with resistive or capacitive shunt feedback. For example, a collector base capacitance of 1.5 pf causes a drop in gain from Point 6, Figure 7b, to Point 14 and a drop to Point 13 in Fig. 8b. Also the effect of reducing the collector base capacitance, for example, by reducing the base pad size can be easily ascertained. As inductive shunt feedback is added, the gain increases to very large values until very small values of inductance are reached when the gain begins to drop approaching essentially zero with a short circuit.

The reverse gain s_{12} increases with any shunt feedback. It changes a relatively small amount for capacitive or resistive feedback, but changes more drastically for inductive feedback.

Point 5, (Figs. 7b and 8b, 100 ohms) gives a gain $|s_{21}|^2$ of about 5 dB at 1 and 2 GHz with about 15 to 10 ohms of input impedance with 45-60 ohms of output impedance and a low reverse feedback $|s_{12}| < 0.2$. More gain could be obtained over this frequency range by using inductive peaking in the shunt feedback.

The same gain, about 5 dB, can be obtained at both 1 and 2 GHz with about 50 ohms (Point 4) of series feedback (Figs. 5b and 6b).

In this case the input impedance is about 10 ohms but with about 60 ohms to 30 ohms of capacitive reactance (Figs. 5a and 6a). The output impedance is 10-20 ohms with 60-150 ohms of capacitive reactance. The reverse feedback goes from 0.2 to 0.4. Additional gain can be obtained with capacitive series peaking.

This technique has been exceptionally useful in obtaining a thorough understanding of the behavior of small signal devices in amplifier and oscillator circuits from low frequencies to the very highest frequencies at which transistors will presently operate. The technique has been used to advantage as an initial or rough synthesizing tool and also as a precise and general analysis technique for very complex circuits.

Although not illustrated, these transformations are particularly well suited for considering distributed impedances. For example, a transmission line terminated by a lumped element is represented on the r plane as a circle about the origin with frequency. This circle also maps onto the s planes as a circle.

Three-Port Measurement System

The three-port measurement system is just an extension of the two-port system, but what we will describe here in detail is the unique three-port broadband system for the measurement of unbonded transistor chips.

A schematic of the system is shown in Fig. 9 and photographs of the actual setup in Figs. 10, 11, 12, 13 and 14. The signal is directed incident on one port and measured reflected from this port and transmitted

out the other two ports. Next the second port is driven and then the third, resulting in the measurement of the 9 scattering parameters. The switching of the signal and measurement ports is controlled by electrical signals triggered either manually or by a computer. The signals are detected by a sampler and compared against a reference. The resulting output is displayed on a polar chart, oscilloscope, etc., or can be fed directly to a computer.

Transistor chips are presently being measured on a production basis for use on hybrid integrated circuits on this equipment. A chip can be measured from 0.1 to 12.4 GHz on this equipment. Almost any information about the device can be obtained; f_{max}' $|s_{21}|^2$, etc., or performance in an amplifier or oscillator. This information can also be obtained as a function of the dc bias conditions. The loading, testing, calculating, unloading and sorting can be done routinely in less than 2 minutes per device. The device is then ready to be bonded down on a microcircuit. It is assured not only that the device will work but that the circuit will perform as required with a very high yield even with many devices per circuit.

CONCLUSION

A practical and accurate technique for measuring unbonded transistor chips from 0.1 to 12.4 GHz has been described.

In order to accomplish this, a new set of parameters, the three-terminal scattering parameters for a transistor, are utilized. Not only can the conventional two-port parameters be obtained simply from the measured quantities, but also the paper shows how the effect of adding a series or shunt impedance to the device can be obtained mathematically by using a simple extension of the basic equation involved.

The data for a conventional microwave transistor is utilized for showing how a mapping technique can be applied which shows visibly at a single glance, at a particular frequency, the effect of adding any series or shunt feedback element. The data and general effects shown are typical of any microwave small signal transistors and the many figures shown are therefore of general use for reference information.

The equipment used to accomplish the measurement of transistor chips is described including a description and pictures of the techniques used to make contact to the transistor chips.

In this paper and one previously published, the foundation has been laid for the precise measurements of transistor chips in terms of useful microwave parameters as well as describing powerful design tools particularly but not limited to the precise but simple design of microwave hybrid thin film circuitry. The utilization of this material in designing microwave circuits such as oscillators and amplifiers will be described in forthcoming articles.

ACKNOWLEDGMENT

The author wishes to express his appreciation to everyone who assisted in preparing and editing this manuscript. Particularly to Mee Chow for the considerable effort required in preparing the artwork, Joan McClung and Roseanne Caldwell for preparing the manuscript and to Larry Rayher for editing the paper.

REFERENCES

1. Linville and Gibbons, "Transistors and Active Circuits," McGraw-Hill Book Co., Inc., New York, 1961.
2. Bodway, George E., "Two-Port Power Flow Analysis of Linear Active Circuits Using the Generalized Scattering Parameters," Hewlett-Packard Internal Report, April 1966.
3. Bodway, George E., "Two-Port Power Flow Analysis Using Generalized Scattering Parameters," *the microwave journal*, Vol. 10, No. 6, May 1967.
4. Kurokawa, K., *IEEE Transactions - MTT*, March 1965, p. 194.

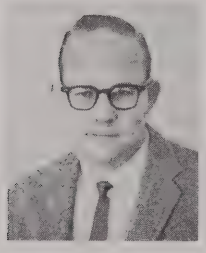

GEORGE E. BODWAY received a B.S. in 1960, an M.S. in 1964 and a Ph.D. in Engineering Physics in 1967 from the University of California at Berkeley. He is presently the Section Manager responsible for the Microcircuits and Solid State Program for the Microwave Division of the Hewlett-Packard Company.

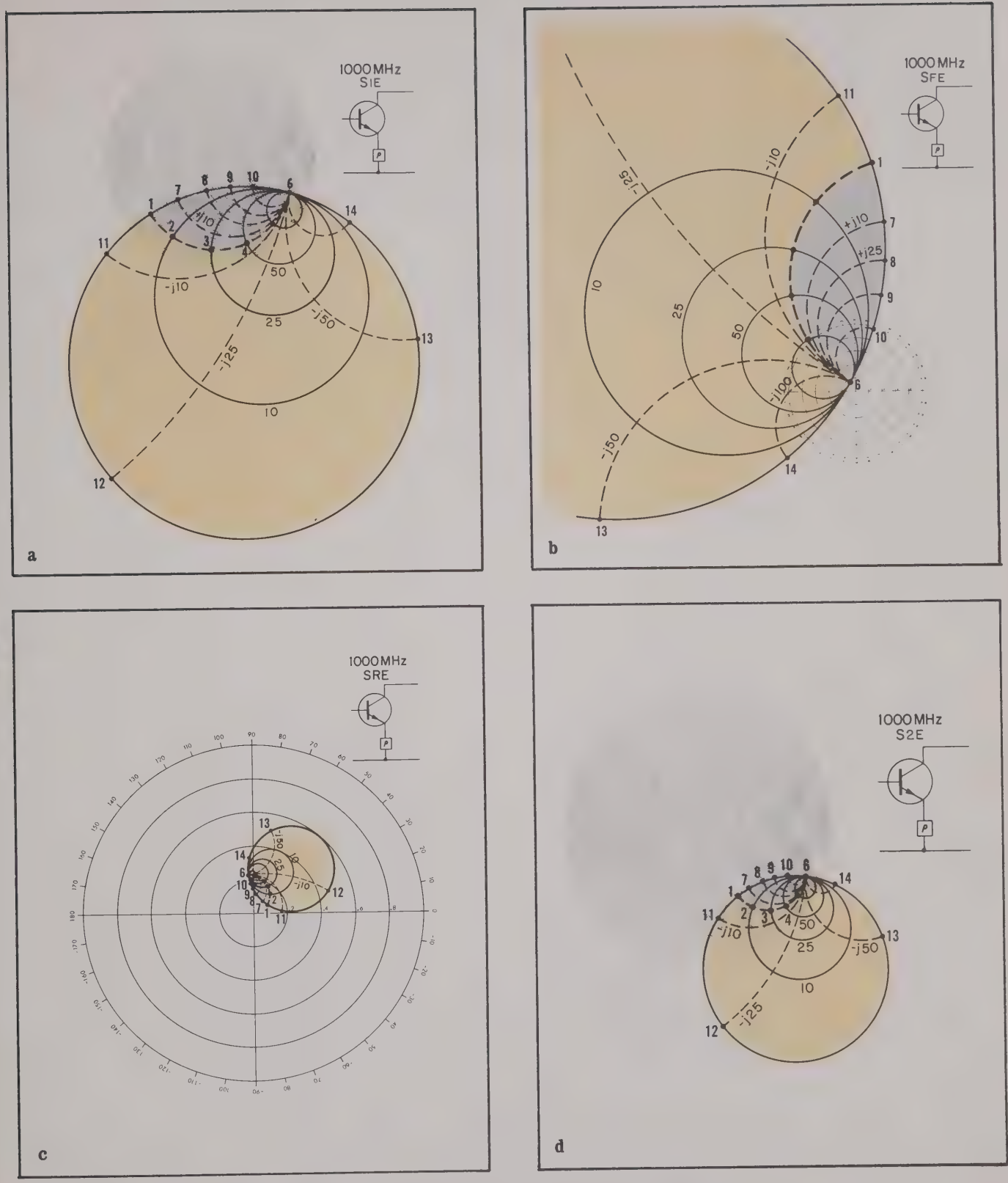

Figs. 5a, b, c and d – Common emitter series feedback impedance mapped onto the s-parameter planes at 1 GHz. The shaded regions correspond to inductive impedance while the colored areas are capacitive.

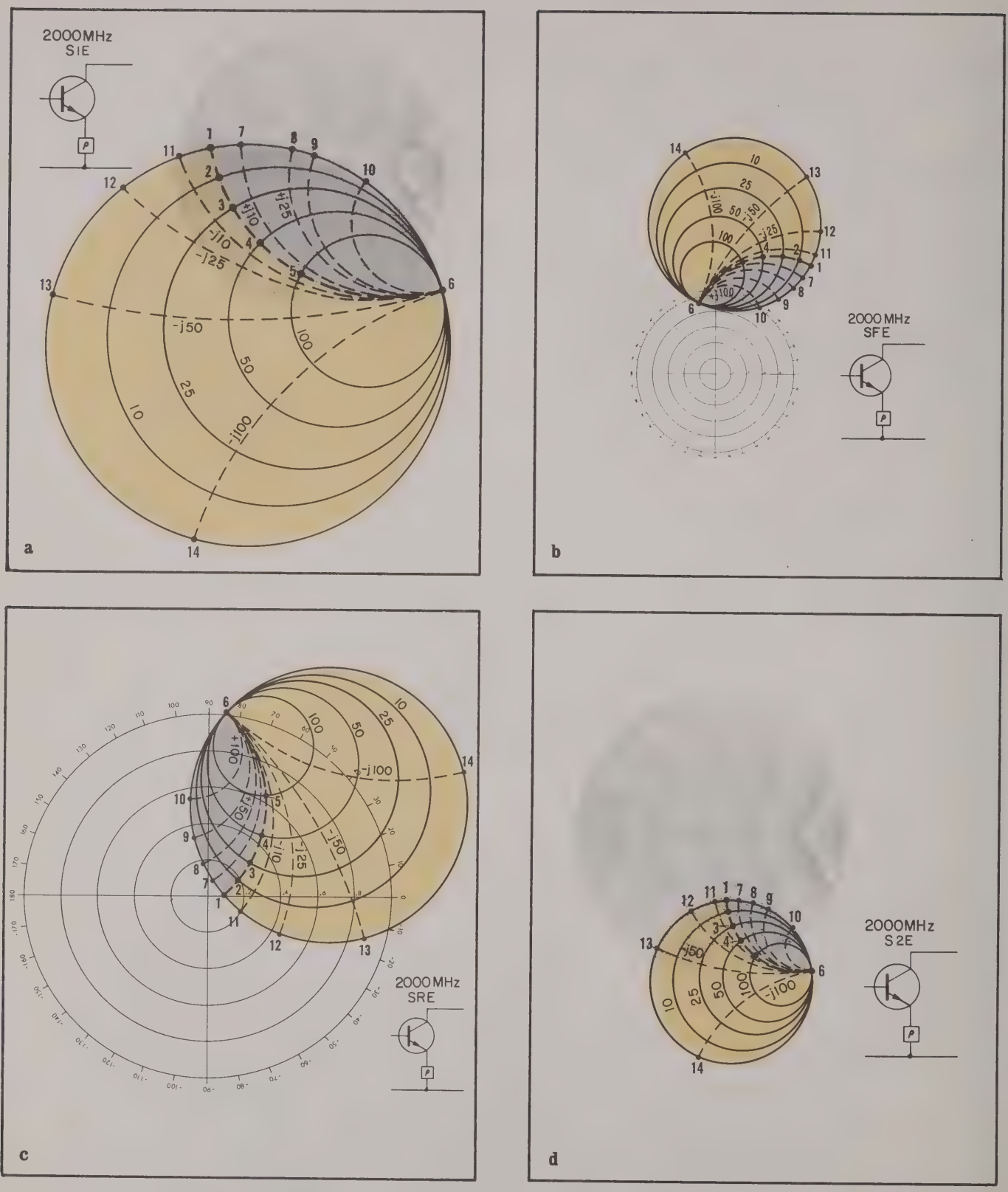

Figs. 6a, b, c and d – Common emitter series feedback impedance mapped onto the s-parameter planes at 2 GHz. The shaded regions correspond to inductive impedances while the colored areas are capacitive.

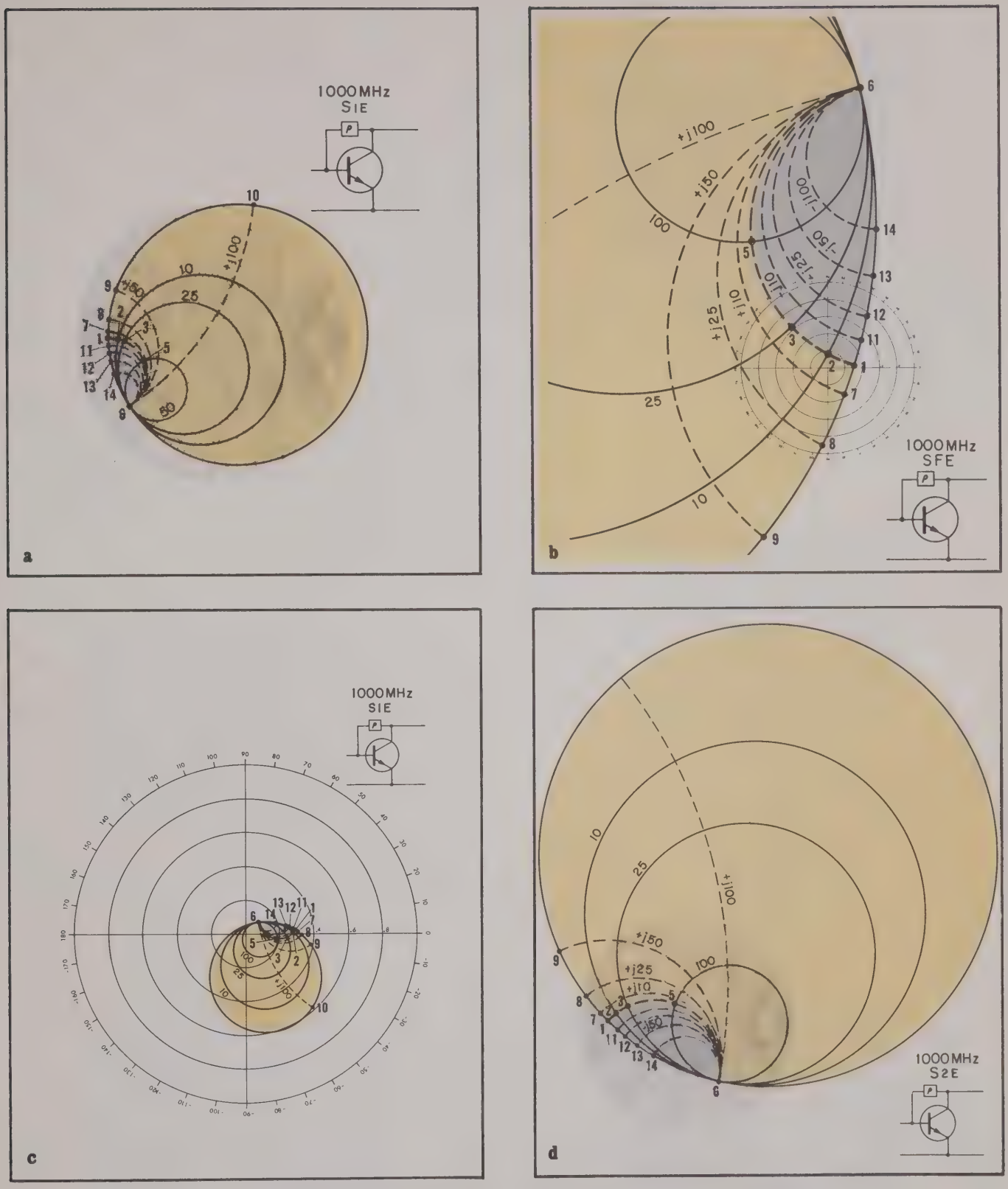

Figs. 7a, b, c and d – Common emitter shunt feedback impedance mapped onto the s-parameter planes at 1 GHz. The shaded regions correspond to inductive impedances while the colored areas are capacitive.

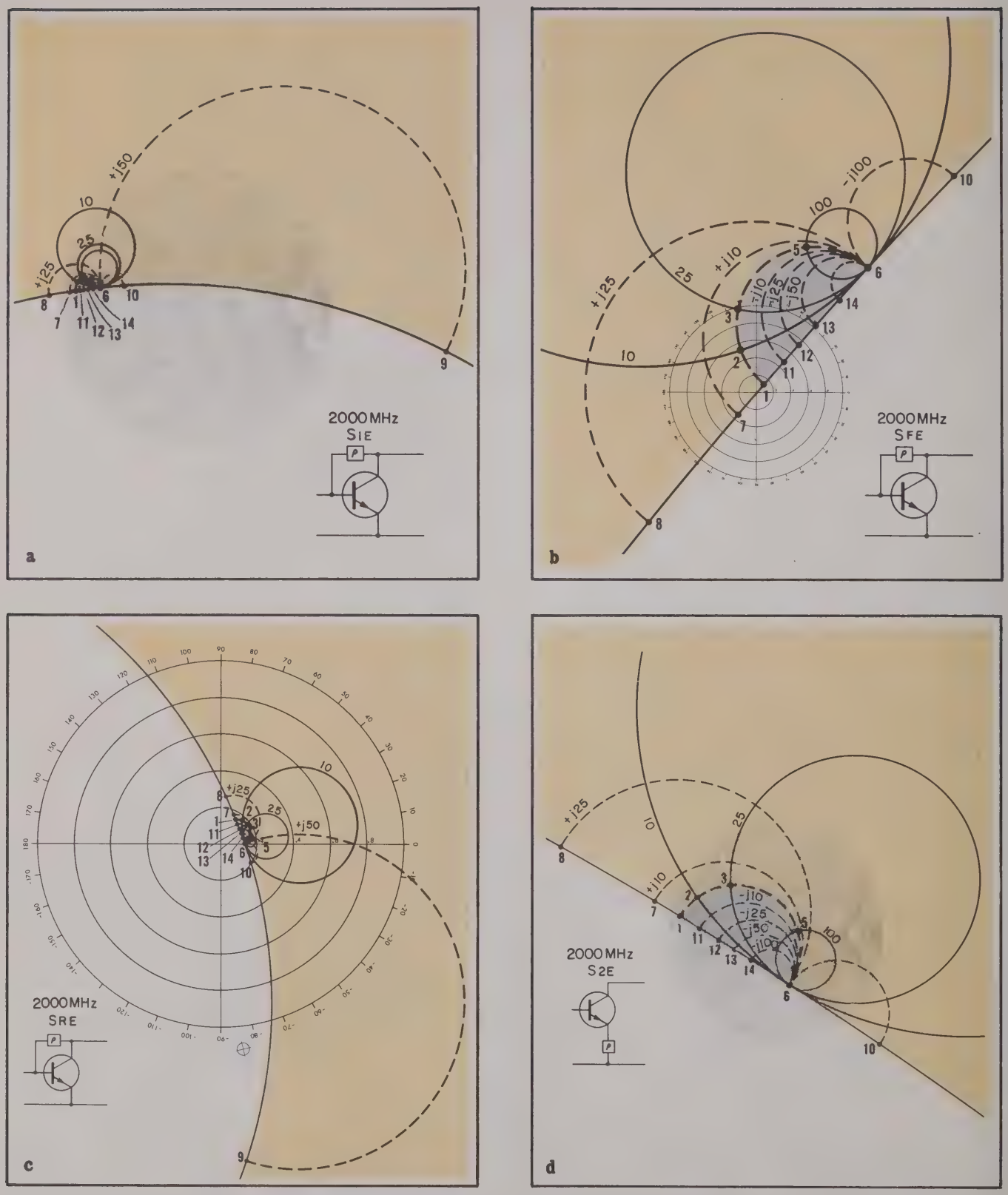

Figs. 8a, b, c and d – Common emitter shunt feedback impedance mapped onto the s-parameter planes at 2 GHz. The shaded regions correspond to inductive impedances while the colored areas are capacitive.

Fig. 9 — Schematic of the rf system used to make the three-port measurements.

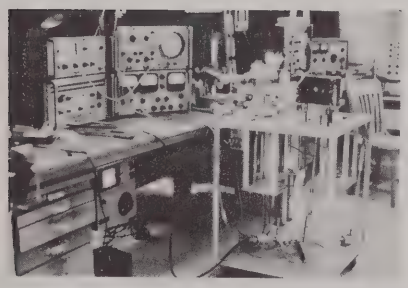

Fig. 10 — This is a photograph of the first system built to measure the three-port scattering parameters of transistor chips.

Fig. 11 — This figure shows the system in more detail. Apparent in the photograph is one of the phase shifters, bottom, the sampler on the left, a microscope at the top, a positioner for making contact to the transistor, right, and the three signal ports terminating in the transistor chip fixture in the center.

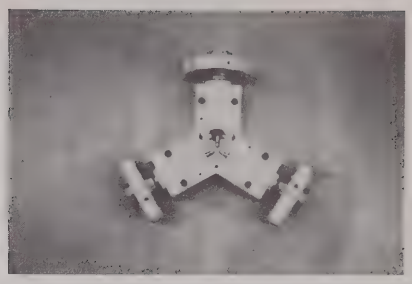

Fig. 12 — This is a close-up view of the fixture used for measuring chips with the cover removed for loading.

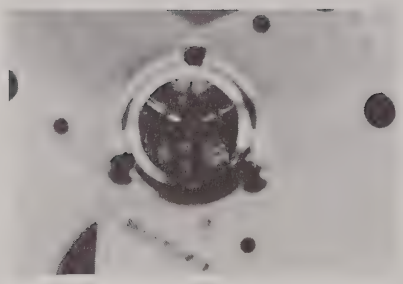

Fig. 13 — This is a close-up picture of the fixture. The three center conductors can be observed converging at the center.

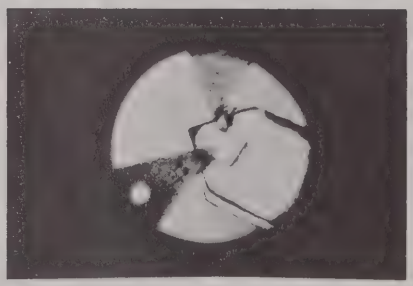

Fig. 14 — This photograph was taken through a microscope and shows one center conductor making contact to the collector (plated gold on the back of the chip) and the base and emitter contacts. This device has contact pads of about 1 mil on a side. Devices with pads 1/2 mil on a side are handled routinely.

APPENDIX

MEASURING S PARAMETERS

Today's interest in s parameters results from the ease with which these vector quantities are measured. One of the standard circuits for measuring s parameters of transistors consists of two dual directional couplers, two biasing tees, and a fixture to hold the transistors. The operation is quite straightforward.

Consider the circuit shown below.

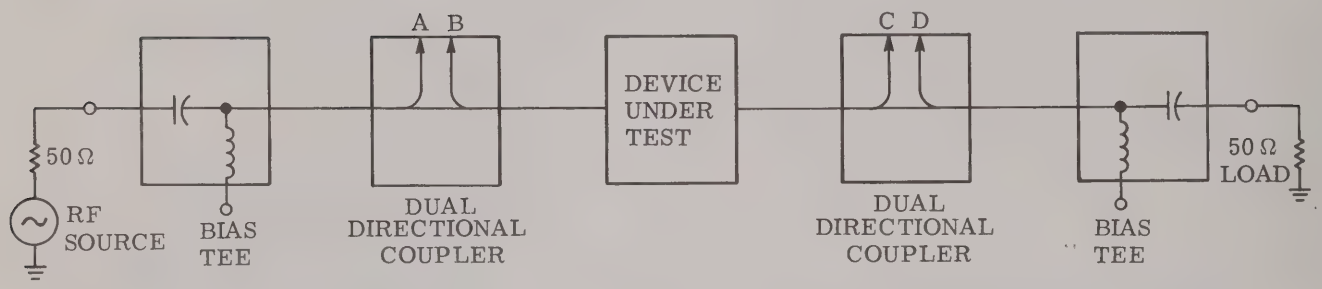

$$S_{11} = \frac{B}{A} \angle \phi_B - \phi_A$$

$$S_{21} = \frac{C}{A} \angle \phi_C - \phi_A$$

The RF source sends a signal down the 50Ω system toward the test device (transistor). The signal out of A is proportional to the signal incident on port 1 of the test device. The signal out of B is proportional to the signal reflected from port 1, and the signal at C is proportional to the signal transmitted through the test device and out of port 2. The 50Ω system on the port 2 side is terminated in the 50Ω load. As a result, the signal at D is zero because none of the signal out of port 2 is reflected back at the test device.

The ratio B/A is the magnitude of s_{11}, and the phase difference between B and A is the phase of s_{11}. Likewise, C and A determine s_{21}. Either the 8405A Vector Voltmeter or the 8410A Network Analyzer is used to detect these coupler outputs.

Similarly, the setup shown below measures s_{12} and s_{22}. The major difference between these two setups is that the 50Ω load and the RF source have been interchanged.

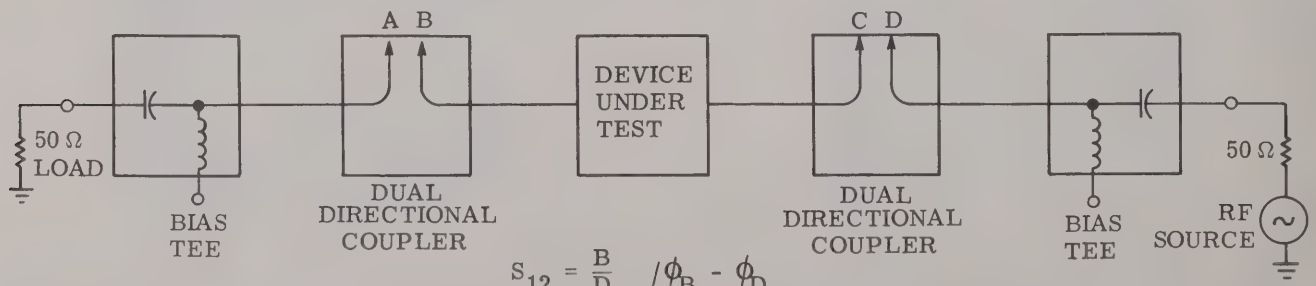

$$S_{12} = \frac{B}{D} \angle \phi_B - \phi_D$$

$$S_{22} = \frac{C}{D} \angle \phi_C - \phi_D$$

These circuits can be constructed from individual components or supplied in a single box. When the circuit is contained in a single box, the tedious job of connecting coax circuitry disappears, and s-parameter measurements can be made by pushing a button. This is the case with the HP 8745A S Parameter Test Set.

The figure below shows diagrams of two different s parameter systems.

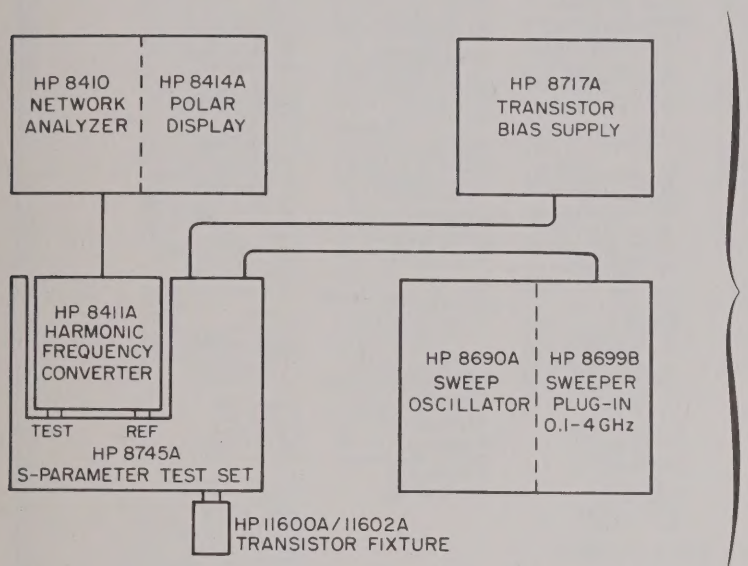

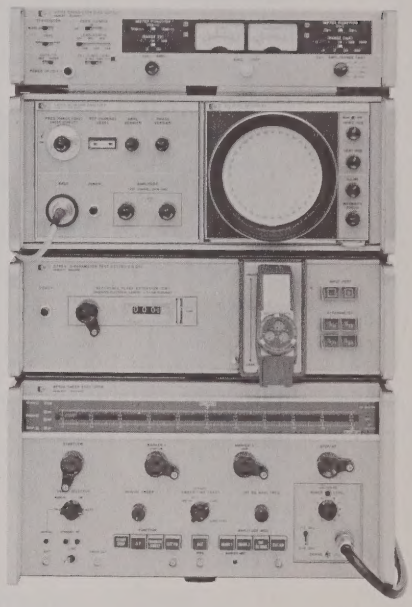

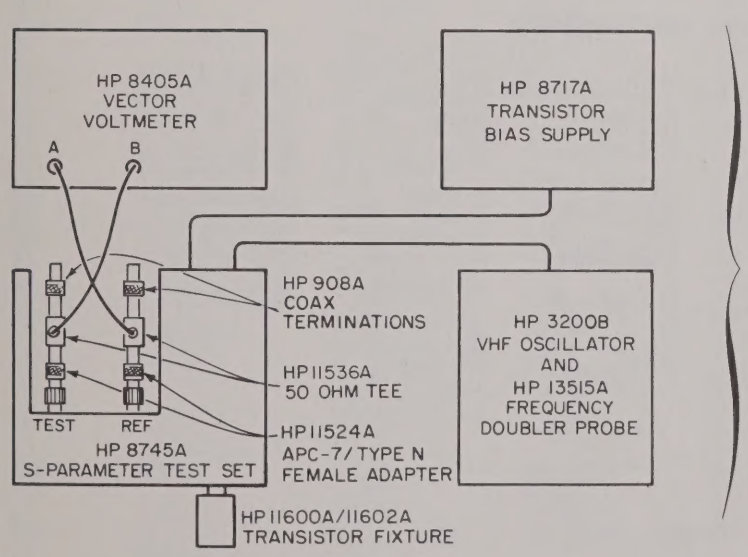

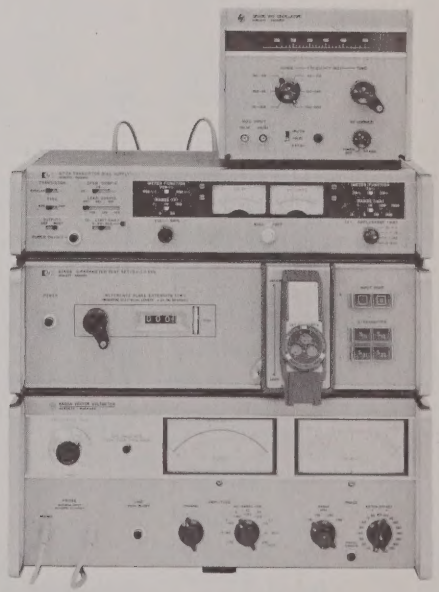

The first system makes swept-frequency measurements from 110 MHz to 2 GHz using an 8410A Network Analyzer. The minimum transistor drive signal required by this system is 22.5 mV.

The second system makes single-frequency measurements using the 8415A Vector Voltmeter. The vector voltmeter is more sensitive than the network analyzer. The minimum transistor drive signal required by this system is 5 mV. This additional sensitivity will compensate for coupler rolloff in the s parameter test set below 100 MHz. As a result, this system can be used down to 14 MHz and still preserve the same transistor signal levels required by the network analyzer system at 110 MHz.

HEWLETT·PACKARD

ELECTRONIC INSTRUMENTATION SALES AND SERVICE

UNITED STATES, CENTRAL AND SOUTH AMERICA, CANADA

UNITED STATES

ALABAMA
P.O. Box 4207
2003 Byrd Spring Road S.W.
Huntsville 35802
Tel: (205) 881-4591
TWX: 810-726-2204

ARIZONA
3009 North Scottsdale Road
Scottsdale 85251
Tel: (602) 945-7601
TWX: 910-950-1282

5737 East Broadway
Tucson 85716
Tel: (602) 298-2313
TWX: 910-952-1162

CALIFORNIA
3939 Lankershim Boulevard
North Hollywood 91604
Tel: (213) 877-1282
TWX: 910-499-2170

1101 Embarcadero Road
Palo Alto 94303
Tel: (415) 327-6500
TWX: 910-373-1280

2591 Carlsbad Avenue
Sacramento 95821
Tel: (916) 482-1463
TWX: 910-367-2092

1055 Shafter Street
San Diego 92106
Tel: (714) 223-8103
TWX: 910-335-2000

COLORADO
7965 East Prentice
Englewood 80110
Tel: (303) 771-3455
TWX: 910-935-0705

CONNECTICUT
508 Tolland Street
East Hartford 06108
Tel: (203) 289-9394
TWX: 710-425-3416

111 East Avenue
Norwalk 06851
Tel: (203) 853-1251
TWX: 710-468-3750

DELAWARE
3941 Kennett Pike
Wilmington 19807
Tel: (302) 655-6161
TWX: 510-666-2214

FLORIDA
P.O. Box 545
Suite 106
9999 N.E. 2nd Avenue
Miami Shores 33153
Tel: (305) 754-4565
TWX: 810-848-7262

P.O. Box 20007
Herndon Station 32814
621 Commonwealth Avenue
Orlando
Tel: (305) 841-3970
TWX: 810-850-0113

P.O. Box 8128
Madeira Beach 33708
410 150th Avenue
St. Petersburg
Tel: (813) 391-0211
TWX: 810-863-0366

GEORGIA
P.O. Box 28234
450 Interstate North
Atlanta 30328
Tel: (404) 436-6181
TWX: 810-766-4890

ILLINOIS
5500 Howard Street
Skokie 60076
Tel: (312) 677-0400
TWX: 910-223-3613

INDIANA
4002 Meadows Drive
Indianapolis 46205
Tel: (317) 546-4891
TWX: 810-341-3263

LOUISIANA
P.O. Box 856
1942 Williams Boulevard
Kenner 70062
Tel: (504) 721-6201
TWX: 810-955-5524

MARYLAND
6707 Whitestone Road
Baltimore 21207
Tel: (301) 944-5400
TWX: 710-862-0850

P.O. Box 1648
2 Choke Cherry Road
Rockville 20850
Tel: (301) 948-6370
TWX: 710-828-9684

MASSACHUSETTS
32 Hartwell Ave.
Lexington 02173
Tel: (617) 861-8960
TWX: 710-326-6904

MICHIGAN
24315 Northwestern Highway
Southfield 48075
Tel: (313) 353-9100
TWX: 810-232-1532

MINNESOTA
2459 University Avenue
St. Paul 55114
Tel: (612) 645-9461
TWX: 910-563-3734

MISSOURI
9208 Wyoming Place
Kansas City 64114
Tel: (816) 333-2445
TWX: 910-771-2087

2812 South Brentwood Blvd.
St. Louis 63144
Tel: (314) 962-5000
TWX: 910-760-1670

NEW JERSEY
W. 120 Century Road
Paramus 07652
Tel: (201) 265-5000
TWX: 710-990-4951

1060 N. Kings Highway
Cherry Hill 08034
Tel: (609) 667-4000
TWX: 710-892-4945

NEW MEXICO
P.O. Box 8366
Station C
6501 Lomas Boulevard N.E.
Albuquerque 87108
Tel: (505) 255-5586
TWX: 910-989-1665

156 Wyatt Drive
Las Cruces 88001
Tel: (505) 526-2485
TWX: 910-983-0550

NEW YORK
1702 Central Avenue
Albany 12205
Tel: (518) 869-8462
TWX: 710-441-8270

1219 Campville Road
Endicott 13764
Tel: (607) 754-0050
TWX: 510-252-0890

82 Washington Street
Poughkeepsie 12601
Tel: (914) 454-7330
TWX: 510-248-0012

39 Saginaw Drive
Rochester 14623
Tel: (716) 473-9500
TWX: 510-253-5981

1025 Northern Boulevard
Roslyn, Long Island 11576
Tel: (516) 869-8400
TWX: 510-223-0811

5858 East Molloy Road
Syracuse 13211
Tel: (315) 454-2486
TWX: 710-541-0482

NORTH CAROLINA
P.O. Box 5188
1923 North Main Street
High Point 27262
Tel: (919) 882-6873
TWX: 510-926-1516

OHIO
25575 Center Ridge Road
Cleveland 44145
Tel: (216) 835-0300
TWX: 810-421-8500

3460 South Dixie Drive
Dayton 45439
Tel: (513) 298-0351
TWX: 810-459-1925

OKLAHOMA
2919 United Founders Boulevard
Oklahoma City 73112
Tel: (405) 848-2801
TWX: 910-830-6862

OREGON
Westhills Mall, Suite 158
4475 S.W. Scholls Ferry Road
Portland 97225
Tel: (503) 292-9171
TWX: 910-464-6103

PENNSYLVANIA
2500 Moss Side Boulevard
Monroeville 15146
Tel: (412) 271-0724
TWX: 710-797-3650

8th Avenue
King of Prussi : Industrial Park
King of Prussia 19406
Tel: (215) 265-7000
TWX: 510-660-2670

TEXAS
P.O. Box 1270
201 E. Arapahoe Rd.
Richardson 75080
Tel: (214) 231-6101
TWX: 910-867-4723

P.O. Box 22813
4242 Richmond Avenue
Houston 77027
Tel: (713) 667-2407
TWX: 910-881-2645

GOVERNMENT CONTRACT OFFICE
225 Billy Mitchell Road
San Antonio 78226
Tel: (512) 434-4171
TWX: 910-871-1170

UTAH
2890 South Main Street
Salt Lake City 84115
Tel: (801) 486-8166
TWX: 910-925-5681

VIRGINIA
P.O. Box 6514
2111 Spencer Road
Richmond 23230
Tel: (703) 282-5451
TWX: 710-956-0157

WASHINGTON
433-108th N.E.
Bellevue 98004
Tel: (206) 454-3971
TWX: 910-443-2303

FOR U.S. AREAS NOT LISTED:
Contact the regional office nearest you: Atlanta, Georgia . . . North Hollywood, California . . . Paramus, New Jersey . . . Skokie, Illinois. Their complete addresses are listed above.

CENTRAL AND SOUTH AMERICA

ARGENTINA
Hewlett-Packard Argentina S.A.C.e.I
Lavalle 1171 - 3°
Buenos Aires
Tel: 35-0436, 35-0627, 35-0431
Telex: 012-1009
Cable: HEWPACKARG

BRAZIL
Hewlett-Packard Do Brasil I.e.C Ltda.
Rua Coronel: Oscar Porto, 691
Sao Paulo - 8, SP
Tel: 71-1503
Cable: HEWPACK Sao Paulo

Hewlett-Packard Do Brasil I.e.C. Ltda.
Avenida Franklin Roosevelt 84-grupo 203
Rio de Janeiro, ZC-39, GB
Tel: 32-9733
Cable: HEWPACK Rio de Janeiro

CHILE
Hector Calcagni P.
Casilla 13942
Estado 215 - Oficina 1016
Santiago
Tel: 31-890, 490-505

COLOMBIA
Instrumentacion
Henrik A. Langebaek & Kier Ltda.
Carrera 7 #48-59
Apartado Aereo 6287
Bogota, 1 D.E.
Tel: 45-78-06, 45-55-46
Cable: AARIS Bogota

COSTA RICA
Lic. Alfredo Gallegos Gurdián
Apartado 3243
San José
Tel: 21-86-13
Cable: GALGUR San José

ECUADOR
Laboratorios de Radio-Ingenieria
Calle Guayaquil 1246
Post Office Box 3199
Quito
Tel: 12496
Cable: HORVATH Quito

EL SALVADOR
Electrónica
Apartado Postal 1589
27 Avenida Norte 1133
San Salvador
Tel: 25-74-50
Cable: ELECTRONICA San Salvador

GUATEMALA
Olander Associates Latin America
Apartado 1226
7a. Calle, 0-22, Zona 1
Guatemala City
Tel: 22812
Cable: OLALA Guatemala City

MEXICO
Hewlett-Packard Mexicana, S.A. de C.V.
Apartado Postal 12-832
Eugenia 408, Dept. 1
Mexico 12, D.F.
Tel: 43-03-79, 36-08-78

NICARAGUA
Roberto Terán G.
Apartado Postal 689
Edificio Terán
Managua
Tel: 3451, 3452
Cable: ROTERAN Managua

PANAMA
Electrónica Balboa, S.A.
P.O. Box 4929
Ave. Manuel Espinosa No. 13-50
Bldg. Alina
Panama City
Tel: 30833
Cable: ELECTRON Panama City

PERU
Fernando Ezeta B.
Avenida Petit Thouars 4719
Miraflores
Casilla 3061
Lima
Tel: 50346
Cable: FEPERU Lima

PUERTO RICO
San Juan Electronics, Inc.
P.O. Box 5167
Ponce de Leon 154
Pda. 3-Pta. de Tierra
San Juan, P.R. 00906
Tel: (174) 725-3342
Cable: SATRONICS San Juan
Telex: SATRON 3450 332

URUGUAY
Pablo Ferrando S.A.
Comercial e Industrial
Avenida Italia 2877
Casilla de Correo 370
Montevideo
Tel: 40-3102
Cable: RADIUM Montevideo

VENEZUELA
Hewlett-Packard De Venezuela C.A.
Apartado del Este 10934
Chacaito
Caracas
Tel: 71.88.05
Cable: HEWPAK Caracas

FOR AREAS NOT LISTED, CONTACT:
Hewlett-Packard Inter-Americas
3200 Hillview Ave.
Palo Alto, California 94304
Tel: (415) 326-7000
TWX: 910-373-1267
Cable: HEWPACK Palo Alto
Telex: 034-8461

CANADA

ALBERTA
Hewlett-Packard (Canada) Ltd.
11745 Jasper Ave.
Edmonton
Tel: (403) 482-5561
TWX: 610-831-2431

BRITISH COLUMBIA
Hewlett-Packard (Canada) Ltd.
304-1037 West Broadway
Vancouver 9
Tel: (604) 738-5301
TWX: 610-922-5059

MANITOBA
Hewlett-Packard (Canada) Ltd.
511 Bradford Ct.
St. James
Tel: (204) 786-7581

NOVA SCOTIA
Hewlett-Packard (Canada) Ltd.
7001 Mumford Road
Suite 356
Halifax
Tel: (902) 455-0511
TWX: 610-271-4482

ONTARIO
Hewlett-Packard (Canada) Ltd.
880 Lady Ellen Place
Ottawa 3
Tel: (613) 722-4223
TWX: 610-562-1952

Hewlett-Packard (Canada) Ltd.
1415 Lawrence Avenue West
Toronto
Tel: (416) 249-9196
TWX: 610-492-2382

QUEBEC
Hewlett-Packard (Canada) Ltd.
275 Hymus Boulevard
Pointe Claire
Tel: (514) 697-4232
TWX: 610-422-3022
Telex: 01-20607

FOR CANADIAN AREAS NOT LISTED:
Contact Hewlett-Packard (Canada) Ltd. in Pointe Claire, at the complete address listed above.

HEWLETT·PACKARD

ELECTRONIC INSTRUMENTATION SALES AND SERVICE

EUROPE, AFRICA, ASIA, AUSTRALIA

EUROPE

AUSTRIA
Unilabor GmbH
Wissenschaftliche Instrumente
Rummelhardtgasse 6/3
P.O. Box 33
Vienna A-1095
Tel: 42 61 81
Cable: LABORINSTRUMENT Vienna
Telex: 75 762

BELGIUM
Hewlett-Packard Benelux S.A.
348 Boulevard du Souverain
Brussels 16
Tel: 72 22 40
Cable: PALOBEN Brussels
Telex: 23 494

DENMARK
Hewlett-Packard A/S
Langebjerg 6
2850 **Naerum**
Tel: (01) 80 40 40
Cable: HEWPACK AS
Telex: 66 40

FINLAND
Hewlett-Packard O/Y
Gyldenintie 3
Helsinki 20
Tel: 67 35 38
Cable: HEWPACKOY-Helsinki
Telex: 12-1563

FRANCE
Hewlett-Packard France
Box No. 6
Quartier de Courtabouef
Boite Postale No. 6
91 Orsay
Tel: 920 88 01
Cable: HEWPACK Paris
Telex: 60048 HEWPACK ORSAY

Hewlett-Packard France
4 Qua des Etroits
69 **Lyon** 5e
Tel: 42 63 45

GERMANY
Hewlett-Packard Vertriebs-GmbH
Lietzenburgerstrasse 30
1 **Berlin W** 30
Tel: 24 86 36
Telex: 18 34 05

Hewlett-Packard Vertriebs-GmbH
Herrenbergerstrasse 110
703 **Böblingen**, Württemberg
Tel: 07031-6971
Cable: HEPAG Böblingen
Telex: 72 65 739

Hewlett-Packard Vertriebs-GmbH
Achenbachstrasse 15
4 **Düsseldorf** 1
Tel: 68 52 58/59
Telex: 85 86 533

Hewlett-Packard Vertriebs-GmbH
Kurhessenstrasse 95
6 **Frankfurt** 50
Tel: 52 00 36
Cable: HEWPACKSA Frankfurt
Telex: 41 32 49

Hewlett-Packard Vertriebs-GmbH
Beim Strohhause 26
2 **Hamburg** 1
Tel: 24 05 51/52
Cable: HEWPACKSA Hamburg
Telex: 21 53 32

Hewlett-Packard Vertriebs-GmbH
Reginfriedstrasse 13
8 **München** 90
Tel: 0811 69 59 71/75
Cable: HEWPACKSA Munich
Telex: 52 49 85

GREECE
Kostos Karayannis
18, Ermou Street
Athens 126
Tel: 230 301
Cable: RAKAR Athens
Telex: 5962

IRELAND
Hewlett-Packard Ltd.
224 Bath Road
Slough, Bucks, England
Tel: Slough 753-33341
Cable: HEWPIE Slough
Telex: 84413

ITALY
Hewlett-Packard Italiana S.p.A.
Viale Lunigiana 46
20125 **Milan**
Tel: 69 15 84
Cable: HEWPACKIT Milan
Telex: 32046

Hewlett-Packard Italiana S.p.A.
Palazzo Italia
Piazza Marconi 25
00144 **Rome** - Eur
Tel: 591 2544
Cable: HEWPACKIT Rome
Telex: 61514

NETHERLANDS
Hewlett-Packard Benelux, N.V.
de Boelelaan 1043
Amsterdam, Z II
Tel: 42 77 77
Cable: PALOBEN Amsterdam
Telex: 13 216

NORWAY
Hewlett-Packard Norge A/A
Nesveien 13
Haslum
Tel: 53 83 60
Cable: HEWPACK Oslo
Telex: 6621

PORTUGAL
Telectra
Rua Rodrigo da Fonseca 103
P.O. Box 2531
Lisbon 1
Tel: 68 60 72
Cable: TELECTRA Lisbon
Telex: 1598

SPAIN
Ataio Ingenieros
Urgel, 259
Barcelona, 11
Tel: 230-69-88

Ataio Ingenieros
Enrique Larreta 12
Madrid, 16
Tel: 235 43 44
Cable: TELEATAIO Madrid
Telex: 2 72 49

SWEDEN
Hewlett-Packard (Sverige) AB
Hagakersgatan 7
431 04 **Mölndal** 4
Tel: 031 - 27 68 00

Hewlett-Packard (Sverige) AB
Svetsarvägen 7
S171 20 **Solna** 1
Tel: (08) 98 12 50
Cable: MEASUREMENTS Stockholm
Telex: 10721

SWITZERLAND
Hewlett Packard (Schweitz) AG
Zurcherstrasse 20
8952 Schlieren
Zurich
Tel: (051) 98 18 21/24
Cable: HEWPACKAG Zurich
Telex: 53933

Hewlett Packard (Schweitz) A.G.
Rue du Bois-du-Lan 7
1217 Meyrin-**Geneva**
Tel: (022) 41 54 00
Telex: 2 24 86

TURKEY
Telekom Engineering Bureau
P.O. Box 376 - Galata
Istanbul
Tel: 49 40 40
Cable: TELEMATION Istanbul

UNITED KINGDOM
Hewlett-Packard Ltd.
224 Bath Road
Slough, Bucks
Tel: Slough 753-33341
Cable: HEWPIE Slough
Telex: 84413

YUGOSLAVIA
Belram S.A.
83 avenue des Mimosas
Brussels 15, Belgium
Tel: 34 33 32, 34 26 19
Cable: BELRAMEL Brussels
Telex: 21790

FOR AREAS NOT LISTED, CONTACT:
Hewlett-Packard S.A.
Rue du Bois-du-Lan 7
1217 Meyrin-**Geneva**
Tel: (022) 41 54 00
Cable: HEWPACKSA Geneva
Telex: 2.24.86

AFRICA, ASIA, AUSTRALIA

ANGOLA
Telectra Empresa Técnica de Equipamentos Eléctricos SAR
Rua de Barbosa Rodrigues 42-1°
Box 6487
Luanda
Cable: TELECTRA Luanda

AUSTRALIA
Hewlett-Packard Australia Pty. Ltd.
22-26 Weir Street
Glen Iris, 3146
Victoria
Tel: 20.1371 (4 lines)
Cable: HEWPARD Melbourne
Telex: 31024

Hewlett-Packard Australia Pty. Ltd.
61 Alexander Street
Crows Nest 2065
New South Wales
Tel: 43.7866
Cable: HEWPARD Sydney

Hewlett-Packard Australia Pty. Ltd.
97 Churchill Road
Prospect 5082
South Australia
Tel: 65.2366
Cable: HEWPARD Adelaide

Hewlett Packard Australia Pty. Ltd.
2nd Floor, Suite 13
Casablanca Buildings
196 Adelaide Terrace
Perth, W.A.

CEYLON
United Electricals Ltd.
P.O. Box 681
Yahala Building
Staples Street
Colombo 2
Tel: 5496
Cable: HOTPOINT Colombo

CYPRUS
Kypronics
19-19D Hommer Avenue
P.O. Box 752
Nicosia
Tel: 6282-75628
Cable: HE-I-NAMI

ETHIOPIA
African Salespower & Agency Private Ltd., Co.
P. O. Box 718
58/59 Cunningham St.
Addis Ababa
Tel: 12285
Cable: ASACO Addisababa

HONG KONG
Schmidt & Co. (Hong Kong) Ltd.
P.O. Box 297
1511, Prince's Building
10, Chater Road
Hong Kong
Tel: 240168, 232735
Cable: SCHMIDTCO Hong Kong

INDIA
The Scientific Instrument Co., Ld.
6, Tej Bahadur Sapru Road
Allahabad 1
Tel: 2451
Cable: SICO Allahbad

The Scientific Instrument Co., Ld.
240, Dr. Dadabhai Naoroji Road
Bombay 1
Tel: 26-2642
Cable: SICO Bombay

The Scientific Instrument Co., Ld.
11, Esplanade East
Calcutta 1
Tel: 23-4129
Cable: SICO Calcutta

The Scientific Instrument Co., Ld.
30, Mount Road
Madras 2
Tel: 86339
Cable: SICO Madras

The Scientific Instrument Co., Ld.
B-7, Ajmeri Gate Extn.
New Delhi 1
Tel: 27-1053
Cable: SICO New Delhi

INDONESIA
Bah Boion Trading Co. N.Y.
Djalah Merdeka 29
Bandung

IRAN
Telecom, Ltd.
P. O. Box 1812
240 Kh. Saba Shomali
Teheran
Tel: 43850, 48111
Cable: BASCOM Teheran

ISRAEL
Electronics & Engineering Div. of Motorola Israel Ltd.
16, Kremenetski Street
Tel-Aviv
Tel: 35021 (4 lines)
Cable: BASTEL Tel-Aviv
Telex: Bastel Tv 033-569

JAPAN
Yokogawa-Hewlett-Packard Ltd.
Nisei Ibaragi Bldg.
2-2-8 Kasuga
Ibaragi-Shi
Osaka
Tel: 23-1641

Yokogawa-Hewlett-Packard Ltd.
Ito Building
No. 59, Kotori-cho
Nakamura-ku, **Nagoya** City
Tel: 551-0215

Yokogawa-Hewlett-Packard Ltd.
Ohashi Building
59 Yoyogi 1-chrome
Shibuya-ku, **Tokyo**
Tel: 370-2281
Telex: 232-2024YHP
Cable: YHPMARKET TOK 23-724

KENYA
R. J. Tilbury Ltd.
P. O. Box 2754
Suite 517/518
Hotel Ambassadeur
Nairobi
Tel: 25670, 26803, 68206, 58196
Cable: ARJAYTEE Nairobi

KOREA
American Trading Co., Korea, Ltd.
P.O. Box 1103
Dae Kyung Bldg.
170 Sejong Ro
Chongro Ku
Seoul (4 lines)
Tel: 75-5841
Cable: AMTRACO Seoul

LEBANON
Constantin E. Macridis
Clemenceau Street
Clemenceau Center
Beirut
Tel: 220846
Cable: ELECTRONUCLEAR Beirut

MALAYSIA
MECOMB Malaysia Ltd.
2 Lorong 13/6A
Section 13
Petaling Jaya, **Selangor**
Cable: MECOMB Kuala Lumpur

NEW ZEALAND
Hewlett-Packard (N.Z.) Ltd.
32-34 Kent Terrace
P.O. Box 9443
Wellington, N.Z.
Tel: 56-409
Cable: HEWPACK Wellington

PAKISTAN (EAST)
Mushko & Company, Ltd.
31, Jinnah Avenue
Dacca
Tel: 80058
Cable: NEWDEAL Dacca

PAKISTAN (WEST)
Mushko & Company, Ltd.
Oosman Chambers
Victoria Road
Karachi 3
Tel: 51027, 52927
Cable: COOPERATOR Karachi

PHILIPPINES
Electromex Inc.
2129 Pasong Tamo
Makati, Rizal
P.O. Box 3419
Manila
Cable: ELEMEX

SINGAPORE
Mechanical and Combustion Engineering Company Ltd.
9, Jalan Kilang
Singapore, 3
Tel: 642361-3
Cable: MECOMB Singapore

SOUTH AFRICA
Hewlett Packard South Africa (Pty.), Ltd.
Hill House
43 Somerset Rd.
Cape Town
Tel: 3-6019
Cable: AUTOPHONE Cape Town
Telex: 7038CT

Hewlett Packard South Africa (Pty.), Ltd.
P.O. Box 31716
30 De Beer Street
Braamfontein, **Johannesburg**
Tel: 724-4172 724-4195
Telex: 0226 JH
Cable: HEWPACK Johannesburg

TAIWAN
Hwa Sheng Electronic Co., Ltd.
P. O. Box 1558
Room 404
Chia Hsin Building
No. 96 Chung Shan North Road, Sec. 2
Taipei
Tel: 555211
Cable: VICTRONIX Taipei

TANZANIA
R. J. Tilbury Ltd.
P.O. Box 2754
Suite 517/518
Hotel Ambassadeur
Nairobi
Tel: 25670, 26803, 68206, 58196
Cable: ARJAYTEE Nairobi

THAILAND
The International Engineering Co., Ltd.
P. O. Box 39
614 Sukhumvit Road
Bangkok
Tel: 910722
Cable: GYSOM Bangkok

UGANDA
R. J. Tilbury Ltd.
P.O. Box 2754
Suite 517/518
Hotel Ambassadeur
Nairobi
Tel: 25670, 26803, 68206, 58196
Cable: ARJAYTEE Nairobi

VIETNAM
Peninsular Trading Inc.
P.O. Box H-3
216 Hien-Vuong
Saigon
Tel: 20.805
Cable: LANBROCOMP Saigon

ZAMBIA
R. J. Tilbury (Zambia) Ltd.
P.O. Box 2792
Lusaka
Zambia, Central Africa

FOR AREAS NOT LISTED, CONTACT:
Hewlett-Packard Export Marketing
3200 Hillview Ave.
Palo Alto, California 94304
Tel: (415) 326-7000
TWX: 910-373-1267
Cable: HEWPACK Palo Alto
Telex: 034-8461

Printed in U.S.A. 30M-11/68

HEWLETT hp PACKARD

PRINTED IN U.S